

Dipartimento di / Department of

Scienza dei Materiali

Dottorato di Ricerca in / PhD program Scienza e Nanotecnologia dei Materiali    Ciclo / Cycle XXXI

# **FUNCTIONALIZATION OF UNSATURATED POLYMERS BACKBONE FOR TYRE COMPOUNDING APPLICATION**

Cognome / Surname Andreosso    Nome / Name Ivan

Matricola / Registration number 709140

Tutore / Tutor: prof. A. Papagni

Supervisor: dr. L. Giannini

Coordinatore / Coordinator: prof. M. Bernasconi

**ANNO ACCADEMICO / ACADEMIC YEAR 2017/2018**



# CONTENTS

List of Abbreviations .....	5
Preface.....	7
Structure of the thesis.....	8
1. POLYMER FUNCTIONALIZATION.....	9
1.1 1,3 Dipolar Cycloaddition .....	12
1.1.1 Nitrones.....	16
1.1.2 Nitrile oxides .....	16
1.2 Thiol-X functionalization .....	18
1.2.1 Free Radical Thiol-Ene/Yne .....	18
1.2.2 Nucleophilic Thiol-Ene Reaction .....	19
1.2.3 Thiol-Disulfide Exchange Reactions .....	19
1.3 Triazolinedione.....	21
1.3.1 Diels-Alder .....	28
1.3.2 Alder-ene reaction .....	29
1.3.3 Electrophilic Aromatic Substitution .....	30
1.3.4 [2+2] Cycloaddition .....	31
1.3.5 Polymer functionalization with Ph-TAD.....	31
2. RUBBER COMPOUNDING.....	33
2.1 Formulation of rubber compounds .....	33
2.1.1 Rubbers .....	34
2.1.2 Fillers .....	36
2.1.3 Antidegradants .....	37
2.1.4 Vulcanizing agents.....	38
2.2 Overview on Filler reinforcement .....	39
2.2.1 Filler-Filler interaction.....	41
2.2.2 Filler-Rubber interaction .....	42

2.2.3	Polymer network effect.....	42
2.2.4	Hydrodynamic effect .....	43
2.3	Filler rubber interaction, the key role of interface.....	43
2.4	Increasing compatibility: state of the art and our proposal .....	45
3.	SYNTHETIC PROCEDURES .....	47
3.1	1,3 dipolar cycloaddition.....	48
3.2	Thoils-ene.....	60
3.3	Triazolidinone .....	68
3.3.1	Oxidation with hypervalent iodine: .....	71
3.3.2	Oxidation with hypochlorite .....	72
3.3.3	Oxidation with nitrogen(IV).....	72
3.4	Polymers backbone functionalization with PhTAD .....	73
3.4.1	Scale Up.....	77
3.4.2	Polybutadiene Functionalization .....	81
3.4.3	Polyisoprene Functionalization .....	91
3.5	Diazeno derivative Synthesis.....	97
4.	FORMULATION AND CHARACTERIZATION OF RUBBER COMPOUNDS .....	106
4.1	General procedures for rubber compounding.....	107
4.1.1	IR compounds.....	110
4.1.2	Functionalized BR-based compounds .....	120
5.	CONCLUSIONS.....	134
6.	APPENDIX A – MATERIAL AND INSTRUMENT .....	137
7.	APPENDIX B – Experimental part .....	141
	Bibliography.....	161

## LIST OF ABBREVIATIONS

AIBN	2,2'-Azobis(2-methylpropionitrile)
ATRP	Atom Transfer Radical Polymerization
BR	Butadiene Rubber
CB	Carbon Black
DA	Diels Alder
DCC	N,N'-Dicyclohexylcarbodiimide
DCM	DiChloroMethane
DEAD	DiEthyl AzoDicarboxylate
DMA	Dynamic Mechanical Analysis
DMSO	DiMethyl SulfOxide
FTIR	Fourier-Transform InfraRed spectroscopy
GPC	Gel Permeation Chromatography
HOMO	Highest Occupied Molecular Orbital
IR	Isoprene Rubber
Me-TAD	4-methyl-1,2,4- triazoline-3,5-dione
$M_n$	Number average molecular weight
$M_w$	Weight average molecular weight
MPTMS	(3-MercaptoPropyl)TriMethoxySilane
NMR	Nuclear Magnetic Resonance
NR	Natural Rubber
LUMO	Lowest Unoccupied Molecular Orbital
ODR	Oscillating Disk Rheometer
PB	PolyButadiene
Ph-TAD	4-phenil-1,2,4- triazoline-3,5-dione
phr	Parts per hundred rubber
PIDA	phenyliodine(III)diacetate
PyDP	bis [4-(1-pyrenyl) butyl]3,3'-disulfanediyl dipropanoate
RAFT	Reversible Addition-Fragmentation chain Transfer
RPA	Rubber Process Analyzer
SemiC	ethyl(anilinocarbonyl)diazencarboxylate

SBR	Styrene-Butadiene Rubber
SN <sub>Ar</sub>	Nucleophilic Aromatic Substitution
TAD	1,2,4- triazoline-3,5-dione
TEA	TriEthylAmine
TESPT	Bis[3-(triethoxysilyl)propyl] Tetrasulfide
Tg	glass transition Temperature
THF	Tetrahydrofuran
TLC	Thin Layer Chromatography
UV	UltraViolet

## PREFACE

When Ford, in 1908, launched the Model T, the very first car produced by an assembly line, he was rewriting the mankind history. Since then, the demand of cars has always been growing, with a rise that seems unstoppable. To date, more than 1.2 billion vehicles are circulating worldwide, and it is estimated that this number is set to increase up to an impressive 2 billion in 2035. At the same time, the demand for tires has consequently increased and the tire industry kept pace investing heavily in research and development, to improve the product in all its components. Important steps have been taken in the understanding of the filler-rubber interactions and of the dynamic mechanical properties connected to them, with attention to the nature of the filler and its functionalization, to make it more compatible with the polymer matrix.

Only recently the idea of a complementary approach attracted more interest and this project was born under this light, with the idea of functionalizing the polymer backbone, introducing functional groups able to make the matrix more compatible with the inorganic fillers used as reinforcing agents.

Thinking of chemical modification of the elastomeric matrix, the main ingredient of any rubber-based composite, is a fascinating but also extremely challenging strategy. The recipes used for compound formulation have been optimized in over one hundred years of research and they have reached a high degree of complexity. During compounding, net of the production process, a dozen of different ingredients synergistically interacts with each other to give to the product the expected properties; we need to be aware that changing the majority component that holds everything together can trigger a cascade process that overturns established conventions, forcing the research to start from scratch in the optimization process.

This is the first collaboration between an industrial partner, like Pirelli, with the research group where I worked, whose background is in organic synthesis. Starting from a clean sheet offers a lot of opportunities, but it has been necessary to invest some time to acquire a basic knowledge of the reactivity of the polymers, to gain practical experience in compound formulation and to learn their mechanical dynamic behavior.

Furthermore, formulation and characterization of the compounds was carried out in the laboratories of our industrial partner, whose equipment are much bigger than the laboratory scale standards. This fact requires working on large quantities of material, in hundreds of grams scale, which has made the production of a functional material difficult and time-consuming, with a consequent slowing down of the research work.

## STRUCTURE OF THE THESIS

The **first chapter** will describe the ideal characteristics that a suitable functionalization should have, using these key parameters as a starting point for the literature research, in order to find some useful reactivity for the purpose of the thesis. They will therefore be individually listed, briefly describing their history and the main characteristics.

The **second chapter** will provide a theoretical introduction on the compound formulation and on their dynamical-mechanical characteristics.

In the **third chapter** the experimental details of the preparation of the precursors, of the coupling agents and of the functionalized materials will be described.

In the **fourth chapter** the results will be presented, in which the chemical, physical and mechanical properties of both the functionalized rubbers and the compounds produced will be reported.

Finally, in the **fifth chapter** conclusions, main results, and future developments to which this thesis will open the doors will be summarized.

At the bottom there is also an additional chapter (i.e. **Appendix**) where instruments, measurement methods and synthetic procedures are described.

# 1. POLYMER FUNCTIONALIZATION

One of the main fields of application of polymers chemistry is the synthesis and development of innovative materials, whose properties can be technologically useful and relevant.

If the twentieth century and the world history were revolutionized by studies that allowed the discovery of new synthetic ways to produce polymers on industrial scale, in the present century the scientific research was deployed in the front line on a new topic, the polymer functionalization.

To carry out a comprehensive study on this topic, it should be done a distinction between pre-polymerization and post-polymerization functionalization.

In the first case it is possible to insert specific functional groups into different chain position: one of the most commonly used strategies concerns the functionalization of the head or of the tail of the polymer (also known as "functionalization in  $\alpha$ - or  $\omega$ - position"); another opportunity is represented by the functionalization of the polymeric backbone acting on the monomers, which must then be polymerized.

The synthesis of a polymer starting from a telechelic polymer, or the use of functionalized chain initiators and/or terminators is one of the hallmarks of the atom transfer radical polymerization (ATRP) and its different form such as the Reversible Addition-Fragmentation chain Transfer polymerization (RAFT).<sup>1</sup>

The adoption of this type of strategy allows to have a functional group in a key position of the polymer chain, but it also has some intrinsic limitations. First of all, the stoichiometry is strongly limited, since it is not possible to insert more than one unit per chain, moreover the library of functional groups, able to support the polymerization conditions without being involved in side reactions, is quite narrow.

As far as the functionalization of monomers is concerned, the advantage of this type of approach is easily identifiable: by working on the single molecules it is possible to resort to a plethora of chemical reactions through the classical organic chemistry synthesis techniques, developed over centuries of research. The access to such a wide range of reactions allows, theoretically, to make a monomer bearing any type of functionalization on the side chain, avoiding the need to operate on the polymer, which is not always possible, especially if working on a high molecular weight macromolecule. The downside is also represented here by the polymerization reaction itself, whose the conditions of which must be compatible with the functionalization introduced, and, even if it was possible to obtain stable functionalized monomers, it would be necessary to study the reactivity

of the monomers from scratch, in order to understand their behavior during the polymerization phase and making a product that shows the desired chemical-physical characteristics.

A chemical modification to be carried out after polymerization is therefore the only valid alternative able to insert specific functional groups on the chain without taking care of the reactivity of the latter during the polymerization stage and, most importantly, without the need to re-optimize the already defined conditions on industrial scale. However, it should be noted that processing and compounding of a chemically modified polymer would be strongly affected by the functionalization itself.

This type of approach, during history, has been perceived as a "surrender" by the scientific community, due to the impossibility of synthesizing a polymer with the characteristics expected according to the known methods. Nevertheless, in recent years the development of new techniques and the introduction of the concept of "click-chemistry" has brought new life to this sector, making possible the creation of a wide range of compounds with different properties, architecture and functionalization thanks to post-polymerization functionalization.

However, patrolling such a vast territory is still complicated since it is necessary to examine countless types of chemical transformations in order to identify the most suited one for the purpose of this thesis. During this project, to narrow down the field and focus on a set of feasible functionalizations, we have chosen to borrow some of the key concepts typical of click-chemistry, according to which an ideal functional group should give rise to a reaction:

- Without any side product or collateral reaction
- Integrable in a process flow
- Easy reaction and simple purification procedures
- Selective functionalization
- Able to run under mild condition
- Versatile
- Not toxic
- Cheap

Matching all these requests is really complicated, and the problem becomes even more difficult to solve if we add the constraints imposed by the substrate we want to use: an olefinic polymeric matrix (Butadiene Rubber (BR), Isoprene Rubber (IR) or Styrene-Butadiene Rubber (SBR)), and the goal we want to pursue: to have a functional group able to compatibilize the inorganic fillers with the polymer.

The ideal functionalization must, therefore, be able to:

- Form covalent bond with rubber matrix
- Interact with target fillers

Finally, since collaborating with an industrial partner, the reactivity used should desirably be new or, at least, never been used for filler-rubber compatibilization.

As mentioned in the preface, the first part of the doctoral project was dedicated to an extensive survey of the literature to identify a range of suitable functionalizations. The most promising candidates appeared to be the three listed below:

- 1,3 dipolar cycloaddition
- Thiol-ene reaction
- Aza-ene reaction

These reactivities will be therefore described in detail in the following dedicated sections, in which the theoretical concepts and their relative reactivity will be introduced.

## 1.1 1,3 DIPOLAR CYCLOADDITION

The first reactivity that appeared to be able to fulfill most of these criteria was a pericyclic reaction such as the 1,3 dipolar addition.

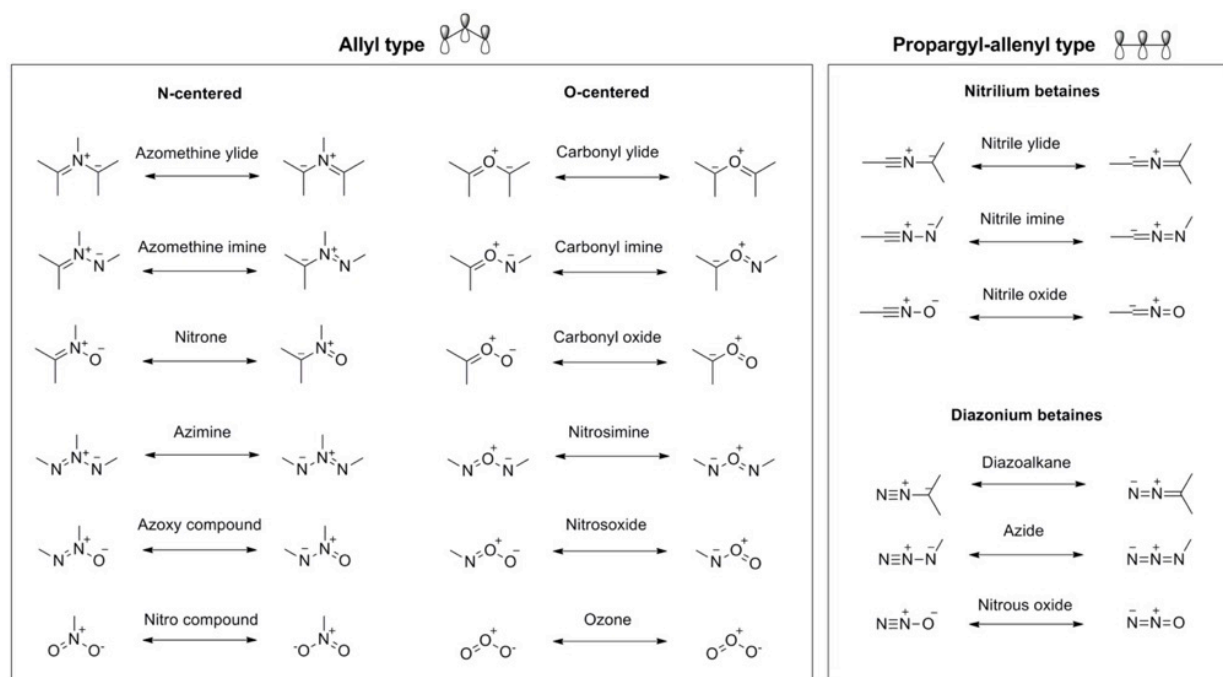
This type of reactivity is based on the chemical reaction between a 1,3 dipole and a dipolarophile with the formation of a five-member-ring.

Although several works, between the late 1800s and early 1900s, proposed reactions that used this type of reactivity,<sup>2-3-4-5-6-7</sup> a detailed description of the reaction mechanism was not provided until the pioneering work of Rolf Huisgen<sup>8</sup> of 1963, who hypothesized a single-step concerted mechanism, thus justifying the stereospecificity of this type of reaction.

Already in 1970, Firestone presented an alternative mechanism that involved the formation of a di-radical intermediate in a two-step mechanism.<sup>9</sup>

The issue is still much debated to date, with arguments in favor of one or the other theory, however the currently most accredited one describes it as a concerted and asynchronous reaction despite there are examples of stepwise mechanism of reactions without catalyst with thiocarbonyl ylides,<sup>10</sup> or nitrile oxides<sup>11</sup>.

With a great scientific interest behind, given by the extraordinary ability to form heterocycles in a stereo- and regioselective way that motivated the extensive use of this type of reactivity for applications in biological-pharmaceutical field, it is possible to find in literature thousands of



SCHEME 1 – CLASS OF POSSIBLE DIPOLES, LISTED BY THEIR GEOMETRY

articles with the more disparate conditions. It is therefore appropriate to analyze the two key players involved in this type of reactivity, namely the 1,3-Dipole and the dipolarophile.

A dipole 1,3 is an organic molecule in which there is a charge separation and 4  $\pi$ -type electrons are delocalized on three atoms (which constitute the dipole).

Depending on the geometry, bent or linear, it is possible to distinguish dipoles in two types: allyl-type or propargyl-type respectively (Scheme 1).<sup>12</sup>

Usually these compounds have in their structure a nitrogen or oxygen heteroatom, or rarely there are dipoles containing sulfur or phosphorus.

Considering the delocalization of the charge on more atoms, it is not correct to assign a unique structure formula, rather it is convenient to represent all the resonance structures. Nevertheless, in the literature there are examples in which the mesomer significantly contributing to the energy of the ground state is determined, both through experiments and computationally.<sup>13-14</sup>

The charge distribution has a direct consequence on the reactivity of these systems: one of the key parameters that directs the reaction is the orbital overlap between the HOMO and LUMO levels of the dipole-dipolarophile couple, as postulated by Sustmann in the '70s.<sup>15</sup>

It is indeed possible to identify three types of behavior depending on the alignment and on the gap of energy levels. In the first type, commonly described as HOMO-controlled dipole (or nucleophilic dipole), we can find dipoles like azomethine ylide, carbonyl ylide, nitrile ylide, azomethine imine, carbonyl imine and diazoalkane.

In this case, the HOMO of the dipole tends to align with the LUMO of the dipolarophile. It is therefore obvious that any electron-tractor substituent, thus able to lower the LUMO, allows an approach of the levels, speeding up the reaction. On the contrary, an electron-donor group will accentuate the spacing between the levels, slowing down (or in the worst case, preventing) the reaction.

The behavior that characterizes dipoles such as nitrile imide, nitron, carbonyl oxide, nitrile oxide, and azide, is instead of the second type, also called HOMO-LUMO-controlled dipole (or ambiphilic dipole), in which the two frontiers molecular orbitals can both move in direction of their target orbital and any substituent helps to close this gap, thus increasing the reaction speed.<sup>16</sup>

Finally, a third type can be identified in which the dipole LUMO is characterized by a low energy value that allows it to align with the HOMO of the target dipolarophile.

Dipoles like nitrous oxide and ozone belong to the third type, which is the LUMO-controlled dipole one (or electrophilic dipole). The introduction of a substituent on the dipolarophile produces an opposite effect to that seen for the reactivity of the first type, where the electron donor groups accelerate the reaction while the attracting groups slow it down.<sup>17</sup>

Obviously, there are several other factors, mainly related to the characteristics of dipolarophile and reaction intermediate, which influence the progress of the reaction that can be summarized as follows:

- **Conjugation of the target molecule:** During the formation of the sigma bonds between the reactants, partial charges are formed which can be stabilized by the aromaticity of the substrate, thus conferring greater stability to the intermediate reaction.
- **Polarizability of dipolarophiles:** The polarizability of the substrate regulates the reactivity of the compound, since an extensive electronic cloud makes the system more prone to exchange electrons.
- **Angle strain & Steric hindrance:** Tensioned systems have higher ground state energy levels, which make the molecule more reactive: in the same way the passage through a reaction intermediate with high steric hindrance can slow down the reaction rate considerably.

The combination of the two effects is evident when considering the isomerism of the dipolarophile that must undergo the reaction, in which the reactivity (and thus the speed of attack) between cis and trans isomers is radically different.

In the above description we often referred to functional groups capable of influencing the reactivity of the substrate; it is evident that, for this doctoral project, the use of an activated dipolarophile could not be contemplated. The starting point has to be necessarily a commercial polymer, belonging to the raw materials commonly used for tires production. The range is, therefore, limited to olefins such as polybutadiene (PB), polyisoprene (IR) or to styrene-butadiene copolymers (SBR), in which the dienophiles are constituted by the double bonds present on the polymeric backbone, either internal or terminal. We focused on the synthesis and on the subsequent coupling to the polymer matrix of variously substituted nitrones and nitrile oxides.

The reasons that led us to consider this reaction as a valid way for our purposes were different: first of all, the possibility of forming covalent bonds with the polymer matrix, introducing a functional

group able to locally modify the polarity of the rubber leaving open the possibility for further chemical modifications of the introduced group. Another very positive aspect is the ability of 1,3 dipolar cycloadditions to react in stereo and regioselective manner giving, in theory, to the operator the chance to selectively functionalize the hooking sites of a certain type (vinyl bonds lateral to the chain).

Having established the parameters imposed by the substrate, we have therefore selected two classes of dipoles to concentrate on, such as nitrones and nitrile oxides.

### 1.1.1 NITRONES

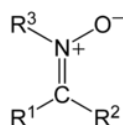


FIGURE 1 – GENERAL STRUCTURE OF NITRONE

A nitronium ion (Figure 1) is a functional group consisting of an N-Oxide of an imine. Its structure can be generically illustrated in figure 1. where R3 represents a substituent different from hydrogen.

This molecule can be produced in several ways, the most common of which are: by oxidation of N,N-disubstituted Hydroxylamines, by oximes, by aromatic nitrous compounds as well as other more exotic ways. In our case we opted for the synthesis starting from N-substituted hydroxylamine.

Once formed, it can attack different substrates to give aldol condensation, dimerization or, more interestingly for our case, 1,3 dipolar cycloadditions.

In the literature there are few but significant examples of attack on non-substituted alkenes to give isoxazoline through an addition process [3 + 2], with the formation of two new bonds, a C-C and a C-O, which guarantee a good stability of the final product. In the examples reported by Huigens, an  $\alpha$ -Phenyl-N-methylnitronium ion reacts with double terminal bonds with a whole series of alkenes, among which 1-heptene or safrole, double non-conjugated, unstressed bonds and without a proximal substituent, with yields between 92 and 95%.<sup>18</sup>

### 1.1.2 NITRILE OXIDES

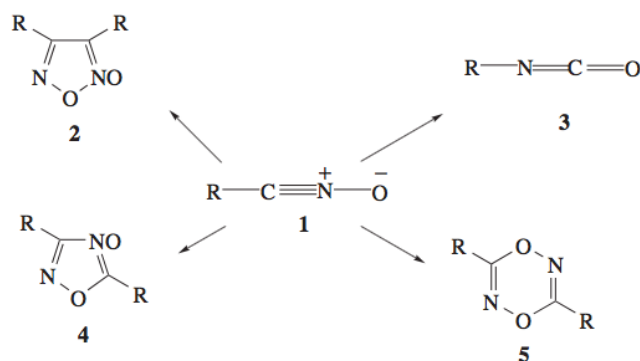
Also nitrile oxides, exactly as nitronium ions, have been widely used in organic chemistry.



FIGURE 2 - GENERAL STRUCTURE OF NITRILE OXIDE

Obviously, this class of compounds has its peculiarities; first of all, a different geometry compared to nitronium ions (Figure 2). In contrast to the latter, in fact, the nitrile-oxides have a linear geometry, which implies a different mechanism of coupling to the dipolarophile.

The preparation of nitrile oxides is slightly more complicated because of their more pronounced reactivity. They must be produced in-situ because, if they do not have a target in their proximity to react with, they can rearrange or dimerize, as described by Torssell<sup>19</sup> and reported in the scheme 2.



SCHEME 2 - POSSIBLE SIDE REACTION OF NITRILE OXIDE IN ABSENCE OF A MOLECULAR TARGET

Clearly in the literature an immense library of substrates has been investigated, which can undergo a dipole 1,3 addition from the nitrile oxides. Focusing the interest to the reactivity of not activated alkenes, these dipoles react with them forming an isooxazoline system albeit with regio- and stereoselectivity problems. In the literature it is reported by Gaisler and coworkers<sup>20</sup> an example of this type of reaction on polymeric substrates, where they have chemically modified cis-polybutadiene (PB) and cis-polyisoprene (IR) by reaction with a nitrile oxide generated in situ by dehydrochlorination of the corresponding hydroximoyl chlorides. This paper is particularly interesting because it demonstrates that it is possible to modify a polymer with this type of reactivity, maintaining the typical selectivity of these systems on double bonds, without using any kind of catalysts that are commonly used to reduce the activation energy barrier that this kind of reactions needs.

## 1.2 THIOL-X FUNCTIONALIZATION

The chemical manipulation of polymers with sulfur-based systems is one of the oldest transformations carried out on polymers since, in the mid-800s, Goodyear proposed a strategy to vulcanize rubber. However, only recently, since the advent of so-called “click-chemistry”, a post-polymerization functionalization based on the chemistry of sulfur<sup>21</sup> has attracted the interest of academic and industrial research.

In general, this type of reactivity is referred to as “Thiol-X modification” and in the literature it is possible to find many books and reviews that deal with the topic. The RAFT polymerization itself, cited above, is one of its declination, but for this project it is possible to limit the description to cases involving interesting reactivity for the substrates under investigation, such as olefins, internal alkenes and polymer terminals. This kind of reactivity will be briefly described:

- Free Radical Thiol–Ene/Yne Reaction
- Nucleophilic Thiol–Ene Reaction
- Thiol–Disulfide Exchange Reactions

### 1.2.1 *FREE RADICAL THIOL-ENE/YNE*

The free-radical addition of thiols is a straightforward tool for the chemical modification of double or triple bonds. This reactivity is widely used in numerous fields of application, like polymerization and curing (vulcanization) reactions and for the modification of polymers,<sup>21-22</sup> including rubber<sup>23</sup> and polybutadiene.<sup>24-25-26</sup>

As suggested by the name, this kind of Thiol-ene reaction type proceeds by radical means. The generation of radicals can be triggered by various factors, such as heat, light or molecules designed for this function (radical initiators), able to form sulfur-centered radical species.<sup>27</sup>

The next step of the reaction is the addition of the radical to an ene-group through an Anti-Markovnikov regioselective reaction, and the subsequent formation of a carbon-centered radical species.

The reaction proceeds by abstracting a hydrogen atom from another thiol molecule producing a sulfur-centered radical species which adds to another ene-group triggering the propagation process.

One of the great advantages of thiol-ene radical addition is the extreme simplicity of the reaction, the variety of systems that can be used to initiate it and the extensive library of substrates on which

it can operate. On the other hand, the sensitivity to oxygen, the stench odor typical of thiols, the need to use large excess of reagents (which must then be removed), and the risk of side reactions promoted by the introduction of radicals in a formed polymer network, limit its potential.

### 1.2.2 *NUCLEOPHILIC THIOL–ENE REACTION*

This reaction, also known as Thiol-Michael, involves the nucleophilic addition of a thiol to an electron-poor olefin in a base-catalyzed process.

Together with the radical-promoted reaction just described, it represents the most widespread thiol-ene reaction.<sup>27-28-29</sup>

If the radical type reaction requires a source of radicals, whatever it is, the thiol-ene nucleophilic reaction is activated using a suitable catalyst.

Depending on the type of substrate on which the reaction must take place, a wide variety of catalysts, including strong bases, metals, organometallics, and Lewis acids, have been used in literature.<sup>30</sup>

Some examples have been reported in which it was possible to avoid the use of a catalyst, but in these cases a highly polar solvent was used to aid the functionalization reaction of nanoparticles surface.<sup>31</sup>

The choice of specific catalysts and the optimized synthetic conditions have been the key to achieve high levels of efficiency for a thiol-Michael addition, with high degrees of conversion under mild reaction conditions.

The reaction mechanism is not too dissimilar to what we have seen in radical-type reactions, with the difference that the active species that is transferred from chain to chain is an anion and not a radical, and the generation of the initial thiolate involves the addition of a nucleophilic alkene catalyst.

### 1.2.3 *THIOL–DISULFIDE EXCHANGE REACTIONS*

This type of reactivity, whose use is widespread in biology or medicinal chemistry, involves the exchange between a molecule containing a disulfide bridge with a thiol bearing a different functionality. The breaking of the S-S bridge leads to the formation of a new mixed molecule, in which one portion retains the initial functionality and the other part is brought from the free thiol.

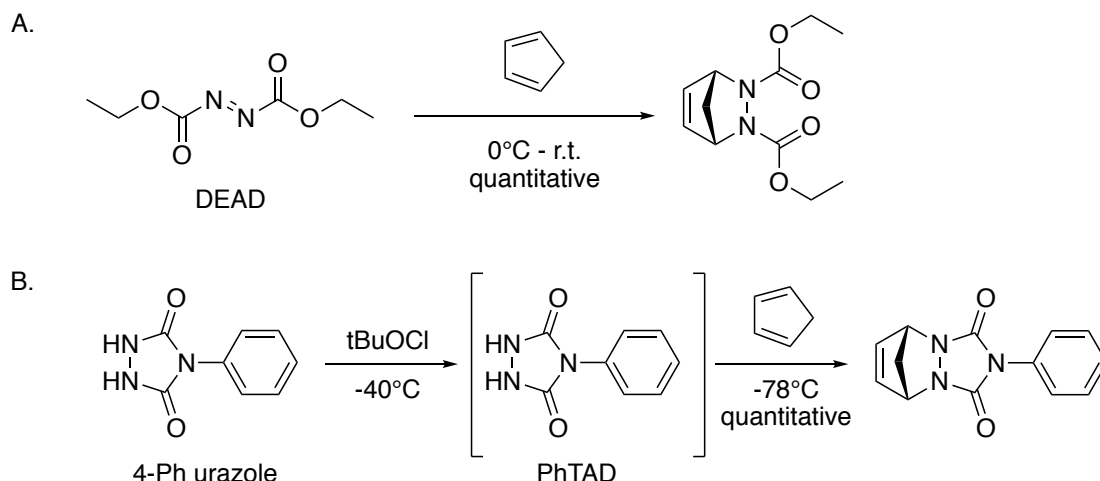
Usually, this type of reaction can proceed at a rather slow rate at room temperature, but it is necessary to use catalysts to release the thiol and allow the reaction to go to completion.



### 1.3 TRIAZOLINEDIONE

The outstanding reactivity of azodicarbonyl derivatives with an unsaturated hydrocarbon substrate was discovered in '20s by Diels and coworkers.<sup>32</sup> For the first time, the authors reported the reaction between diethyl azodicarboxylate (DEAD) and cyclopentadiene with quantitative yields at room temperature without using any other reagent (scheme 3a).

That pioneering work was the background for the description of the famous Diels-Alder reaction, for which the two scientists were awarded the Nobel Prize in Chemistry in 1950.<sup>33</sup> However, DEAD is not the oldest example of dienophile in literature, in fact already in 1894 Thiele and Stange<sup>34</sup> synthesized an even more reactive species, a 4-phenyl-1,2,4- triazoline-3,5-dione ("triazolinedione" or PhTAD) but, due to its elaborated synthesis and purification, this kind of compound was not included, as dienophile, in the early stage of investigation.



SCHEME 3 – A) FIRST EXAMPLE OF ADDITION OF AZODICABONYL DERIVATIVE ON A UNSATURATED SUBSTRATE. B) OXIDATION PROCEDURES OF 4-PHENYL-URAZOLE AND SUBSEQUENT ADDITION TO PENTADIENE

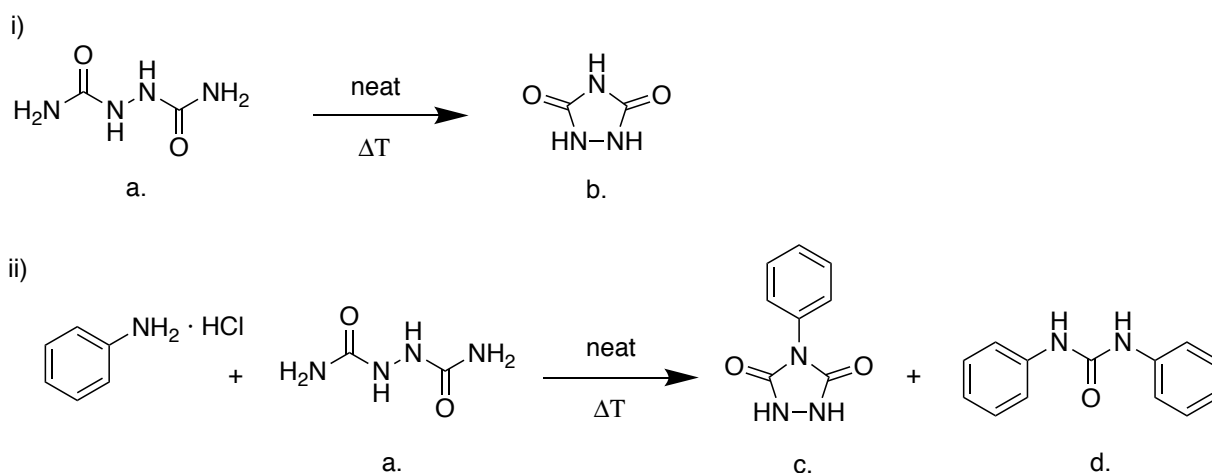
Just in '60s, Cookson et al.<sup>35-36</sup> isolated this reagent in its crystalline form and, thanks to his major contribution, in the subsequent years TAD chemistry attracted considerable interest, that lasts even today (scheme 3b). In order to fully understand how fast the reaction between PhTAD and a dienic system is, we can compare the speed of this molecule with a similar Diels–Alder-type reaction: DEAD<sup>37,38,39</sup> and tetracyanoethylene<sup>40,41</sup> are respectively 30000 and 1000 times slower, so - on this basis - triazolinediones can be considered one of the most reactive class of dienophiles<sup>38,42</sup> and enophiles.<sup>43</sup> A further parameter, able to afflict their already prominent reactivity, is the nature of the substituent in position 4-. As reported by Cookson et al. in 1975,<sup>44</sup> an electron-poor substituent, like a 4-nitrophenylic group, can dramatically increase the electrophilicity of the molecules, making it so reactive that it cannot be isolated.

Although not all TAD derivatives are easy to handle, if stored properly in a dark, cold and dry environment (-18°C), they are quite stable over the long run.<sup>35</sup>

TAD chemistry was reviewed several times in literature starting from '80s, describing from time to time all the reactions investigated along years. The most recent one, published by Du Prez et al. in 2016,<sup>45</sup> gives an overview of different synthetic strategies of TAD reagents and summarizes the novel and various applications of this class of reactants. A detailed description of all the synthetic methods, reactions and possible applications of the TAD chemistry would go beyond the purpose of this thesis, so, after a brief introduction on the synthesis of this system, I will focus the attention on the modification and synthesis of polymers reviewed by Butler and coworkers in 1980, eventually describing a novel and interesting application in a totally different contest like biochemistry.<sup>37,44</sup> In 1887 Pinner reported, for the very first time, the synthesis of a new molecule based on the reaction between phenylhydrazine and urea. The resulting product was influenced by the ratio between the two reactants: using a stoichiometric amount of them, the reaction led to the formation of 1-phenyl-semicarbazide, while an excess of urea allowed the formation of a cyclic compound. Besides this compound, the scientist produced a series of substituted five-member heterocyclic and named them "urazole" (Scheme 5). This kind of intermediate plays a key role in the synthesis of TADs, because almost all the possible synthetic routes involve this derivative in an oxidation step. However, various methods have been investigated to produce it. In the past, the most applied synthetic strategy was based on the hydrazodicarboxamide derivative.<sup>34</sup>

Heating this compound (Scheme 4, **a**) at 200°C in a solvent-free environment causes the loss of an ammonia molecule, giving the unsubstituted urazole (Scheme 4, **b**).

Similarly, heating bis-urea in neat condition with a stoichiometric amount of aniline hydrochloride, allowed Thiele to isolate for the first time a 4-phenyl urazole in satisfactory yields.

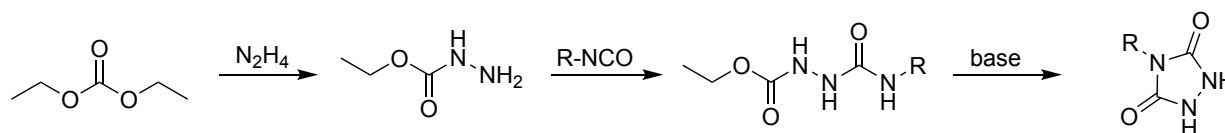


SCHEME 4 – SYNTHETIC METHOD PROPOSED IN LITERATURE FOR THE PRODUCTION OF URAZOLE

The first step of the proposed mechanism was the formation of a 1-arylbiurea, then, after the loss of ammonia, the intermediate undergoes a cyclization followed by another loss of ammonia.<sup>46</sup>

Unfortunately, that reaction did not afford satisfactory yields due to the simultaneous formation of diphenylurea; moreover, the separation of products from the unreacted species was not a trivial topic.

During the following years several researches were focused on the improvement of the synthesis methodology.



SCHEME 5 - SYNTHETIC STRATEGY FOR THE PREPARATION OF 4-SUBSTITUED URAZOLE FROM SEMICARBAZIDE

Only 70 year later, in 1961, Zinner and Deucker<sup>36</sup> published an alternative synthetic strategy through a semicarbazide intermediate (Scheme 5). This approach starts from reaction between two inexpensive reagents such as hydrazine and diethylcarbonate; the condensation product obtained (ethyl carbazate) is one of the two building blocks for the final product. This compound can easily react with a highly reactive species like isocyanate in excellent yields (>95%) at room temperature in a day, or just in few hours if heated. Solvent is not a key parameter because this reaction can even run in neat conditions, grinding the reactants with a mortar, but, if chosen wisely, the solvent can really help during the workup procedures. Usually, in a hydrophobic environment, like toluene, a hydrophilic compound such as semicarbazide precipitates, so it can be easily collected by filtration and used without any other purification step.

The resulting compound can be converted in the corresponding urazole by simple intramolecular

cyclization with a base under mild conditions, a complete conversion of the reagents and high yield can be achieved in few hours.

Considering major advantages, like the dramatical improvement in the overall yields and the easiness of purification, this convenient strategy was extensively used, starting from '70s. However, this synthetic path is limited by the availability and the reactivity of isocyanates, for 4-substitued semicarbazides. To synthesize an exotic 4-substitued urazole is therefore necessary reconsidering the whole synthetic route.

Once obtained the desired urazole, the very next step is the most critical one, the oxidation of the aza bridge. In the beginning the oxidation of urazole moieties was an analytical test, to confirm the successful synthesis of the desired urazole; the appearance of a bright pink-red color, typical of azo compounds, was the clear evidence of the oxidation. As stated before, before Cookson procedure, nobody was able to isolate the oxidized form, but nevertheless several oxidation methods were developed. Despite urazole can be easy oxidized by many oxidants, the reaction is not as straightforward as might seem, in fact there are some issues to face off. First of all, an ideal reaction should oxidize chemoselectively the azo bridge, leave others functional group intact and form just one oxidation products, without side products, allowing eventually to recover the target compound. This second quest is very deceitful because of the highly reactivity nature of TADs, which forces to be particularly careful during the purification process.

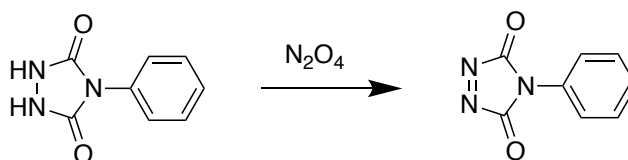
In view of this, identifying a general method is extremely hard, so the best approach should be evaluated from time to time. For example, in some cases the best option is an “*in-situ*” oxidation, without removing the oxidant species and bypassing purification steps, while for other applications it is mandatory to isolate the final TAD.

In the next paragraphs some of possible oxidation methods reported in literature will be described, grouping them by the type of chemical species used.

It was again Thiele in his seminal work the first to report a nitrogen-(IV)-mediated oxidation. In order to solve a silver salt of 4H-urazole he added this compound to concentrated nitric acid; instead of the dissolution of his adduct, he observed the appearance of a bright red color, ascribable to oxidation phenomena. With the same procedures, the oxidation of 4-phenylurazole was attempted, but the instability of the product in such an acid environment made it impossible to isolate.<sup>34</sup> Several research groups tried to optimize this reaction<sup>47</sup> but only in 1973 Ried and coworkers set up a methodology able to give 70% yields on a large-scale batch (40 g) by addition of HNO<sub>3</sub>.<sup>48</sup>

However, TAD produced with this protocol are not so stable for long periods, neither if stored in a dark and cold environment, probably because of the presence of water residues, acidic protons and side-products of oxidation, which can react with the product again. Moreover, in order to isolate the TAD compound it was necessary to carry out an aqueous extraction and it is known that this chemical species is sensitive to hydrolysis.

To overcome this limitation, Strickler and Pirkle proposed an innovative and straightforward protocol by using gaseous (over 20 °C) dinitrogen tetroxide (N<sub>2</sub>O<sub>4</sub>), which establishes equilibrium with NO<sub>2</sub>, the dehydrated form of nitric acid (Table 1). The resulting reactant is a good oxidant and can transform the urazole into the corresponding TAD making the isolation of the product much easier, so it can be collected just by evaporation of the solvent.<sup>49,50</sup>



Oxidants	Conditions	Yield %
HNO <sub>3</sub> conc.	CHCl <sub>3</sub> – 0°C	70
NO <sub>2</sub> /N <sub>2</sub> O <sub>4</sub>	DCM – 0°C	86
NO <sub>2</sub> /N <sub>2</sub> O <sub>4</sub>	DCM – 90 min, -10°C	94
N <sub>2</sub> O <sub>4</sub> sol.	EtOAc – 12 min, r.t.	95

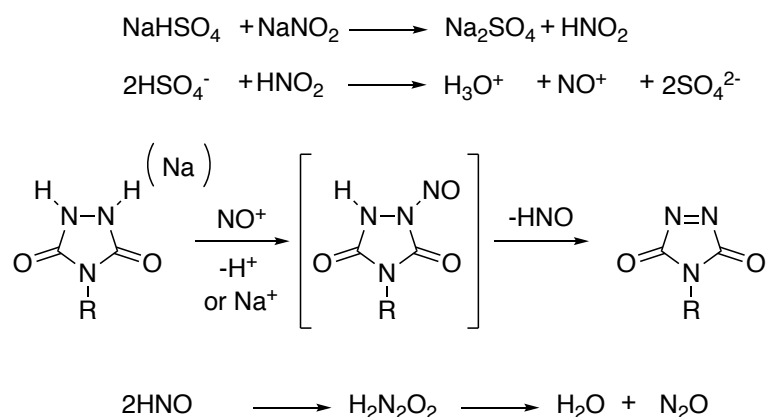
TABLE 1 – OXIDATION OF URAZOLE TO PHTAD WITH NITROGEN (IV) REACTANTS.

Despite of the reliability and the easiness of this approach, the usage of N<sub>2</sub>O<sub>4</sub> is not recommended for several reasons. First, it is a highly toxic and corrosive gas, whose cost is quite high in its pure form, and, last but not least, the severe shipping procedures to be complied in order to get it. Mallakpour and coworkers,<sup>51</sup> however, investigated a method that would allow the formation of a limited amount of N<sub>2</sub>O<sub>4</sub> in the reaction mixture. They started from an easy lab procedure, collecting the fumes produced by heating on a flame a dried lead nitrate powder, then they focused their research on an heterogeneous oxidation procedures with supported nitrogen (IV) oxide species or by the usage of insoluble inorganic salts, in order to generate the desired gas in situ.

The cited example attracted our interest for the very simple workup procedure; in fact, the authors

achieved a total conversion of starting 4-phenyl-urazole into the corresponding oxidized form using, as oxidizing agent, a mixture of  $\text{NaNO}_2$ ,  $\text{NaHSO}_4 \cdot \text{H}_2\text{O}$  and wet Silica powder, with dichloromethane as solvent, at room temperature.

After a 1-hour reaction, all insoluble reagents and waste products were filtered off and, after removal of volatiles, the product was isolated with an excellent yield (96%). In that article they also proposed the mechanism of oxidation of the urazole precursor as follows in scheme 6:



SCHEME 6 - PROPOSED MECHANISM FOR THE OXIDATION OF URAZOLE COMPOUNDS

At the beginning of the reaction, the formation of the nitrous acid ( $\text{HNO}_2$ ) takes place, this species evolves into a nitrosonium ion after the interaction with hydrogen sulfate ion. Once the effective oxidant is formed, urazole can be transformed in the target molecule. In the first step, the substrate undergoes an exchange between a proton (or a sodium cation) and a nitrosonium ion, while in the second step the real oxidation occurs with simultaneous loss of an azanone ( $\text{HNO}$ ) molecule. The last step is the recombination of two equivalents of the leaving group into nitrous oxide and water.

As previously reported, this procedure ensures many advantages with few drawbacks mainly related to the incompatibility with electron rich substrate due to the possible competitiveness electrophilic aromatic substitution. Anyway, with proper modification of the original recipe, this was the method of election chosen for most of the oxidation experiments performed during this project.

Over the years, many different methods of oxidation have been developed, ranging from nitrogen(IV) and nitrogen(V) oxide-based to halogen-mediated oxidation ( $\text{Cl}_2$  or  $\text{Br}_2$ ), up through hypochlorites ( $t\text{-BuOCl}$  or  $\text{CaOCl}$ ), in-situ generator of halogen species (DBH or NBS), Chalcogen mediated homogeneous oxidation (phenylseleninic acid, diphenylselenoxide or di(*p*-methoxyphenyl)telluroxide ending with metal ion/metal oxide-mediated oxidation ( $\text{KMnO}_4$ ,

BaMnO<sub>4</sub>, Ph<sub>3</sub>BiCO<sub>3</sub>).

I would like to dedicate few words to the description of a further type of oxidation performed by hypervalent iodine compounds. This kind of reactivity was reported for the first time by Moirarty et al. in an article published in 1987, where they oxidized, under mild conditions, a 4-substituted urazole with phenyliodine(III)diacetate (PIDA) and pentafluoroiodobenzene bis trifluoroacetate.<sup>52</sup>

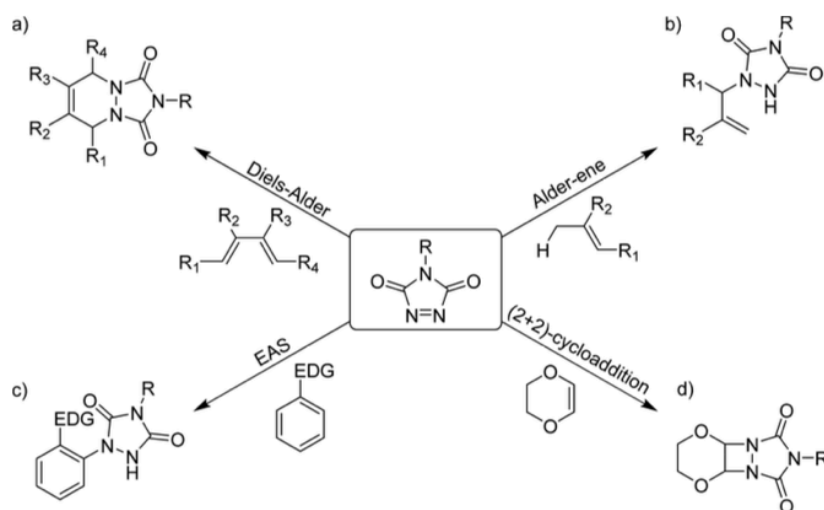
This reaction is easy and straightforward, proceeds at r.t. in less than 30 minutes and the side products are represented by inert iodobenzene and acetic acid. Once removed the solvent medium, the desired TAD can be crystallized from a non-polar solvent like hexane. In order to proceed with a reaction on a lab scale, this method is a valuable alternative to N<sub>2</sub>O<sub>4</sub> and it was employed several times at the beginning of the project, in order to have a double check on the oxidation methods and in the preliminary experiments made to set up a reproducible protocol.

After describing the possible synthetic routes, the next paragraph will report an overview of the peculiar reactivity of TADs. If we look at the chemical structure, TADs can recall the most known class of maleimides, a very powerful toolbox in organic chemistry, which find application in several fields, including click chemistry.<sup>53</sup> Furthermore, this class of compounds, like maleimides, can be involved in pericyclic reaction on a larger number of substrates, thanks to their enhanced reactivity, including simple olefins.<sup>40-54-55</sup>

In terms of reactivity TAD possesses a higher thermodynamic thrust than maleimides, resulting in a completely irreversible reaction and a lower control on reactivity and selectivity during the process, as it can be observed in the reaction between TAD and thiols or amines. Other similarities could be recognized comparing TADs and singlet oxygen reactivity.<sup>56-57-58</sup> As oxygen, this reagent can easily perform Diels-Alder, Alder-ene and [2+2] cycloaddition reaction on several substrates, even with electron rich or non-polarized olefins. One of the reasons of this match between so different molecules can be ascribed to the peculiar arrangement of their highest occupied molecular orbital (HOMO) and lowest unoccupied molecular orbital (LUMO), which are really close in energy.<sup>59</sup>

This unique feature allows TAD to react in the same way with substrates bearing delocalized  $\pi$ -orbitals rather than localized ones or ionic nucleophiles. At the same time, TADs have a valuable advantage in terms of stability, compared to singlet oxygen, so they can be isolated and stored for weeks, while the counterpart can live less than a millisecond in organic solvents. Lastly, as an added value, TAD can be chemically modified, so it is possible to introduce a functional group on the substrate instead of simple oxygenation.

As perfectly illustrated by Du Prez,<sup>45</sup> TAD reactivity can be summarized as follows, as shown in the scheme; independently from the substrate, there is always the formation of a nitrogen-carbon bond (Scheme 7). Each conjugation reaction will be briefly described.



SCHEME 7 - POSSIBLE REACTION OF PH-TAD

### 1.3.1 *DIELS-ALDER*

Diels-Alder (DA) is one of the most known reactions in the world and it can be easily considered one of the most efficient ways for the formation of intermolecular bonds. One of the most important features of this reactivity is the high level of control on the chemo-, stereo-, and regioselectivity of the final product that can be achieved.<sup>60</sup>

This reaction can be described as a concerted pericyclic reaction and, to be completed, it generally requires high temperatures that can be lowered using an appropriate catalyst.<sup>61</sup>

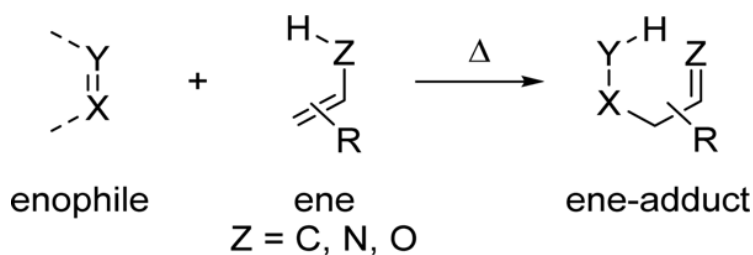
Under certain condition, the DA reaction can be reversed; it is a highly atom economical process, and, at least in theory, the bond-forming process can be reversed, giving the original reactants, this specific reaction being commonly named retro-Diels–Alder (rDA).<sup>62</sup>

This is a very versatile toolbox, in fact, exploiting this aspect, it is possible to protect temporary some dienes,<sup>63</sup> use the dienophile as a diene scavenger on a complex reaction mixture,<sup>64</sup> or trigger a chemical transformation taking and releasing reaction intermediates.<sup>65</sup>

Although the discovery of TADs occurred earlier than the DA-type reactivity, they were not used as dienophiles till Cookson's contribute. But, immediately after that time, TADs gained the reputation of the fastest dienophiles that could be isolated. Focusing on the reaction between triazolinediones and an enophile, like cyclopentadiene, it is evident that the reaction runs instantly with quantitative yield also at low temperature (-78°C).

### 1.3.2 ALDER-ENE REACTION

The Alder-Ene reaction (AE), also referred as “Ene reaction”, by definition, is a chemical reaction between an alkene bearing an allylic hydrogen (the ene) and a compound containing a double bond (the enophile) (Scheme 8). It was described for the first time by Alder in 1943,<sup>66</sup> and it can be classified as a transfer pericyclic reaction. It takes place when a 1,5 prototropic transposition occurs, along with the migration of the ene double bond, and the resulting product is a substituted alkene with the double bond shifted in the allylic position.<sup>67</sup>

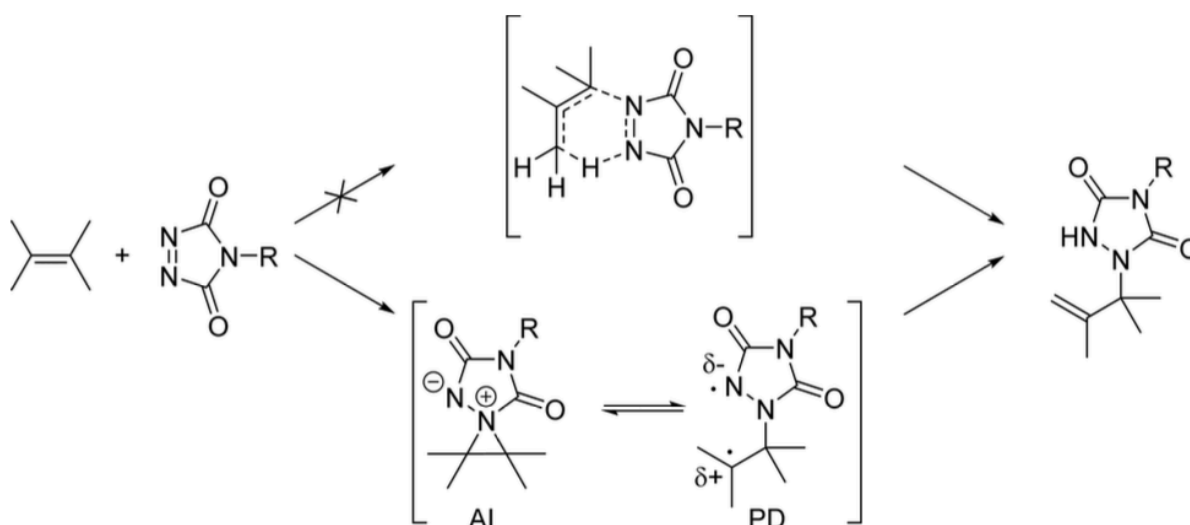


SCHEME 8 - GENERAL FORMULA FOR ADDITION REACTION BETWEEN DIPOLE AND DIPOLAROPHILE

Typically, this reaction requires high temperature to be activated, or strongly activated substrates, due to a highly ordered transition state with relatively poor orbital overlap,<sup>68</sup> which results in a higher enthalpy and entropy of activation which is reflected in a very slow rate of conversion. Because of this, alder-ene reaction had received little attention in literature, despite its great potential.

To soften the otherwise drastic reaction conditions, many researchers have proposed the use of Lewis acids. With this strategy high yields can be achieved at lower temperature, however the problem of regioselectivity limits the possible application of this kind of reactivity to intramolecular application.<sup>69</sup>

Nevertheless, the discovery of a highly reactive enophiles like TADs led to a renewed interest to intermolecular ene reaction making possible a selective and reliable reaction at low temperature (r.t. or even at -78 °C) with quantitative yields.



SCHEME 9 - PROPOSED REACTION MECHANISM OF PHTAD ADDITION

The reaction mechanism has not been fully understood, but the currently accredited hypothesis is based on the formation of a zwitterion adduct of aziridinium imide (AI)<sup>70-71</sup> followed by proton displacement (Scheme 9).

An interesting alternative was proposed by Squillacote and co-workers, which provides for the formation of a di-radical intermediate (PD), probably stabilized by the solvent reaction.<sup>72-73</sup>

Despite the high reactivity of the TAD compounds, the final product is very stable and only few examples in the literature have been found concerning reversibility through a retro-Alder-ene<sup>56</sup> reactivity.

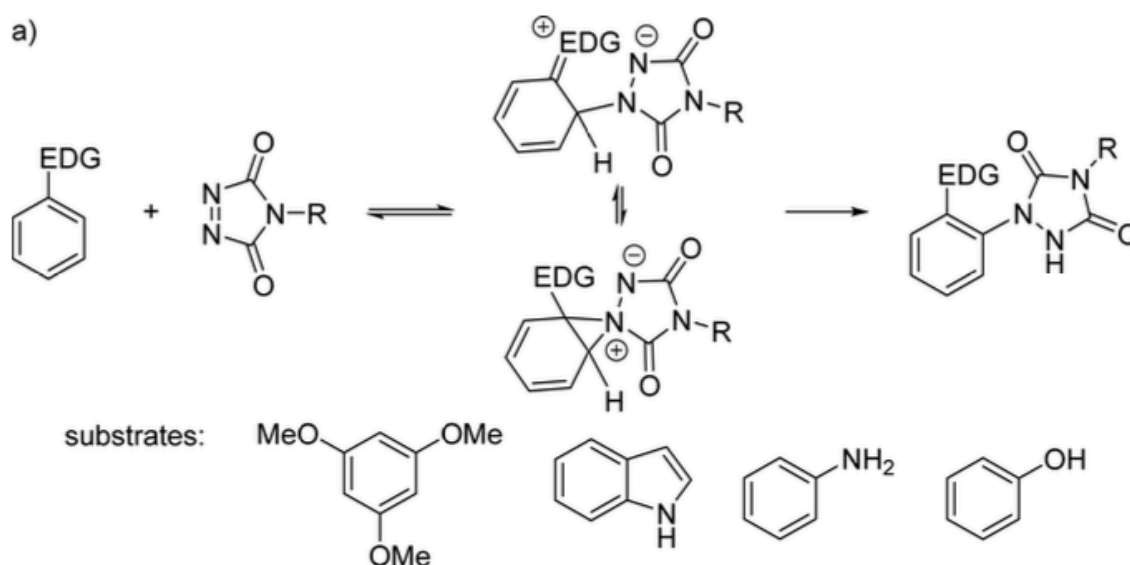
### 1.3.3 ELECTROPHILIC AROMATIC SUBSTITUTION

A third type of reaction that TADs can make is an electrophilic aromatic substitution (EAS) reaction on electron-rich activated substrates, such as aniline derivatives, phenols or indoles.

Also, in this case, the reaction mechanism is not completely clear, nevertheless it has been demonstrated that the reaction passes through the formation of a charge transfer complex.<sup>74</sup> Furthermore, the presence of a proton able to transfer from the substrate to the urazole is mandatory for the success of the reaction (Scheme 10).

This type of reactivity is particularly interesting because allows reactions on the cited substrates with good selectivity without using catalysts, and this makes this strategy attractive for biological application, where the control of metal impurities is a critical point. Recently it has been shown that

the TAD compounds are able to label tyrosine residues of the proteins<sup>75,76,77</sup> and it can be considered a key enabling technology for the functionalization of bio-organic substrates.



SCHEME 10 – POSSIBLE MECHANISM FOR EAS ADDITION REACTION.

#### 1.3.4 [2+2] CYCLOADDITION

The last type of reactivity involving TAD is represented by a 2 + 2 pericyclic addition reaction. A classic addition 2 + 2 is generally prevented by the steric impediment that does not allow the approach of the  $\pi$ -bonds in an antarafacial way. However, the geometrical configuration of TAD system makes it possible to approach certain substrates (such as ketenes)<sup>78</sup> and consequently the reaction.

#### 1.3.5 POLYMER FUNCTIONALIZATION WITH PH-TAD

One of the most interesting applications of TAD chemistry is the chemical modification of polymers. The possibility of inserting functionalities into the polymer matrix in a simple, fast and versatile way has been explored in both academic<sup>40,79</sup> and industrial sector.<sup>80,81,82</sup> Butler and Williams were among the most active researcher in this sector and reported the results obtained in the functionalization of a series of technologically interesting polymers, such as PB, IR and SBR. This kind of functionalization is particularly interesting for several reasons: first because it occurs already at room temperature and, conversely, too high temperatures can trigger detrimental side

reactions. A second fundamental aspect is given by the fact that the addition of the TAD does not involve the loss of the double bond, therefore the macroscopic properties of the rubber, such as  $T_g$ , are not macroscopically compromised (within a certain amount of functionalizing). Furthermore, the great reactivity of the system ensures that a very high degree of conversion of the reaction is achieved in a very short time, regardless of the concentrations involved, and without the formation of any by-product, greatly simplifying the purification procedures.

Finally, the introduction of an urazole unit on the polymeric backbone allows to alter the local polarity of the system, giving it new and peculiar characteristics.

Butler, in his studies, realized that it was possible to heavily functionalize the polymeric substrate, up to 400%, completely distorting its chemical-physical characteristics.<sup>83,84</sup>

Nevertheless, even if the level of functionalization is under 5% mol, it is possible to observe secondary supramolecular aggregation phenomena within the polymeric matrix, due to the strong hydrogen bond interaction established between the functional groups.<sup>85,86</sup>

As an evidence of the importance of this property, the ability of urazole units of self-recognizing within a polymer matrix has been thoroughly investigated with an encircling characterization (SEC,<sup>87</sup> rheology,<sup>88</sup> IR,<sup>89</sup> birefringence,<sup>90</sup> light scattering,<sup>91</sup> DMA<sup>92</sup>).

Furthermore, the proton of the N-H bond has a discrete acidity ( $pK_a \approx 5$ ) and is subject to further chemical modifications to customize this effect. Obviously, replacing the proton with a different functional group will prevent supramolecular aggregation.<sup>93</sup>

## 2. RUBBER COMPOUNDING

This chapter will describe the types and the characteristics of rubbers, fillers, vulcanization ingredients and the other chemicals used for the preparation of rubber compounds, then an introduction on the reinforcement effect of fillers in a rubber matrix will be given.

### 2.1 FORMULATION OF RUBBER COMPOUNDS

Formulation is an industrial process consisting of the set of operations necessary to mix together the appropriate ingredients according to a recipe. Each formulation has a different mix of components according to the properties required for the final composite.

<i>Ingredient</i>	<i>phr</i>
Crude rubber	100
Filler	50
Softener	5
Antioxidant	1
Stearic acid	1
Zinc oxide	5
Accelerator	1
Sulphur	2
<i>Total</i>	<i>165</i>

TABLE 2 - GERNERAL TIRE FORMULATION

A generalized rubber formula is given in Table 2.

The main ingredient of a rubber compound is obviously the rubber itself. Generally, one, two or more polymers are mixed together to have a fine-tuning of the characteristics required for the final product. The total amount of rubber parts is used as a reference, defined in 100 parts, and all other ingredients that will be added are weighted from that.

Each component that is added clearly has its own specific function in the economy of the final composite, some are useful during the process phase, others during curing and others still affect the specific characteristics of the product.

In addition to rubber, we can find dozens of ingredients that can be grouped into classes according to their purpose, such as fillers (like silica or carbon black), plasticizers and softeners (oil extenders, processing aids), antioxidants (radical scavenger, antiozonants, antiaging), vulcanizing agents and

vulcanization mediators (sulfur, accelerator, activators, co-activators), in addition to a series of special ingredients (pigments, antistatic agents, flame retardants) useful for specific purposes.

The formulation process is not trivial, as each ingredient, in addition to fulfilling the function for which it was added, should be theoretically inert during the other mixing phases, but they are able to interact in several different ways<sup>94,95,96</sup> (Figure 3).



FIGURE 3 - INGREDIENTS COMMONLY USED IN TIRE INDUSTRY

### 2.1.1 RUBBERS

With the generic term “rubber” we describe a polymeric material, capable of undergoing significant deformations and returning to its original size once the stress which caused the deformation has ended.

The polymer chains, which chemically constitute the rubber, are macromolecules whose molecular weight is typically high ( $M_n > 100,000$ ), able to return to their initial position after elongation under mechanical stress thanks to the links present between different chains, generated by their peculiar random coil arrangement. For these unique elastic properties it is possible to refer to this material also with the term "elastomer".<sup>76-77</sup>

The elastomers used in the rubber industry can be divided into two categories: natural or synthetic rubber materials.

Natural rubber (NR), according to standards UNI 7703, is obtained coagulating latex harvested from some tropical trees. In 2017 the world production of NR was estimate in 13.5 millions of

metric tons and the largest source of commercial NR comes from *Hevea brasiliensis* tree. Natural rubber latex is a colloid where the continuous phase is water and the dispersed phase is mostly a *cis*-1,4-polyisoprene polymer – with a molecular weight between 100,000 and 1,000,000 Daltons. As a natural product, a small percentage (up to 5% of dry mass) of other materials, such as proteins, fatty acids, resins, and salts could be found along with the polymer.

Besides natural rubber, we can find a much wider group of synthetic rubbers. They are artificial elastomers, produced by the polymerization of monomers obtained from petroleum-derived hydrocarbons. The rubber market is growing year by year, in 2017 the production was stood at 29 billions of kilograms and over 60% was synthetic, with a global revenue generated of 29 billion US\$. Considering the plethora of existing synthetic polymers, a general description of them would go beyond the aims of this thesis, therefore only those that have had relevance will be described.

The synthetic homologue of the natural rubber is the poly isoprene (IR) and only with the discovery of the stereospecific catalysts it has been possible to synthesize it with quality standards suitable for the industry.

Depending on the polymerization conditions, the isoprene monomer can be added in various ways that can lead to the formation of four possible isomers: 1,4-*cis*, 1,4-*trans*, 1,2 and 3,4 (Figure 4).

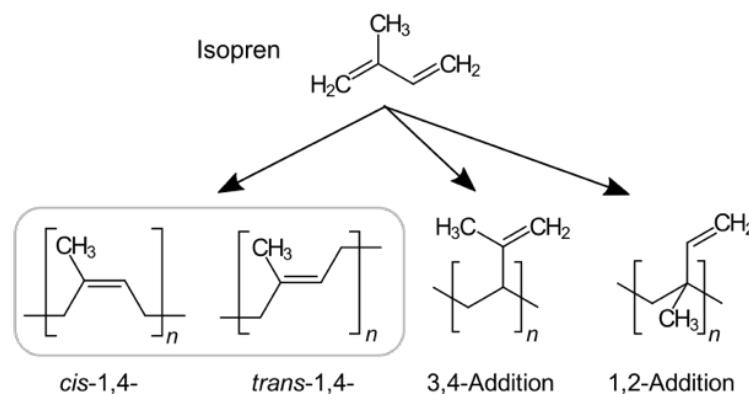


FIGURE 4 - ISOPRENE MOLECULE AND STRUCTURE OF ALL FOUR POSSIBLE ISOMERS OF IR

In the last two examples, the polymerization introduces a stereogenic center, which theoretically can lead to three pure polymeric structures: isotactic, syndiotactic and atactic. Among all possible structures, the only ones synthesizable are 1,4-*cis* (synthetic equivalent of NR), 1,4-*trans* (synthetic equivalent of gutta-percha) and 3,4 atactic. However, each of the isomers could be detected as polymerization impurities.

1,4-*cis* polyisoprene is one of the most widely used polymers for the mechanical and elastic

properties that give to vulcanized compounds, especially for the ability to withstand loads, which make it suitable for applications in heavy vehicles tires or carcasses and sidewalls in car tires.

Another example of general-purpose elastomers, such as NR and IR, is butadiene rubber (BR).

About 10% of yearly global rubber production is constituted by polybutadiene, 70% of which is used in tires industry.

As in the case of IR, butadiene can polymerize in different ways but, since it does not have a lateral substituent, it has fewer accessible configurations. This allows the formation of only three isomers: 1,4-cis, 1,4-trans and the polymer given by 1,2 addition. This latter structure introduces, as for IR, a stereogenic center in the polymer chain with three possible types of vinyl structures: isotactic, syndiotactic and atactic.

Depending on the polymerization conditions, it is possible to isolate polymers with different microstructures, either pure or made by a blend of different isomers.

In this project, a mainly cis- polybutadiene was used; it is a soft and easily soluble material. It has excellent dynamic characteristics, low hysteresis, good resistance to abrasion and high resilience.

The production of pure BR compound is not trivial; indeed, commonly, compounds are formulated using blends with NR or SBR.

BR-based vulcanized compounds have better characteristics compared to NR or SBR composites like enhanced abrasion resistance, flexibility at low temperature, high temperature resistance, low deformation resilience and ozone resistance, however adhesion to the other components of the tire, resistance to tearing and mechanical characteristics are lower.

As just illustrated, all the elastomers share common features but each one has peculiar characteristics that significantly influence the final properties of a composite. Nevertheless they can be extensively modified adding proper ingredients during the mixing process.

### 2.1.2 *FILLERS*

Fillers are the most abundant compounding ingredients added to polymer matrix, typically in a proportion ranging from 30 to 70 phr (parts per hundred rubber). Generally, their physical aspect is a powder, added to the mixture to improve its mechanical properties or to lower the cost of the final product. Fillers can be divided into two main groups: carbon black and non-black fillers.

Carbon black (CB) is a pigment produced by the incomplete combustion of heavy petroleum products. It is certainly the oldest filler used in tires compounding and even today it is still widely used. There are many types of CB that can be classified by their morphological characteristics such as particle size, surface area, size and shape of the aggregates.

In fact, CB presents a variegated microstructure, the primary particles of colloidal dimensions are fused together into clusters, called aggregates. They interact with each other forming agglomerates with a complex structure under the driving force of weak interactions. A common feature of CB-based fillers is their ability to give the compound a high resistance to abrasion and wear while having excellent heat conduction properties.

In the literature there is a broad library of non-black fillers, such as clays, zinc, titanium and magnesium oxide, mica, talc, barites and carbonates. However, the most important one is certainly silica; this filler can provide extremely high reinforcement values, but only since 1980, with the discovery of coupling agents<sup>97</sup> (e.g. alkyl silane), it started to replace the CB in the compounds formulation. Thanks to this breakthrough, silica has been able to guarantee excellent mechanical performances, enhancing wet grip, lowering the rolling resistance without losing tear, abrasion and heat resistance.

### 2.1.3 ANTIDEGRADANTS

One of the main problems afflicting elastomeric products is the loss of performance over time, especially if it occurs due to causes not strictly related to their use. Exposure to atmospheric agents, such as moisture, oxygen, ozone, light and heat, in fact, can trigger degradation phenomena to the surface that compromise the stability and significantly affect the aging process of the product.

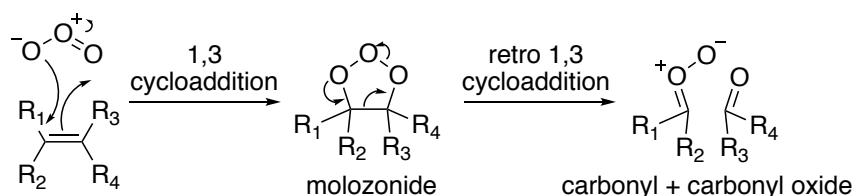


FIGURE 5- OXIDATIVE DEGRADATION MECHANISM

To prevent this situation, additives are added during rubber compounding, in quantities ranging from 1 to 4 phr. Typically, antioxidants and radical scavengers are introduced. They can delay, hinder or even inhibit oxidation by oxygen and ozone (figure 5), which can break the polymer

chains.

#### 2.1.4 *VULCANIZING AGENTS*

The most important discovery in rubber technology was undoubtedly made by Charles Goodyear in 1839, who developed a method to make natural rubber pliable, waterproof, moldable and solvent resistant by sulfur addition and heat treatment.

Vulcanization is a chemical process in which bonds are formed among the molecules of a polymeric matrix, randomly arranged to form a lattice. The introduction of these bridges radically transforms the elastic properties of the material, making it technologically relevant.

The protocol developed by Goodyear, with vulcanization carried out just with sulfur, was not particularly efficient, in fact, the process was completed by adding 8 phr of sulfur and leaving the system at 140 °C for 5 hours. Over time, industrial research has pushed to develop system able to enhance the process, make it faster, homogeneous, with a better quality of the final polymeric network, also lowering the amount of sulfur required.

To describe the huge range of molecules useful for this purpose, it is convenient to group them according to their function:

**Vulcanizers:** they are responsible for the actual formation of intermolecular bridges; generally elemental sulfur is used.

**Accelerants:** they interact with vulcanizers, their function is lowering the activation energy of the process from 210kJ/mol (for sulfur alone) to 80-125 kJ/mol, with a consequent drastic reduction of the time needed to complete the process. There are over 100 different types of accelerators, each one characterized by a different curing and/or scorch time, which can be classified according to the chemical nature: class 1 sulfenamide (CBS), class 2 thiazole (MBT), class 3 guanidines, class 4 thiurams, class 5 dithiocarbamates and class 6 dithiophosphates.

**Activators:** they are metal oxides and the most used is ZnO. They can form complexes with accelerators and co-activators, influencing the curing rate and the cross-linking efficiency.

**Co-activators:** usually they are organic molecules that react with the activators, forming complexes containing the cations necessary for the reaction with the accelerators. They promote solubilization of the activator in the polymer, making the cations more available. The most important and popular type of organic activators is stearic acid.<sup>98</sup>

## 2.2 OVERVIEW ON FILLER REINFORCEMENT

To fulfill the technical and market demands, a rubber must have certain characteristics: for example, it must guarantee a good grip both in dry and wet conditions, must have a high resistance to consumption and abrasion, have a low rolling resistance, give precise feedback to the driver during the steering phase. Together with the construction of the tire itself and the tread pattern design, the parameter that most determines these characteristics is the composition of the compounds used in tire fabrication. The task is particularly complicated because some desired features are in contrast with each other, an example is the "magic triangle" on which research is focusing, trying to improve some qualities like traction in wet condition and rolling resistance without losing wear resistance.

It is therefore evident that rubber alone cannot satisfy all these requirements and needs to be mixed, as mentioned, with components capable of improving its properties. The composition of the composite material will be therefore closely related to the type and quantity of filler introduced, but its final characteristics will not simply be the sum of the contribution of the individual ingredients, but rather their mutual interaction will determine these features.

The behavior of a rubber-based composite material is complex, but it is possible to assimilate it to a viscoelastic material and, to describe it, some basic theoretical concepts will be introduced.

Applying a tangential deformation  $\gamma(t)$  with an angular frequency  $\omega$ , the equation describing its behavior is:

$$\gamma(t) = \gamma_0 \sin(\omega t)$$

with  $\gamma_0$  corresponding to the maximum value of strain and  $t$  to the time.

To  $\gamma(t)$ , an out-of-phase sinusoidal stress is correlated, described by the equation:

$$\sigma(t) = \sigma_0 \sin(\omega t + \delta) = (\sigma_0 \cos \delta) \sin(\omega t) + (\sigma_0 \sin \delta) \cos(\omega t)$$

Where  $\delta$  is the phase angle.

We can therefore define  $G'$ ,  $G''$  as follows:

$$\sigma(t) = \gamma_0 [G' \sin(\omega t) + G'' \cos(\omega t)]$$

$$G' = \frac{\sigma_0}{\gamma_0} \cos \delta$$

$$G'' = \frac{\sigma_0}{\gamma_0} \sin \delta$$

With  $G'$  the component in phase of the shear modulus, that represents the elastic modulus (storage modulus) and describes the reinforcement contribution given by the filler to the polymer matrix, while  $G''$  describes the viscous modulus and accounts for dissipative phenomena (loss modulus).

From these relationships we can then draw up the complex equation that describes the shear modulus  $G^*$ :

$$G^* = G' + iG''$$

and the phase angle formula:

$$\tan \delta = \frac{G''}{G'}$$

This last value is particularly important because it is directly related to the hysteretic behavior of the mixture, primary cause of rolling resistance, that is the energy consumed per unit of distance traveled.

The values of  $G'$ , of  $G''$  and therefore also of  $\tan \delta$  depend on both the temperature and the frequency, and by analyzing their behavior it is possible to obtain valuable information about the mechanical dynamic characteristics of the material.

As previously mentioned, the mechanical behavior of a composite material is strongly influenced by the addition of the filler. The reinforcement contribution to the mixture will be therefore partly dictated by the intrinsic nature of the filler naturally, by its chemical nature, by the particle size, by their aspect ratio, by their aggregation state and by their surface reactivity.

In force of this, it is essential understanding, predicting, or even dominating, the various types of interactions that are established. We must focus on the filler-filler and filler-rubber interaction next to the hydrodynamic effects and the polymer network contribution that we will analyze individually in the next paragraphs.

The final reinforcement effect will be the sum of the individual contributions, as shown in Figure 6.

On the Y axis, the shear modulus ( $G^*$ ) is reported as a function of the deformation. The interpretation of these curves was provided by Payne, in whose work the dependence of  $G'$  and  $G''$  from the strain is investigated by correlating it with the size of the filler aggregates in the composite.

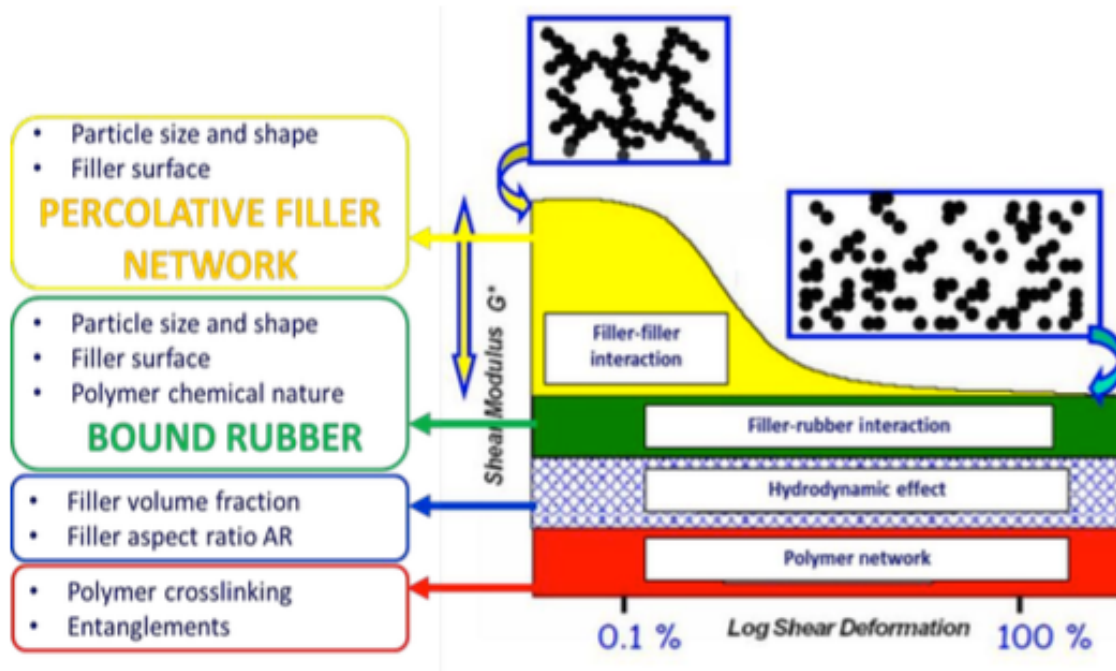


FIGURE 6 - MODEL OF STRESS-STRAIN CURVE OF A RUBBER NANOCOMPOSITE, EACH CONTRIBUTION IS REPRESENTED WITH A DIFFERENT COLOR – IMAGE ADAPTED FROM WEHMEIER (EVONIK) VKRT 2008

### 2.2.1 FILLER-FILLER INTERACTION

Payne suggested that the breaking of the filler network of an sheared sample follows a sigmoidal-like pattern that decreases from an initial value ( $G'_0$ ) at low strain to a plateau ( $G'_\infty$ ) for higher shear deformation.<sup>99-100</sup>

This breakdown is caused by the destruction of the weak forces that hold together the filler particles (such as hydrogen bonds and Van der Waals interactions), unlike the covalent bonds that are created at the interface between the polymer matrix and the filler.

The difference between these two values  $G'_0$  and  $G'_\infty$  is commonly referred as Payne effect, and is one of the most important parameters to keep under control. This effect is associated with the

dissipated energy by the system during the breakdown of the filler network, and consequently with the rolling resistance of the compound and its heat generation.

Several other models have been proposed to explain this type of interaction, and among the most recent the theories the one proposed by Klüppel and collaborators stands out. They suggest two alternative approaches, a link-blob-nodes (LBN) model and one based on cluster-cluster aggregation (CCA).<sup>101-102</sup>

They constitute a more complete approach not limited to the interaction among the filler particles but taking into account also the filler-rubber interaction.

### 2.2.2 *FILLER-RUBBER INTERACTION*

The main actor of the reinforcing action in a composite material is the filler-polymer interaction. It is a shear-independent contribution and it is related to the superficial interaction established between the filler particles and the rubber that surrounds them. Often in the literature we refer to this layer with the name of bound rubber, a misleading term because it leads us to think that the matrix is connected through chemical bonds to the surface of the particles. This is true only if a coupling agent, able to form such bridges (silane-silica systems), is used, but it is more correct to describe this portion of rubber as immobilized rubber; moreover, precisely because of this intimate interaction between the two components, the local mechanic properties are twisted.

Medalia and Kraus proposed a model in which they hypothesized that the rubber could be trapped inside a filler cage, with an elastic behavior like the filler itself at low strain values.<sup>103-104</sup>

Smith and Pliskin gave a similar, but slightly different, reading of the phenomenon: according to them, the rubber coated the filler agglomerates, to form a chemisorbed shell on the surface of the filler.<sup>105-106</sup>

### 2.2.3 *POLYMER NETWORK EFFECT*

This contribution is independent from the elongation and can be considered as the mutual interaction between polymeric chains, which are physically linked through entanglements or real chemical bonds introduced into the polymeric network after the vulcanization process.

The equation describing this contribution is rather simple:

$$G_0 = \nu \cdot K_b \cdot T$$

With  $K_b$  Boltzmann constant,  $T$  temperature and  $\nu$  the concentration of elastically active chains per unit volume.

#### 2.2.4 HYDRODYNAMIC EFFECT

The hydrodynamic effect is a consequence of the increase of viscosity determined by the addition of particles. The first to theorize this behavior was Einstein who described the viscosity variation as follows:

$$\eta = \eta_0(1 + k_e\phi)$$

with  $\eta$  viscosity of the suspension,  $\eta_0$  viscosity of the pure liquid,  $k_e$  coefficient factor linked to the shape and aspect ratio of the filler and  $\phi$  volume fraction of the filler.

This hypothesis is true by applying fairly strong approximations to the system, such as spherical particles, total surface wettability and diluted particle concentration.

This equation was then modified semi-empirically by Guth and Gold to make it suitable for the description of reinforced tires:

$$\eta = \eta_0(1 + 2.5\phi + 14.1\phi^2)$$

in which the parameter  $\phi^2$  accounts for the effect given by a dense solution of particles.

Finally, considering also the aspect ratio of the particles, Guth further corrected the equation introducing the parameter “ $a$ ”:

$$G' = G'_0(1 + 0.67a\phi + 1.62a^2\phi^2)$$

### 2.3 FILLER RUBBER INTERACTION, THE KEY ROLE OF INTERFACE.

In summary, the main part of the speech concerns the filler-rubber interaction, which must be maximized at the expense of filler-filler interactions. All the theories and modeling that analyze this theme converge on one point: the interface that is formed between the organic and inorganic component is crucial and it is the first responsible for the rheological behavior of the final product.

Given the importance of the role played at the interface, the best thing is to try to understand what kind of affinity exists between the surface of the filler and the rubber, with attention to the surface reactivity and functional groups exposed by the particles. It is therefore evident that it is not possible to treat the various fillers in the same way, but it is necessary to distinguish between Silica and CB which, as mentioned, constitute the two most used filler categories.

Silica is one of the most studied and used materials on the planet so there are tons of articles and books in the literature that describe its characteristics. For the purposes of this thesis, the superficial structure and its compatibility with the polymeric matrices will be briefly discussed.

The silica used in the mixing phase is an amorphous silica, mainly consisting of spherical particles produced in a pyrogenic way. The size of the primary particles depends on the reaction conditions, but they usually do not exceed 50 nm in diameter, which aggregate into more complex structures, called string of pearls structure, with dimensions between 50 and 500 nm, which cannot be destroyed in the mixing phase,<sup>107</sup> able to aggregate in clusters composing the aforementioned filler network, of micrometric dimensions.

The driving force of the aggregation phenomena consists of weak attractive forces, such as hydrogen bonds, VdW forces, or dipole-dipole interactions that the terminal polar groups exert each other.

The particles surface is in fact decorated with silanol units of various kinds<sup>108</sup> (such as isolated silanols, geminal silanols, vicinal silanols or siloxanes). They are weak Brönsted acids, but they are also stronger than aliphatic silanols or hydrocarbon alcohols, and thanks to this feature they are able to establish hydrogen bonds with polar molecules such as water, amines, alcohols or other silanol groups.<sup>109-110</sup> This marked surface polarity makes the silica particularly hydrophilic, a characteristic that certainly does not help the dispersibility of the particles in a hydrophobic matrix such as polymers.

Surface energy, according to the interpretation of Donnet et al.,<sup>111</sup> can be described as the sum of two components:

$$\gamma_s = \gamma_s^d + \gamma_s^p$$

With  $\gamma_s^d$  describing the tendency of silica to be dispersed in the rubber (hence the dispersion component name) and  $\gamma_s^p$  the aggregation surface energy. These two values can be measured by evaluating the interaction of silica particles (nominally at infinite dilution) with a variable polarity

probe.

Thanks to this type of technique<sup>112-113</sup> it has been possible to evaluate the dispersibility of silica in the most common polymeric matrices, which can be qualitatively represented by this scale of values:

NBR>SBR>NR>BR>high vinyl BR>EP(D)M>IIR.

Where NBR is the acronym of nacrilonitrilebutadiene rubber, IIR is butyl or isobutylene isoprene rubber and EP(D)M is ethylene propylene diene rubber.

## 2.4 INCREASING COMPATIBILITY: STATE OF THE ART AND OUR PROPOSAL

Although carbon black based fillers are inherently more compatible with the polymer matrix, due to their non-polar nature, the composites obtained still have a hysteretic character and a marked Payne effect. For years they have been the technological standard used in industry, without the use of any type of compatibilizer. Only recently various treatments have been proposed (chemical, plasma, ozone, electrochemical, and heat treatment)<sup>114</sup> capable of oxidizing the carbon black surface to obtain a better compatibility with more polar polymeric matrices.

To overcome the limits imposed by the nature of carbon black and move to a more environmentally sustainable production, over the course of time research has focused on the progressive replacement of carbon-based fillers in favor of silica-based fillers.

However, the use of silica alone is not enough to guarantee the required performances, not without the use of a coupling agent capable of modifying the surface energy of the particles, in order to increase their dispersion in the polymer matrix.

The decisive step in this direction was the discovery of bifunctional organosilanes, able to graft to the surface, reacting with the hydroxyl groups of silica, and at the same time able to bind covalently to the polymer in the vulcanization phase.

Of the more than 100 compounds synthesized by Wolff and collaborators,<sup>111</sup> only two were useful for the purpose, in particular the bis (triethoxysilylpropyl) tetrasulfide (TESPT) (see molecular structure reported in figure 16, page 61).

All these methods, together with much of the literature, move in the direction of making the filler more compatible with the polymer matrix. Our approach, however, has been radically different and unusual: the ambitious goal that we set was to modify the polymer matrix to make it more compatible with the filler, but without modifying it too much in its fundamental properties.

Taking advantage of the features deemed appropriate to our intentions, we moved on several fronts trying to explore this path.

As for the functionalization through PhTAD, the basic idea was to make the polymer matrix locally more polar by introducing functional groups capable of forming hydrogen bonds with the filler. In addition to a direct increase of the number of interaction points between filler and polymer, we wanted to exploit a second effect of compatibilization in the mixing phase. In fact, recalling the type of interaction that exists between the filler particles, adding a functionalizing agent with a competitive interaction mechanism compared to weak interaction forces acting between polar groups, would have had to reduce the tendency of the particles to aggregate with each other.

This idea was corroborated by the work carried out by Peng and collaborators in which they claim that the introduction of functional groups capable of generating hydrogen bonds improved the performance and the silica dispersibility compared to the same unmodified rubber.<sup>115</sup>

On the other hand, about functionalization with carbon black, we were inspired by several literature works that highlighted the affinity between polycyclic aromatic compounds with activated carbon. Except for a different surface area, the type of chemical interaction because of VdW or  $\pi$ - $\pi$  stacking is similar, so by exploiting this affinity the objective was to synthesize a bifunctional molecule able to interact with the filler and at the same time able to bind the polymer in the curing phase in the same ways of TESPT.

### 3. SYNTHETIC PROCEDURES

In this chapter will be described the synthetic procedures exploited during this research.

After overviewing the literature for a few months, in agreement with the industrial partner, we started testing the synthetic routes chosen. As mentioned in the preface, neither me nor the research group in which I worked, were familiar with the topic in question either as a knowledge of the reactivity involved or as an experience in the handling of polymers. The starting point was necessarily to test literature recipes, gain experience with the synthesis procedures, and tailor them in order to functionalize a polymeric substrate.

With the objective of functionalizing the double bonds of the PB polymer backbone, a model system was chosen as a benchmark for laboratory-scale reactivity.

The choice fell on a commercial polymer, POLYVEST® 130 (purchased from Evonik), a stereospecific, low viscous and unsaponifiable polybutadiene oligomer, with a mean molar mass of 4,600 g/mol, with a high content of 1,4-cis double bonds (Figure 7). The microstructure of this compound is so composed:

- 1,4-cis double bonds approx. 77% (p)
- 1,4-trans double bonds approx. 22% (n)
- 1,2-vinyl double bonds approx. 1% (m)

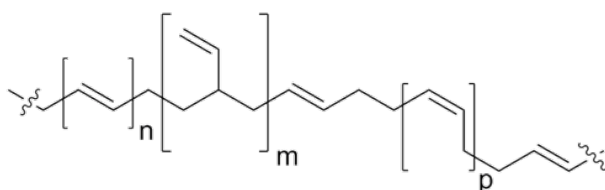


FIGURE 7 - STRUCTURE OF POLYVEST, WITH (N) OF 1,4 TRANS UNITS, (M) NUMBER OF 1,2 VINYL UNITS AND (P) NUMBER OF 1,4 CIS UNITS.

This polymer presents a variegated composition, which allows us to have a qualitative idea of the selectivity of the double bonds touched by the chosen reaction. Polyvest is a viscous transparent liquid and has a good solubility in both aliphatic and aromatic solvents.

In this way it has been possible to use it on a laboratory scale, overcoming the characteristic problems of solubility and viscosity that can be observed by dissolving a long chain polymer in an organic solvent.

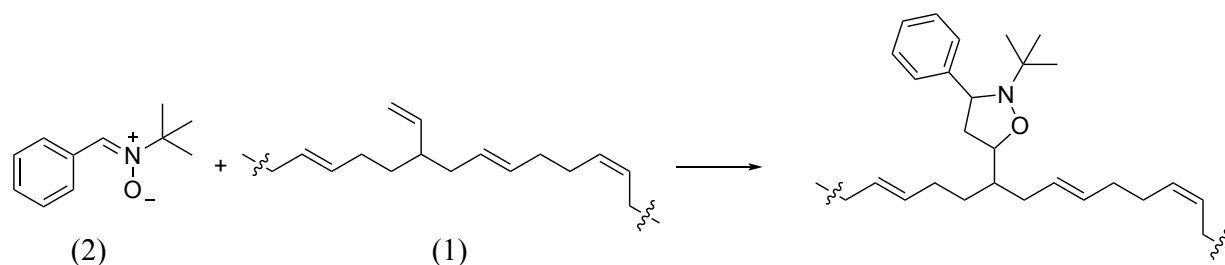
The most important aspect of this feature is the chance of analyzing the addition products to the double bonds of the PB by means of NMR spectroscopic techniques.

Obviously the choice to focus on a model system is just a starting point for the study of the actual reactivity and behaviour of the polymer matrix used for real applications. In fact, against the advantages mentioned above, it is necessary to underline how the mobility of the polymer chains, inter- and intra-chain aggregation phenomena, the distribution of the reactive sites, the diffusion of the reactants in the reaction environment and other technologically relevant parameters will significantly differ from the oligomer used.

In the next paragraphs the reactions on the model systems will be described and, after having identified the most useful reaction for our purposes, we will then list the single synthetic steps to produce the functionalizer and the subsequent coupling to the polymer. Finally, all the tests carried out in the compound will be summarized, describing the logical pathway that has led us to develop the research in the direction agreed with the industrial partner.

### 3.1 1,3 DIPOLAR CYCLOADDITION

First, the solubility of Polyvest was tested in organic solvents such as DCM and Toluene, considering the concentration of 0.33 g/ml and 0.25 g/ml respectively as to the upper limit to be approached before incurring into issues like non-homogeneous stirring due to the excessive viscosity of the system. All reactions carried out on the oligomeric substrate will therefore present a concentration lower than these values. The first type of reactivity tested was the 1,3-dipolar cycloaddition between a nitron and the model polybutadiene. The first dipole tested was an N-tert-Butyl- $\alpha$ -phenylnitron (2), available in our stock (Scheme 11). As reported in section 1.1, this type of reactivity should be selective on the vinyl double bonds of polybutadiene, therefore the molar quantities of the introduced dipole will be calibrated to them.<sup>116</sup>



SCHEME 11 - REACTION SCHEME OF 1,3 DIPOLAR CYCLOADDITION BETWEEN N-TERT-BUTYL-PHENYLNITRON (2) AND POLYVEST (1)

Entry	Ratio eq. (2): vinyl double bonds	Temperature (°C)	Time (h)	Yield
1	1:1	r.t.	20	-
2	1:1	40	24	-
3	1:1	110 <sup>a</sup>	6	-
4	10:1	40	24	-

TABLE 3 – REACTION CONDITION FOR THE ADDITION OF COMPOUND (2) TO (1), <sup>A</sup> MW ASSISTED (200W)

The polymer was then precipitated in methanol, centrifuged, dried and then analyzed by NMR spectroscopy. Unfortunately, no reaction was observed (Table 3). This behavior was attributed to the electron donor nature of the tert-butyl group, able to reduce the reactivity of the dipole. This hypothesis was corroborated by a Yokohama patent<sup>117</sup> in which the authors claim that it is possible to functionalize the double bonds of the butadiene part of an SBR polymer, with a nitron bearing one or more electron attractor groups (Figure 8).

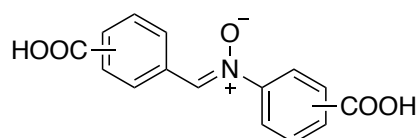
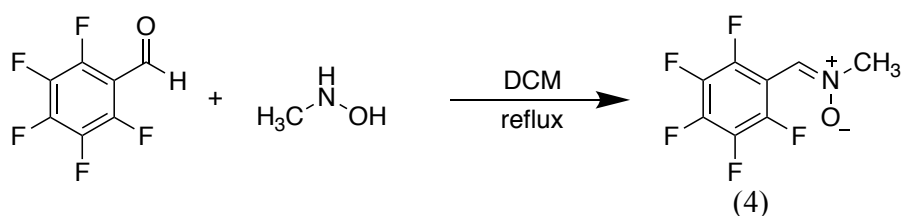


FIGURE 8 - GENERIC MOLECULAR STRUCTURE OF THE NITRONS PROPOSED BY YOKOHOAMA FOR THE FUNCTIONALIZATION OF THE VINYL DOUBLE BONDS IN AN SBR COPOLYMER.

Moving on the same direction we have synthesized a nitron whose aromatic ring was perfluorinated, with an electron attractor behavior, in order to promote the cycloaddition reaction (Scheme 12). As reaction conditions we used the procedure published by Badoiu and coworkers.<sup>118</sup>



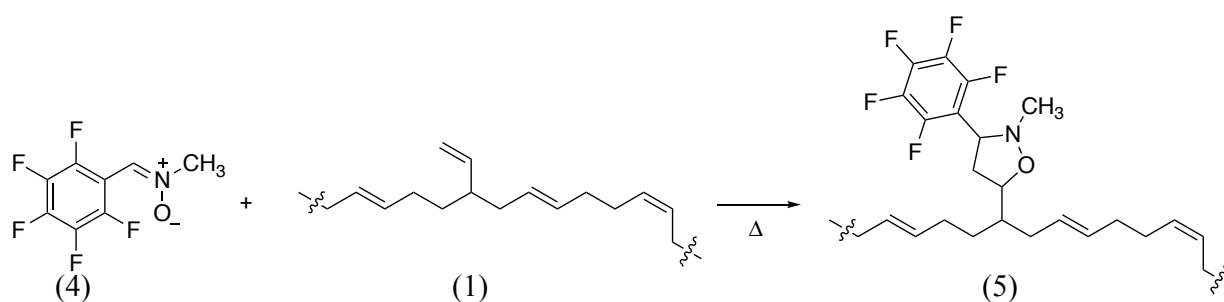
SCHEME 12 - REACTION SCHEME FOR THE SYNTHESIS OF N-METHYL- $\alpha$ -PENTAFLUOROPHENYLNITRONE

The reaction proceeds with excellent yields, as shown in the table, and the N-methyl- $\alpha$ -pentafluorophenylnitron (4) was isolated after a filtration on silica pad (Table 4).

Entry	Reaction time (h)	Yield (%)
1	8	86
2	14	98

TABLE 4 - REACTION YIELDS OF N-METHYLPENTAFLUOROPHENYL NITRONE (4)

The compound (4) was then added to the PB oligomer, varying the reaction temperature, the solvent, the energy source and the vinyl-nitrone ratio as shown in the table 5.



SCHEME 13 - REACTION SCHEME FOR THE SYNTHESIS OF COMPOUND (5)

Entry	Solvent	Ratio eq. (4): vinyl double bonds	Temperature (°C)	Time (h)	Functionalization Yield (5) %
1	DCM	1:1	r.t.	20	-
2	DCM	1:1	40	24	-
3	DCM	10:1	40	24	12 <sup>b</sup>
4	DCM	10:1	110 <sup>a</sup>	6	<5 <sup>b</sup>
5	1,2 - DCE	100:1	83	6	20 <sup>b</sup>

TABLE 5 - REACTION CONDITION FOR THE SYNTHESIS OF COMPOUND (5);

<sup>a</sup>MW ASSISTED (200W); <sup>b</sup> YIELDS OF ADDITION ON VINYL DOUBLE BONDS DETERMINATE BY NMR SPECTRA ANALYSIS

In the first instance, the mildest reaction conditions were replicated, i.e. at room temperature with a stoichiometric ratio of 1:1, but also in this case it was not possible to observe any kind of variation in the reaction mixture. Increasing the temperature and letting the reaction run for 24 hours in refluxing DCM does not seem to have a significant effect, however, under the same conditions but

increasing up to 10 times the ratio between dipole and dipolarophile it is possible to notice the occurrence of a double peak at 4.03 and 4.05 ppm respectively, ascribable to the protons residues of the five member ring formed after the addition to the vinyl double bond (multiplet at 4.98 ppm) – (figure 9). They represent the only diagnostic signals of the coupling, since it is not possible to trace the signals of the other protons due to the superimposition of those signals (like N-CH<sub>3</sub> proton signal shifted to 2.90 ppm) with the characteristic signals of Polyvest.

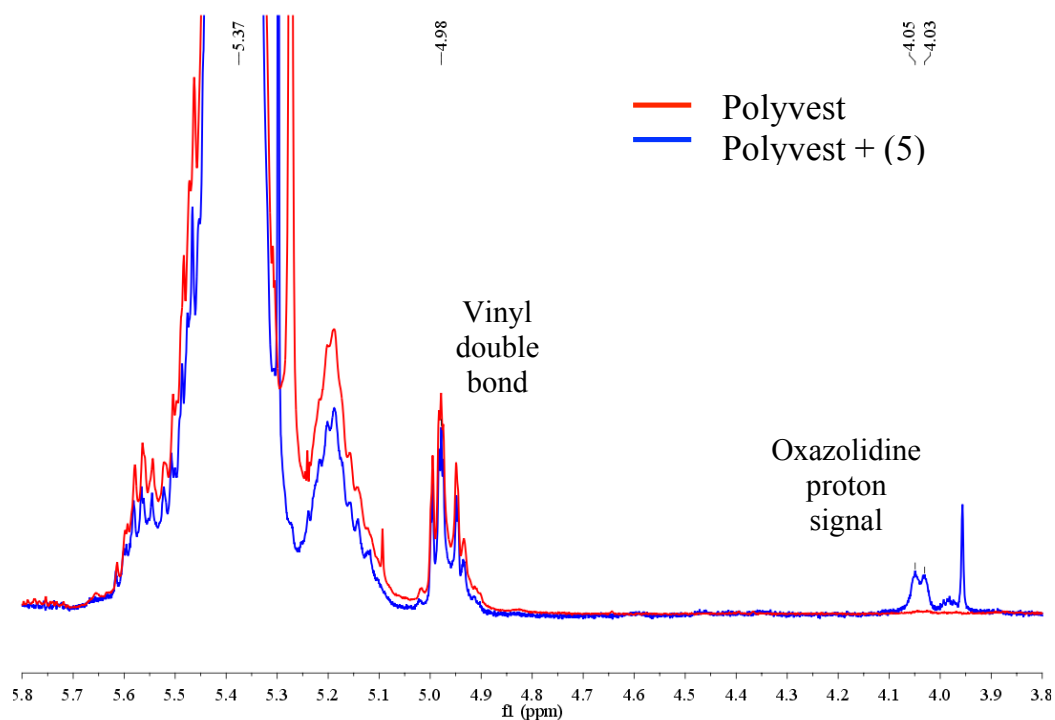


FIGURE 9 - SUPERIMPOSED 1H-NMR SPECTRA OF POLYVEST (1, RED LINE) AND ADDUCT (5, BLUE LINE).

The presence of a split peak rather than a singlet was attributed to the two regioisomers that could be formed during the reaction, as shown in the figure 10, with R polymer backbone. To promote the reaction, the temperature was raised, by irradiating the sealed vessel with microwaves.

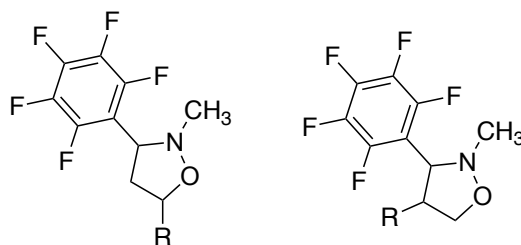
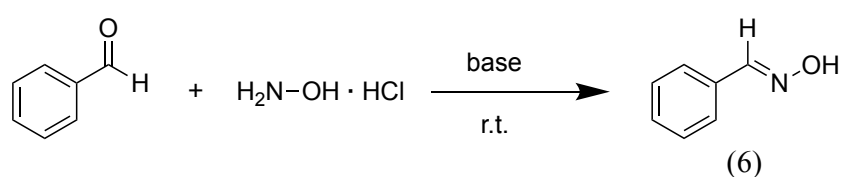


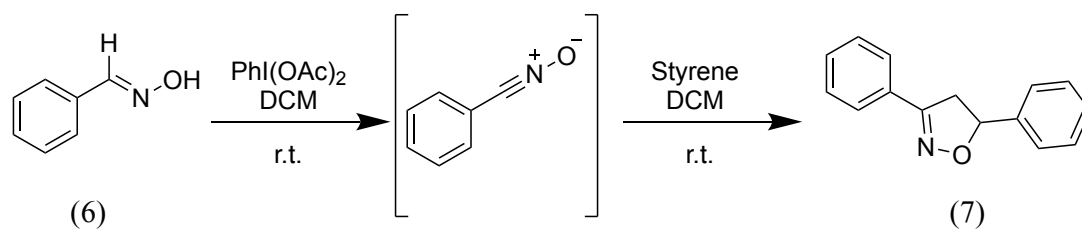
FIGURE 10 -POSSIBLE REGIOISOMER FORMED DURING 1,3 DIPOLAR CICLOADDITION OF COMPOUND (4) ON POLYMER.

However, contrary to expectations, the formation of the product has decreased. Probably, stimulation through microwaves promotes competitive reactions compared to the desired one. Following the course of the reaction by TLC, it is possible to see the appearance of several spots, which are not compatible with the expected product, while the starting dipole is consumed as the reaction proceeds. Using conventional heating in combination with a higher boiling point solvent, such as 1,2 dichloroethane ( $\approx 84\text{ }^{\circ}\text{C}$ ), and a very large excess of nitron compared to vinyls, it is possible to push the reaction in the desired direction, with a maximum estimated conversion in 20% (determined by  $^1\text{H-NMR}$  spectra analysis). A low conversion requires an accurate polymer purification process (see appendix B, synthesis of (5)) to remove the unreacted dipole and by-products. Despite the partial solubility in methanol of the unreacted nitron, traces of the dipole are still present, as we can see from the residual peak at 3.96 ppm in figure 10. Nevertheless, this result is still positive, since here we report, for the first time, the coupling of the nitron (4) to a polymeric matrix through a 1,3 dipolar cycloaddition activated by the temperature, without catalysts. Moreover, despite the use of a large excess of reagent, it is possible to notice how the reaction is selective, reacting only with the vinyl bonds, leaving the structure of the internal bonds intact. To increase the reactivity of the system, it was therefore decided to change the class of dipoles, moving from the family of the nitrons to the nitrile oxides one. The first step was therefore the synthesis of the corresponding oxime, to be converted later and in situ for the reaction with the polymeric substrate. Using a literature procedure reported in a patent,<sup>119</sup> benzaldehydeoxime was synthesized (6) treating with a base (typically sodium hydroxide) benzaldehyde and hydroxyl amine chlorohydrate (Scheme 14).



SCHEME 14 - REACTION SCHEME FOR THE SYNTHESIS OF OXIME (6)

Once the oxime has been synthesized (6) it has been decided to test its reactivity on a styrene monomer to check the procedure found in the literature for in situ production of the corresponding nitrile oxide by the use of an oxidizing compound such as phenyliodine (III) diacetate (PIDA),<sup>120</sup> (Scheme 15).



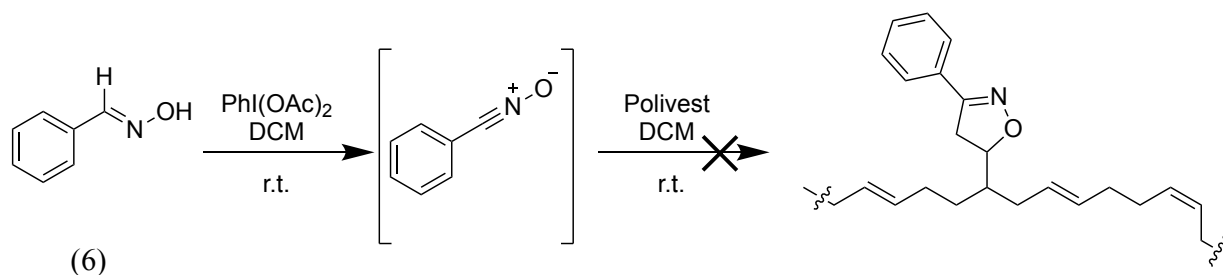
SCHEME 15 - FORMATION REACTION OF NITRIL OXIDE AND SUBSEQUENT ADDITION TO STYRENE

The proposed system for the preparation of nitrile oxides by hypervalent iodine is very interesting because it allows to obtain the desired product in a one pot, easy and straightforward reaction; in contrast to the more traditional methods that included a first step of chlorination of the starting oxime and subsequently a dehydrochlorination step.

Entry	Solvent	Temperature (°C)	Time (h)	Yield (7) %
1	DCM	r.t.	3	42
2	THF	r.t.	3	40

TABLE 6 - REACTION CONDITION OF ADDITION TO STYRENE

As reported in table 6, the yield of product formation (7) is not very high (42% in DCM) but it must be considered that the substrate is not activated, and the reaction conditions are mild. Furthermore, from the collected data it is evident that the solvent does not significantly influence the reaction yield. The NMR characterization of Isooxazoline (7) allowed us to identify the characteristic signals of the newly formed ring, giving us an idea of where the signals of the protons of the product will fall once hooked onto the polymeric substrate (Scheme 16).

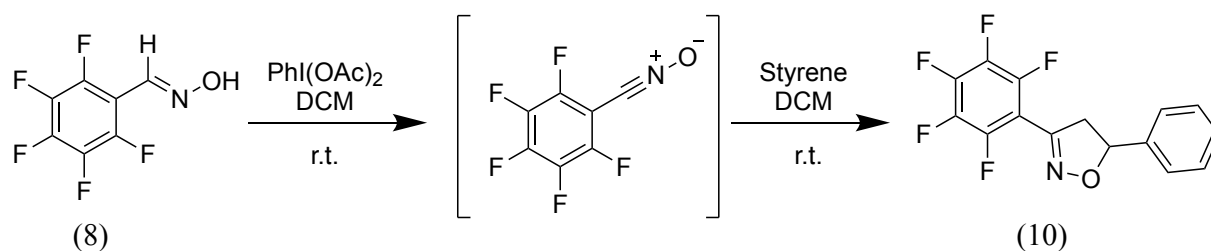


SCHEME 16 – POSSIBLE REACTION BETWEEN NITRIL OXIDE GENERATED IN SITU AND POLYVEST

As in the case of nitrone, the unsubstituted nitril oxide is not able to react with the butadiene oligomer despite the use of a 1:1 stoichiometric ratio between functionalizer, and the repeating units, corresponding to 100 times the number of vinyl double bonds. For this reason, it was decided

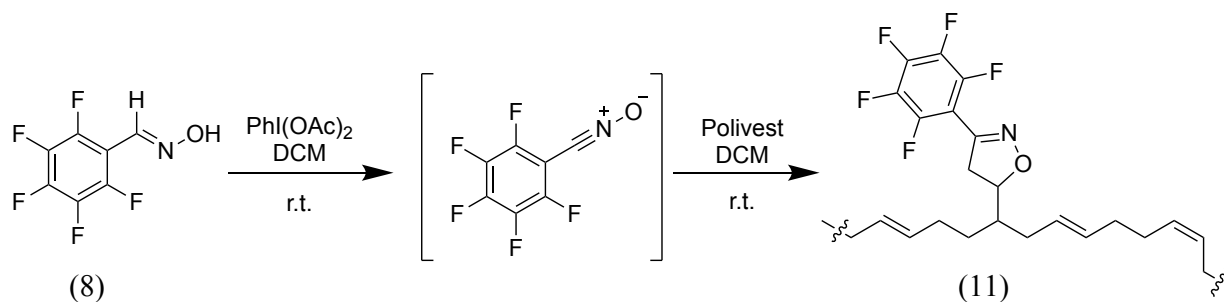
to proceed with the same strategy adopted for the nitrones: increase the electron attractor behavior of the aromatic ring of the oxime by replacing the hydrogen with fluorine.

To accomplish this task, the literature procedure proposed by Van Delft and coworkers was used.<sup>121</sup> Also in this case, to verify the effective formation of the nitrile oxide starting from the corresponding oxime, the reaction was tested on the styrene monomer (Scheme 17).



SCHEME 17 - PROCEDURE FOR THE SYNTHESIS OF 3-(PENTAFLUOROPHENYL)-5-PHENYL-4,5-DIHYDROISOXAZOLE (10)

The successful formation of the product (10), with a yield equal to 61%, confirms the initial hypothesis, i.e. the greater reactivity compared to the non-fluorinated nitrile oxide. In order to obtain the functionalized product, the oxime (8) was then reacted with a ratio of 1:1 with respect to the total double bonds of the polymer (Scheme 18).



SCHEME 18 - OXIDATION OF PENTAFLUORO PHENYL OXIME TO NITRILE OXIDE AND SUBSEQUENT CYCLOADDITION TO PB OLIGOMER

The polymer was recovered precipitating it into methanol, and a spectroscopic characterization was carried out, both with FTIR and <sup>1</sup>H-NMR. As we can see from the FTIR spectrum, the addition product (red line) carries both the main peaks of the polybutadiene oligomer (black line) and the peaks deriving from the pentafluorurate oxime (blue line), Figure 11.

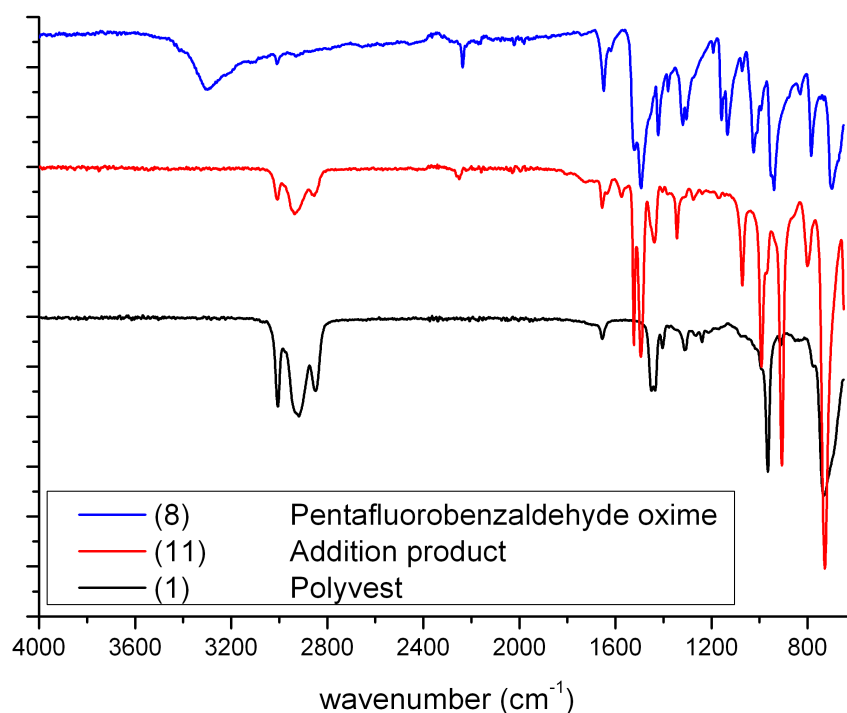


FIGURE 11 - COMPARISON BETWEEN FTIR SPECTRA OF REACTANTS AND ADDITION PRODUCT (11)

By observing the black line obtained by recording the FTIR spectrum of the unmodified Polyvest it is possible to recognize some typical bands of the roto-vibrational modes of polybutadiene. The spectral region between 2800 and 3050  $\text{cm}^{-1}$  is ascribable to the asymmetric stretching of the  $-\text{CH}_2$  and to the stretching of the  $=\text{C}-\text{H}$  bonds; besides those bands there are peaks at 1440  $\text{cm}^{-1}$ , 967  $\text{cm}^{-1}$  and 722  $\text{cm}^{-1}$ , respectively representative of the bending of  $-\text{CH}_2$ , C-C torsion and  $-\text{CH}_2$  rocking. These bands are clearly recognizable also in the addition product (red line) together with the emerging bands between 1400 and 1525  $\text{cm}^{-1}$  and between 900 and 1000  $\text{cm}^{-1}$  whose pattern, even if shifted, is attributable to the starting oxime (blue line), with the exception of the 3300  $\text{cm}^{-1}$  band characteristic of the stretching of  $-\text{OH}$  group, which is lost during the reaction.

The successful functionalization is also evident from the NMR analysis, depicted in the Figure 12, where we note the presence of two imported bands with chemical shift between 3.2 and 4.8 ppm that emerge in a free zone of polybutadiene oligomer signals.

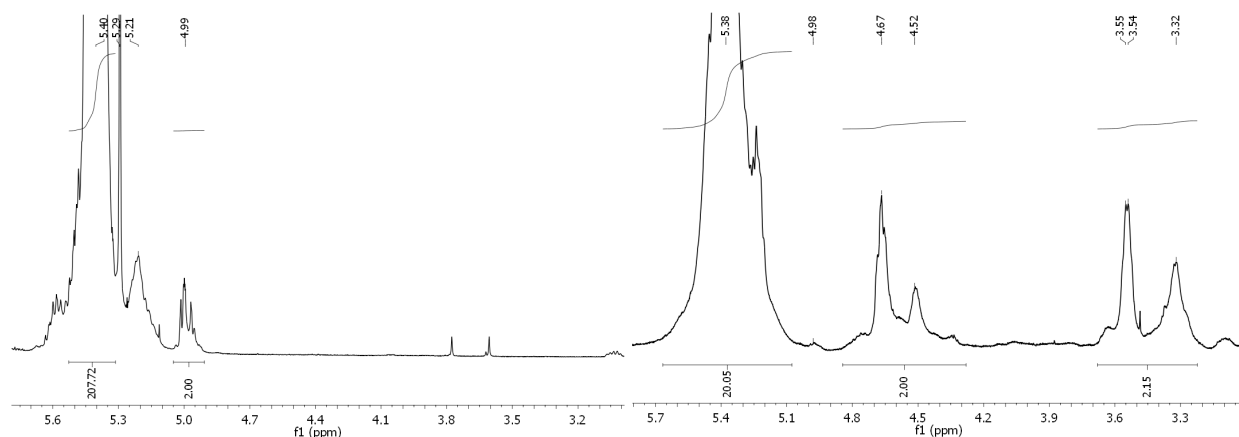
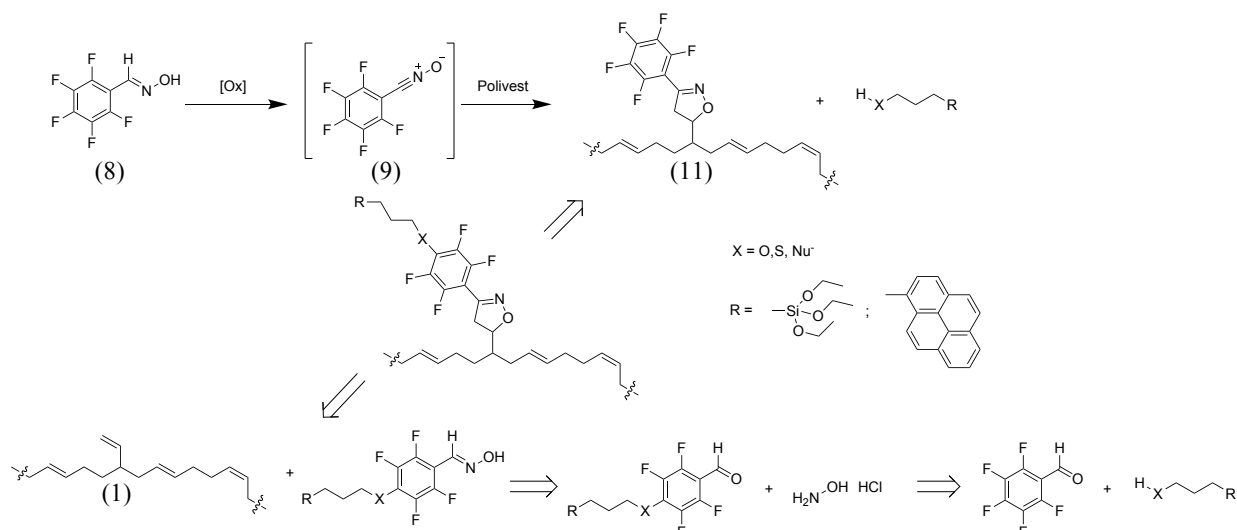


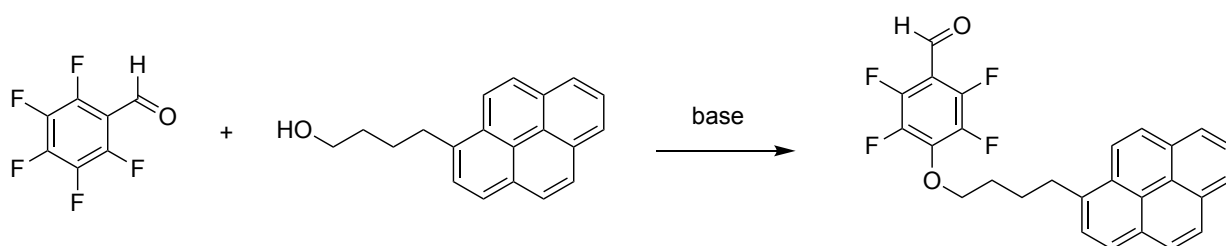
FIGURE 12 - COMPARISON BETWEEN  $^1\text{H}$ -NMR SPECTRA OF PRISTINE POLYMER AND ADDITION PRODUCT (11)

Observing the spectra, it is also possible to notice the selectivity of the reaction on the vinyl double bonds. The peak at 4.99 ppm in fact is diagnostic of the 1,2 cis isomers of polybutadiene and completely disappears at the end of the reaction. Although the preferential attack occurs on the just mentioned substrate, using a very large excess of dipole, as in this case, the reaction does not stop, continuing also on the inner double bonds of the polymer skeleton, up to an estimated functionalization of about 20%. A final consideration that can be made is that the coupling on the internal double bonds is not regioselective as indicated by the literature for this type of reactivity, which could determine the shape of the visible band in the NMR spectrum of the product (11). As previously mentioned, the decision of introducing a fluorinated system into a polymer matrix was also prompted by the need of having an electronwithdrawing substituents on the aromatic ring to enhance the reactivity of the system. However, the choice of a fluorinated substituent was made with the prospect of further modification of the system through an aromatic nucleophilic substitution reaction ( $\text{S}_{\text{N}}\text{Ar}$ ). Performing a second reaction step on a substrate, already bound to the polymeric matrix, presents considerable operational difficulties. The reaction conditions required for a  $\text{S}_{\text{N}}\text{Ar}$  are incompatible with the strongly apolar nature of the polymer matrix, both for its insolubility and for the subsequent purification step. This aspect can be represented by a small retrosynthetic scheme, in which the two theoretically plausible pathways are illustrated, but it is possible to divide the synthesis of the functional group from the addition reaction only in the second case (Scheme 19).



SCHEME 19 - RETROSYNTHETIC ANALYSIS FOR THE PRODUCTION OF A SUBSTITUED FUNCTIONAL GROUP

The nucleophilic aromatic substitution takes place thanks to the action of a nucleophile, usually activated by a base, and it is therefore evident that one side of the molecule must contain this functionality. On the other hand, if we want to compatibilize an inorganic filler, we should introduce a functional group able to interact with it. For silica-based fillers, a valid alternative can be represented by an ethoxysilane, just like TESPT, able to react with the surface hydroxyl groups of silica nanoparticles. On the contrary, to make carbon black compatible, the idea was to use a system capable of establishing weak interactions ( $\pi$ - $\pi$ ) with the large surface area of CB. In literature,<sup>122,123</sup> the interaction between the pyrene derivatives and carbon black particles is documented; keeping these considerations in mind, the synthesis of the key intermediate was attempted through an aromatic nucleophilic substitution synthesis by reacting pentafluorobenzaldehyde and 1-pyrenbutanol as shown in the diagram below (Scheme 20).



SCHEME 20 -EXPECTED  $\text{S}_{\text{N}}_{\text{AR}}$  ON PENTAFLUORO BENZALDEHYDE

Unfortunately, the reaction did not give the desired result because it was possible to isolate the replacement product (12), but the aldehyde group was probably reduced by a reaction mechanism like that of the haloform (Figure 13). To avoid the formation of this side product, the reaction was

attempted without the presence of the base: unfortunately this attempt did not give a good result, probably due to a low nucleophilic nature of the hydroxyl group of pyren-butanol.

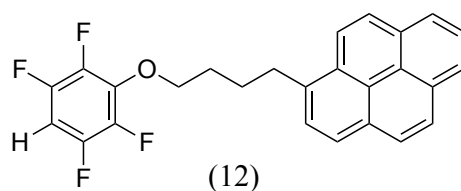
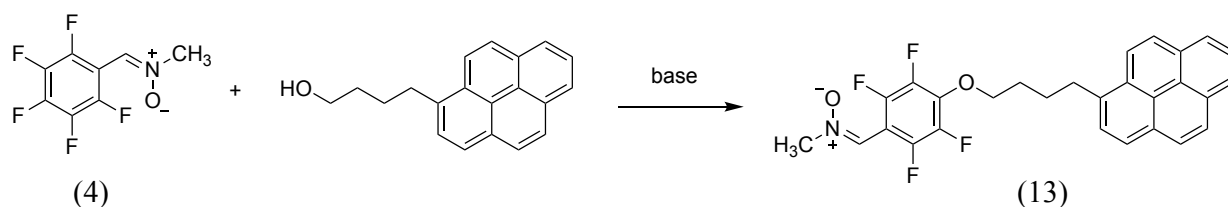


FIGURE 13 - UNEXPECTED ISOLATED PRODUCT

Since it was not possible to perform the reaction on pentafluorobenzaldehyde without any protective group and, at the same time, in order to avoid increasing the already numerous synthetic steps involved, the nucleophilic aromatic substitution was attempted on the already formed dipole, and the chosen substrate was N-methyl- $\alpha$ -pentafluorophenylnitron (4), (Scheme 21).



SCHEME 21 - SUBSTITUTION ATTEMPT ON PERFLUOROPHENYL-N-METHYLNITRON

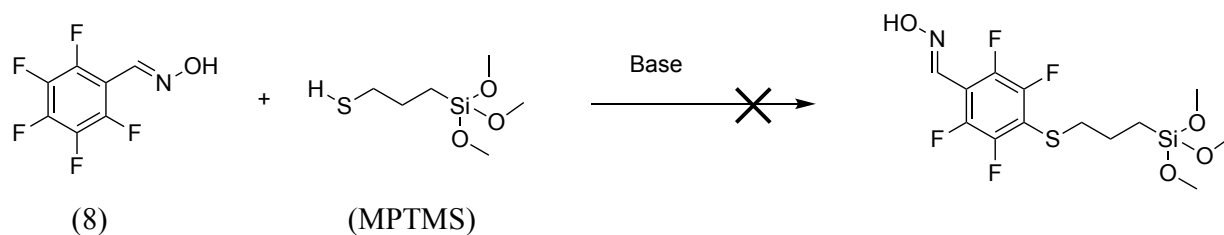
Several reaction solvents were tested, which could promote aromatic nucleophilic substitution. In the case of THF and DMSO the reaction was controlled by TLC every hour for the first 4 hours of reaction but, not observing any change, they were left to react overnight without any difference (Table 7).

Entry	Solvent	Base	Temperature (°C)	Time (h)	Yield (13) %
1	THF	t-ButOK	r.t.	18	n.r.
2	DMF	t-ButOK	r.t.	5	0
3	DMSO	t-ButOK	r.t.	18	n.r.

TABLE 7 - REACTION CONDITION FOR THE SYNTHESIS OF PRODUCT (13) – N.R. NO REACTION OBSERVED

Only in the case of the reaction in DMF it was possible to observe a fast proceeding of the reaction that led to the disappearance of the initial reagents. Unfortunately, despite the products formed could be isolated by a purification process with a chromatographic column, it was not possible to identify the desired compound (13). A possible way to promote the aromatic nucleophilic substitution reaction could be the use of molecules with a more pronounced nucleophilic character

than a hydroxyl moiety, for example a thiol. The proof of concept reaction was the addition of a (3-Mercaptopropyl) trimethoxysilane (MPTMS) to the oxime (8), (Scheme 22).

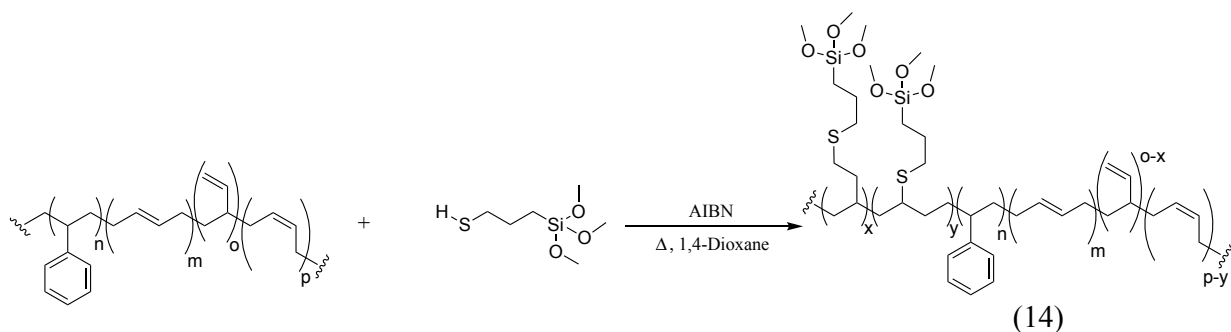


SCHEME 22 -  $S_NAR$  REACTION OF A THIOL ON A PERFLUORINATED SUBSTRATE

The reaction was carried out in DMF dry, with triethylamine (TEA) dry as base. The choice of this reagents was driven by the fear that the presence of water and a protic base could trigger condensation phenomena of the siloxane units. Unfortunately, no reaction could be observed, indicating that, obviously, the base is not strong enough to trigger the reaction, which would require an optimization not addressed in this thesis, preferring instead the investigation of other types of reactivity.

## 3.2 THIOILS-ENE

As described in chapter 1.2, a second opportunity of coupling to the unsaturated double bonds of a polymeric matrix is offered by the thiols-ene chemistry. If we want to improve compatibility between rubber and filler it is necessary that the thiol introduced into the compound has a functional group capable of interacting, covalently or not, with the inorganic component. Inspired by the chemistry of TESPT, the current standard for the compatibilization of silica, the functionalizer chosen as a model was the (3-Mercaptopropyl) trimethoxysilane (MPTES), a bifunctional molecule in which there is a siloxanic group able to bind to the surface of silica particles, just like TESPT, and a thiol capable of reacting with the double bonds of the polymeric backbone. Among the various types of reactions available, the one that seemed most suitable for our purposes was the Free Radical Thiol-Ene reaction. It is a very simple and direct reactivity, which can be carried out in non-polar solvents (able to dissolve the polymer) and without the need for acid catalysis, as for the Nucleophilic Thiol-Ene Reaction. On the other hand, to be activated, the reaction needs a source of free radicals. We can identify mainly 3 different activation system: UV irradiation,<sup>124</sup> exposure to high temperatures or radical initiators (AIBN).<sup>125</sup> Although UV irradiation represents a fascinating alternative, thanks to the ability of generating free radicals in a clean way, this approach has not been considered in this discussion, because of the impossibility of accurately determining the number of radicals introduced. Furthermore, an optically active molecule (such as pyrene) would act as an energy funnel, inhibiting the process of generating radicals. The chosen source of radicals was therefore an economic radical initiator, extremely known in literature, such as the AIBN, capable of activating at reasonably low temperatures,  $\approx 50$  °C. The solvent chosen for the functionalization tests was therefore dioxane (b.p. 101 °C). It is good to remember that thio-ene radical functionalization proceeds through an Anti-Markovnikov regioselective reaction, with the addition to the less substituted carbon. This could be seen in a different kinetics of addition to the double bonds of the polybutadiene part of the polymer, in particular in-chain double bonds are 10 times less reactive than vinyl double bonds and may promote an intermolecular cross-linking of chains.<sup>126,127</sup>



SCHEME 23 - FUNCTIONALIZATION OF POLYMER THROUGH A THIO-ENE FREE RADICAL CYCLOADDITION

To test both the merits of the idea and the versatility of this type of approach, the addition reaction was attempted on different polymeric substrates, with different degrees of functionalization (Scheme 23, Table 8).

In addition to Polyvest, described at the beginning of chapter 3, two other polymers have been tested:

- BR40 - neocis, a commercial regioregular polybutadiene with a high content of cis-bonds (over 97% of the total mass) and high molecular weight ( $\approx 480,000 \text{ g}\cdot\text{mol}^{-1}$ ), produced by Versalis, useful for testing the behavior of the present functionalization on a polybutadiene polymer with a technological relevance for the production of rubber compounds.

- Ricon 100 - a low molecular weight ( $\approx 4,500 \text{ g}\cdot\text{mol}^{-1}$ ) copolymer of butadiene and styrene, produced by Cray Valley, whose composition, as reported in Table 8, is 27% Styrene w/w and 73% w/w of B, of which 70% consists of 1,2-B. In this case the choice has been made in order to test the reactivity of a different nature polymer, through a test on a model oligomer similarly to Polyvest.

Entry	Polymer	n (%wt)	m+p (%mol)	o (%mol)	MPTES eq.	AIBN eq.
1	Polyvest	0	99	1	0.1	0
2	Polyvest	0	99	1	0.01	0.001
3	Polyvest	0	99	1	0.1	0.01
4	Polyvest	0	99	1	0.2	0.02
5	BR40 - Neocis	0	97 cis	0.1<	0.2	0.02
6	SBR Ricon 100	27	27	73	4.7	0.47

TABLE 8 - REACTION CONDITION OF THIO-ENE FREE RADICAL REACTION

First, we made a blank reference without a radical initiator and, as expected, it was not possible to find traces of the adduct in either IR or NMR spectra. Although the samples were subjected to the same type of purification treatment, the results of the functionalization both on Polyvest (entry 2-3-4) and on BR40 (entry 5) were misleading and it was not possible to find a direct correlation between the molar ratios of the reagents with the collected NMR spectra. This is probably due to the poor reactivity of the internal double bonds that prevents a fast addition of thiols, which allows free radicals to undertake different reaction pathways, producing side reactions and interchain crosslink. These considerations are based on the observation of some physical properties of the material, the most evident being the variation of solubility in organic solvents. In fact, the polymer tends to swell rather than melt, making the collection of an NMR spectrum in solution extremely difficult. On the contrary, much better results have been obtained by functionalizing an oligomeric copolymer such as Ricon 100 (entry 6). Using the signals of the styrene aromatic protons as an internal standard and, comparing the non-functionalized pristine (red line) polymer with the reaction product (black line), it is immediately evident that a diagnostic peak at 3.57 ppm of chemical shift is present, ascribable to the 9H of the methoxy-siloxanic group, which corresponds to a decrease of the integral relative to the peak of the 1,2-PB vinyl protons at 4.95 ppm (Figure 14).

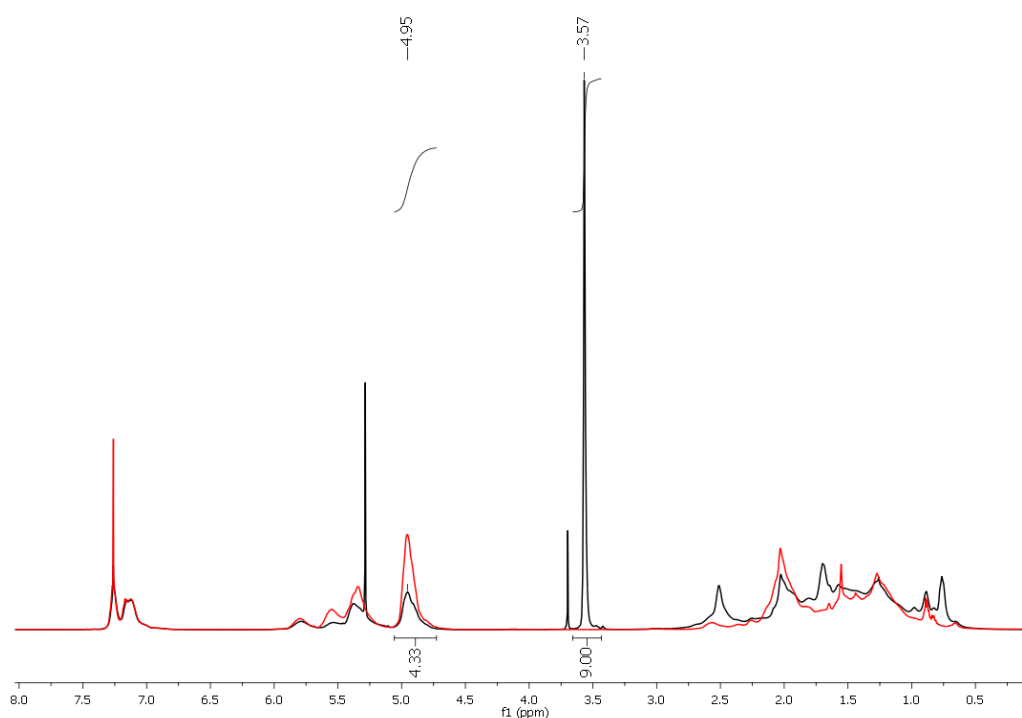


FIGURE 14 - <sup>1</sup>H-NMR SPECTRA OF PRISTINE (RED LINE) AND FUNCTIONALIZED (BLACK LINE) SBR OLIGOMER

Calculating the amount of functionalizer inserted in the polymer matrix based on the integration of the vinyl residue signals with the aromatic protons of the polystyrene results a yield of 98%.

This is also qualitatively confirmed by the FTIR analysis (Figure 15) in which it is possible to recognize, beside the asymmetric  $\nu_a$  (Si-OCH<sub>3</sub>) and symmetric  $\nu_s$  (Si-OCH<sub>3</sub>) stretching at 2943 and 2840 cm<sup>-1</sup>, all the other modes of this group appearing at 1190, 1084 and 811 cm<sup>-1</sup>.<sup>128</sup>

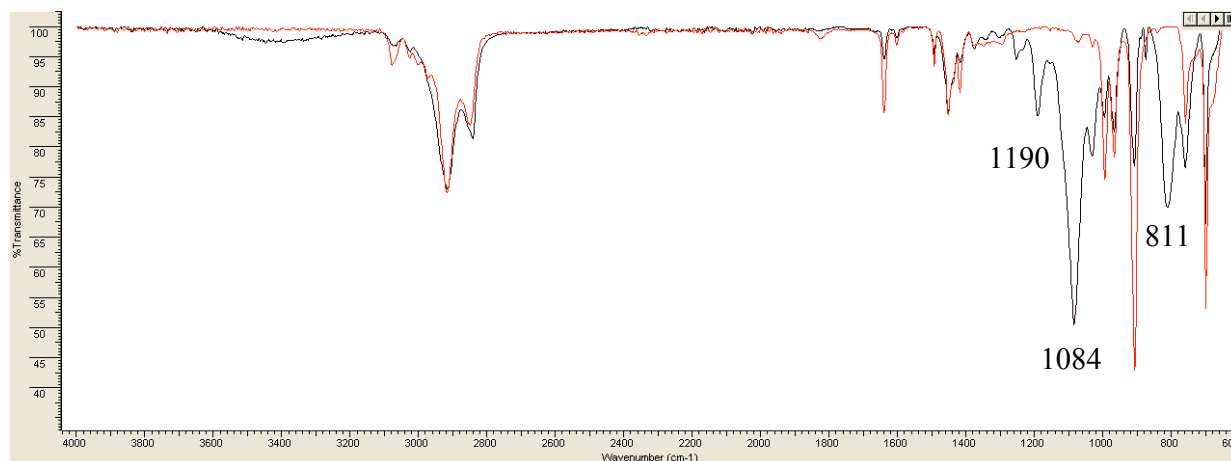


FIGURE 15 - FTIR SPECTRA OF PRISTINE (RED LINE) AND FUNCTIONALIZED (BLACK LINE) SBR OLIGOMER

This reaction demonstrates that it is possible to introduce a functional group capable of forming covalent bonds with the silica under mild reaction conditions, allowing a preferential functionalization on the vinyl double bonds. Unfortunately, this type of functionalization does not allow us to ignore two problems that seriously compromise the application in the industrial field. Firstly, introducing siloxane functional groups before the mixing phase compromises the processability of the composite. In fact, when silanization occurs during the rubber compounding, the filler becomes directly linked to the polymer matrix. This would cause a sudden raise of the viscosity of the system, preventing its correct mixing process. Secondly, as already mentioned above, introducing free radicals into a highly unsaturated system, such as a polymer, is not trivial at all, since it involves cyclization and crosslink phenomena, which can vary the intrinsic characteristics of the rubber in a detrimental way. In agreement with the industrial partner, we then moved to another front, in order to dodge the limits imposed by the free radical functionalization just described, moving on into the furrow track of sulfur chemistry, recycling the idea to compatibilize the CB through weak interactions, as unsuccessfully attempted with 1,3 dipole additions.

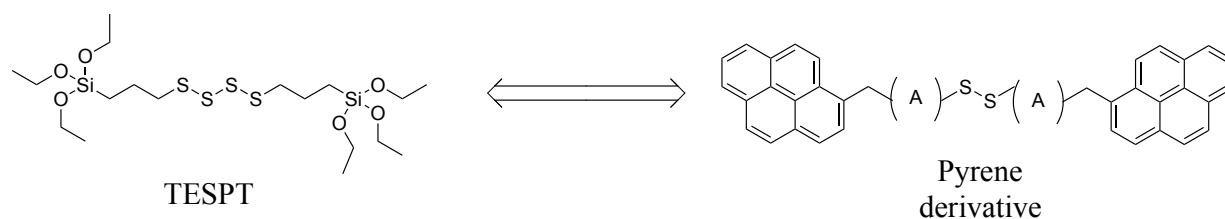
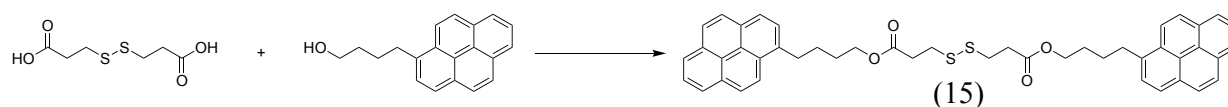


FIGURE 16 - MOLECULAR STRUCTURE OF TESPT (LEFT) AND PYRENE ANALOGUE (RIGHT)

The basic idea was the synthesis of a TESPT homologue, with a central core consisting of a sulphur bridge able to open during the vulcanization phase (figure 16) and functional groups at the edges constituted by pyrene derivatives. As previously described (paragraph 3.1), the choice of using a pyrene derivative is given by its ability to exhibit  $\pi$ - $\pi$  stacking with the surface or with the internal layers of CB,<sup>121-122</sup> here used as filler, in order to maximize the interaction.

The first synthetic route explored led us to the synthesis of a pyrenic derivative, the bis [4-(1-pyrenyl) butyl]3,3'-disulfanediyldipropanoate (PyDP), obtained through an esterification between a tiopropildicarboxyle acid with two molecules of 1-pyrenbutanol (Scheme 24).

The product (15) was initially synthesized by means of a Steglich esterification,<sup>129</sup> however the presence of unreacted dicyclohexylcarbodiimide (DCC) made the product purification procedure difficult, heavily affecting the overall yield (<35%). Considering the amount of product necessary for an effective functionalization during rubber compounding and, above all, the high price of pyren butanol, we decided to perform a Fischer esterification,<sup>130</sup> which led to the synthesis of the target molecule with an excellent yield (> 90%).



SCHEME 24 - ESTERIFICATION OF PYREN DERIVATIVE

The Steglich esterification is a variation of an esterification with DCC as a coupling reagent and 4-dimethylaminopyridine (DMAP) as a catalyst, while Fischer esterification is a more conventional reaction made by refluxing a carboxylic acid and an alcohol in the presence of an acid catalyst, the para-toluen sulfonic acid in this case.<sup>131</sup>

To verify the actual interaction between the synthesized pyren-derivative and the surface of the CB commonly used in compound application, an optical characterization of the sample was performed.

The loss of fluorescence by a molecule, the PyDP in this case, could be due to several factors, in this particular experiment it was exploited to monitor the degree of internalization of the pyrene derivative within the filler structure, in order to estimate the minimum amount of filler necessary to have a complete interaction between the carbon planes, or on the surface, of the CB and the compatibilizer proposed. The evaluation of residual fluorescence of the unbound PyDP was performed as follows:

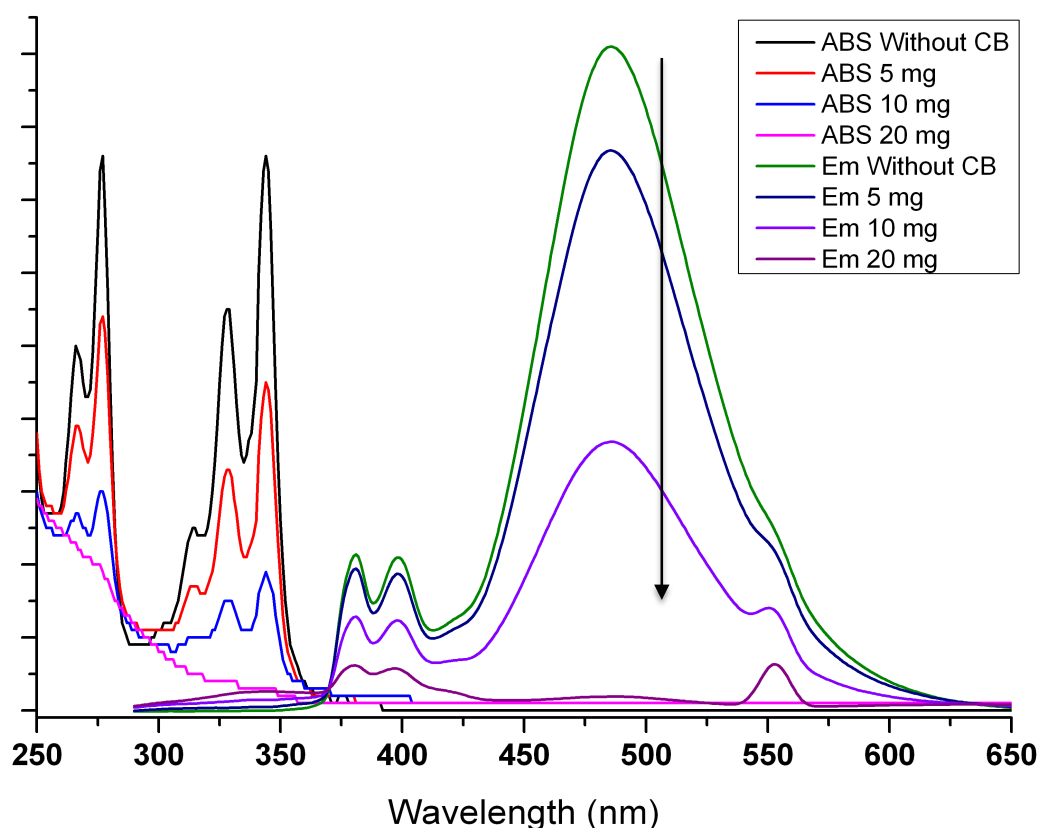
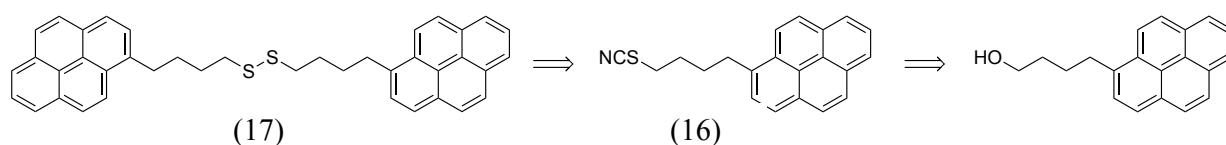


FIGURE 17 - UV AND EMISSION SPECTRA OF PYDP IN DCM IN PRESENCE OF CB

A PyDP solution (15) was prepared in DCM at a known concentration ( $2.5 \cdot 10^{-4}$  M) and its absorption and emission spectrum was recorded. 5 mg of CB N326 were added to the system, leaving the solution under stirring for 30 minutes. After taking an aliquot, the particles larger than 200 nm were filtered off and a new spectrum was recorded. The procedure was repeated adding more carbon black, until the complete disappearance of the characteristic absorption and emission signals, as shown in Figure 17.

From the calculations made, it emerged that the desirable internalization of PyDP on CB occurred at the concentration of 1 g of functionalizing every 11 g of CB N326, which makes it possible to hypothesize its effective use as coupling agent in a compound. To produce a standard laboratory-

scale mixture ( $\approx 50$  g total) with a small mixer, as described in the dedicated chapter, the amount of filler to be included was between 10 and 15 g, along with about 1g of compatibilizer, quantities quite comparable with those found in the experiment just described. After having tested this pyrene derivative in mixture, we tried to synthesize a new pyrenic derivative with the intent of removing the ester group from the molecular structure of the compound. This part of the molecule is potentially the most problematic one, as it could act, like other esters, as a plasticizer during formulation or, in the worst case, it could open or hydrolyze, neutralizing the synthetic effort to constrain the sulfur bridge with a pyren-unit.



SCHEME 25 - RETROSYNTHETIC ANALYSIS OF THE BIS-[4-(1-PYRENYL)-BUTYL]-DISULFIDE (PYS)

The most convenient approach to obtain a disulfur bridge seems to be the coupling between two thiocyanate units (Scheme 25), which is in turn produced from the same starting substrate of the derivative (15). To realize the first part of the synthesis we were inspired by procedures known in the literature for the conversion of primary alcohols to thiocyanates using heteroaromatic azo compounds under Mitsunobu conditions proposed by Iranpoor and coworkers,<sup>132</sup> although in our experience not all the articles gave the reported results.<sup>133</sup>

For the second part we used the very simple and direct method proposed by Burns and coworkers for the preparation of disulfides from acyclic bis-thiocyanate, through a cleavage of thiocyanates with Tetrabutylammonium fluoride (TBAF).<sup>134</sup>

Entry	Solvent	Azo group	Temperature (°C)	Time (h)	Yield (16) %
1	ACN	DEAD	r.t.	18	87%
Entry	Solvent	Base	Temperature (°C)	Time (h)	Yield (17) %
1	THF	TBAF	r.t.	18	98%

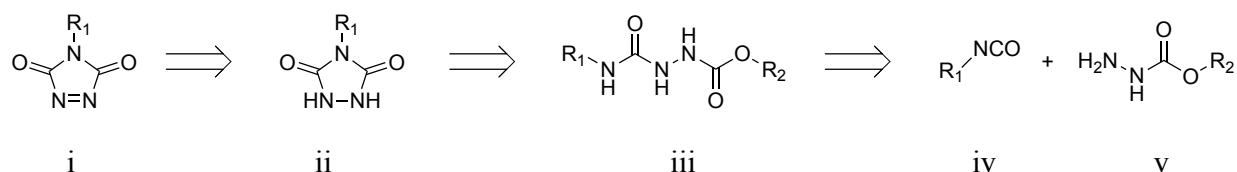
TABLE 9 - REACTION CONDITION FOR THE SYNTHESIS OF THE INTERMEDIATE (16) AND PYS (17)

Both reactions have been successful with excellent yields, guaranteeing the quantity necessary to carry out a formulation test of a compound with CB as filler (Table 9). For the synthetic details, see the experimental appendix.

Unfortunately, despite the effort made to synthesize these two molecules, none of them has led to an effective functionalization of the carbon black in the mixture, in any case further studies are still underway in order to synthesize different pyrene derivatives with a tailored and more reactive anchor group.

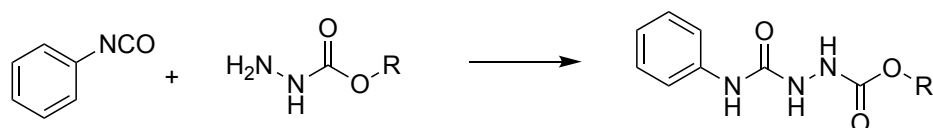
### 3.3 TRIAZOLIDINONE

As reported in section 1.3, the chemistry of TADs has attracted our interest for its outstanding reactivity with non-activated dipoles. The great reactivity of this system allows to minimize the operational difficulties of the addition phase to the polymeric substrate. Most of the work was therefore centered on the synthesis of PhTAD and, since nobody in the literature had ever tried to evaluate its ability to compatibilize silica-based fillers, on the optimization of its use to produce tire compounds.



SCHEME 26 - RETROSYNTHETIC ANALYSIS FOR THE PRODUCTION OF TAD

The literature survey showed that the most convenient synthetic procedure was the one proposed for the first time by Zinner and Deucker, which involved the synthesis of a semicarbazide intermediate as a key step. The retrosynthetic analysis of TAD (i) is articulated in several steps, the most important one is obviously the last one: the oxidation of the corresponding urazole (ii) obtained from intramolecular cyclization, in the alkaline condition, of semicarbazate (iii). The latter is synthesized from the addition of a carbamate (v) and an isocyanate (iv) carrying the functionality that we will then find in position 4- in the final product (Scheme 26). Inspired by the work of Mallakpour group<sup>135</sup>, different methodologies and different starting substrates were tested to achieve the desired phenyl urazole (16).



SCHEME 27 - GENERAL SCHEME OF REACTION BETWEEN PHENYL ISOCYANATE AND CARBAZATE WITH -R= -ET OR -TBUT

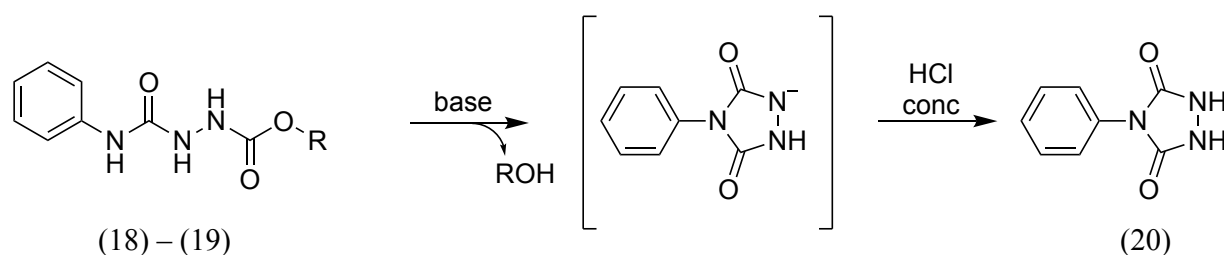
The reaction is simple and straightforward, with yields always higher than 88%. It can be carried out both in solution and in neat conditions, grinding the reagents with a mortar. The residue R seems to be irrelevant for the addition of the phenyl isocyanate carbamate, however the reaction conditions influence the purity of the final compound (Scheme 27). In neat conditions, in fact, the

reaction has a much faster course, due to direct contact of the reagents. However, in NMR spectra it is possible to identify impurities probably formed due to hydrolysis of isocyanates because of atmospheric moisture, whose separation is very complicated. On the contrary, a reflux reaction in an organic solvent, such as toluene, is slower but grants higher yields, with a considerably higher degree of purity (Table 10).

Entry	-R	Solvent	Temperature (°C)	Time (h)	Yield %	Product
1	-Et	- <sup>a</sup>	- <sup>a</sup>	0.5	88	<b>18</b>
2	-t-But	- <sup>a</sup>	- <sup>a</sup>	0.5	91	<b>19</b>
3	-Et	Toluene	110	3	98	<b>18</b>
4	-t-But	Toluene	110	3	95	<b>19</b>

TABLE 10 - REACTION CONDITION FOR THE PRODUCTION OF PHENYLSEMICARBAZIDE

The next intramolecular cyclization step can be completed using different bases, both inorganic, such as potassium hydroxide (KOH), and organic such as sodium ethoxide (NaOEt), depending on the nature of the solvent used to dissolve the semicarbazate. The base deprotonates the amide nitrogen and makes a nucleophilic attack to the carbonyl of the ester group, the molecule forms a five-member ring cycle and after a rearrangement the alcohol ROH is expelled. The final product (16) is then simply recovered by acidifying the solution with concentrated hydrochloric acid, the phenyl urazole in fact precipitates and the crystals can be recovered by filtration (Scheme 28, Table 11).



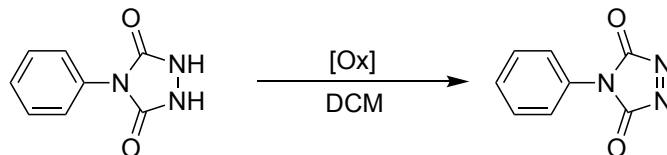
SCHEME 28 - SYNTHESIS OF PHENYL URAZOLE

Entry	Substrate	Base	Solvent	Temperature (°C)	Time (h)	Yield %
1	18	NaOH	H <sub>2</sub> O	100	5	35
2	18	KOH	H <sub>2</sub> O	100	3-5	79-98 <sup>a</sup>
3	19	KOH	H <sub>2</sub> O	100	5	-
4	19	NaOEt	EtOH	79	5	<5

TABLE 11 - REACTION CONDITION FOR THE SYNTHESIS OF PHENYL URAZOLE; <sup>A</sup> WORST AND BEST RESULTS ACHIEVED IN OVER 10 REACTIONS

The synthesis of the compound (18), key intermediate for the synthesis of the most studied functionalizer in this project, was performed several times (over 10) with an average yield of 90% just when the cyclization of ethyl-semicarbazate was performed in aqueous solution with KOH as a base; NaOH in fact, allows the formation of the desired urazole but with a significantly lower yield. By changing the leaving group, from ethoxide to tert-butoxide, the behavior is radically different, in this case it is evident how the function of the carbazate substituent is fundamental. A bad leaving group like t-butoxide prevents cyclization. In the case of entry 3 (compound 15), in the normal concentrations at which we operate, the substrate is totally insoluble even in an alkaline aqueous environment, and this completely hinders the reaction. The solubility problem can be overcome by using ethanol as reaction solvent and sodium ethoxide as a base, nevertheless the yield remains low due to the just mentioned reasons.

PhTAD was prepared by oxidizing the corresponding phenyl urazole. As reported in the introduction, this passage is the most chemically critical one, the TAD compounds are in fact sensitive to moisture, to nucleophiles, to heat and, albeit in a limited way, also to light. Different oxidation systems have been tested, as reported in Table 12, which will be analyzed individually in the next paragraph.



Entry	Substrate	Oxidant	Solvent	Time (h)	Yield %
1	20	PhI(OAc) <sub>2</sub>	DCM	0.25	n.d. <sup>a</sup>
2	20	H <sub>3</sub> IO <sub>6</sub> ·H <sub>2</sub> O / Kbr	DCM	0.5	69
3	20	Ca(OCl) <sub>2</sub>	DCM	0.5	40
4	20	NaNO <sub>2</sub>	DCM	2	52-88

TABLE 12 - REACTION CONDITIONS FOR THE OXIDATION OF PHENYLURAZOLE TO THE CORRESPONDING PhTAD; <sup>a</sup> N.D. NON DETERMINATED - THE REACTION TOOKS PLACE BUT IT WAS NOT POSSIBLE TO ISOLATE THE PRODUCT DUE TO THE IMPURITIES PRESENT IN THE REACTION MIXTURE.

The common denominator of these oxidation systems inspired by the literature is that, despite the attention we used during the synthesis and purification phases, in our hands the yield has always

been lower than reported. Nonetheless, all these methods represent a viable alternative for the oxidation of urazoles.

### 3.3.1 *OXIDATION WITH HYPERVALENT IODINE:*

#### • **Oxidation with PIDA**

The first tested reaction, i.e. the one with  $\text{PhI}(\text{OAc})_2$ , is also one of the simplest from the operational point of view.<sup>52</sup> It consists in simply suspending the substrate in DCM (Phenyl urazole is insoluble in the solvent) and adding the oxidant in an equimolar ratio, under vigorous magnetic stirring. Almost instantaneously the appearance of the reaction mixture moves from a white-milky suspension to a clear solution with an intense red color. Within 15 minutes after the addition of the oxidant, it is no longer possible to trace particulates, a sign that the starting urazole has been completely transformed into the expected product. The main problems related to this type of reaction are due to the by-products that are created by the reduction of PIDA: an equivalent of Iodobenzene and two equivalents of acetic acid. Iodobenzene is a high-boiling liquid (188 °C) which cannot be removed from the reaction mixture except by chromatographic column, which is not applicable for TAD purification. Moreover, acetic acid, if left in contact with the functionalizer, is able to deteriorate it, which prevents the possibility of storing it. This type of reactivity is therefore extremely reliable, but it does not allow to isolate and therefore characterize the oxidation product, restricting its application field to in-situ applications.

#### • **Oxidation with periodic acid ( $\text{H}_5\text{IO}_6 \cdot \text{H}_2\text{O}$ )**

Inspired by a procedure found in the literature,<sup>136</sup> a second type of hypervalent iodine containing oxidizer was tested. Also in this case, the reaction took place in heterophase by putting in suspension the substrate with two equivalents of periodic acid in the presence of 0.2 eq of KBr and a catalytic amount of water. The product was then washed from the salts by extracting the reaction mixture with water. The organic layers were subsequently collected and dried. The isolated product was analyzed by IR spectroscopy and the collected data match with the commercial reference. However the purple color, typical of the PhTAD powder, is darker and, if stored for a few days, the mixture tends to degrade, probably due to iodine impurities that are not eliminated in the purification process. The yield is quite good, however, the choice of this type of oxidation is to be discouraged if we intend to functionalize a polymer, in order to avoid introducing impurities that could bind to the polymer matrix, altering its characteristics.

### 3.3.2 OXIDATION WITH HYPOCHLORITE

- **Oxidation with  $\text{Ca}(\text{OCl})_2$**

Another type of extremely economical oxidizer capable of oxidizing phenyl urazole is calcium hypochlorite. The reaction does not guarantee an exceptional yield (40%) but the procedure is extremely linear. It is in fact sufficient to suspend in DCM the substrate and excess oxidizing powder (2.2 eq) to allow the reaction to proceed. In a short time, the suspension assumes the characteristic pink-red color, but unlike in the case of oxidation with PIDA, it is more complicated to understand exactly when all the reagent is consumed, as it remains suspended with the oxidizing powder. At the end of the reaction, the oxidant (together with possible reagent residues) is removed by filtration and the product is collected from the organic phases after washing it three times with water. Extraction obviously is not the best procedure to undergo the PhTAD, as it risks degrading it, however it is necessary to eliminate the residues of bleach passed in the organic phase.

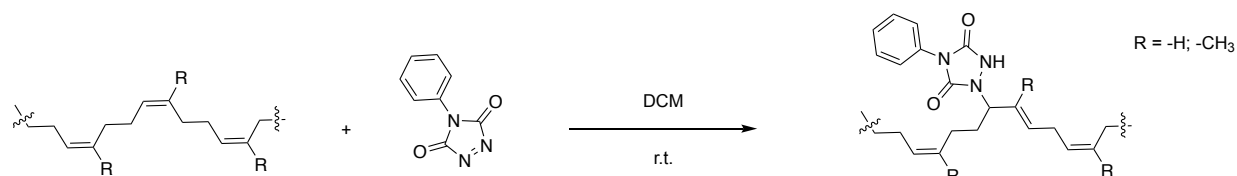
### 3.3.3 OXIDATION WITH NITROGEN(IV)

- **Oxidation with  $\text{NaNO}_2$**

This type of reaction was carried out based on the synthesis procedure proposed by Mallakpour and collaborators.<sup>51</sup> In this case the reaction uses  $\text{N}_2\text{O}_4$  gas as oxidating agent. However, handling an extremely toxic gas like this is difficult, the most convenient alternative is therefore to generate it in situ through an heterogeneous system, by reacting an inorganic salt such as  $\text{NaHSO}_4$  with  $\text{NaNO}_2$  on a 50% w/w wet silica substrate in DCM. According to the authors, the yield should be higher than 95%, however in our hands the results were more modest, around 50% and, after a small optimization of the procedure, we achieved yields of the order of 80%. We have indeed noticed that conducting the reaction in a hermetically sealed vessel, which does not allow the formed gas to escape from the reaction environment, makes it possible to increase yields of 10%. Furthermore, limiting the use of water at 25-30% w/w compared to silica allows to achieve the best yields. The addition of sodium nitrite is made in portions every 30 minutes over a period of 2 hours. At the end of the reaction all non-soluble inorganic salts are filtered, the solvent is removed by cold reduced pressure distillation, and the product can be collected. This method was by far the most used for the oxidation of phenyl urazole to PhTAD, the main functionalizing compound under study for the rheological properties in the mixture. In addition, given the storage difficulties, the PhTAD used for the functionalization of the compounds was freshly produced every time a batch of polymer was prepared.

### 3.4 POLYMERS BACKBONE FUNCTIONALIZATION WITH PhTAD

Not having a solid background neither with the chemistry of TAD, nor with the functionalization of polymers, after having synthesized the PhTAD, the starting point was to try to make it react with different polymers to understand if the use of this compound could be simple and advantageous as described in the literature (Scheme 29).



SCHEME 29 - FUNCTIONALIZATION OF PB WITH PhTAD

The first functionalized polymer (Table 14 entry 1) was the Polyvest, our model system, with a molar ratio between double bonds of the PB and PhTAD of 100:1, or seen in other terms, with a 1:1 ratio compared to vinyls present in the chain. After dissolving the polymer and the PhTAD in DCM, the two solutions are mixed and immediately the purple color, typical of the functionalizing, vanishes, sign of the addition to the double bonds of the polymer matrix. All this happens in air, at room temperature and in a really short time. From this simple experiment it is possible to find different unique characteristics of this type of reactivity. In fact, in a <sup>1</sup>H-NMR spectroscopic analysis it is possible to notice how the conversion is total and does not involve the double bonds of the vinyl type. The two protons of the vinyl double bonds (c), which have a characteristic chemical shift at 5 ppm, are in fact unaltered with respect to the pristine polymer. Furthermore, it can be seen how the phenyl ring signals of PhTAD (d, 7.37-7.52 ppm) are comparable in intensity to the signals of vinyl bonds, as imposed by the quantities of functionalizer added at the beginning of the reaction (Figure 18).

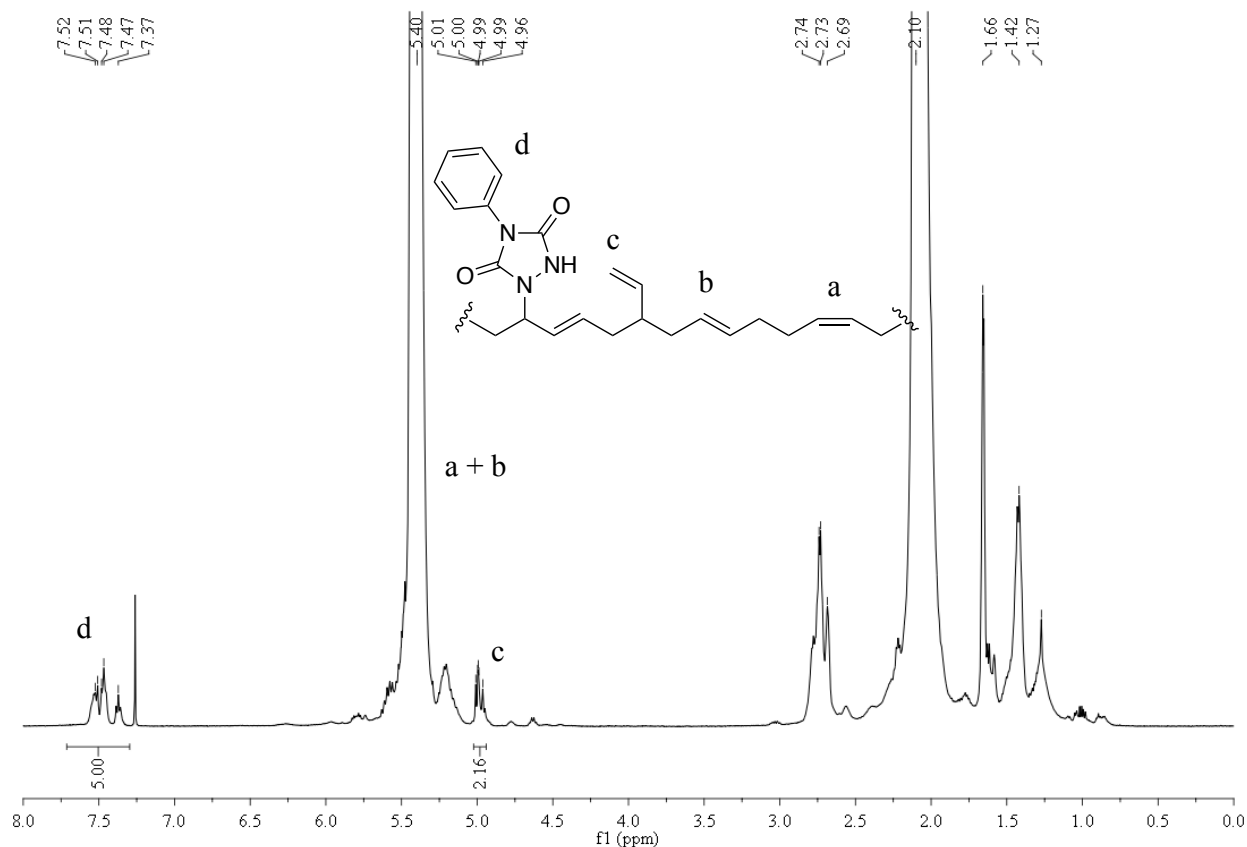


FIGURE 18 - NMR SPECTRA OF FUNCTIONALIZED POLYVEST WITH PHTAD

This is known in the literature,<sup>137,138,139,140</sup> where the scale of reactivity of the TAD indicates that which the kinetic of addition to the internal double bonds of the cis type is 6 times faster than to the trans type and, above all, 90 times faster to vinyl terminal ones (Table 13).

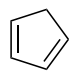
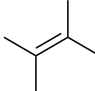
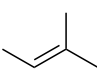
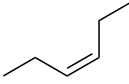
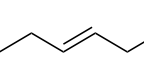
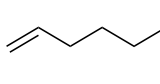

Substrate							
$K_2$ ( $M^{-1}s^{-1}$ )	160000	333	6.5	0.89	0.15	0.01	0.0007

TABLE 13 - KINETIC CONSTANT OF ADDITION OF PHTAD ON DOUBLE BONDS

Once it was verified that the addition ran as expected with the model oligomer, we tested the system on a high molecular weight high-cis polybutadiene, the BR40 Neocis, used by the industry in the formulation of the Table 14 entry 2 compounds.

In this case the PB solubility is an obstacle to a characterization by NMR spectroscopy in solution, however a valid alternative is offered by the observation of the reaction itself and by FTIR

spectroscopy. For this product, the signal that confirms the successful functionalization is the stretching of the carbonyl groups to  $1703\text{ cm}^{-1}$  (Figure 19).

Entry	Polymer	Styrene (%wt)	PB cis/trans (%mol)	PB Vinyl (%mol)	PhTAD:PB double bond ratio
1	Polyvest	0	99	1	0.01
2	BR40 - Neocis	0	97 cis	0.1<	0.01
3	S-SBR 17272	26	76	24	0.01

TABLE 14 - FUNCTIONALIZATION OF DIFFERENT POLYMERIC SUBSTRATES WITH PHTAD

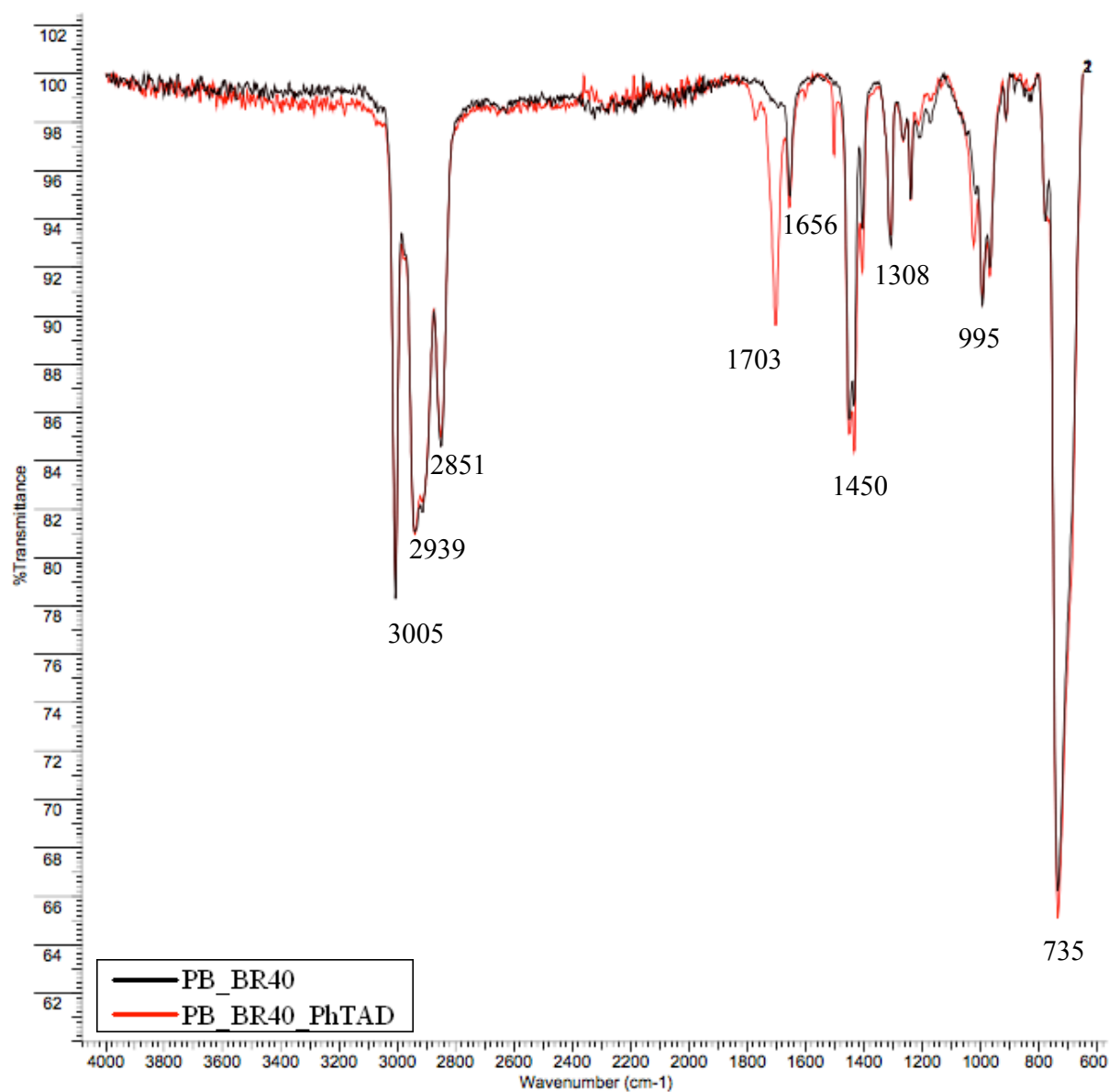


FIGURE 19 - FTIR SPECTRA OF FUNCTIONALIZED PB WITH PH TAD

Since the part of the polymer involved in the aza-ene reaction is always the butadiene portion, the styrene-polybutadiene copolymers are also a substrate that can be used for this type of reaction. Nevertheless, for confirmation, the addition of the PhTAD functionalizer to an S-SBR has been attempted, specifically the commercial copolymer S-17272, in which 26% w/w consists of styrenic units and the remaining part of PB, whose microstructure consists of 24% of vinyls (Table 14 entry 3). Even if with some difficulties, in this case it was possible to carry out both an NMR and FTIR analysis of the addition product. The first shows the appearance of the phenyl ring signals present on the functional group (red line, 7.46 ppm), in the second we find the peak associated with the vibrational modes of the carbonyl groups ( $1702\text{ cm}^{-1}$ ) (Figure 20).

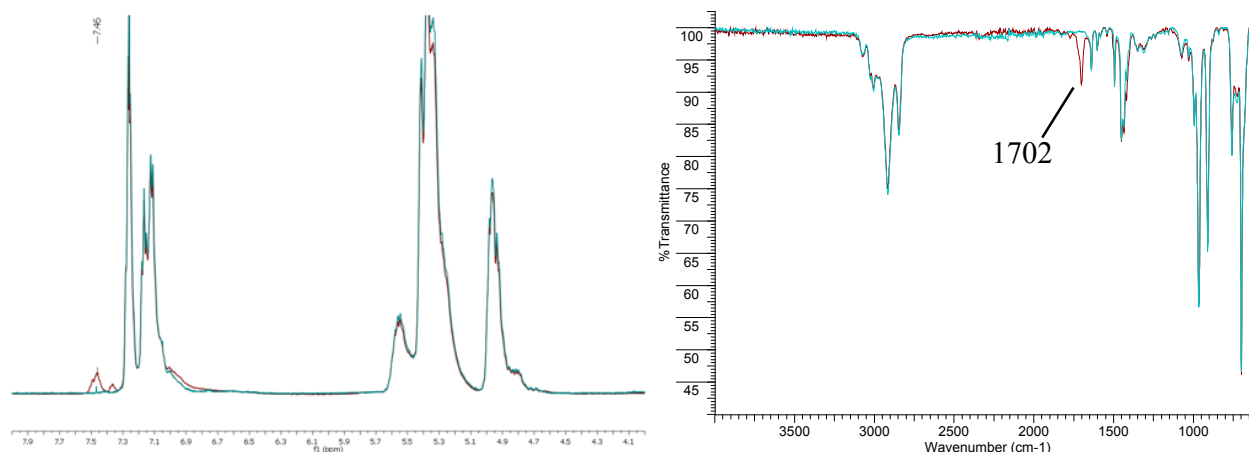


FIGURE 20 -  $^1\text{H-NMR}$  SPECTRA (LEFT) AND FTIR SPECTRA (RIGHT) OF SBR COPOLYMER FUNCTIONALIZED WITH PHTAD

Although an absolute quantification of the reaction yield is not possible, the disappearance of the starting reagent, along with the spectroscopic characterization performed, allow to state that, for low PhTAD concentrations ( $< 1\text{ phr}$ ), the overall yield is over 95%, in agreement with data reported in the literature.<sup>37,84</sup>

### 3.4.1 SCALE UP

After becoming familiar with model systems and having tested the effectiveness of functionalization, we began to scale up the reactions, starting from synthesizing an amount of polymer sufficient for the compound test. Treating a minimum of 40 grams (up to 120 g) of rubber at a time is not trivial at all, because it is not possible to achieve a sufficiently high dilution without using an excessive amount of solvent. This means that the high viscosity of the system must be remedied by means of an agitation method of the solution capable of providing enough shear force to the system to homogenize it properly. The developed synthetic protocol provided a polymer concentration in the reaction solvent of about 40 mg/mL, inside a 3 L sized reactor, stirred with a mechanical rotor-stator system. The polymer, to be dissolved in the reaction solvent (DCM) within a reasonable time, must be crumbled into small pieces, about 5 mm<sup>3</sup> in size. Nevertheless, even in this way, a complete dissolution of the polymer takes 4 to 8 hours, which makes the whole procedure very time-consuming.

Once the polymer is dissolved, at the same time, the functionalizer is prepared and dripped into the reaction mixture over a period of 15 minutes. As the PhTAD is added to the reaction, the solution moves to the typical red color that distinguishes the TADs, followed by a quick bleaching (less than an hour), passing through a soft pink to a yellowish color at the end of the reaction. The polymer is then left under stirring for 3 hours more, to guarantee complete conversion of the initial reagent. At the end of the reaction the polymer must be recovered, but also the purification cannot be carried out in the same way if it is carried out on a laboratory scale or on a large scale. Given the total conversion of the reagents and the extremely high efficiency of the addition reaction, the first idea was to remove the solvent simply by evaporating it under reduced pressure. However, at those concentrations, a long chain polymer with polar functional groups therein behaves like a non-ionic surfactant, making the procedure extremely difficult. To recover (and at the same time purify) the polymer successfully, a more classical approach to the handling of polymers has been used: the use of a solvent non-solvent that can precipitate it. Specifically, methanol is the most commonly used solvent for this purpose and, for optimal results, a volume 2 to 10 times greater than the solvent in which the polymer is dissolved should be used. This would have involved the use of huge quantities of solvents and, of course, the production of an identical amount of chemical waste to dispose of. Not having at our disposal neither these volumes of solvent, nor equipment to treat it, also to meet the needs of the company with regard to toxicity, a procedure that involved the use of only 500 - 700 ml of EtOH has been developed.

In a 2 L flask containing 500 mL of EtOH, 700 mL of initial solution was poured; the flask was then placed under stirring in vacuo. Proceeding with this approach, ethanol alters the surface tension of the polymer solution in DCM, allowing the chlorinated solvent to leave the reaction environment without foaming. As the evaporation proceeds, the polymer concentrates and precipitates into alcohol. Once the DCM has been removed, it is possible to recover the polymer and add another aliquot of starting solution, until the complete purification of the product. The recovered functionalized polymer will still contain part of the reaction solvent inside. The next step is to place the rubber mass in a beaker with fresh ethanol ( $\approx$  200 mL) and let it stand overnight, allowing the polymer to release the incorporated DCM by diffusion. The next day the residue is filtered and dried in a vacuum oven heated to 40 °C for at least 12 hours.

This protocol was specifically designed for a seminal approach. In order to verify the feasibility on a technologically relevant scale, albeit on prototype stage, we opted for a procedure that requires the use of a massive amount of toxic solvents (such as DCM). From a corporate point of view, while not representing an insurmountable problem, this can hinder the future development of this technology. This issue could be overcome by functionalizing the polymer immediately after its synthesis, when it is still dissolved in the reaction solvent (typically cyclohexane) or, in the best case scenario, avoiding the constraint of functionalization in a solvent medium, achieving a functionalization on the polymer matrix in bulk, during the compounding phase. The procedure just described was the method of choice used for the functionalization of PB BR40 (or, since it went out of production, its counterpart CB25 with the same characteristics) and isoprene SKI3 produced (Table 15).

<b>Entry</b>	<b>Polymer</b>	<b>PhTAD (phr)</b>
1	BR40	0.3
2	BR40	0.5
3	BR40	1.5
4	BR40	3
5	BR40	5
6	CB25	0.5
7	CB25	0.75
8	CB25	1.2
9	IR SKY3	0.5
10	IR SKY3	2

11	IR SKY3	5
----	---------	---

TABLE 15 - FUNCTIONALIZED POLYMER MATRIX FOR TIRE COMPOUNDING APPLICATION

Although, up to now, the description of the stoichiometric ratios between reagents or, in this case, between the functionalizing agent and the polymer has been expressed in moles, conventional measurement unit in the chemical field, from this moment the amount of functionalizer will be compared to the polymer using phr as a unit of measurement, for a more comfortable and homogenous treatment with the language used in the description of compounding and formulation process.

In particular, for PB, we should considered that 1 phr of PhTAD corresponds to a stoichiometric ratio of 324:1 between double bonds and functionalizing agent.

The synthesized polymeric matrices were then analyzed with different basic techniques, to evaluate the impact of functionalization on the chemical-physical properties on the polymer.

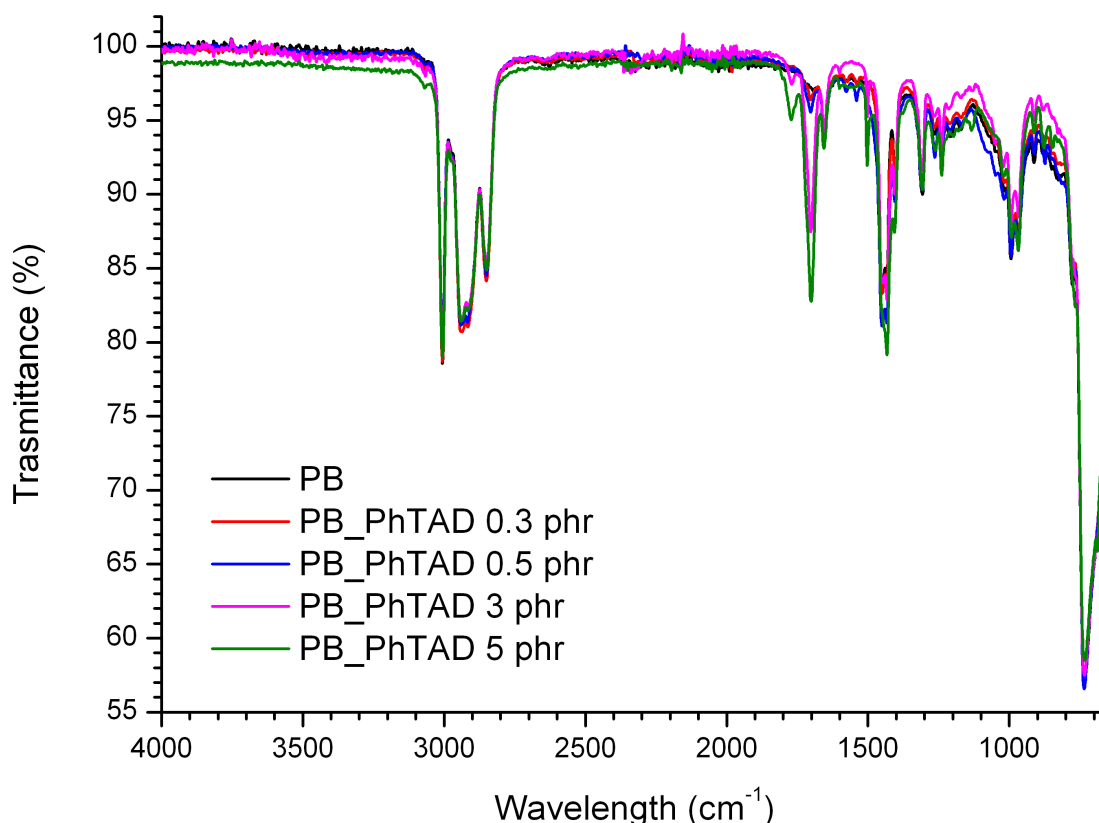


FIGURE 21 - FTIR SPECTRA OF PB FUNCTIONALIZED WITH AN INCREASING AMOUNT OF PHTAD

First, through an FTIR analysis it was possible to verify the effective functionalization (Figure 21, 22). Considering the peak related to the stretching of the carbonyl group ( $\approx 1700\text{ cm}^{-1}$ ), it is possible to see how the transmittance value faithfully reflects the degree of functionalization inserted, a sign

that the reaction is not influenced, in the studied range, by the quantity of functionalizer added. Moreover, for the most concentrated samples, it is also possible to identify the rising of a weak peak at  $1500\text{ cm}^{-1}$ , attributable to the bending of the N-H bond that is formed following the reduction of the functionalizer from PhTAD to urazole.

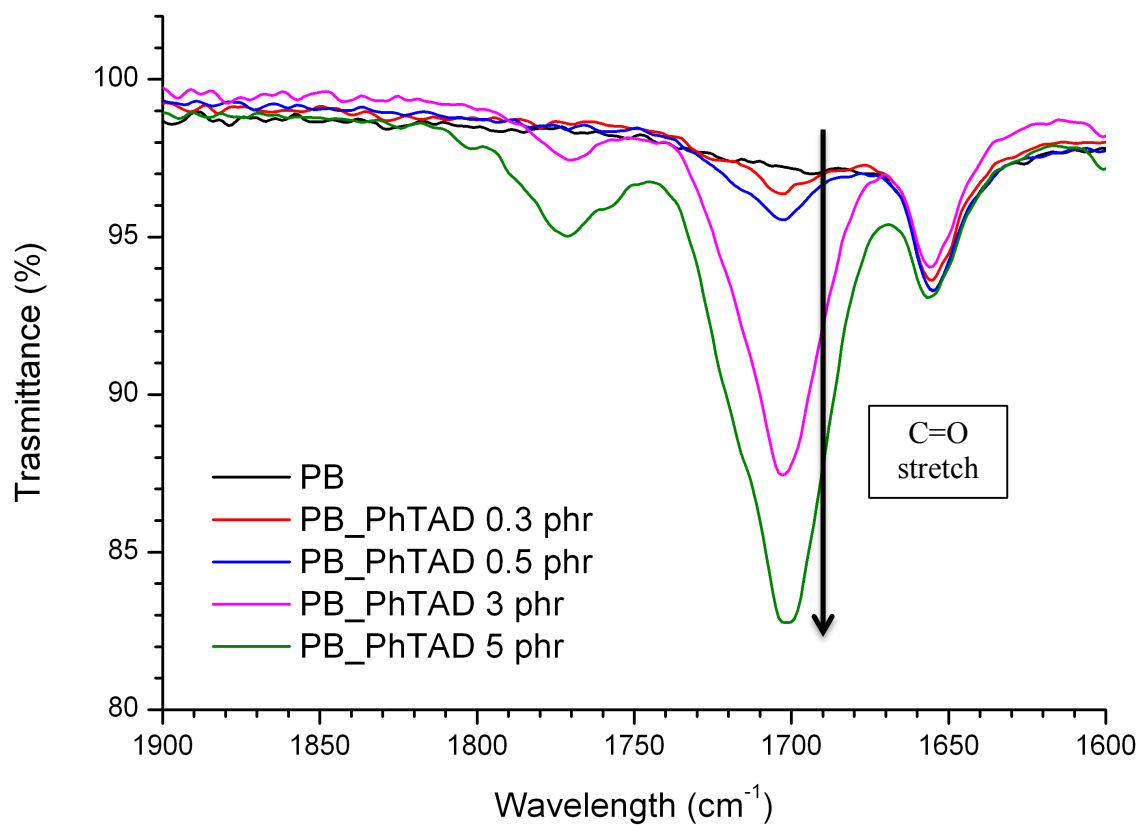


FIGURE 22 - EXPANSION OF THE FTIR SPECTRA CENTERED ON THE CARBONYL VIBRATIONAL MODE

### 3.4.2 POLYBUTADIENE FUNCTIONALIZATION

By observing the polymer recovered from the reaction as the quantity of functionalizer increases, it is possible to notice how it seems to be more and more stiff, compact, spongy and way lot less sticky. Usually such variations of the physical characteristics of the polymer just described are indices of an increase of the glass transition temperature ( $T_g$ ). However, as can be inferred from the data shown in table 16, the difference in values between pristine and functionalized polymer is too small to justify such a different appearance and behavior.

Entry	1	2	3	4	5	6	7
Polymer	BR40	BR40	BR40	CB25	CB25	CB25	CB25
PhTAD phr	0	0.5	5	0	0.5	0.75	1.2
$T_g$ (°C)	-107.9	-106.8	-101.7	-105.4	-104.3	-105.0	-103.9

TABLE 16 - GLASS TRANSITION TEMPERATURE OF DIFFERENT FUNCTIONALIZED PB

Not being able to analyze each single sample produced, the choice of the samples to be analyzed was made with the intent of underlining as much as possible the differences between the samples. The value that most deviates from the non-functionalized polymer data is the most functionalized one (5 phr, table 16 entry 3), recording an increase of 6 °C when compared to the initial  $T_g$ . Except for some small fluctuations, it is evident that the introduction of PhTAD into the rubber matrix shifts the glass transition temperature to higher values, which indicates that the polymer chains are less mobile. The cause of this behavior can be ascribed to the phenomenon already observed by Freitas and coworkers.<sup>88,89</sup> They stated that, if the amount of TAD exceeds 0.5% mol (corresponding to 1.7 phr), recognition and self-aggregation phenomena occur between the amine groups and the carbonyl groups of the functionalizer, as shown in figure 23.

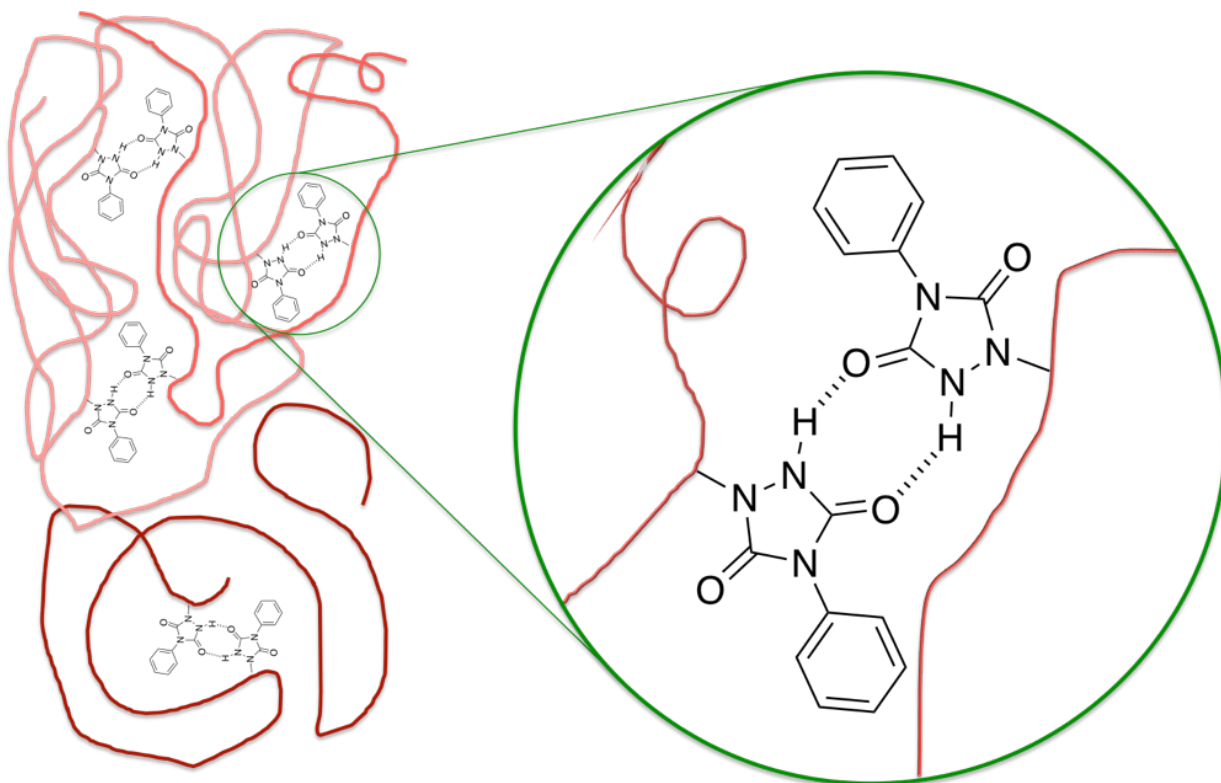


FIGURE 23 - ILLUSTRATION OF RECOGNITION AND INTERCHAIN AGGREGATION PHENOMENA

However, in our case it seems evident that already with a ratio of 0.5 phr this type of phenomenon happens, altering in a significant way the initial properties of the rubber. Continuing in the characterization of the thermal properties of the polymers through the use of calorimetric techniques and plotting the thermograms in a graph, we can see an endothermic peak at temperatures close to 0 °C, due to the melting of the microcrystalline phase of the PB. Contrary to the behavior of  $T_g$ , the melting peak moves in the opposite direction, towards lower temperatures, as the degree of functionalization of the rubber increases (Figure 24).

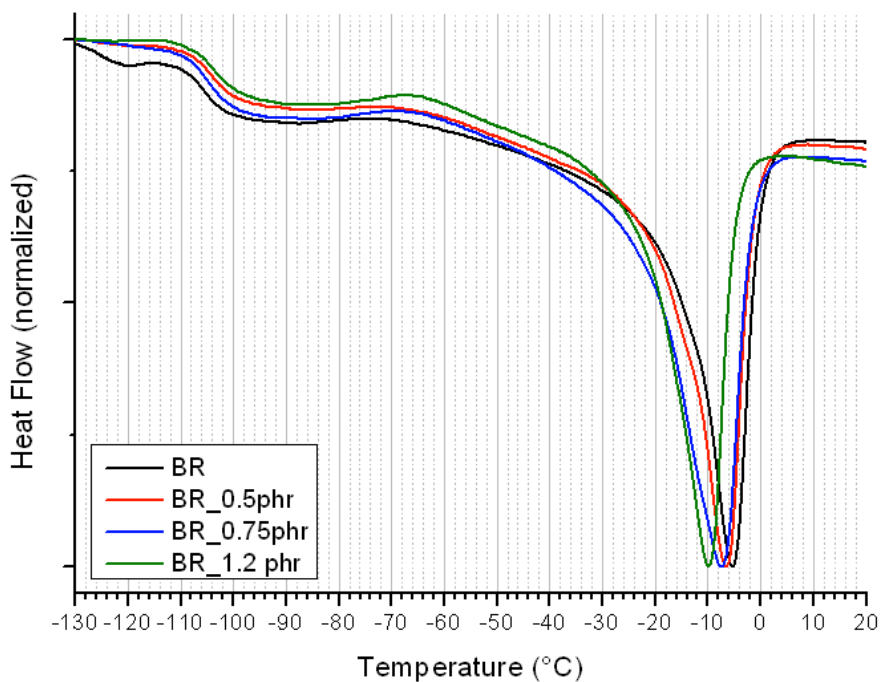


FIGURE 24 - THERMOGRAMS OF FUNCTIONALIZED PB SAMPLES

This is consistent with what has been described, in fact, the introduction of a functional group able to shift a double bond in the alpha position could interfere with crystallization phenomena among the polymer chains, which lowers the energy necessary to melt the crystalline domains (Table 17).

Entry	4	5	6	7
Polymer	CB25	CB25	CB25	CB25
PhTAD phr	0	0.5	0.75	1.2
T <sub>m</sub> (°C)	-9.9	-7.5	-6.6	-5.3

TABLE 17 - T<sub>M</sub> PEAKS OF FUNCTIONALIZED PB

Butler, in the course of his studies, has also investigated the thermal stability of adducts, although on samples with a way higher functionalization degree, concluding that they remained stable up to temperatures around 200 °C, and then decomposed. However, in order to subsequently use them in the mixture, it was decided to test their stability through a thermogravimetric analysis.

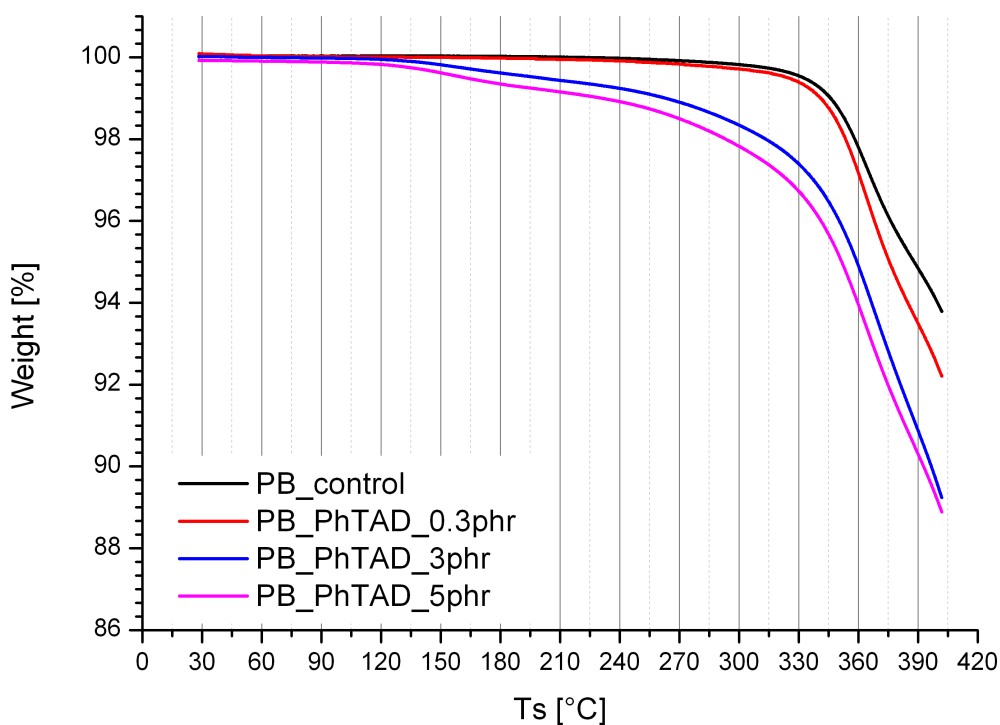


FIGURE 25 - THERMOGRAVIMETRICAL ANALYSIS OF FUNCTIONALIZED PB

Sample	PB_BR40 Control	PB_PhTAD 0.3 phr	PB_PhTAD 3 phr	PB_PhTAD 5 phr
Weight Loss (%) @140°C	0	-0.01	-0.12	-0.29
Weight Loss (%) @170°C	0	-0.03	-0.32	-0.57
Temperature (°C)	350	301	338	351
Weight Loss (%)	-1.2	-0.3	-3	-5

TABLE 18 - WEIGHT LOSS AT DIFFERENT TEMPERATURES OF FUNCTIONALIZED PB SAMPLES

Table 18 shows the data related to the thermograms shown in the graph (figure 25). It can be noted that up to 140 °C (temperature at which the mixing phase is commonly performed) there is no significant weight variation in the samples analyzed. Going up to 170 °C (maximum temperature to which the compounds are exposed during vulcanization phase), a very low weight loss is detectable. Even if it was completely caused by a detachment of the urazole from the polymer matrix, it would be less than 10% compared to the amount of functionalizer introduced. To achieve a weight loss equal to the percentage of PhTAD it is necessary to go much further with the temperature, over 300

°C, however, at those temperatures, other competitive degradation phenomena take place, with a significant weight loss (-1.2% for the control polymer).

Weight loss accounts for possible detachment of the adduct, but if chemical changes occur within the system, which do not involve weight loss, it would be impossible, only with the use of calorimetric techniques, to assert that these compounds are stable after an exposition to high temperatures, an essential factor for their subsequent use in a compound. To dispel any doubt, a combined approach was adopted: a Polyvest sample was initially functionalized with 2 phr of PhTAD, and, after a purification step by ethanol precipitation, both FTIR and <sup>1</sup>H-NMR spectra were recorded. The sample was then subjected to a thermal treatment (Figure 26) that simulated both temperatures and process times of a mixing process. The thermal ramp set by the experiment is shown in blue while the red line is the actual temperature reached by the sample. At the end of the test, the polymer was recovered and spectroscopic analyzes were performed again. During the thermal treatment, the compound lost less than 0.5% of its weight (green line), and this is due to the evaporation of ethanol trapped between the polymer chains, as easily deduced from the comparative analysis of the NMR spectra, in which peaks at 1.25 ppm and 3.72 ppm are missing (Figure 27).

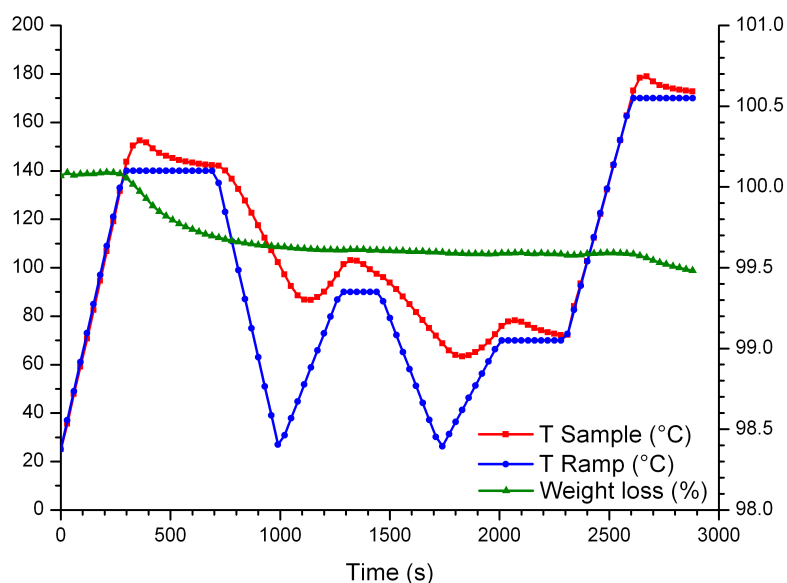


FIGURE 26 - THERMAL TREATMENT OF FUNCTIONALIZED PB OLIGOMER WITH 2 PHR OF PHTAD; SAMPLE TEMPERATURE (RED LINE), RAMP TEMPERATURE (BLUE LINE) AND WEIGHT LOSS (GREEN LINE) ARE PLOTTED AS FUNCTION OF TIME.

On the contrary, the position of the peaks and the ratios between the integrals of the characteristic signals of PhTAD are unchanged, which proves, beyond any reasonable doubt, that this system is stable enough to be tested in a compound.

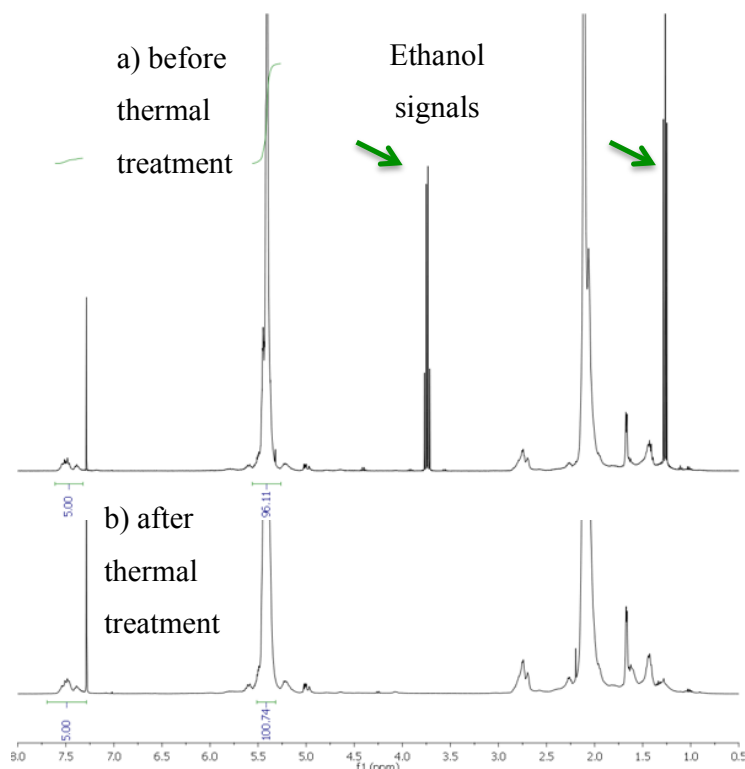


FIGURE 27 - <sup>1</sup>H-NMR SPECTRA OF FUNCTIONALIZED PB OLIGOMER BEFORE (A) AND AFTER (B) THERMAL TREATMENT.

After examining the issue concerning the thermal stability of the system, we focused on the study of mechanical properties. Specifically, we tried to better understand the impact that the formation of hydrogen bonds has on the rheological properties of the polymer matrix. The rubber samples were then evaluated with an Oscillating Disk Rheometer (ODR) operating in shear mode at different temperatures and through swelling tests (Table 19). For the experimental details of these tests, see the dedicated section in the appendix, however the results confirm the observations made on the polymer recovered after the reaction.

Sample	Q (%)	q	f (%)
BR40	SOLUBLE		
BR_PhTAD_0.3 phr	SOLUBLE		
BR_PhTAD_0.5 phr	2760	40	42
BR_PhTAD_3 phr	410	6	11
BR_PhTAD_5 phr	440	6	18

TABLE 19 - SWELLING TEST OF FUNCTIONALIZED PB SAMPLES

The non-functionalized control sample dissolved completely in the solvent (Toluene) used for the analysis, as was expected, in less than 12 hours; a sample functionalized with 0.3 phr of PhTAD was also totally soluble but it took 24 hours. A significant difference was found in the functionalized samples with an amount of PhTAD equal or greater than 0.5 phr. In the case of 0.5 phr, the sample reached a swelling ratio (Q) of over 2500%, i.e. it incorporated a quantity (in weight) of solvent of 27 times its initial weight, with an extractable fraction (f), that is the weight loss of the sample given by the removal of the unbounded polymer chains, of 42%. Samples with a functionalization level of 3 and 5 phr provide a very similar response, with values of Q ranging from 410 to 440% and f between 11 and 18%. The main difference between the two systems is the solvent uptake speed: in the case of the PB\_3phr already after 24 h it had reached an equilibrium situation around 400%, while the sample functionalized with 5 phr reached the maximum swelling ratio after 76 h. These data are quite surprising also as absolute values, since they are very similar to the common values found in sulfur vulcanized PB compounds.<sup>141</sup>

These data indicates that, due to functionalization, a solid polymeric network is formed, whose characteristics recall those of a cured compound. In this case, however, the driving force that governs the process was the hydrogen bonds interaction. To have a proof of the strength of these bonds, rheological properties were tested with an ODR. The instrument probe is a cone-shaped disk, embedded in the rubber sample. The probe oscillates with a small angle while the specimen is heated under pressure. With this system both G' (stored modulus) and G'' (loss modulus) can be measured as a function of the strain set by the user.

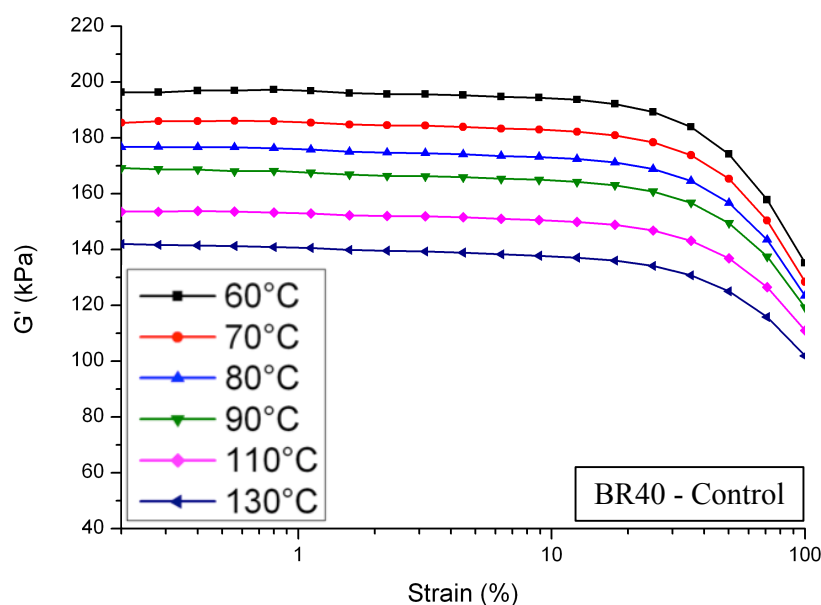


FIGURE 28 - STRAIN SWEEP TEST AT DIFFERENT TEMPERATURE OF NON-FUNCTIONALIZED PB

First of all a non-functionalized sample was tested as a reference (Figure 28), the experiment consists of a series of strain sweep measurements at different temperatures (from 60 °C to 130 °C), observing the  $G'$  progression in function of the strain, in a range between 0 and 100%. It is evident that as the temperature increases, there is a corresponding reduction in the storage modulus, as an effect of the increased mobility of the polymer chains.

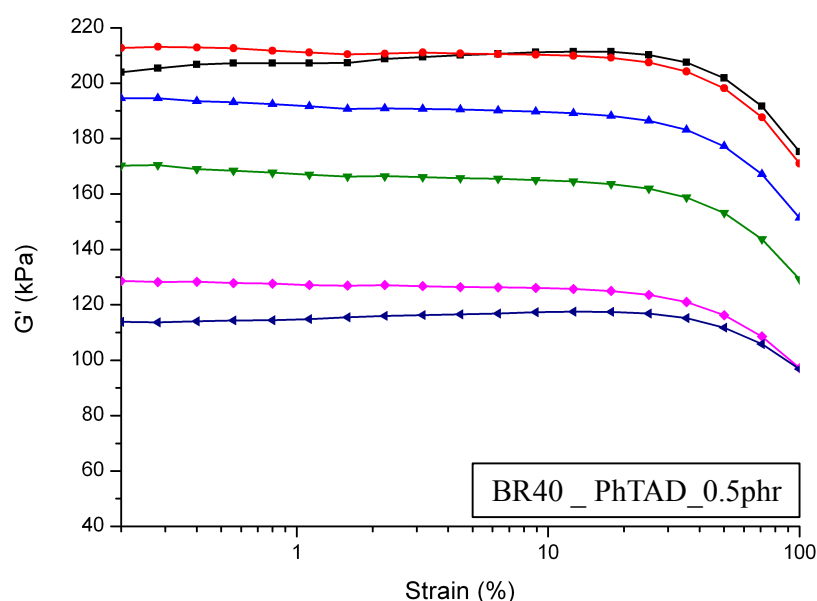


FIGURE 29 - STRAIN SWEEP MEASUREMENT OF 0.5 PHR FUNCTIONALIZED PB SAMPLE AT DIFFERENT TEMPERATURES

By replicating the same experiment on the functionalized PB 0.5phr (Figure 29), it was possible to observe various interesting behaviors. First of all, it is possible to notice how the absolute value of  $G'$  does not deviate much from the non-functionalized homologue, but its evolution with temperature variations is not trivial. The  $G'$  curve varies very little from 60 (black line) to 70 °C (red line), a sign that the urazole molecules are still able to bind together via hydrogen bonds. By increasing the temperature up to 90 °C (green line), we are providing energy to the system which responds becoming softer in a similar way to what we saw for the pristine BR40. However at 110 °C (pink line) the value suddenly collapses and then stabilizes: this can be explained by the breaking of the previously formed hydrogen bonds.

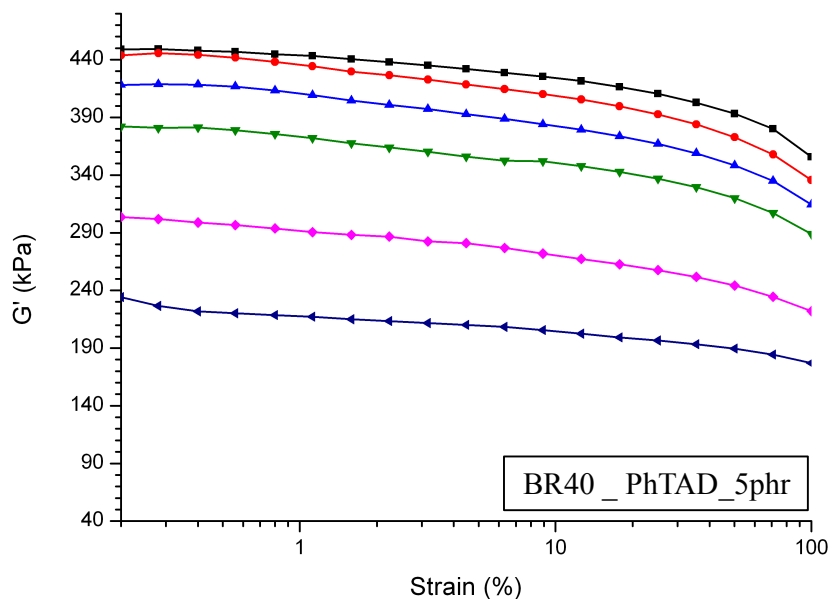


FIGURE 30 - STRAIN SWEEP MEASUREMENT ON A FUNCTIONALIZED PB WITH 5 PHR OF PHTAD

With the same experimental setup, the sample of BR40 functionalized with 5 phr of PhTAD was tested. As can be seen from the graphs shown in the Figure 30, its behavior is more accentuated as absolute values but identical as general trend. Starting from an initial value of  $G'$  two times higher compared to the BR\_PhTAD\_0.5phr, even in this case up to 90 °C the decrease in the value of  $G'$  is constant but contained, till the drastic drop above 110 °C. It should be noted, however, that the minimum value reached at 130 °C is comparable to the curves recorded at 60-70 °C of the sample at 0.5 phr. Probably this is due to a partial break of the hydrogen bonds formed during the synthesis.

In order to better evaluate the trend of  $G'$  values as the temperature varies, it is possible to process the previously proposed spectra with a small mathematical cosmetic. As can be seen in the figure below (31.a), setting a deformation (9% of strain in this example) and reporting the  $G'$  data at the tested temperatures, the plot referred to the pristine PB shows a linear decrease, as opposed to the functionalized samples which present a step. This is even more evident if we look at the graph of the first derivative (figure 31.b) calculated starting from this data. The minima of the function correspond to the temperature at which the breaking of the largest number of hydrogen bonds present in the functionalized polymer matrix occurs. The minimum varies its position based on the amount of functionalizing agent present, however we can see how the temperature range affected by this phenomenon is between 80 °C and 110 °C.

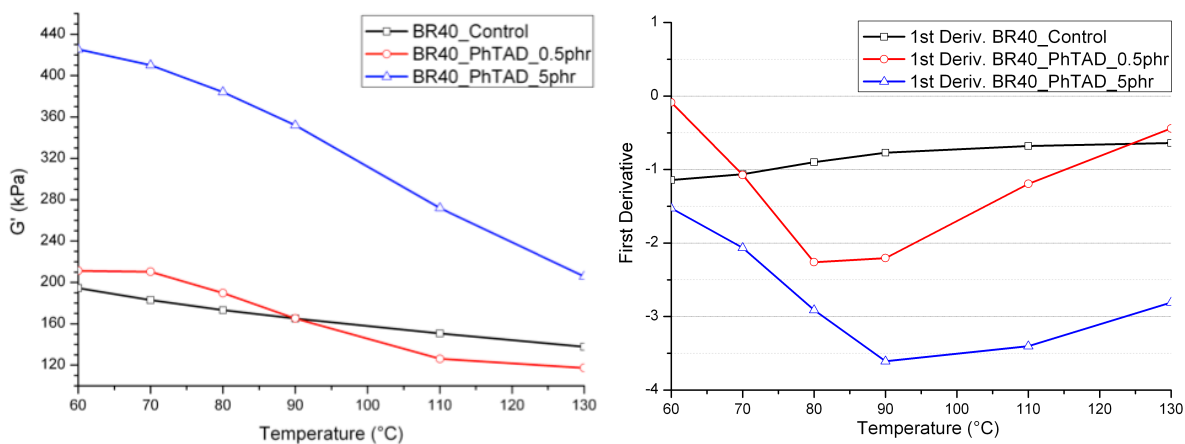


FIGURE 31- A)  $G'$  VALUES IN FUNCTION OF THE TEMPERATURE; B) FIRST DERIVATIVE PLOT

In addition to the  $G'$ , there is another experimental data able to corroborate the hypothesis of an effective crosslink given by the cumulative effect of weak interactions, in accordance with what has already been observed through the swelling tests. We are referring to the values of the  $\tan\delta$  of the various samples analyzed (Figure 32).

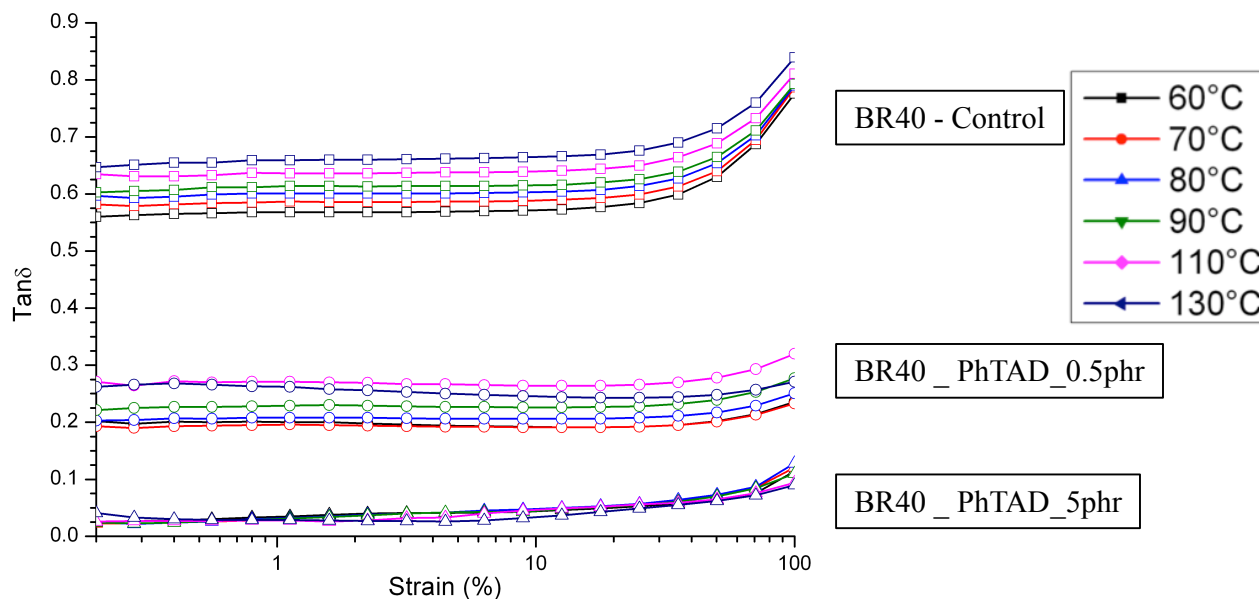


FIGURE 32 - COMPARISON BETWEEN  $\tan\delta$  AT DIFFERENT TEMPERATURE AND DEGREE OF FUNCTIONALIZATION

We can see how, increasing the degree of functionalization, the mean value of  $\tan\delta$  drastically decreases and at the same time the effect of temperature is less and less pronounced. A decrease in the  $\tan\delta$  is certainly a desirable feature in a compound for applications in the automotive sector as it

accounts for the hysteretic behavior of the compound and it is directly related to the rolling resistance of the final product, with obvious benefits in terms of fuel consumption and tire wear.

### 3.4.3 *POLYISOPRENE FUNCTIONALIZATION*

An entirely different story is the functionalization of isoprene rubber (IR). Although in literature Butler and co-workers have reported the possibility of functionalizing this polymer matrix, without particular issues, in our experience the process of functionalization produced unexpected results, extremely impacting on the rheological properties of the polymer. First of all, the morphological differences between PB and IR have to be considered. In the case of the high cis PB (BR40 / CB25), taking into account the small amount of 1,4 trans and 1,2 vinylic double bonds present, combined with their low reactivity (table 13), we can firstly state that the functionalization through PhTAD occurs almost exclusively on cis-type bonds. The possibility of coupling with this system is therefore only one, since the two positions, from which the functionalizer could tear off an hydrogen atom, are statistically and energetically equivalent. Conversely, if we look at the IR structure (Figure 33), even considering only 1,4 cis- units, we can see how the PhTAD can take the needed proton from different points of the chain, forming different isomers. Moreover, we should also add all the other possible isoprenic units present in the chain the PhTAD could react with. In fact, if the 1,2 units are not reactive to the addition of the functionalizer, since they have not an allylic hydrogen, and the 1,4 trans units have a slower kinetics, we cannot neglect the possibility of coupling with 3,4 isomers. It is even much more reactive, going to expose off-chain functionalization and statistically presenting more allyl hydrogens to which the PhTAD could get, with a subsequent rearrangement of the structure to a tetra-substituted double bond. The heterogeneity that is induced in the system will therefore have an impact on the properties of intra- and inter-chain aggregation, altering significantly the behavior of the functionalized polymer from pristine one (Figure 33).

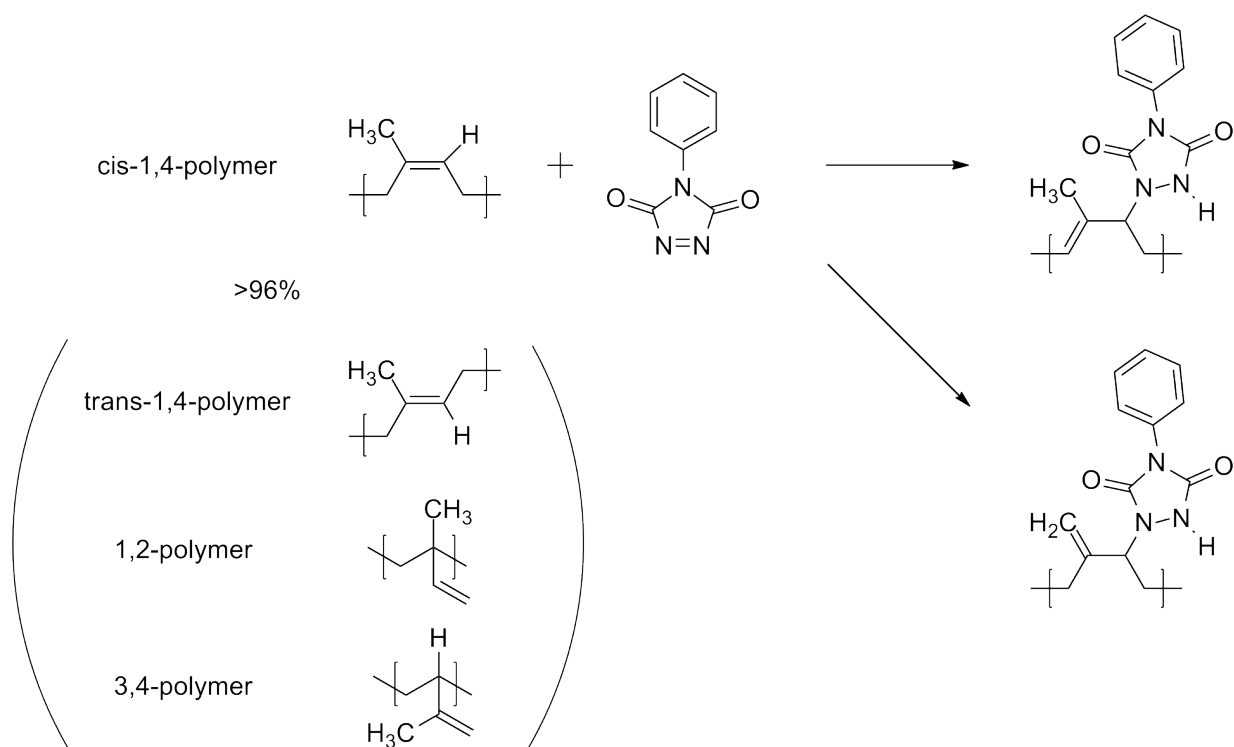


FIGURE 33 - ISOPRENE RUBBER MICROSTRUCTURE AND POSSIBLE WAYS OF FUNCTIONALIZATION WITH PhTAD

With this assumption, three batches of isoprene were then prepared with an increasing amount of PhTAD, as reported in table 20.

Entry	Polymer	PhTAD (phr)
1	IR SKI3	0
2	IR SKI3	0.5*
3	IR SKI3	2
4	IR SKI3	5

TABLE 20 - SYNTHESIZED BATCH OF IR RUBBER WITH AN INCREASING AMOUNT OF PhTAD.  
\*POLYMER USED AS RECEIVED, WITHOUT ANY FURTHER PURIFICATION

The SKI 3 isoprene polymer is a synthetic commercial polymer which looks like a dark rubber (Figure 34a) due to the residues of metal catalysts used for its production. In addition, traces of stearic acid may also be present within it. These impurities, theoretically, should not interfere with functionalization reactions, however, given the complexity of data interpretation, it was preferred to remove them when possible, using previously purified rubber by means of a dissolution-precipitation process in ethanol (Figure 34b).



FIGURE 34 - A) SAMPLE OF COMMERCIAL SKI3 IR BEFORE PURIFICATION. B) SAMPLE OF PURIFIED IR.

The problem immediately visible after the functionalization process was the dramatic change in consistency. As the amount of functionalizer added increases, the polymer softens and becomes extremely sticky. For the functionalization with 0.5 phr this phenomenon was limited and it was possible to recover the polymer by precipitation and then use it as a base for the formulation of a compound. The following step was trying to do the same operation with polymers with 2 and 5 phr. However, if in the first case the consistency allowed a minimum workability, in the case of the 5 phr, once precipitated, the polymer was totally impossible to process.

The hypothesis advanced to explain this phenomenon was an oxidative degradation of the polymer triggered by the functionalization process, that led to a depolymerization of the rubber. To study this phenomenon more in detail, several characterizations were performed, starting from a FTIR spectroscopy (Figure 35).

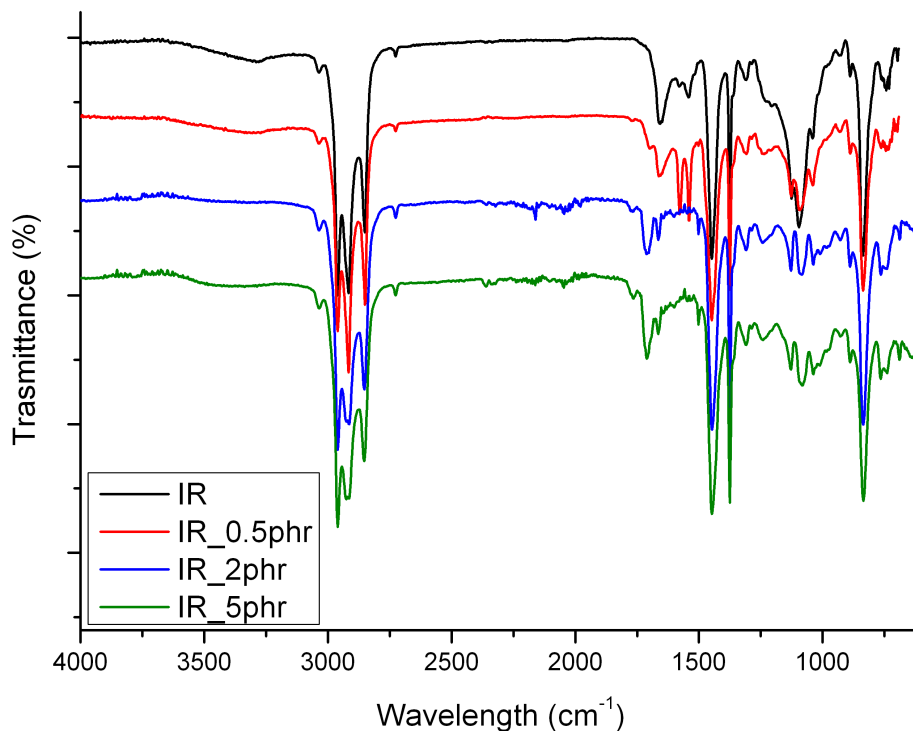


FIGURE 35 - FTIR SPECTRA OF FUNCTIONALIZED ISOPRENE RUBBER. REFERENCE SAMPLE (BLACK LINE), FUNCTIONALIZED ONE WITH 0.5 PHR OF PHTAD (RED LINE), 2 PHR (BLUE LINE) AND 5 PHR (GREEN LINE).

As it can be seen in the graph at the top, similarly to what we have seen with the PB, there are two characteristic carbonyl peaks at 1700 and 1764  $\text{cm}^{-1}$ , in addition to the weak bending peak of the N-H bending at 1500  $\text{cm}^{-1}$  present only in the two highly functionalized samples (blue and green lines). As anticipated in table 20, entry 2, in the FTIR spectrum of the sample at 0.5 phr (red line) two sharp peaks at 1541 and 1579  $\text{cm}^{-1}$  are visible and they can be ascribed to the stearic acid indicated in the supplier's data sheet.

To verify the average chain length, a GPC analysis was performed which showed the following results (Table 21):

Entry	Polymer	PhTAD (phr)	Mw	Mn	D
1	IR SKI3	0	1'490'000	840'900	1.772
2	IR SKI3	0.5*	415'000	172'100	2.412
3	IR SKI3	2	488'700	124'900	3.912

TABLE 21- GPC ANALYSIS RESULTS OF SELECTED SAMPLES OF FUNCTIONALIZED IR

Where  $M_w$  mass-average molar mass,  $M_n$  is the number-average molar mass and D polydispersity, defined as  $M_w/M_n$ .

Although these data seem to indicate that indeed a depolymerization may have occurred, with a reduction in the chain length of a factor 4, compared to similar experimental evidence, Butler provided an entirely different explanation of the phenomenon. He observed that, by functionalizing a polymer with 1% mol of TAD (PhTAD or MeTAD) and analyzing it by GPC, the average chain length of its samples decreased by a factor 10. He correlated this phenomenon with the effect of hydrogen bond established by urazole residues, able to drastically reduce the average hydrodynamic volume of the polymer, a parameter that regulates the retention time of the specimen during a GPC analysis. This theory seems to be confirmed by comparing the thermograms of a non-functionalized IR sample and one functionalized with 0.5 phr of PhTAD (Figure 36).

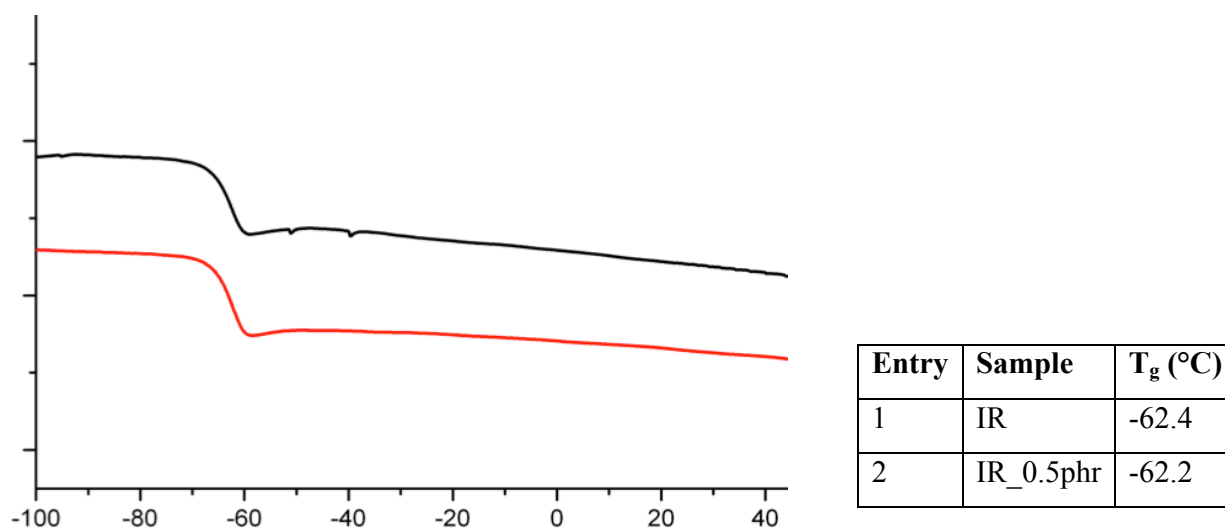


FIGURE 36 - DSC ANALYSIS OF IR SAMPLES, NON-FUNCTIONALIZED (BLACK LINE) AND FUNCTIONALIZED ONE WITH 0.5 PHR PHTAD (RED LINE)

By calculating the glass transition temperature of the polymer (Figure 36) it can be seen that there is no real difference between the two analyzed samples. Although the effects on the glass transition temperature are not remarkable considering polymer with high molecular weight, Flory and Fox described this relationship according to the following equation:

$$T_g = T_{g,\infty} - \frac{K}{M_n}$$

Where:

- $T_{g,\infty}$  is the maximum value of  $T_g$  that can be achieved at a theoretical infinite molecular mass
- $K$  is an empirical parameter that is related to the free volume present in the polymer sample.

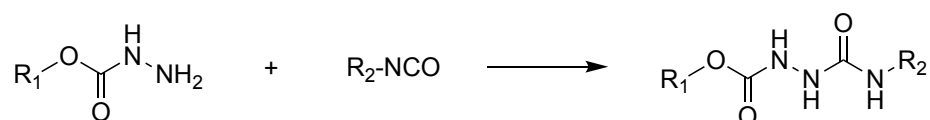
By shortening the chains, it would be reasonable to expect also a slightly decrease in the glass transition temperature but, in our case, this condition does not occur, showing instead an opposite behavior.

If all these data seem to point in the same direction as Butler's conclusions, the rheological properties of the compounds produced from these substrates (paragraph 4.1.1) will allow further clarification on this topic.

### 3.5 DIAZENE DERIVATIVE SYNTHESIS

One of the main advantages of TAD chemistry is actually one of its biggest technological limits: we are talking about the extremely high reactivity that these systems show. In fact, the TADs are extremely quick to react and the addition reaction to the double bonds of the polymeric backbone completes its course in a few minutes. This entails an inherent difficulty in exploiting this type of reactivity since it must necessarily run on the polymer dissolved in a solvent. Obviously, the longer the polymer chains are and the less soluble it is. Therefore, avoiding the need to work in solution and moving instead to an in-bulk functionalization would be desirable. In this case the diffusion of the functionalizer inside the polymer matrix would be a fundamental step to have an homogeneous distribution of the functional groups once the reaction has occurred. With this objective, the best strategy to follow has been to investigate the possibility of synthesizing a dipolarophile system with reduced reactivity, triggered by an external stimulus, in our case the high temperature during the mixing phase. Retracing the path that led us to study the TAD, it was evident that the solution to the problem could be the use of their corresponding open form.<sup>142</sup>

Starting from the most simple and commercially available form, azodicarboxylate (DEAD), a library of analogous substrates was synthesized, thus attempting to make them react with the model polybutadiene oligomer. Below we will summarize the synthesized semicarbazates both for the preparation of urazoles (Table 22) and those synthesized specifically for the purpose. In the following paragraphs their oxidation and, for those tested, also the addition to the polymer will be described.



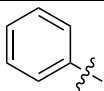
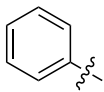
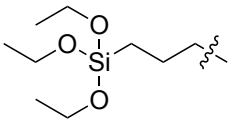
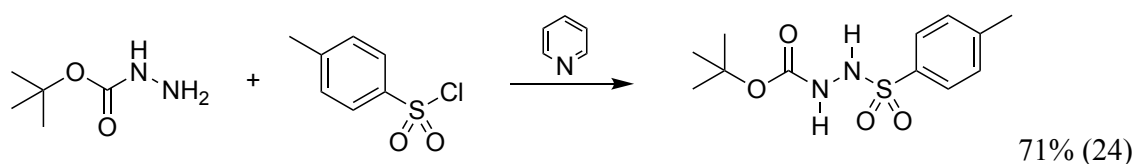
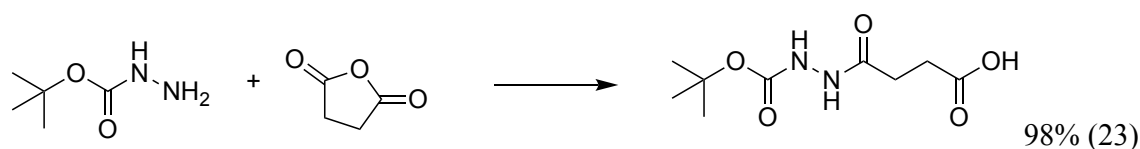
Entry	R1	R2	Solvent	Temperature (°C)	Time (h)	Yields %	Compound
1	-Et		Toluene	110	3	98	18
2	-tBut		Toluene	110	3	95	19
3	-Et		Toluene	0 -> r.t.	8	62	22

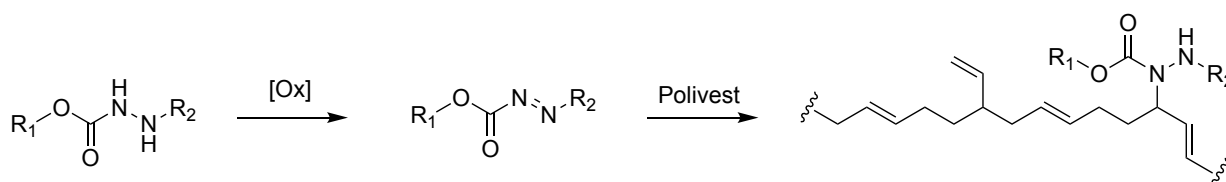
TABLE 22 - REACTION CONDITIONS FOR THE SYNTHESIS OF SEMICARBAZATES.

The reaction procedure of semicarbazates (18) and (19) has already been described, unlike the compound (22) presented here for the first time.

Besides these, there are other types of reactions able to generate compounds with an azo bridge capable of being oxidized, where the carbazate reacts with other compounds such as anhydrides or a sulfonyl chloride instead of isocyanate.<sup>143</sup>

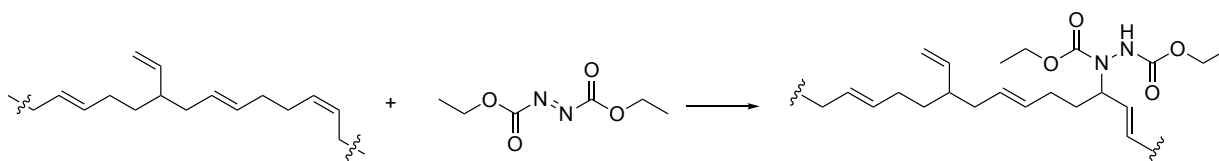


Once the semicarbazate has been synthesized, it can be oxidized in situ, according to the methods previously described for the oxidation of the urazoles. Usually, for the sake of simplicity, oxidation with PIDA was used, without isolating the oxidized intermediate and afterwards additions were attempted on the double bonds of the polybutadiene oligomer. (Scheme 30, Table 24).



SCHEME 30 - GENERIC SYNTHESIS PROCEDURE FOR THE ADDITION OF A DIAZENE DERIVATIVE ON A POLYMER MATRIX

As proof of concept we tested DEAD as the first dipolarophile, due to the applications found in literature and its fairly reactive nature (Table 23).



Eq. Double bond	Eq. DEAD	Solvent	Temperature (°C)	Time (h)	Overall functionalization %
1	0.1	DCM	r.t	2	>90

TABLE 23 - REACTION CONDITION FOR THE FUNCTIONALIZATION OF POLYVEST WITH DEAD

After dissolving the polymer in DCM, DEAD has been added, the reaction takes place quickly and the progress can also be seen by the naked eye following the discoloration of DEAD from a bright orange to a pale yellow.

This type of reaction, like PhTAD, involves the internal double bonds of the polymer, leaving the vinyl bonds unaltered, so they can be taken as an internal standard to determine the overall functionalization.

At the end of the reaction, after purifying the product three times according to the standard procedure, a  $^1\text{H-NMR}$  spectrum was recorded (Figure 37).

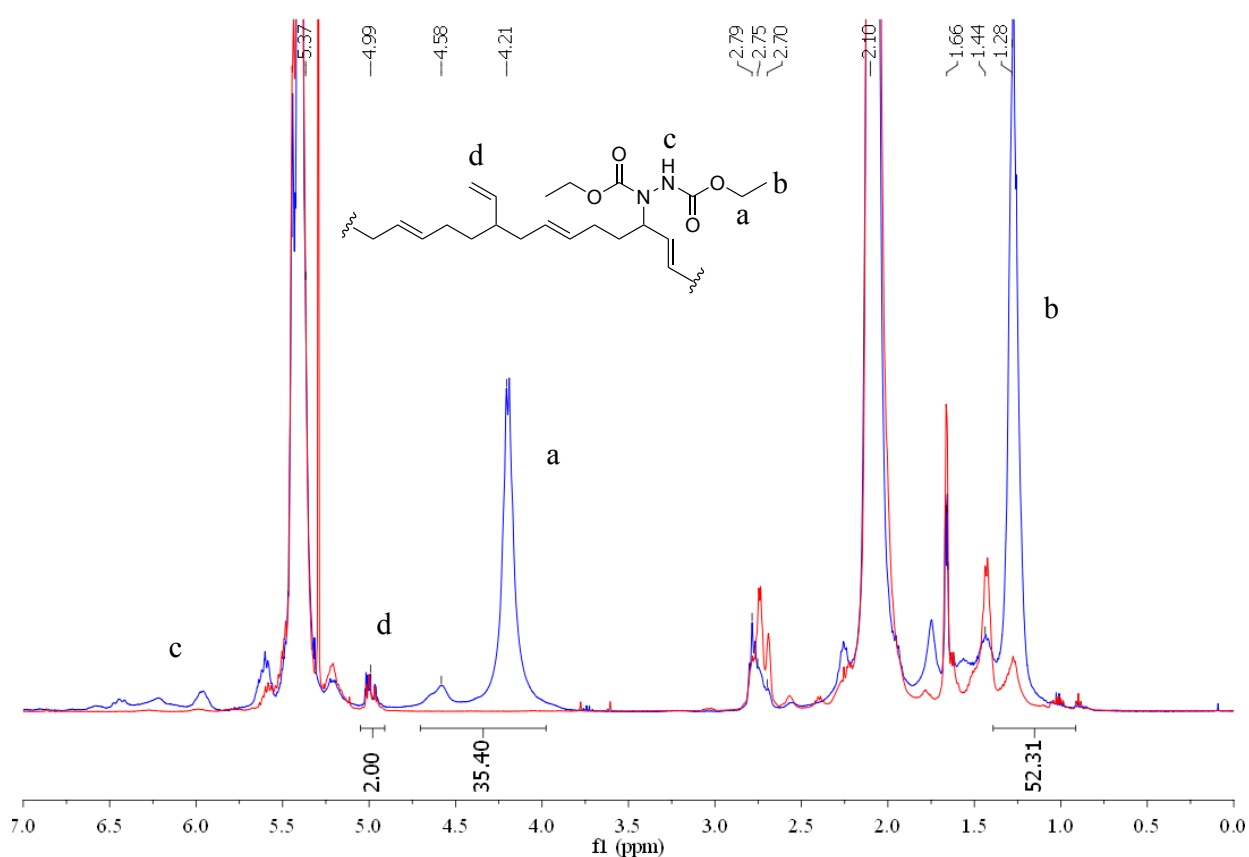


FIGURE 37 -  $^1\text{H-NMR}$  SPECTRA COMPARISON BETWEEN THE ADDITION PRODUCT (BLUE LINE) AND POLYVEST (RED LINE)

As it can be seen from the overlapping of the sample spectra (blue) and the polyvest reference (red), it is possible to notice how the anchoring of the functionalizer on the polymer chain has been almost total.

In fact, the signals of the ethyl residue are clearly visible at 1.28 ppm (b) and 4.21 ppm (a), in addition to a very wide peak at 4.58 ppm given by possible regio-isomer formed in the addition process.

Finally, it is possible to notice the presence of broad signals with chemical shift higher than 6 ppm (c), ascribable to the hydrazide hydrogens given by the reduction of the azo bridge of DEAD.

For confirmation, an FTIR spectroscopic analysis was carried out, that allowed to identify a broad band given by the commingling of the typical peaks of the carbonyl groups at 1713 and 1759  $\text{cm}^{-1}$ .

Having therefore verified the feasibility of an aza-ene reaction also for this type of structures, several compounds have been tested with the intent of finding a functionalizer capable of creating analogous adducts but with a slower reaction kinetics and, consequently, controllable through the temperature.

Entry	Substrate	Solvent	Eq. substrate	Eq. double bond	Temperature ( $^{\circ}\text{C}$ )	Time (h)	Overall functionalization <sup>a</sup> %
1	18	DCM	1	30	r.t.	48	0
2	18	DCM	1	30	40	24	0
3	19	DCM	1	10	40	24	0
4	18	Toluene	1	30	70	36	30
5	18	Toluene	1	10	110	18	39
6	22	DCM	1	50	40	120	0
7	23	Toluene	1	10	r.t.	24	-
8	23	Toluene	1	10	110	24	30
9	24	DCM	1	30	r.t.	24	n.d.

TABLE 24 - REACTION CONDITIONS FOR THE FUNCTIONALIZATION OF PB OLIGOMER BY DIAZENE DERIVATIVES

Starting from the same reaction conditions used for the functionalization of the PB oligomer with DEAD, it has been made reacting with ethyl(anilinocarbonyl)diazene-carboxylate (SemiC), the corresponding oxidized open structure of PhTAD (Table 24, entry 1). Unfortunately, after 48 hours of reaction, the mixture had the same initial color. The polymer was then recovered, as expected, without any trace of the addition product. To promote the reaction, the temperature was then raised to 40  $^{\circ}\text{C}$ , the boiling point of the DCM (Table 24, entry 2-3). However, even in these cases, the reaction did not take place.

It was therefore decided to change the reaction solvent (moving to toluene) to be able to reach higher temperatures.

The progress of the reaction was followed by UV-Vis spectroscopy, observing the evolution of the 327 nm band, characteristic of the azo bridge (Figure 38).

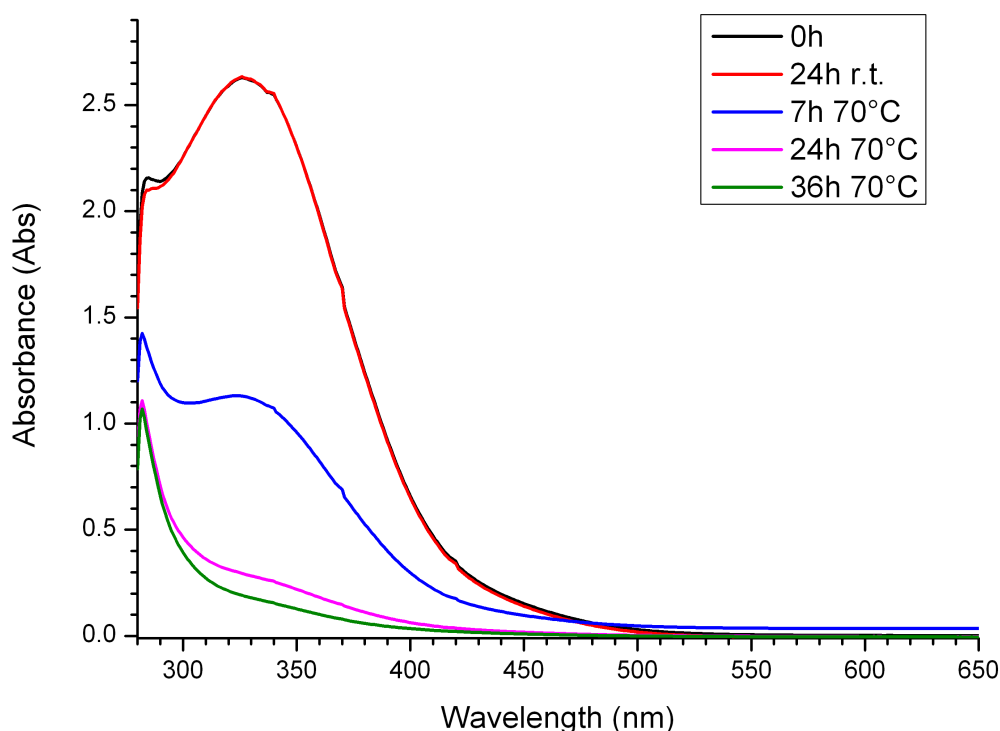


FIGURE 38 - EVOLUTION OF UV VISIBLE BAND ABSORPTION OF REACTION MIXTURE BETWEEN POLYVEST AND COMPOUND 18.

As it can be seen, 24 hours at room temperature have no effects on the reaction, but, when the solution is heated, a drastic reduction in the intensity of the absorption band is noted. After 36 h at 70 °C, the reaction almost completely lost its initial color, from a strong orange to a soft brown.

The polymer, after purification, was analyzed by FTIR and NMR spectroscopy. Analyzing the data obtained from this analysis, it was possible to compare the area of the integrals of the peaks of the ethyl residue with that of the vinyl bonds taken as internal standard, obtaining the amount of functionalizer anchored to the polymer, just like for the reaction with the DEAD.

In this case (table 24, entry 4) only 30% of the introduced functionalizer was actually anchored on the polymer.

By refluxing the reaction in toluene (110 °C) (Table 24 entry 5), the discoloration of the solution was faster, so that it was possible to significantly reduce the reaction time from 36 h to 18 h, while increasing the overall functionalization of the 39%.

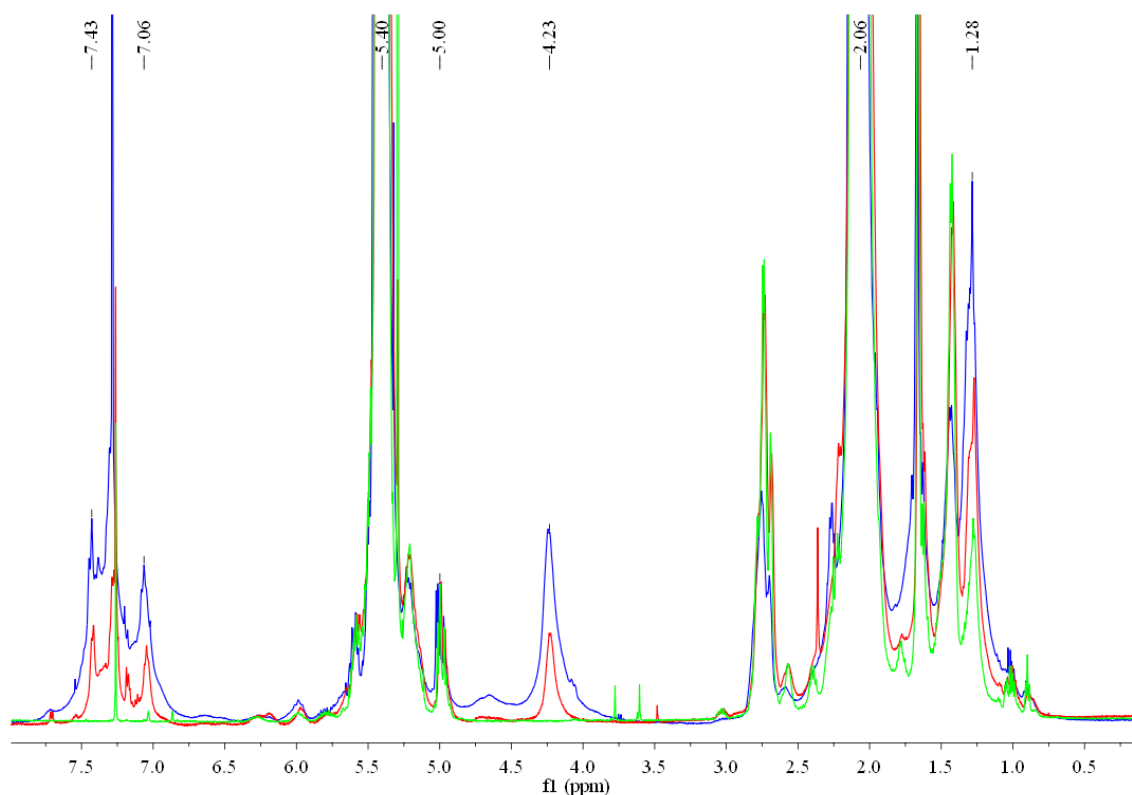


FIGURE 39 –  $^1\text{H-NMR}$  SPECTRA COMPARISON BETWEEN PB OLIGOMER: PRISTINE POLYMER (GREEN LINE, ENTRY 4 (RED LINE), ENTRY 5 (BLUE LINE)

The increasing functionalization found through NMR spectroscopy (Figure 39) was also confirmed by the FTIR data, as can be seen from the peaks of the carbonyl group in the area between  $1491\text{cm}^{-1}$  and  $1507\text{cm}^{-1}$  (Figure 40).

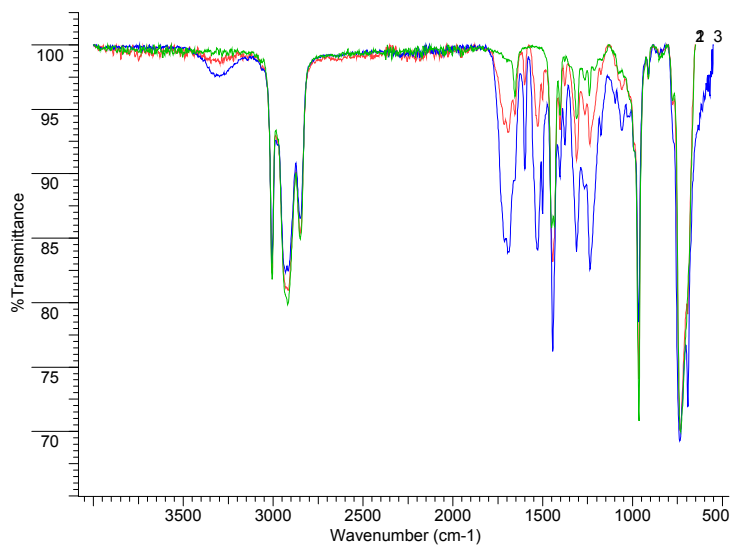


FIGURE 40 – FTIR SPECTRA OF PRISTINE OLIGOMER (GREEN LINE), ENTRY 4 (RED LINE) AND ENTRY 5 (BLUE LINE)

To finish this overview on the graft semicarbazates on the polymeric chain, other more exotic compounds were also tested, with specific functional groups.

For example, the reaction between the polyvest and a functionalizer bearing a siloxane group has been tested (Table 24, entry 6). In this case, however, to prevent any condensation reaction, the reaction was held at 40 °C for one week, but it was not possible to observe a functionalization despite the reaction mixture had almost completely bleached, a sign that the substrate was reduced before it could perform its function. The best result was the functionalization of the polymer with tert-butyl [(4-methylphenyl) sulfonyl] diazenecarboxylate (substrate 23, Table 24, entry 7-8) which, although being inactive at room temperature, reached a total functionalization of 30% after being refluxed in toluene for 24 hours. Finally the 4-[(tert-butoxycarbonyl)diazenyl]-4-oxobutanoic acid (substrate 24, Table 24, entry 9) was anchored to the model system, however the interpretation of the NMR spectrum was particularly complex as the aliphatic peaks of the molecule in large part overlap with the much more intense peaks of the polymer, thus making it impossible to quantify the reaction yield (Figure 41).

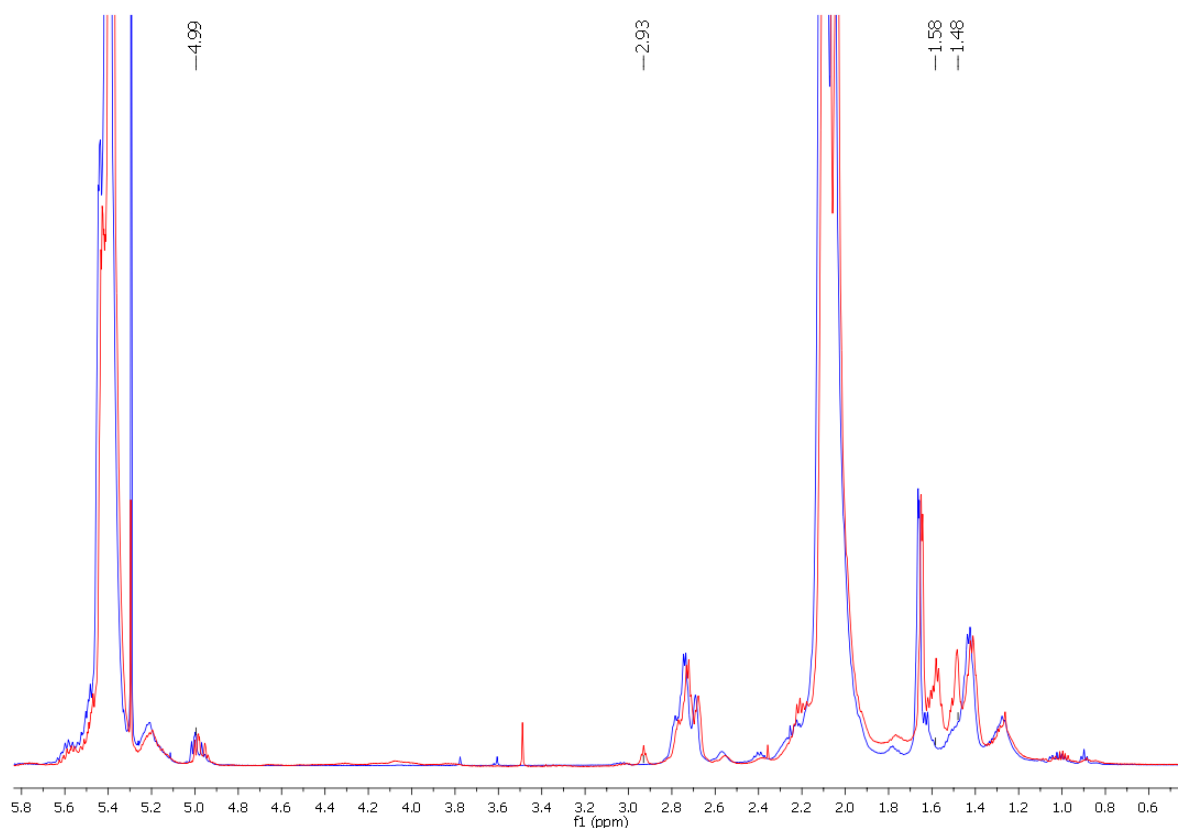


FIGURE 41 - <sup>1</sup>H-NMR SPECTRA OF PRISTINE POLYVEST (BLUE LINE) AND FUNCTIONALIZED ONE (RED LINE) WITH COMPOUND 24.

This functionalization approach has a particular relevance, because it opens a new and unexplored line of research.

As mentioned at the beginning of this dissertation, this doctoral project was born with the intent of making a screening through the possible functionalizations that can be implemented on a polymeric substrate in an easy, fast, versatile way and that are able to meet the processability requirements needed for the production of compounds.

So the possibility of introducing into the polymer chain a customizable functionalizing agent, which whose azo bridge reaction is activated simply by temperature, without the use of particular synthetic procedures or optimized catalysts, is a fundamental step in the desired direction.

After the good results achieved both in terms of overall functionalization and addition speed, it was therefore decided to raise the bar of the difficulty, moving from a functionalization on a model system in solution to a bulk functionalization, directly in the internal mixer, on a long chain polybutadiene polymer, to make a mixture with and to evaluate its properties.

The chosen substrate was therefore the one that best behaved during the test phase (Table 24, substrate 18, entry 4-5).

With the idea of obtaining a modification of the polymer in the order of about 1 phr of SemiC, a batch of functionalizing agent was prepared in a quantity doubled with respect to the desired one. Once isolated, the product was kneaded at room temperature, using an open mixer, with the polymer matrix.

The thus obtained mixture was then inserted into the inner mixer chamber, operating at 140 °C at 60 rpm.

At preset times ( $t = 0, 5 \text{ min}, 10 \text{ min}, 30 \text{ min}, 60 \text{ min}$ ) sample aliquots were taken in order to analyze them by IR spectroscopy and to be able to visualize the behavior of the mixture.

After 60 minutes the rubber started to become darker, a sign that some detrimental phenomenon was taking place. The mixing process was then stopped and the rubber was discharged.

The samples collected at different reaction times were immersed in DCM, in order to dissolve and reprecipitate them, to remove the excess of non-reacted functionalization.

During this test it immediately became clear how functionalization actually took place (Figure 42). The samples collected within 5 minutes from the beginning of the heating process dissolved without any problem in the chlorinated solvent, starting from 10-minute-heating it was possible to notice how the polymer matrix resisted the dissolution, swelling enough to completely fill the volume of the beaker at its disposal.

The polymeric network gained more force proportionally with the increase in reaction time, with a consequent reduction in the amount of solvent incorporated.

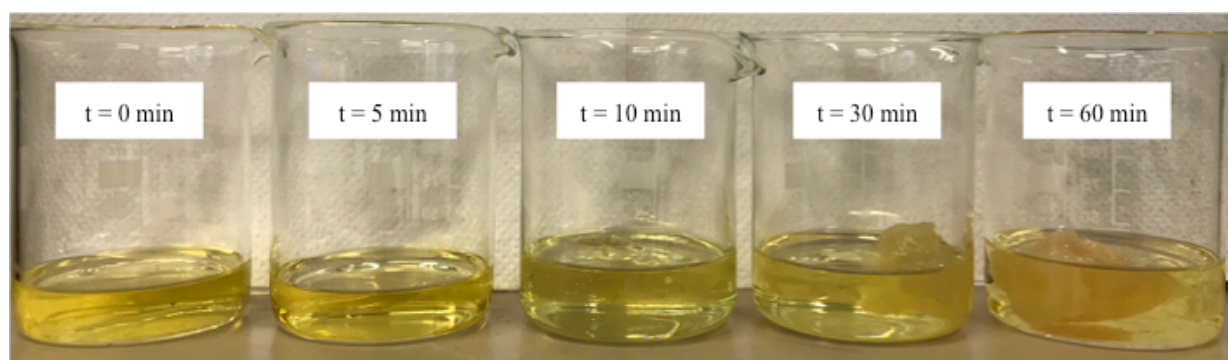


FIGURE 42 -SWELLING TEST OF CB25 FUNCTIONALIZED WITH SEMIC AT DIFFERENT REACTION TIMES.

After purifying the samples, the FTIR spectra shown in the figure below were recorded (Figure 43).

Although not as pronounced as in the model system (where the quantity of functionalizer was much greater), when focusing on the area of the peaks of the carbonyls it is possible to notice how the functionalization increases with the increase of the reaction time, reaching a value that can be roughly approximated between 0.75 up to 1 phr.

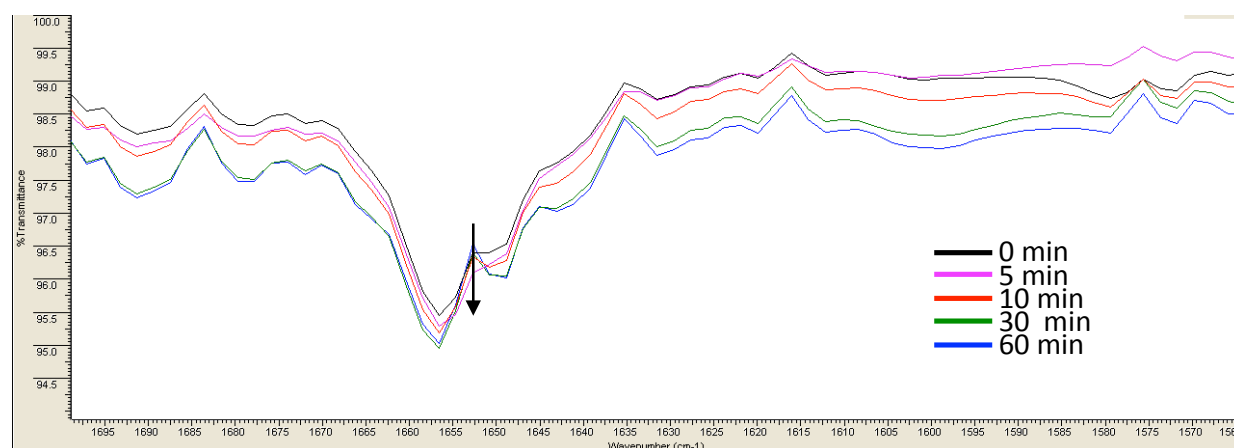


FIGURE 43 - FTIR SPECTRA OF SAMPLES OF CB25 FUNCTIONALIZED WITH SEMIC AT DIFFERENT REACTION TIMES.

## 4. FORMULATION AND CHARACTERIZATION OF RUBBER COMPOUNDS

In this chapter the compounds formulation procedures and the characterization of their rheological properties will be described and finally an interpretation of the collected data will be provided.

As described in the previous chapters, this doctoral project was created to be the forerunner research for the chemical modification of commercial polymers for tire compounding applications. After a careful screening of the possible functionalizations able to link to the unsaturated bonds of a polymer matrix, an important step to comply with the initial requests was to replicate the same reactions, moving from a lab scale functionalization reaction to a larger one, able to produce a satisfactory amount of modified rubber for a real compound test.

Taking into account all the respective synthetic difficulties of the functionalization strategies identified and, at the best of our knowledge, not having found any evidence in the literature about the use of polymer matrixes functionalized with this compound, the PhTAD fulfilled the most of criteria that we aimed to. So this was the compound used as a model system for trying to shed light on the impact that this type of functionalization is able to generate on the final composite.

The basic idea was in fact to change the local polarity of the polymer chains in order to allow a better interaction with the polar components of the compound, silica first and foremost, but, as we will see, the principle could be extended to all the other ingredients introduced (Figure 44).

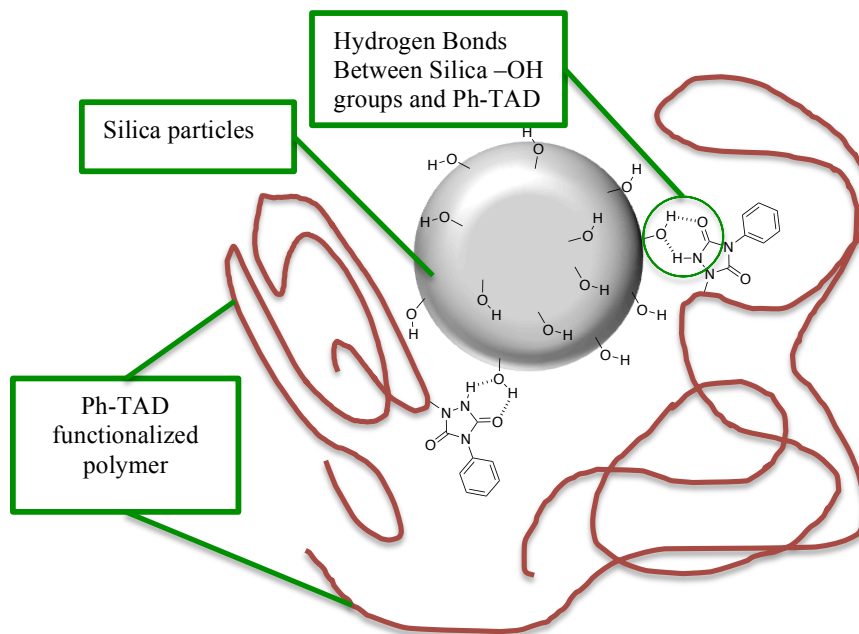


FIGURE 44 - ILLUSTRATION OF POSSIBLE INTERACTIONS BETWEEN FUNCTIONALIZED POLYMER AND SILICA SURFACE NANOPARTICLES

#### 4.1 GENERAL PROCEDURES FOR RUBBER COMPOUNDING

##### **Materials:**

IR SKI3 - Group II Isoprene Rubber from Nizhnenkamsk; BR40 neocis 97% 1,4-cis polybutadiene from Eni Versalis; BUNA CB25  $\geq$  96% 1,4-cis polybutadiene; Functionalized rubber earlier synthesized; Silica Rhodia Zeosil MP 1165; Carbon Black N326 from Cabot; Bis[3-(triethoxysilyl)propyl] Tetrasulfide (TESPT) Si69 from Evonik; *N*-(1,3-dimethylbutyl)-*N'*-phenyl-*p*-phenyldiamine Santoflex (6PPD) from Flexsys; ZnO from Zincol Ossidi; Stearic acid Stearina TP8 from Undesa; *N*-Cyclohexyl-2-benzothiazolesulfenamamide (CBS) from Lanxess and Sulfur from Redball superfine.

Except for some specific compounds, whose formulation procedure will be described together with the dynamic mechanical properties, the method, the components used and their proportions will be reported here.

Two different internal mixers were used to prepare the uncured compounds, one of which is the Brabender Plasti-corder lab station, present in the Pirelli laboratories, equipped with a mixing chamber of 50 mL, while during the abroad period at the Deutsches Institut für

Kautschuktechnologie (DIK) a Thermo Haake PolyLab Rheomix 600 with a 58-mL-mixing chamber was used. In both cases the filling factor was kept constant in order to keep the mixing process homogeneous.

The mixing procedure for a non-black filler is divided into three steps, each of which is performed at a different temperature, in order to be sure that the desired reactions occur at the right point of the process. Too high temperatures in the presence of the vulcanizing pack could in fact lead to premature vulcanization, while too low temperatures during the first phase could, for example, prevent proper silanization of the surface of the silica particles used as fillers.

During the first step, the polymer is placed inside the mixing chamber previously heated to 140 °C. After a short mastication of about 30 s the filler and the compatibilizer (TESPT), if needed, are added. The reaction is left in mixing conditions (140 °C, 60 rpm) for 3 minutes, in order to let the reaction between the coupling agent and silica happen, thus preventing secondary reactions with the other components to be inserted, as the ZnO. After this time, ZnO, Stearic Acid and a static antioxidant such as 6PPD are inserted. The compound is then dumped after 7 minutes of overall mixing.

During the second step the vulcanizing pack is added to the mixture produced during the first phase, in particular the mixture recovered from the previous step is inserted into the mixing chamber at a temperature of 90 °C at 60 rpm. After a short mastication, 30 s, CBS and Sulfur are added and the compound is mixed for another 2 minutes and 30 s for a total of 3 minutes.

After dumping the mixture thus obtained, the third step is performed, consisting of 5 passages in a two rolling mill, to homogenize the distribution of the components inside the composite.

Table 25 below shows the ratios among the components added to the mixture.

Compound	Step 1						Step 2	
	Polymer	Filler	TESPT	6PPD	Stearic Acid	ZnO	S	CBS
Phr	100	v.a.	8%w/w	2.5	1	2	1	3

TABLE 25 - GENERAL LIST OF INGREDIENTS AND RATIOS FOR RUBBER COMPOUNDING

The main component in a compound is undoubtedly the polymer matrix, in our case the amount of rubber used for each test is about 35 g. What has been generally referred to as rubber may consist of a single polymer or a blend of two or more distinct polymers.

The filler is then added to this mass, in our case Silice Rhodia Zeosil MP 1165 or CB N326, whose quantity is variable according to the needs. In particular, mixtures with 0, 10, 35 and 50 phr of fillers were produced in order to evaluate their different rheological behavior.

In the case of CB, no coupling agent has been added, except for the two pyrene derivatives of our production that will be reported in the dedicated paragraph.

In the case of silica, a coupling agent such as TESPT can be added in an amount equal to 8% by weight with respect to the amount of silica inserted, a quantity commonly used as a benchmark in the silica-based recipes of industrial compounds.

It is evident that an industrial process, refined by years of research and development, is a particularly effective system in carrying out the required task. Therefore, comparing with the rheological standards imposed by this type of compatibilizer is an extremely demanding challenge, so the work that will be described will have to be read in the perspective of showing how a new and totally different approach can have a potential in this sector. This research is nothing more than a starting point for future studies with the aim of better understanding the problems related to the use of a functionalizing agent, in order to start closing the gap of knowledge that today prevents a technologically relevant application.

The compounds produced with a polymer functionalized by PhTAD will then be compared with a reference compound made with and without TESPT, in order to have a direct comparison of the effects given by the functionalization.

All ratios with the other components of the compound have been left unchanged from the original recipe that the industrial partner provided us.

#### 4.1.1 IR COMPOUNDS

Given the amount of components involved and the mutual interactions that these components must necessarily interlace with, the most convenient choice was to start from a single polymer compound. Although most laboratory-scale functionalization tests have been performed on a polybutadiene oligomer, making a pure BR compound is not trivial. Pure BR compounds show good abrasion resistance, flexibility at low temperatures, resistance to high temperatures and low ozone oxidizability, however the adhesiveness to the other tire components, the tear resistance along with modest mechanical properties make BR unsuitable for a stand-alone usage in tire construction: for these reasons it is always mixed with other types of rubbers.

So we started from the production of a series of pure IR compounds, using silica as filler (Table 26).

Entry	Polymer	PhTAD (phr)	Silica (phr)	TESPT (8% w/w)	Label
C1	IR	0	0	NO	IR_0
C2	IR	0	10	YES	IR_10_Sil
C3	IR	0	10	NO	IR_10
C4	IR	0	35	YES	IR_35_Sil
C5	IR	0	35	NO	IR_35
C6	IR	0	50	YES	IR_50_Sil
C7	IR	0	50	NO	IR_50
C8	IR	0.5	35	YES	IRf_35_Sil
C9	IR	0.5	35	NO	IRf_35
C10	IR	2	35	NO	IRf2_35

TABLE 26 - LIST OF IR-BASED COMPOUNDS.

All the compounds have been characterized with ODR: through this analysis it has been possible to collect the values of  $G'$ ,  $G''$  and  $\tan\delta$  of the pre and post curing compounds. Moreover, the optimal vulcanization times were then obtained, along with some technologically relevant values such as  $S'$ ,  $ML$ ,  $MH$ , where  $S'$  is the torque measured during vulcanization process,  $ML$  is the minimum torque reached from a compound heated under pressure, giving a measure of the stiffness and viscosity of an unvulcanized compound, while  $MH$  is the maximum torque recorded in plateau curve.

Those parameters were then used for the realization of vulcanized 2-mm-thicks strips, useful for a subsequent characterization of the elastic properties by means of a stress-strain test.

The graph shows the standard compounds made without any compatibilizer with an increasing amount of filler (Figure 45). The values thus obtained of  $G'$  and  $\tan\delta$  will be the comparison term with the compounds functionalized with PhTAD.

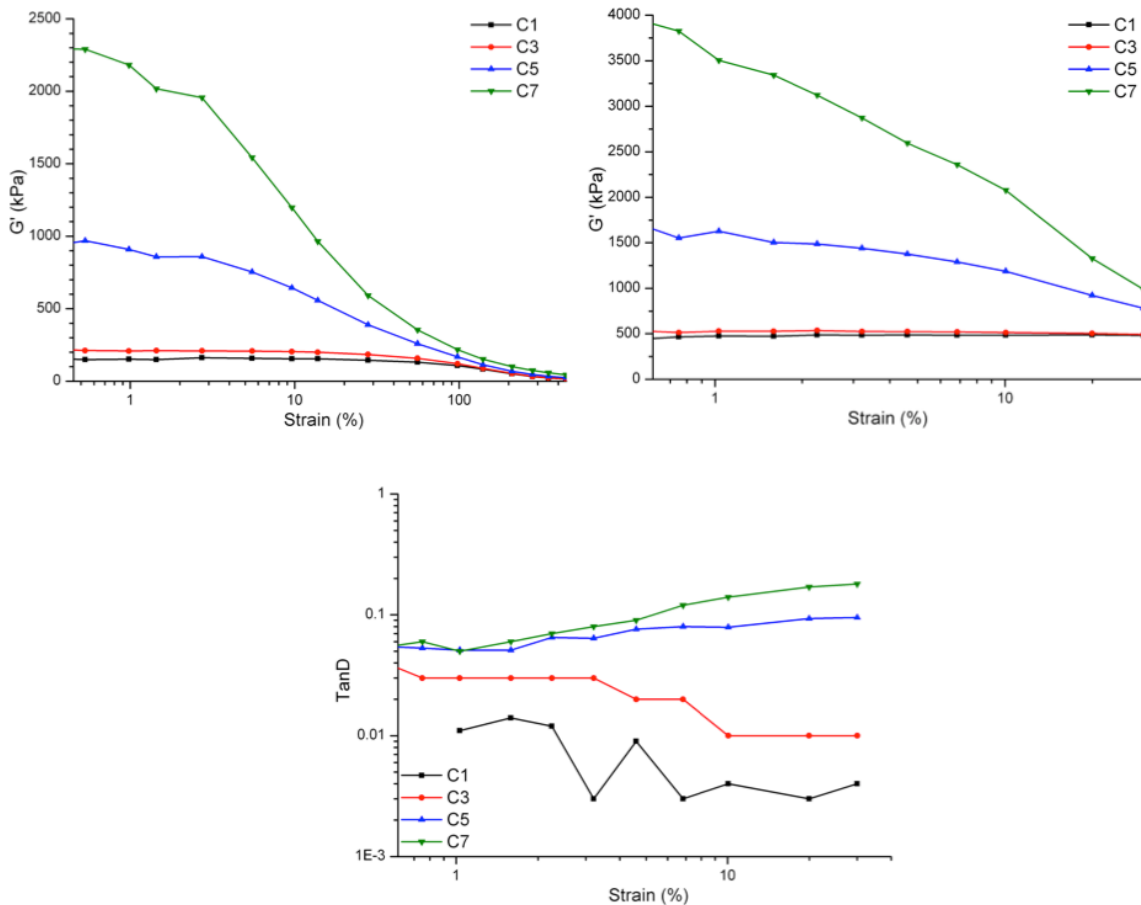


FIGURE 45 – UPPER LEFT: STORAGE MODULUS  $G'$  VS STRAIN OF UNCURED SAMPLES; UPPER RIGHT: STORAGE MODULUS  $G'$  VS STRAIN OF CURED SAMPLES; BOTTOM: TAND VS. STRAIN OF CURED SAMPLE. C1 BLACK LINE, C3 RED LINE, C5 BLUE LINE, C7 GREEN LINE

Recalling what has been described on the dynamic-mechanical behavior of a compound in paragraph 2.2, it is immediately evident that a mixture with the higher amount of fillers will have an higher reinforcement modulus  $G'$ , given by the sum of the hydrodynamic effect, filler-rubber interaction and filler-filler interactions. The latter are particularly important with low strain but, increasing the deformation, they are destroyed, producing the so-called Payne effect, with direct consequences on the hysteretic behavior of the mixture, as evidenced by values of  $\tan\delta$ .

The data of the compounds with TESPT can be read in a very similar way, even if the absolute values are quite different (Figure 46).

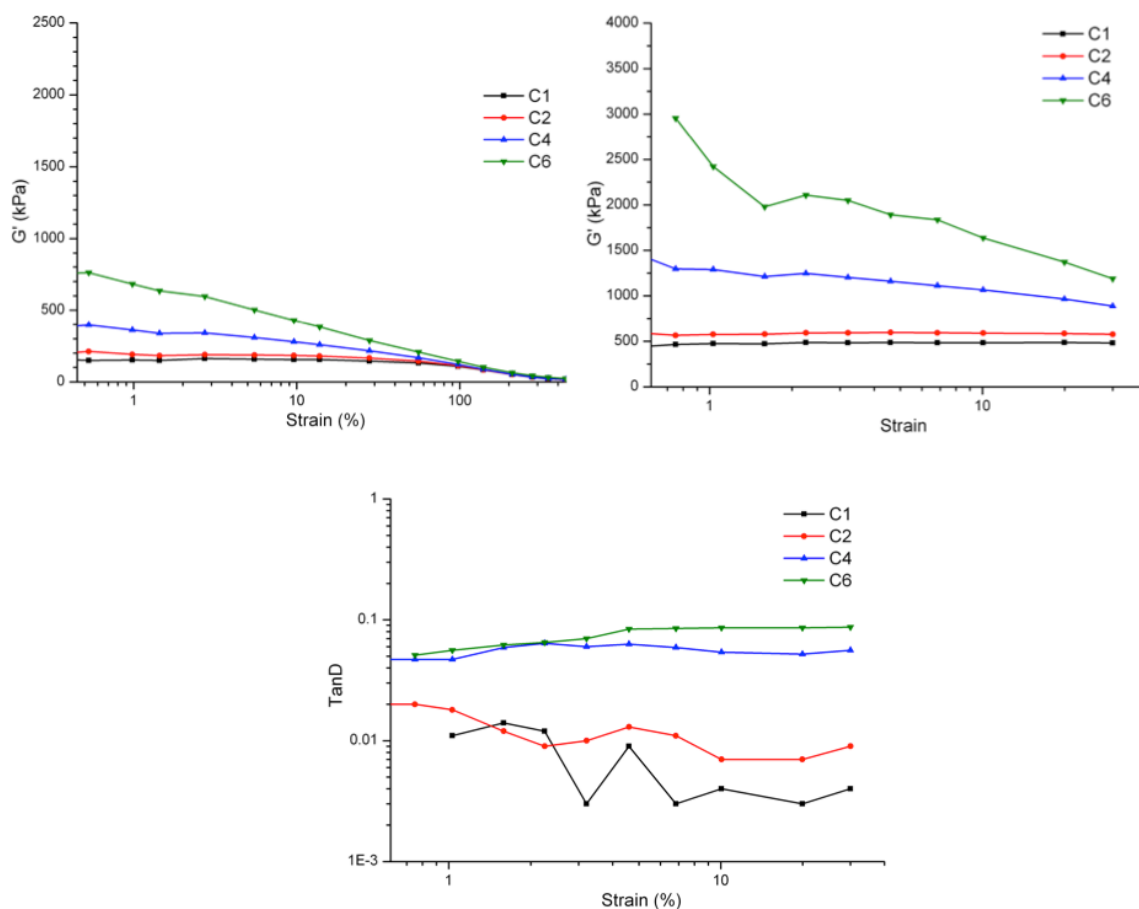


FIGURE 46 - UPPER LEFT: STORAGE MODULUS  $G'$  VS STRAIN OF UNCURED SAMPLES; UPPER RIGHT: STORAGE MODULUS  $G'$  VS STRAIN OF CURED SAMPLES; BOTTOM:  $\tan\delta$  VS. STRAIN OF CURED SAMPLE. C1 BLACK LINE, C2 RED LINE, C4 BLUE LINE, C6 GREEN LINE

First of all, we can see how, by maintaining the ordinate axis with the same proportion of the compounds shown previously (C1, C3, C5, C7), the values of  $G'$  of the uncured samples are extremely different. During the first mixing phase TESPT reacts with the surface of the silica, along with the passivation of the surface there is a reduced filler-filler interactions.

Looking at the graph of the cured sample, it can be seen that the reinforcement modulus is less affected by the increase of the strain. This effect, combined with lower values of  $G''$ , is reflected in a reduction of  $\tan\delta$  and, consequently, of the rolling resistance.

Comparing the C4 and C5, non-functionalized compounds, with their C8 and C9 homologues, in which the isoprene rubber is functionalized with 0.5 phr of PhTAD, we can begin to delineate the effect that this chemical modification produces inside a compound (Figure 47).

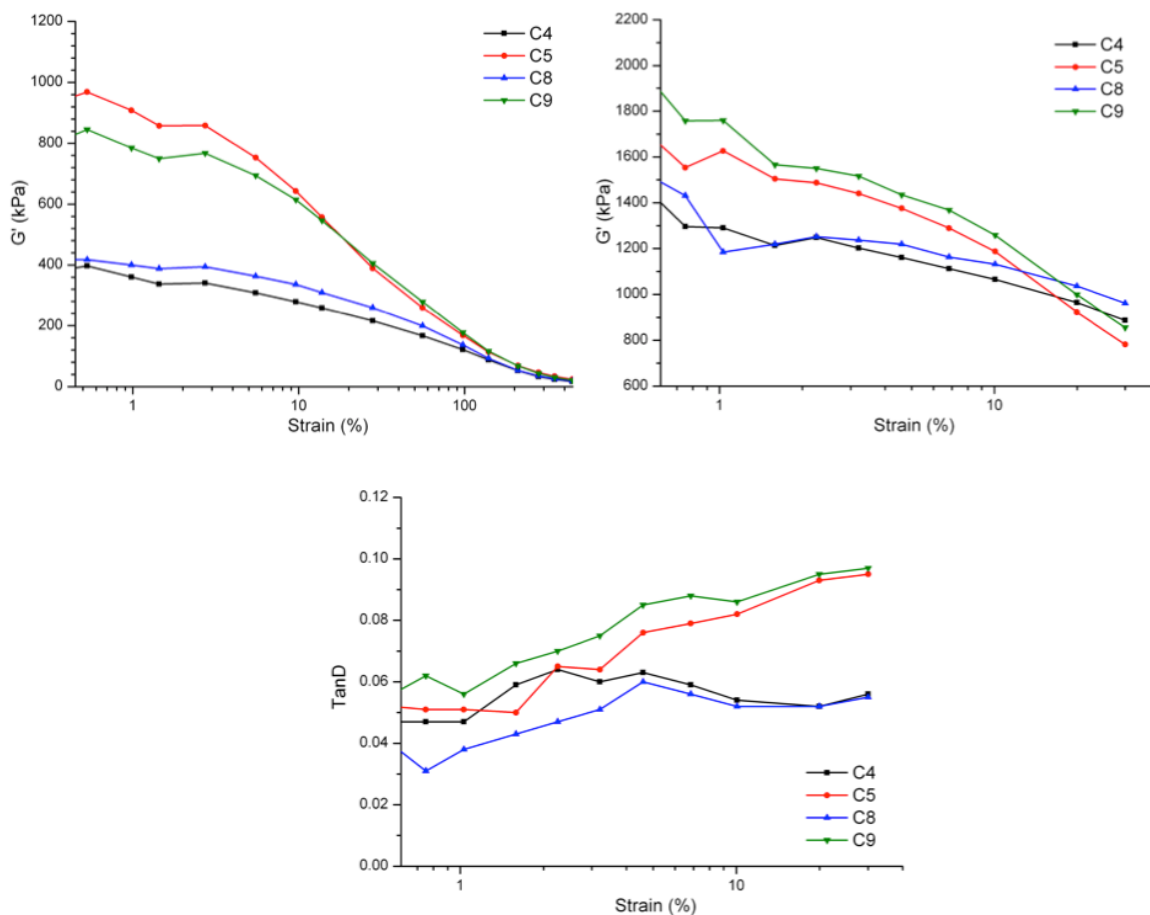


FIGURE 47 - UPPER LEFT: STORAGE MODULUS  $G'$  VS STRAIN OF UNCURED SAMPLES; UPPER RIGHT: STORAGE MODULUS  $G'$  VS STRAIN OF CURED SAMPLES; BOTTOM:  $\tan D$  VS. STRAIN OF CURED SAMPLE. C4 BLACK LINE, C5 RED LINE, C8 BLUE LINE, C9 GREEN LINE

Observing the behavior of the C5 and C9 uncured compounds we can see how the functionalization reduces  $G'$  at low strain (<3%), by 10-12%. Furthermore, by increasing the deformation, the loss of reinforcement, given by the breaking of the filler-filler interactions, is more pronounced, albeit slightly, in the non-functionalized sample.

The comparison between the curves of the compounds in which the TESPT was added is more difficult to read.

In this case the functionalized sample C8 has a slightly higher  $G'$  than C4 but the general behavior of the mixture is clearly due to the coupling effect given by the TESPT.

More interesting, from the technological point of view, are the reinforcing properties in the cured compound. The behavior of C5 and C9 compounds is opposite to what happened before vulcanization process. In this case the functionalized compound exhibits an higher value of  $G'$  compared to the reference sample but with an almost identical Payne effect. Even if we are far from the compatibilizing, this is still an interesting result, a clue of an effective interaction between silica and the urazole residue introduced in the chain.

The same or similar result is also obtained by looking at the compounds C8 and C9, with a slight increase in the value of  $G'$  independent form the strain (net of the fluctuations. Strain values lower than 1% should not to be considered particularly significant).

Also  $\tan\delta$  of these last two compounds is peculiar: C8 compound has reached the lowest value, despite the fact that its  $\Delta S'$  is lower than C4 (12.93 and 13.36 respectively) which, in theory, should lead to a lower quality of final polymer network (Table 27).

<b>Compound</b>	<b>Label</b>	<b>S' min (ML)</b>	<b>S' max (MH)</b>	<b>Time start (min:sec)</b>	<b>Time S' 90% (min:sec)</b>
C1	IR_0	1.100	7.33	04:39	09:04
C2	IR_10_Sil	1.304	9.17	04:01	08:38
C3	IR_10	1.57	8.80	03:48	06:06
C4	IR_35_Sil	2.13	15.49	02:51	04:42
C5	IR_35	4.283	15.88	01:50	02:35
C6	IR_50_Sil	3.119	20.84	02:15	03:50
C7	IR_50	7.67	22.22	01:14	02:12
C8	IRf_35_Sil	2.29	15.22	02:39	03:59
C9	IRf_35	3.78	16.33	02:01	02:43
C10	IRf2_35	0.06	2.83	02:32	02:58

TABLE 27 - VULCANIZATION PROCESS RESULTS OF LISTED COMPOUNDS

After vulcanization process, the tensile behavior of these compounds was also studied, with the results shown in the graph and in the table below (Figure 48, Table 28).

	C1	$\sigma$ C1	C3	$\sigma$ C3	C5	$\sigma$ C5	C9	$\sigma$ C9	$\Delta\%$ vs.C5	C7	$\sigma$ C7	$\Delta\%$ vs.C7
Stress (MPa) @ 50%	0.59	0.01	0.68	0.01	0.71	0.01	0.88	0.01	24	0.86	0.01	2
Stress (MPa) @ 100%	0.85	0.01	0.98	0.03	0.93	0.01	1.21	0.02	31	1.11	0.05	8
Stress (MPa) @ 200%	1.35	0.02	1.56	0.06	1.49	0.01	2.09	0.04	41	2.2	0.4	-3
Stress (MPa) @ 300%	2.01	0.03	2.31	0.09	2.46	0.02	3.53	0.06	43	4.1	0.8	-14
Stress (MPa) @ 500%	6.7	0.3	7.6	0.3	7.0	0.1	10.0	0.2	43	10.3	0.1	-3
Load at break (MPa)	8.0	1.6	14.1	1.7	23.4	0.8	24.7	0.9	6	10.3	1.2	139
Elongation at break (%)	512	12	565	16	764	10	714	11	-7	500	61	43

TABLE 28 - RESULT OF TENSILE STRESS-STRAIN TEST OF CURED IR COMPOUNDS

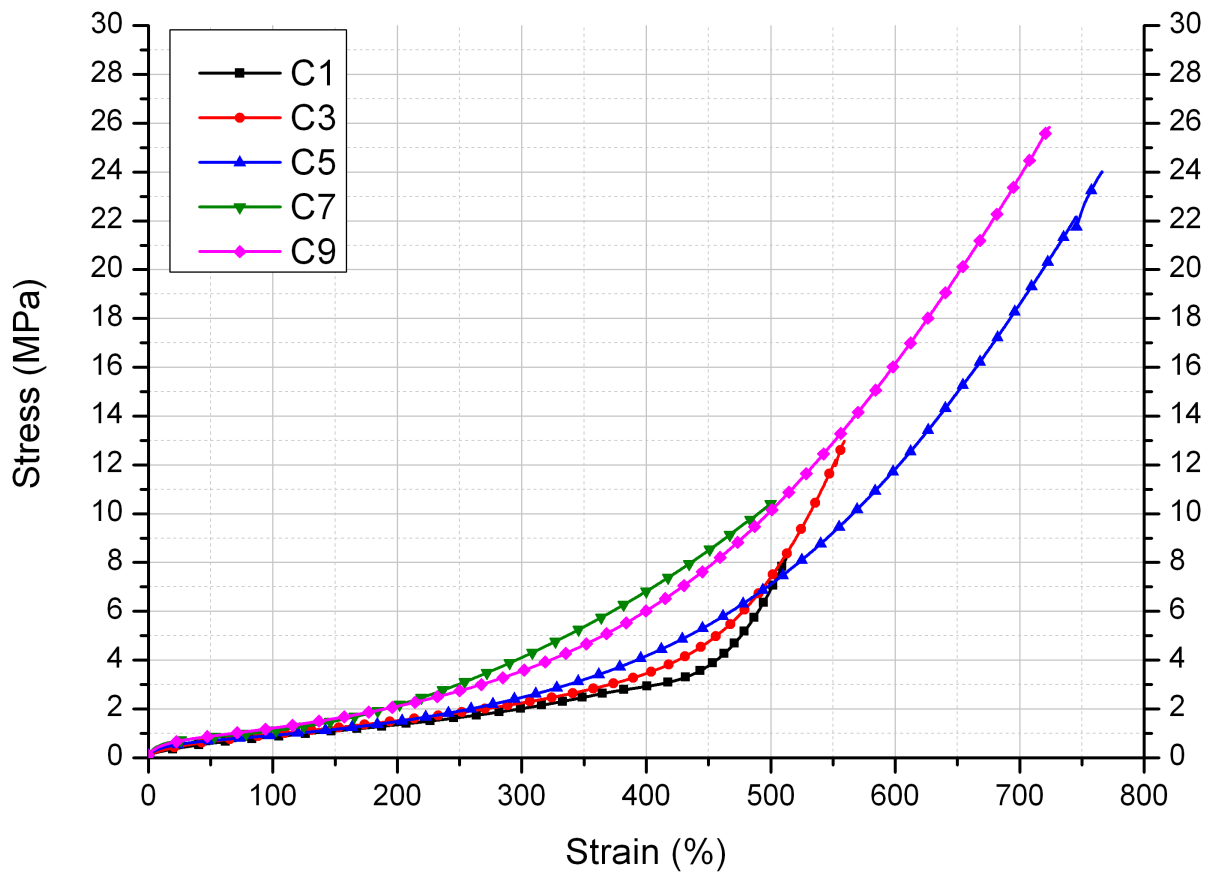


FIGURE 48 - TENSILE STRESS-STRAIN PROFILE OF CURED IR COMPOUNDS. C1 - BLACK LINE; C3 - RED LINE; C5 - BLUE LINE; C7 - GREEN LINE; C9 - PINK LINE.

As it can be seen, functionalization has a noticeable effect on the mechanical behavior of the compound. C9 (pink line), functionalized with 0.5 phr of PhTAD, when compared with the C5 with equal amount of filler, presents:

- Increased stiffness of the sample through the whole elongation (+ 24-43%)
- Slight increase in load at break (+ 6%)
- Marginal loss of elongation at break (-7%)

One of the most encouraging data comes from the fact that the C9 has an elastic behavior very similar to C7, but with elongation and breaking loads 130% and 40% higher respectively.

Working in the same way with the compounds in which TESPT was also present, we can see that the overall data are better, as it could be expected after the analysis carried out with the RPA. Anyway, considering the two compounds with the same amount of silica (C4 and C8), we can see the same trend of the previous pair where the functionalized compound had an higher tensile strength, but in this case we lost something in terms of load at break and maximum elongation (Table 29).

	<b>C1</b>	<b><math>\sigma</math> C1</b>	<b>C2</b>	<b><math>\sigma</math> C2</b>	<b>C4</b>	<b><math>\sigma</math> C4</b>	<b>C8</b>	<b><math>\sigma</math> C8</b>	<b>C6</b>	<b><math>\sigma</math> C6</b>
Stress (MPa) @ 50%	0.59	0.01	0.74	0.01	1.19	0.01	1.26	0.01	1.42	0.02
Stress (MPa) @ 100%	0.85	0.01	1.13	0.02	2.00	0.03	2.23	0.03	2.48	0.01
Stress (MPa) @ 200%	1.35	0.02	2.11	0.06	4.67	0.07	5.03	0.06	6.37	0.04
Stress (MPa) @ 300%	2.01	0.03	3.8	0.1	8.7	0.1	9.2	0.1	11.7	0.1
Stress (MPa) @ 500%	6.7	0.3	-	-	22.3	0.4	23.4	0.4	26.1	0.3
Load at break (MPa)	8.0	1.6	13.9	1.0	31.4	1.2	28.8	1.4	31.8	1.6
Elongation at break (%)	512	12	486	13	594	7	555	15	565	20

TABLE 29 - RESULTS OF TENSILE STRESS-STRAIN TEST OF CURED IR COMPOUNDS WITH TESPT

On these basis, we decided to increase the load of PhTAD, sure that this could have a positive impact on the compound. However, as mentioned in paragraph 3.4.3, when increasing the amount of PhTAD to 2 phr or even 5 phr, the polymer became totally intractable, losing its thermoplastic properties.

This phenomenon was also described by Butler. In fact, when he tried to functionalize up to 1% and 5% mol/mol an isoprene rubber, he was not able to cast a useful film, attributing this behavior to the presence of hydrogen bonds, able to upset the topology of the polymer chains.

In our experience, we have been able to formulate a compound (C10) with an high amount of PhTAD, whose results are summarized in the graphs below, using C1, a not loaded compounds, as a comparison term (Figure 49).

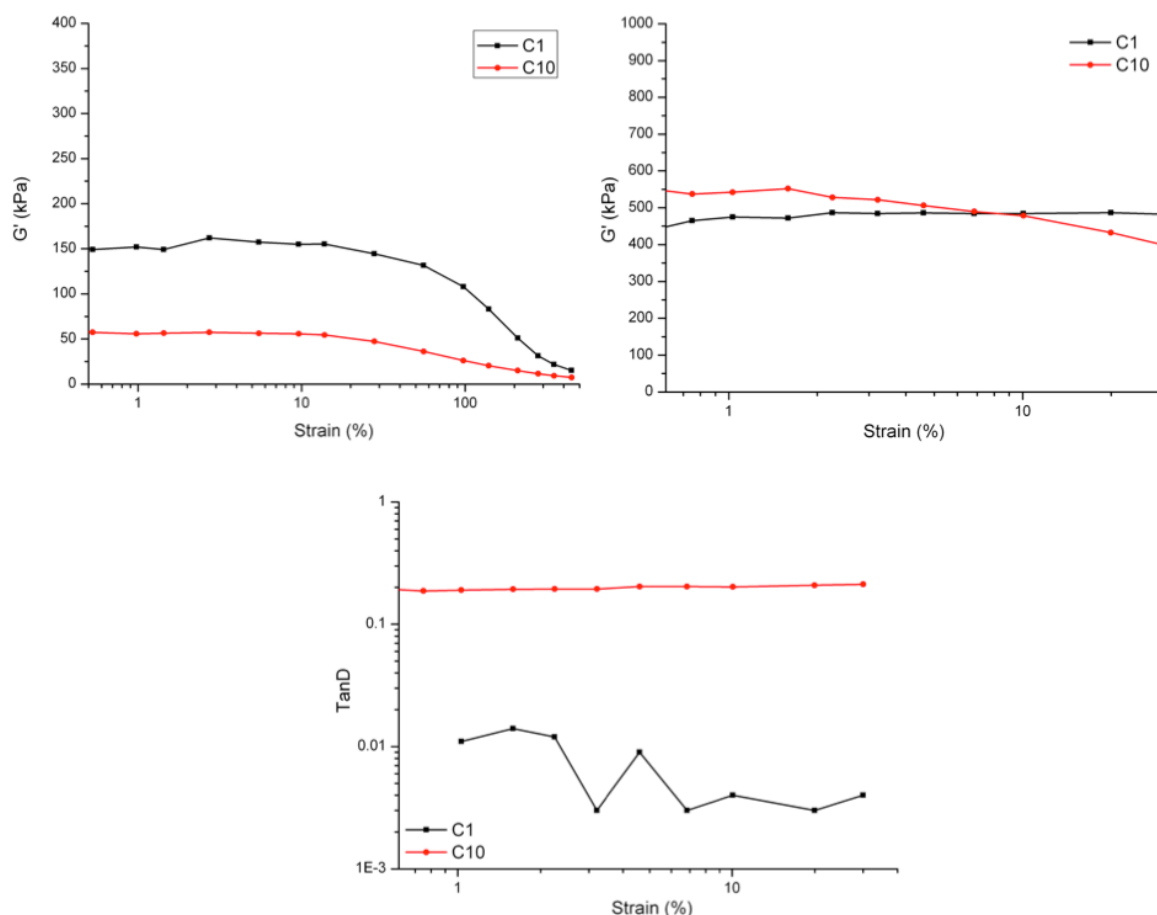


FIGURE 49 - UPPER LEFT: STORAGE MODULUS  $G'$  VS STRAIN OF UNCURED SAMPLES; UPPER RIGHT: STORAGE MODULUS  $G'$  VS STRAIN OF CURED SAMPLES; BOTTOM: TAND VS. STRAIN OF CURED SAMPLE. C1 BLACK LINE, C10 RED LINE.

From the analysis of the obtained results it is really difficult to claim that such a revolution of the rheological properties of the polymer is only due to the presence of hydrogen bonds which, instead, on other rubbers like the PB, have a diametrically opposed effect by stiffening the polymer matrix.

In particular, looking at the trace of the uncured compound, it can be seen that the sample C10 has a G' lower than a rubber without filler, indicating that the contribution given by the polymeric network has failed, with the only contribution left given from the hydrodynamic effect deriving from the introduction of 35 phr of silica in a reduced viscosity matrix.

	<b>C1</b>	<b>σ C1</b>	<b>C10</b>	<b>σ C10</b>
Stress (MPa) @ 50%	0.59	0.01	0.49	0.03
Stress (MPa) @ 100%	0.85	0.01	0.81	0.04
Stress (MPa) @ 200%	1.35	0.02	1.63	0.08
Stress (MPa) @ 300%	2.01	0.03	2.7	0.1
Stress (MPa) @ 500%	6.7	0.3	-	-
Load at break (MPa)	8.0	1.6	3.8	0.8
Elongation at break (%)	512	12	382	39

TABLE 30 – RESULTS OF TENSILE STRESS-STRAIN TEST OF CURED IR COMPOUNDS

#### 4.1.2 FUNCTIONALIZED BR-BASED COMPOUNDS

Unable to continue with IR functionalization but with a clear evidence of the ability of urazole residue to interact with the silica, we continued to investigate the TAD functionalization changing the polymer substrate. We chose a very well-known substrate like 1,4 cis-polybutadiene and we started functionalizing it on a larger scale, in order to be able to study its behavior in a compound. However, as previously mentioned, the production of pure BR compounds is not recommended, therefore, the adopted strategy was to produce compounds in which the polymer matrix consisted of a blend composed 50% by 1,4-cis-PB and 50% by 1,4 cis-IR.

This type of approach worsens the situation, since we introduce a further variable into an already complex system but, on the other hand, the payoff is very interesting.

As a first approximation, we can consider 1,4-cis-Polybutadiene and 1,4-cis-Polyisoprene as two immiscible polymeric phases. If you want to formulate a compound with a blend of two polymers like those, you will inevitably collide with the intrinsic compatibility of the filler in each of the two phases. In fact, the distribution of the filler will not be homogeneous, with a preferential migration in the most congenial phase, minimizing its surface energy.

The absence of any control, or only a marginal one, over the chance to perform a selective load on a specific polymer phase imposes heavy technological limits in the application of polymeric blends.

Our aim was to use our system as a tool able to selectively functionalize only a part of the polymer matrix, in order to unbalance the natural distribution of the filler, forcing it towards its less congenial phase.

We therefore started by functionalizing the BR with an increasing amount of PhTAD. Once the functionalized rubber has been obtained, it has been mixed with an identical quantity of non-functionalized IR, evaluating the final properties of the composite.

As in the case of pure IR-based compounds, different parameters have been investigated such as:

- amount of functionalizer (0.3 phr, 0.5 phr, 0.75 phr, 1.2 phr, 3 phr, 5 phr)
- type of filler (Silica 1165, CB N326)
- amount of filler (0 phr, 10 phr, 35 phr, 50 phr)
- formulation procedure (masterbatch)

- components of the vulcanizing pack (ZnO, Stearic Acid, CBS and Sulfur)

Each sample was analyzed with RPA and, according to the experimental tasks, the compounds were analyzed by DSC, DMTA, Stress strain test, swelling tests, and optical and electron microscopy (TEM).

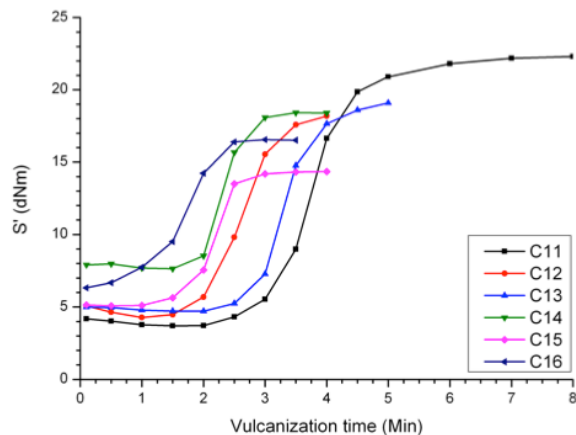
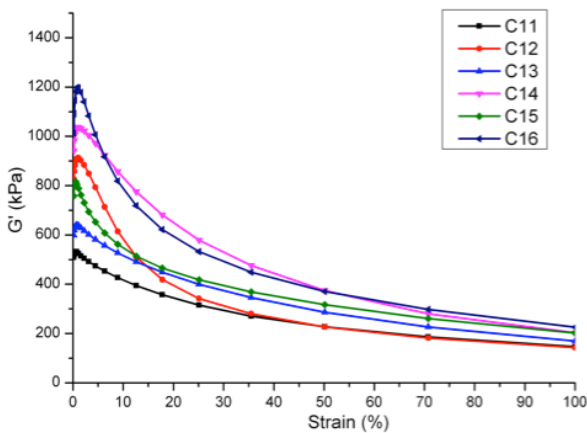
In the following, the keys experiments able to focus the problems encountered during the project will be shown.

Different amount of functionalizer:

In section 3.4.2. we have seen how the amount of functionalizer can affect the mechanical properties of the polymer. Here we can see how these changes affect the properties of a composite material, in particular we will refer to the compounds produced with PB functionalized to 0.5 and 5 phr (Table 31).

Entry	Polymer A (50 phr)	Polymer B (50phr)	PhTAD on B (phr)	Silica (phr)	TESPT (8% w/w)
C11	IR	BR	0	35	YES
C12	IR	BR	0	35	NO
C13	IR	BR	0.5	35	YES
C14	IR	BR	0.5	35	NO
C15	IR	BR	5	35	YES
C16	IR	BR	5	35	NO

TABLE 31 - LIST OF BR-BASED BLENDS WITH DIFFERENT AMOUNTS OF PHTAD



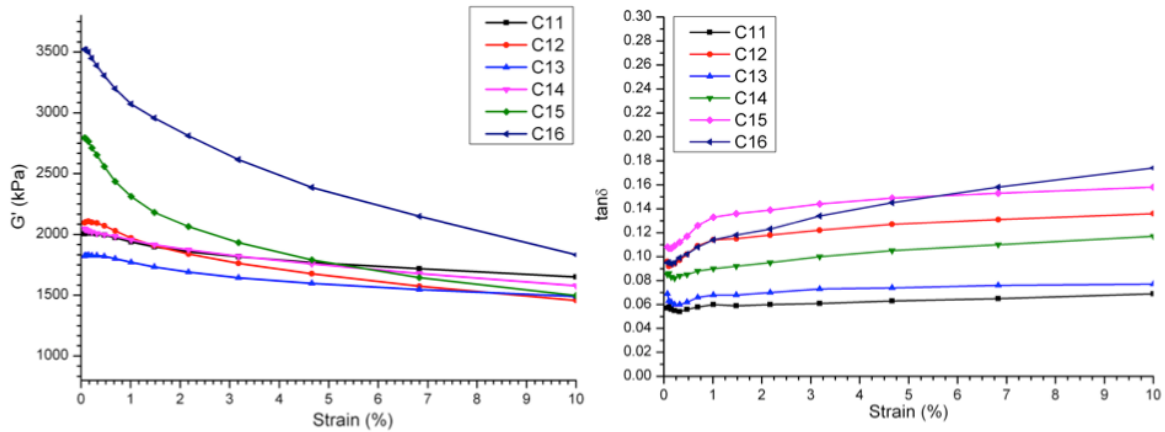


FIGURE 50 - RPA ANALYSIS OF DIFFERENT FUNCTIONALIZED COMPOUNDS. UPPER LEFT: UNCURED SAMPLES, UPPER RIGHT: VULCANIZATION CURVES, BOTTOM LEFT:  $G'$  VS. STRAIN OF CURED COMPOUND, BOTTOM RIGHT:  $\tan\delta$  VS. STRAIN OF CURED SAMPLES.

Starting from the strain-sweep measures (Figure 50) of the non-vulcanized compounds, we can see that the best compatibilization effect is definitely given by the C11 compound, that is the industry standard of reference in which the TESPT (black line) is present. C12, red line, of a similar composition but without the coupling agent, presents instead a decidedly higher form with a low strain, which is immediately lost as the deformation increases, a sign that the weak bonds that connect the particles to each other have been lost irreversibly.

As in the case of IR, the functionalized compounds 0.5 phr C13, blue line, and 5 phr C15, green line, have roughly the same trend of the reference sample with the curve translated upwards. In the case of the BR, especially for the sample with a higher degree of functionalization, a significant contribution to the value of  $G'$  can derive from the intrinsic rigidity of the functionalized polymer matrix, as we have seen in the graphs related to the variable temperature strain sweep in the previous chapter.

The behavior of the compounds formulated without the addition of silane C14, C16 is particular and different from what is observed with IR. In this case the curves not only have reinforcement values, with low strain, much higher than their non-functionalized counterpart, but this trend is conserved along the whole deformation even if in an increasingly less evident manner.

Already from these data (then confirmed by the tests carried out in the course of the research) we can begin to draw some lines of the general picture: it is clear that the functionalization is not irrelevant for its introduction into the mixture, moreover, with the increase of the degree of functionalization, the PB tends to stiffen, with a consequent increase in the value of  $G'$  at low strain.

Looking at the curves of vulcanization (stopped at 90% of their maximum S' (MH)) some important trends that we will described are evident:

The functionalization causes a decrease of  $\Delta S'$ , as the result of the sum of two different effects: the increase of ML and the reduction of MH. The growth of the value of ML can be easily accounted for the greater rigidity of the starting polymer matrix as mentioned before, while the reduction of the value of MH could probably be ascribed to a worse quality of the final polymer network. In addition to the absolute values of S', however, it is also interesting to notice how the kinetics of vulcanization is heavily influenced by the presence of the functionalizer, contrary to what was found with Pure IR based compounds.

From these initial findings it seems clear that the functionalizer under investigation not only manages to interact with the silica but can also interfere with the vulcanization process with obvious and evident repercussions on the final quality of the polymer network and the final properties of the composite.

This particular aspect of the research will also be resumed later with specific tests to understand these interactions.

Although all samples without TESPT have a non-negligible Payne effect, it is still possible to state that the principle behind this approach is correct. It is undeniable that the system is able to interact non-trivially with the fillers present in the polymer matrix. Nevertheless, it is clear that, to achieve some good results with this type of reaction, a low loading of PhTAD is recommended. In particular, if we look at the G' curves as a function of the strain of the C12 and C14 samples, we can see how the latter manages to have a similar pattern to the C11 reference standard and better than the blend without any type of coupling agent, while C16 did not show a valuable result.

Stress and strain profiles of the samples just described were collected and the results summarized in the table below:

<b>Sample</b>	<b>C11</b>	<b>C12</b>	<b>C13</b>	<b>C14</b>	<b>C15</b>	<b>C16</b>
Stress (MPa) @ 100%	2.2	1.1	2.9	2.2	1.2	1.1
Stress (MPa) @ 300%	9.8	2.7	-	6.9	3.8	2.6
Load at break (MPa)	10.6	17.5	8.1	7.2	8.1	3.2

Elongation at break (%)	308	797	218	312	458	345
-------------------------	-----	-----	-----	-----	-----	-----

TABLE 32 - RESULTS OF TENSILE STRESS TEST PERFORMED ON CURED SAMPLES

It is interesting to note that the functionalized C14 compound, after a 100% imposed deformation, produces the same stress as the industrial standard, and a similar load at break, another sign that the interaction between filler and functionalizing, in the right conditions, presents potential.

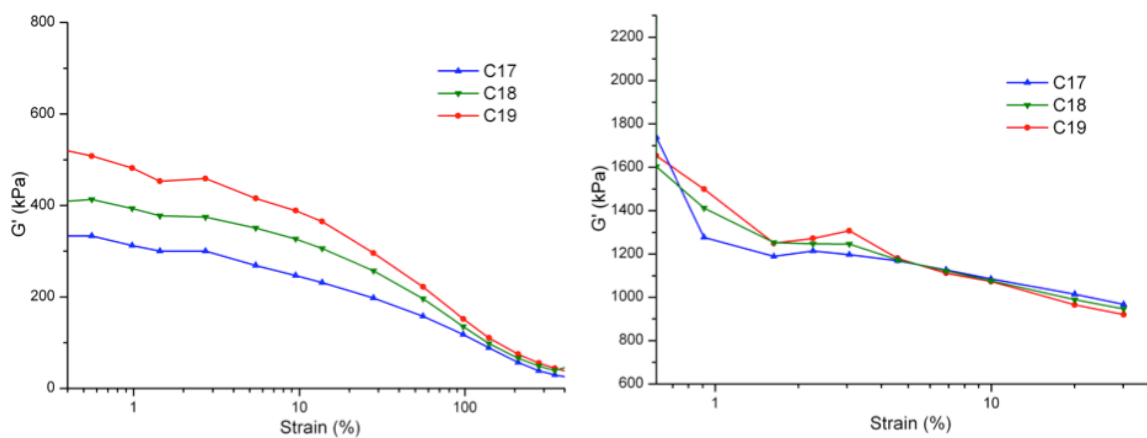
**Different nature of the filler:**

Despite the indications that corroborated the idea of a filler-rubber interaction mediated by hydrogen bonds, with those experiments it was not possible to totally unravel the doubt. As we have seen, the introduction of PhTAD into a compound produces tangible effects on the kinetics of vulcanization, therefore, to understand if the observed phenomena were attributable or not to this fact, a specific experiment was set up.

Using a carbon-based filler instead of silica, the docking sites the functionalizer should interact with should fail. In this way, in principle, it would have been possible to separate the phenomena linked to vulcanization and those linked to the effect of compatibilizer (Table 33, Figure 51).

Entry	Polymer A (50 phr)	Polymer B (50phr)	PhTAD on B (phr)	CB N326 (phr)	TESPT (8% w/w)
C17	IR	BR	0	35	NO
C18	IR	BR	0.75	35	NO
C19	IR	BR	1.2	35	NO

TABLE 33 - LIST OF FUNCTIONALIZED COMPOUNDS WITH CB N326 AS FILLER



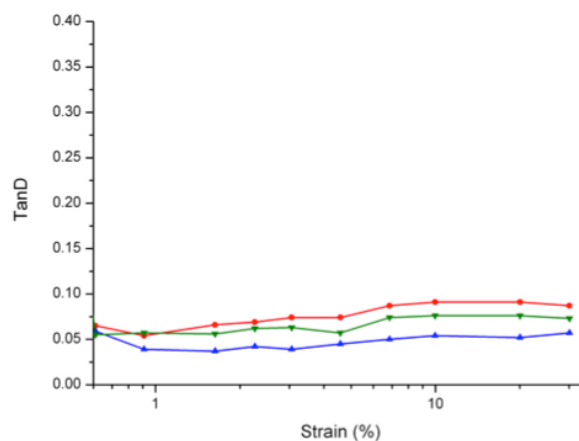


FIGURE 51 - PLOT OF RPA ANALYSIS OF FUNCTIONALIZED COMPOUNDS WITH N326 AS FILLER - UPPER LEFT: UNCURED SAMPLES, UPPER RIGHT, G' VS. STRAIN OF CURED SAMPLES, BOTTOM TAND VS. STRAIN ON CURED SAMPLES.

From a general point of view, the experiment gave the expected result, but observing the data in detail it is possible to make further considerations. First of all, in the graph related to the uncured sample, we can see how the amount of functionalizing stiffens the polymer matrix, probably due to the molecular recognition between the pending urazole units. There is also to consider the fact that the analysis was carried out at 70 °C which, according to what we saw in paragraph 3.4.3, would not be enough to break the polymer network held together by hydrogen bonds.

Once the compounds have been vulcanized, the three curves converge towards a common value, without appreciable differences. This indicates that, after heating the sample, the functionalizer does not interact with the filler, behaving like the standard reference.

However, by analyzing the timing and kinetics of vulcanization, there are many similarities with the experiments reported at the beginning of this section (Table 34). Also in this case, in fact, the process is altered by the presence of the functionalizer in a similar way to what has been previously seen.

Sample	C17	C18	Sample	C17	C18
S' (ML)	1.76	2.52	Stress (MPa) @50%	1.2	1.3
S' (Max)	16.78	13.99	Stress (MPa) @100%	2.0	2.3
T10	3:00	2:38	Stress (MPa) @200%	4.7	5.5
T90	4:47	3:25	Load at break (MPa)	15.1	9.9
			Elongation at break (%)	411	288

TABLE 34 - LEFT: VULICANIZATION RESULT, RIGHT: TENSILE STRENGHT TEST

Taking samples C17 and C18 as a reference, we note (Table 34) that the  $\Delta S'$  is significantly reduced ( $\approx -20\%$ ) and the vulcanization has a much faster course.

The analogies continue also in the tensile behavior of the two samples, with the more rigid and less deformable C18, in line with the other functionalized compounds.

### **Distribution of the filler in the polymer matrix:**

Despite having gathered encouraging data, there were still many questions that needed to be answered in order to reach a complete comprehension of the topic.

In particular, we tried to understand how the filler was distributed in each phase of the functionalized polymer blend. To do this, six compounds were prepared (three loaded with silica and three without filler), including two formulated with the PB functionalized in bulk described in paragraph 3.5, and other two compounds with the corresponding cyclized molecule, with almost the same degree of functionalization (0.5 phr of PhTAD) (Table 35).

<b>Entry</b>	<b>Polymer A (50 phr)</b>	<b>Polymer B (50phr)</b>	<b>Coupling Agent (CA)</b>	<b>Amount of CA (phr)</b>	<b>Silica (phr)</b>
C20	IR	BR	SemiC	≈0.75	0
C21	IR	BR	SemiC	≈0.75	35
C22	IR	BR	PhTAD	0.5	0
C23	IR	BR	PhTAD	0.5	35
C24	IR	BR	None	0	0
C25	IR	BR	None	0	35

TABLE 35 - LIST OF PB/IR BLEND COMPOUNDS FOR DMTA

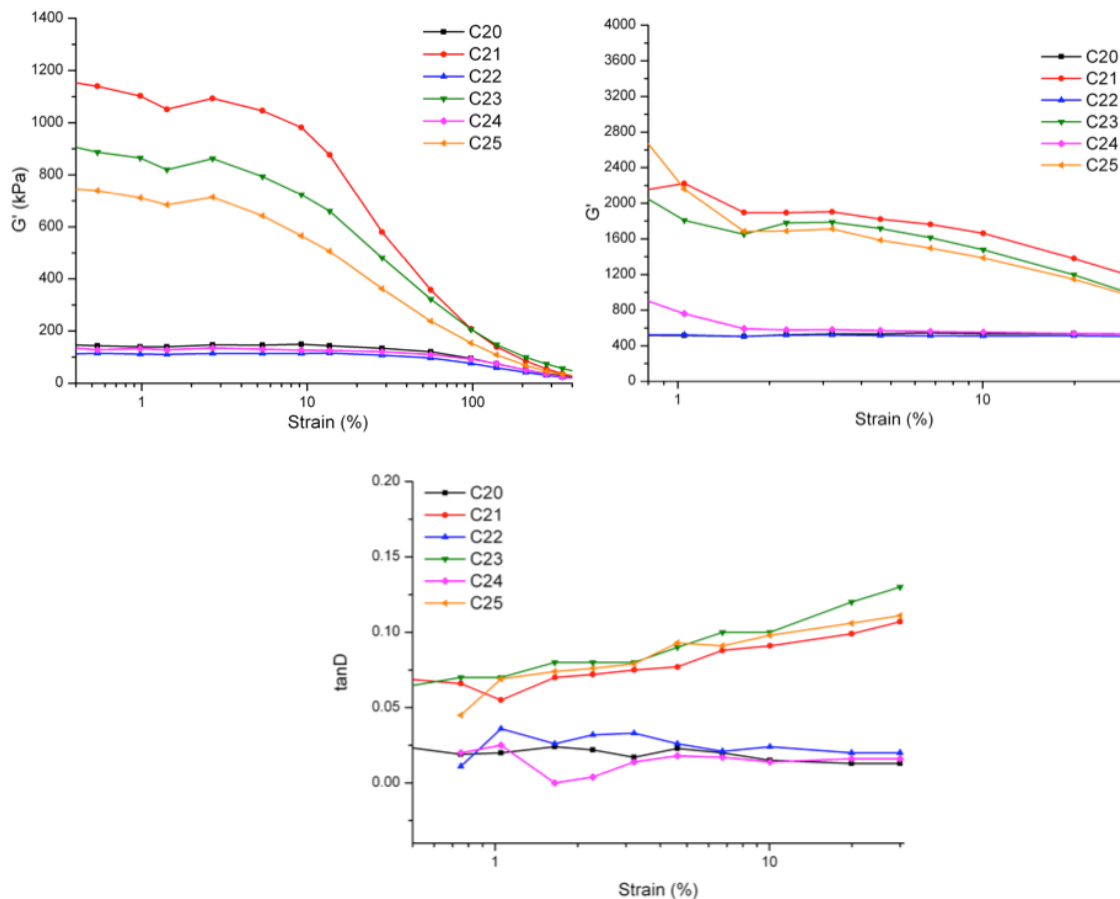


FIGURE 52 - RPA STRESS STRAIN TEST. UPPER LEFT: UNCURED SAMPLES; UPPER RIGHT:  $G'$  VS. STRAIN OF CURED SAMPLES, BOTTOM:  $\tan\delta$  VS STRAIN OF CURED SAMPLES.

As expected, the RPA curves of the compounds without fillers are extremely similar, since the functionalization is contained within 1 phr and the only contribution to  $G'$  is provided by the polymer network (Figure 52).

The situation is slightly different if we refer to the loaded compounds: the properties of the three vulcanized compounds seem much more similar than for the raw ones, in any case, the functionalized compounds have a storage modulus higher than the pristine blend, with comparable values both as a Payne effect and as a  $\tan\delta$ . Moreover, the thermally functionalized polymer with SemiC turns out to be the best of the three samples analyzed.

According to what reported in the literature by Klüppel,<sup>144</sup> it is possible to calculate how much filler is inside each of the phases in a binary system of immiscible polymers. Within certain approximations, this is possible because the dissipated energy ( $G''$  max) increases linearly with the volume fraction of filler contained in it.

$$G''_{max} = G_0 + \alpha \phi_F$$

Where  $\phi_F$  is the volume fraction of filler content in the polymer matrix and  $G_0$  is the maximum dissipated energy for an unfilled compound.

Then, after calculating the coefficients needed for the analysis of the contributions of the single polymer phases in a blend, a temperature dependent dynamic-mechanical analysis was performed on C20-C25 compounds according to the operating parameters stated in the appendix (Figure 53, 54).

The experiments were performed on a range of temperature between -120 °C and +40 °C but, for reasons of clarity, in the graphs below will be report only the relevant part of the collected data.

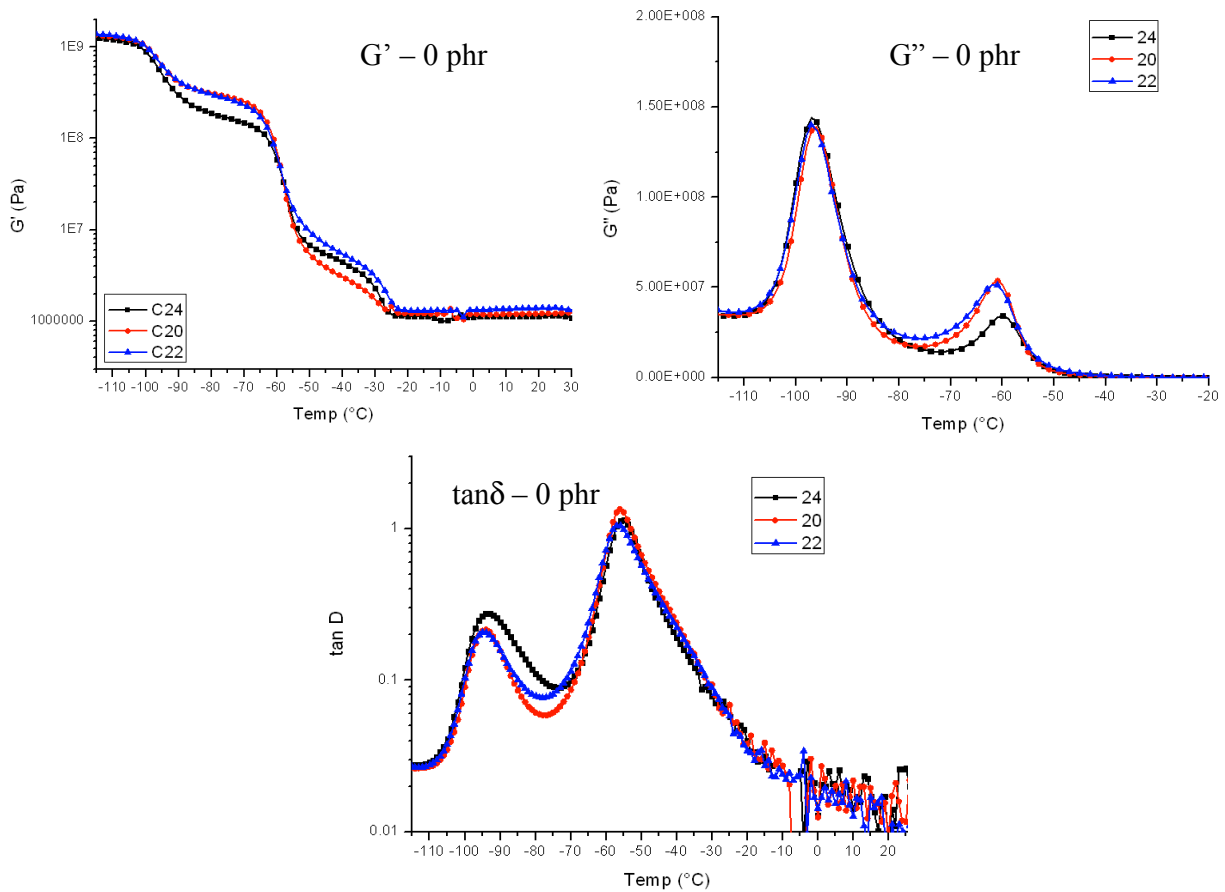


FIGURE 53 - DMTA ANALYSIS OF FUNCTIONALIZED BLENDS WITHOUT FILLER.

The data obtained from this analysis were unexpected and particularly complicated to rationalize.

For sake of simplicity, the analysis of the spectra will be given dividing the samples according to the presence (or absence) of the filler inside the matrix.

The best option is to start from samples without fillers, in order to observe only the behavior due to the polymer matrix.

As it can be seen in the graph of  $G'$ , we have a first drop in the value of the storage modulus corresponding to the glass transition temperature of the PB, so in the area between  $-90\text{ }^{\circ}\text{C}$  and  $-70\text{ }^{\circ}\text{C}$  there is an interphase zone, where the two functionalized polymers appear to be more rigid than the non-functionalized one. This is consistent with the presence of hydrogen bonds in the polymer matrix. The second step, around  $-60\text{ }^{\circ}\text{C}$ , is due to the glass transition temperature of the IR, so we can find a second interphase zone (between  $-50\text{ }^{\circ}\text{C}$  and  $-20\text{ }^{\circ}\text{C}$ ), where the trace of one of the two functionalized polymers (C20) is below that of the non-functionalized one. This anomaly in the behavior may be due to interface phenomena between the different phases of the polymer domains, able to immobilize part of the chains by delaying or accelerating the loss of the storage modulus, or may be related to a different crystallization of BR part induced by both temperature and functionalization.

Moving to the graph of the dissipated energy  $G''$ , the first thing that can be noticed is that the two polymers are still distinct, so the introduced functionalization is not able to alter in depth the miscibility of the two phases. Each of the two peaks represents the contribution to the dissipated energy ( $G''$ ) given by the single polymer phase, respectively at  $-97\text{ }^{\circ}\text{C}$  we find the peak relative to the BR and at about  $-60\text{ }^{\circ}\text{C}$  the one relative to the IR phase. Contrary to expectation, despite the fact that only the BR phase was involved in the functionalization, we can see how both the position and the shape of C20 and C22 are identical to the non-functionalized reference sample C24.

If what has just been described is unexpected, the data relative to the IR part of the compound, not involved in any step of the functionalization process, in which the maximum absolute value of the peak increases by about 50%, are even more surprising.

A possible explanation for this phenomenon is linked to what has been observed in the vulcanization process of the previously described compounds. In fact, if the polarity of the macromolecule is locally modified, from the theoretical point of view, this would allow a migration towards that position of all the ingredients present in the compound.

A decrease in the amount of vulcanizing agents in the IR phase would cause an upper-left shift of the peak, exactly as in our case but, associated with it, there should also be a rigid translation downward and to the left of the graph of  $G'$ , which does not seem to happen.

It is however clear that these phenomena occurring at the interface have a heavy influence on the quality of the final product and the issue deserves a thorough investigation with specific experiments concerning the diffusion of vulcanizing agents across different polymer phases, which is beyond the aim of this project.

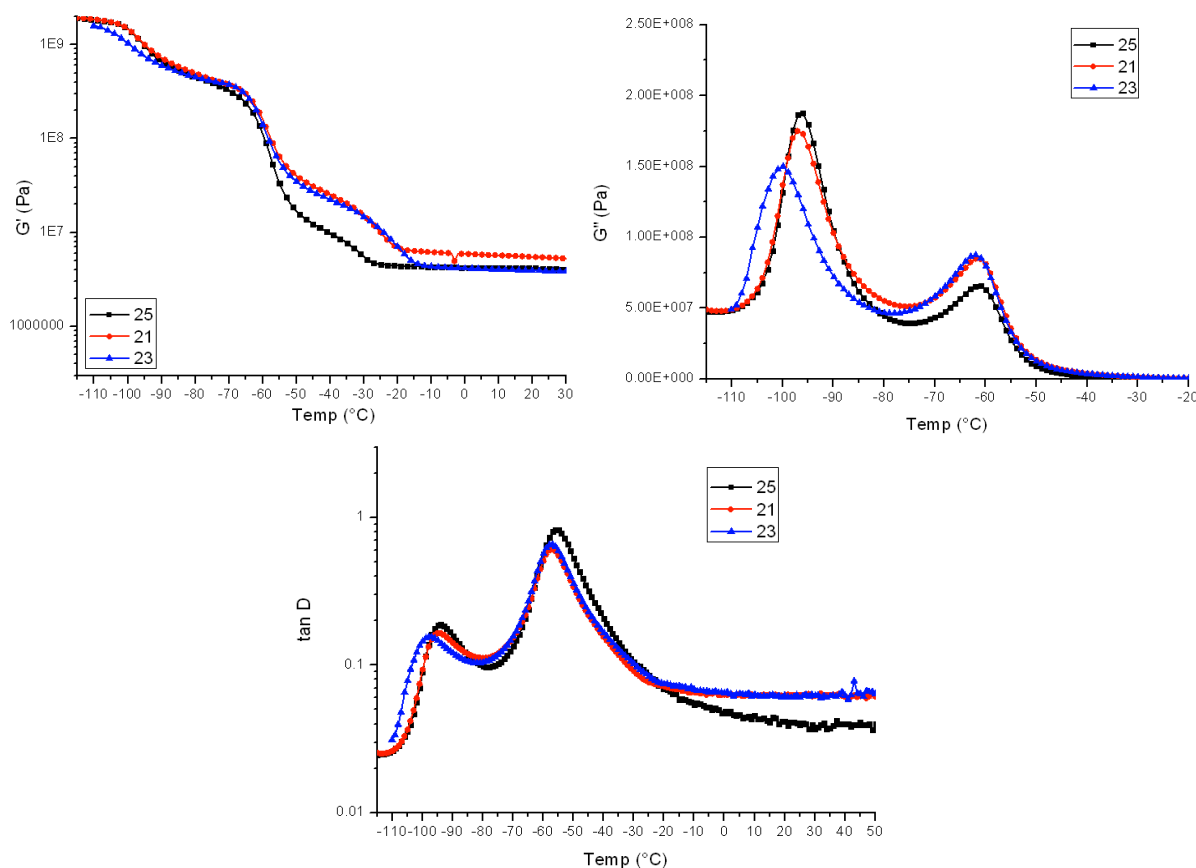


FIGURE 54 -DMTA ANALYSIS OF FUNCTIONALIZED POLYMER BLENDS FILLED WITH 35 PHR OF SILICA.

Focusing on the samples with a similar composition but filled with 35 phr of silica, we could notice the difference of behavior of  $G'$  compared to the unfilled compounds. In addition to the obvious increase of the storage modulus due to the presence of the filler, we can see also in this case the two drops corresponding to the glass transition temperature of each polymer phase.

The behavior of the compounds in the temperature range between -50 °C and -20 °C is very different. In this case the two functionalized compounds retain a residual value of  $G'$  higher than

the reference. This phenomenon could be explained only in part with the temperature induced crystallization of BR, while the effect of the functionalizer and its interaction with the filler is more likely to be the cause of this particular behavior.

If possible, the interpretation of data relating to  $G''$  is even more complicated. Usually the addition of filler to a compound causes the increase of the absolute value and the widening of the peak corresponding to the polymer phase in which the filler has been incorporated. However, sample 23 (and only marginally 21) presents a totally unexpected behavior: functionalization with PhTAD has left the absolute value  $G''$  unchanged, while the position of the maximum is shifted to lower temperatures. This is not consistent with the addition of the filler and allows us to assume a non-optimal distribution of silica inside the polymer phases.

Similarly to samples unfilled, also in this case the peak relative to the IR phase presents a different behavior between the functionalized compound and the reference one. This unique behavior makes impossible to estimate, according to the methods known in literature, the amount of filler presents in each polymer of the blend. For this reason the best option to understand the silica distribution in the compound was to perform a morphological characterization through TEM images (Figure 55).

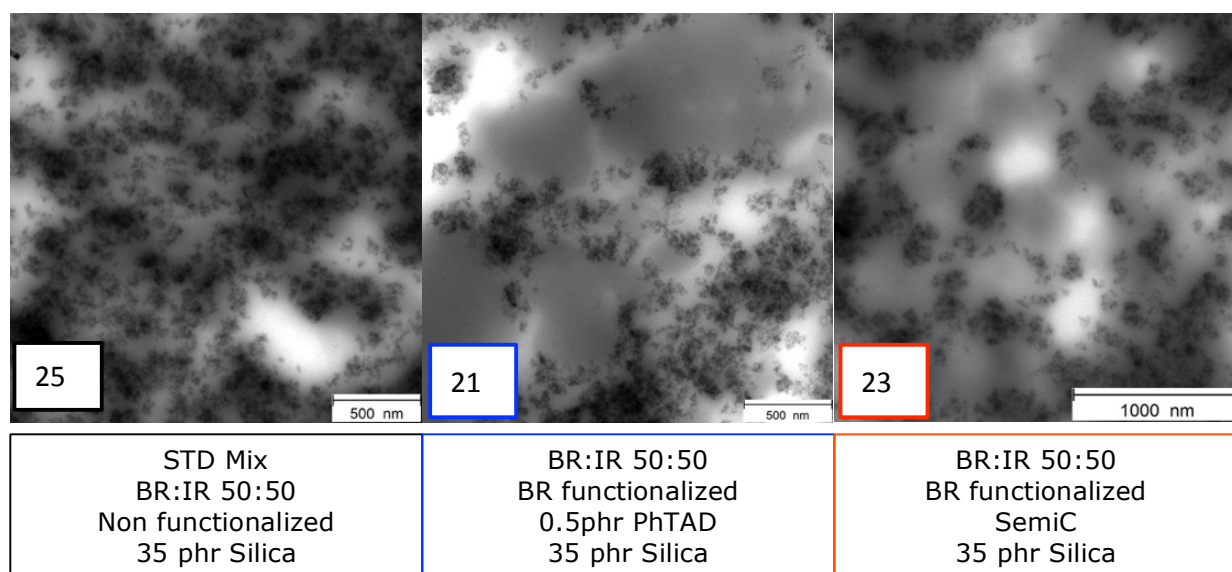


FIGURE 55 - TEM MICROGRAPHS OF SAMPLES 25 – NON FUNCTIONALIZED, 21 – BR FUNCTIONALIZED WITH 0.5 PHR OF PHTAD AND 23 – BR FUNCTIONALIZED WITH SEMIC.

Of over twenty images collected for each sample, only three are shown as a representative example. As can be seen from the picture the non-functionalized compound (black) has a quite homogeneous distribution of the filler. Both the functionalized compounds (blue and red), on the other hand, have

a non homogeneous filler distribution probably due to a different shape and distribution of the polymer domains in the blend. In fact two areas with a different phase contrast can be identified, indicating that we are observing the two polymers which are the constituents of the compound. The appearance of these domains is consistent with the hypothesis advanced during the analysis of DMA data about the interference of the functionalizer during the vulcanization process. The fact that two different, immiscible, polymers have different curing times is known,<sup>145</sup> starting from this, it is reasonable to expect that, by concentrating part of the vulcanizing pack in one of the two phases due to the variation of the local polarity (of the BR in our case), the whole curing process may be modified, leading to an unexpected segregation of the filler.

## 5. CONCLUSIONS

This project was created to act as a trailblazer to a new line of research, scarcely investigated in literature due to the intrinsic difficulty related to the functionalization of polymeric backbone starting from commercially available olefins, for tire applications. When a totally new project is started, especially if, as in this case, the group's background is totally different, the research must begin from scratch.

The first part of my PhD activity was therefore spent extensively surveying the literature and focusing on the state of the art of the topic. Once done, it was therefore necessary to search through the reactions typical of organic chemistry in order to identify a series of suitable families of reactants, able to meet the stringent requirements imposed by the poor substrate reactivity and, indirectly, by its processability. In agreement with the industrial partner, financier of the project, three roads have been explored:

- The addition to the double bonds of the polymer matrix through 1,3-dipolar cycloaddition reactions
- Thio-ene reactions, mainly based on the use of sulfur radicals
- Alder-ene reactions

We started from the addition of 1,3-dipole. One of the main advantages of this type of reaction is the selectivity to the vinyl double bonds present on a polymer chain. In addition, this system allows the formation of a substituted 5-member ring, the ideal substrate for the introduction of further functionalizations.

Several dipoles have been tested, both allyl type (bended) as nitrones, and propargyl-allenyl type (linear) such as nitrile oxides prepared in situ starting from the corresponding oxime. Through the use of strongly electron-acceptor fluorinated systems, in both cases (N-methyl- $\alpha$ -pentafluorophenylnitrone and pentafluorobenzaldehydeoxime), it was possible to obtain an addition product with satisfactory yields. To the best of our knowledge, this is one of the first examples of 1,3-dipole cycloaddition on a commercial polymer using fluorinated systems.

Then we moved to thio-ene type functionalization; several tests were performed, exploiting the reactivity of sulfur radicals. Although it is a well-known type of reactivity, it has some

disadvantages that limit its use, first of all, the need to introduce free radicals into the reaction environment, which can cause a premature cross-linking of the rubber matrix. After verifying the strengths and weaknesses of each reactivity, the most promising one should have been based on an Alder-Ene reaction, which involves the interaction between an olefin (bearing an hydrogen atom in an allyl position) and an electron-poor enophile.

The enophilic compound we studied as a model system was 4-phenyl-1,2,4-triazoline-3,5-dione (PhTAD).

This system, once anchored on the polymer, has a free hydrazidic hydrogen, able to locally modify the polarity of the matrix and, at the same time, able to interact through hydrogen bonds with inorganic fillers such as silica. The research activity was therefore focused on the chemical modification, with PhTAD, of commercial olefins. These modified polymers, with different amounts of functionalizer, were then characterized by a multitechnical approach (DSC, TGA, FT-IR and swelling tests) and subsequently tested into compounds.

The rheological properties of the compounds obtained were evaluated both with an oscillating disk rheometer (ODR), by dynamic mechanical analysis at variable temperatures (DMTA) and by analyzing stress-strain curves.

It was therefore attempted to resolve the critical issues that emerged when using PhTAD as a functionalization agent. First of all, it was necessary to optimize the synthesis of this molecule, despite the huge amount of oxidative procedures that have been reported in literature.

Then several degrees of functionalization were tested on different polymeric matrices and those produced on a larger scale were also tested in rubber compound. The best results were achieved with the functionalization of a IR matrix with 0.5 phr of PhTAD. In that case the tensile strength behavior of the functionalized polymer was significantly better than the non-functionalized one.

Usually the functionalization of a polymer matrix can produce composites in which the values of the  $G'$  modulus are comparable with those of the industrial standards reference, which are based on the use of compatibilizing agents such as TESPT, along with a slight contextual deterioration of the values such as  $\tan\delta$  or the Payne effect, indicating an effective interaction between the polymer matrix functionalized with silica fillers, even if not yet optimal.

Moreover, one of the major intrinsic problems to be solved in the use of a molecule such as PhTAD lies in its high reactivity, which makes it impossible to operate in bulk, directly on the pristine polymer.

The last part of the project was then dedicated to the synthesis of functionalizers of a similar nature, based on diazenics derivatives, but less reactive, in order to make the reaction occur on the polymer directly in the formulation phase, at the temperatures normally used to process compounds ( $\approx 140$  °C), thus avoiding the difficulty due to operating in solution.

In particular, the successful functionalization of a model oligomeric system with ethyl (anilincarbonyl) diazenecarboxylate has allowed to demonstrate the validity of the idea of a thermally stimulated mass functionalization, opening to the possibility of using other molecular systems, that can be specifically tuned to perform a specific function within the compound.

## 6. APPENDIX A – MATERIAL AND INSTRUMENT

All the chemical reagents used for the synthesis and functionalization of rubber matrix were purchased from Fluorchem, except 1-pyrenbutanol purchased from Aldrich and used without any further purification.

Several instruments have been used for the chemical and physical characterization of the samples produced.

### **Nuclear Magnetic Resonance (NMR) Spectroscopy:**

<sup>1</sup>H-NMR spectra were recorded by using a Bruker AMX-500 spectrometer operating at 500 MHz and a Bruker AVANCE III HD operating at 400MHz.

### **Optical spectroscopy:**

UV-VIS absorption spectra were recorded by using a Jasco V570 spectrophotometer.

Emission fluorescence spectra were recorded by using a Jasco FP6300.

IR spectra were collected with a PerkinElmer FTIR spectrophotometer Spectrum 100 working in ATR (Attenuate Total Reflectance) mode.

All the spectra were collected with a resolution of 4 cm<sup>-1</sup>, in the mid-range infrared region between ranging from 4000 cm<sup>-1</sup> to 550 cm<sup>-1</sup>. Each sample spectra reported is the average of 16 scans after baseline subtraction.

Morphological characterization of cured compounds was performed on a Zeiss Libra 120 Zeiss TEM, operating at 120 kV as accelerating voltage in order to avoid the rupture of the polymer matrix. Images were recorded with 25000x, 10000x and 5000x magnification.

The most critical aspect was the preparation of the sample. In order to produce ultrathin slices, the polymer must be cooled below its glass transition temperature. Since the analyzed samples were composed by a rubber blend of 50:50 BR:IR, the cutting procedure were performed with a Leica EM UC6 cryo-Ultramicrotome cooled with liquid nitrogen at -130 °C equipped with a diamond knife. The thickness of the sections was approximately 100 nm.

These experiments were performed in the lab of the Deutsches Institut für Kautschuktechnologie (DIK) – Hannover – Germany, by Dr. Viktor Rose, in collaboration with prof. Ulrich Giese.

### **Thermal characterization:**

In order to determine the thermal behavior, in particular the glass transition temperature ( $T_g$ ) of polymers, both functionalized or in their pristine form, several thermograms were recorded.

The temperature ramps were set in accordance to the nature of the polymer (or compound) analyzed, ranging from  $-135\text{ }^\circ\text{C}$  (with PB) or  $-90\text{ }^\circ\text{C}$  (with IR) to  $+120\text{ }^\circ\text{C}$  at  $10\text{ }^\circ\text{C}/\text{min}$ . The temperature reported are always referred to the second scan recorded, in order to reset the thermal history of the sample. The thermograms were recorded with two different instruments: a Mettler-Toledo DSC 1 STAR<sup>e</sup> System (sample analyzed at University of Milano-Bicocca) and a 2920 Modulated DSC from TA Instruments (sample analyzed at DIK).

Besides differential scanning calorimetry (DSC), the thermal properties, in particular the thermal stability, of the functionalized samples were investigated through thermogravimetric analysis (TGA). The thermograms were recorded with a Mettler Toledo TGA/DSC1 Star System.

### **Rubber functionalization and rheological compound characterization:**

- Rubber functionalization

In order to functionalize a polymer matrix, the polymer mass were dissolved in a 3 L reactor equipped with an IKA EUROSTAR 20 digital overhead stirrer, the impeller used was a collapsible blade impeller (R 1352 centrifugal stirrer, IKA).

- Compound formulation

For blend preparation two different internal mixers were used, a Brabender Plasti-corder lab station, present in the Pirelli laboratories, with a mixing chamber of 50 mL, and a Thermo Haake PolyLab Rheomix 600 at Deutsches Institut für Kautschuktechnologie (DIK), with a 58-mL mixing chamber. In both cases the filling factor was kept constant in order to keep the mixing process homogeneous.

- Oscillating Dish Rheometry (ODR)

The uncured samples were analyzed with a Rubber Process Analyzer (RPA 2000, Alpha Technologies) operating in shear stress mode. A typical experiment was structured as following:

A strain-sweep test was carried out at  $70\text{ }^\circ\text{C}$  with an imposed strain ranging from 0.2 up to 400% of elongation at 10 Hz, recording  $G'$ ,  $G''$ ,  $G^*$  and  $\text{Tan}\delta$  values. The sample was then heated up to  $170\text{ }^\circ\text{C}$  and cured, recording the values of  $S'$ . After a delay of 5 min at  $70\text{ }^\circ\text{C}$  was performed a new

strain-sweep test on the cured sample. This test was carried out at 70 °C from 1% to 10% of elongation at 1 Hz.



The specimen for this test was cut using a Constant Volume Rubber Sample Cutter (Cutter 2000 from alpha technologies).

- Vulcanization process

After establishing the optimal vulcanization time with RPA, the uncured samples were vulcanized by heating them to 170 °C in a vacuum hydraulic press in a 2-mm-thick metal mold. The vulcanization press was a Rucks KV207.00.

- Stress strain test

Stress-strain measurements were performed on dog-bone shaped specimens (Type 2) according to DIN 53 504 from vulcanized flat sheets. The equipment used in this test was a Zwick/Roell Z010. Each results reported in the dissertation are referred to the average result of five samples tested. The samples were stretched at a constant traction rate of 200 mm/min till failure. Ultimate tensile strength, elongation at break and load at different elongation were recorded.

This characterization was carried out in DIK's laboratories.

- Dynamic Mechanical Thermal Analysis (DMTA)

Test specimens were deformed in torsion on a dynamic analyzer (ARES 3A5 Rheometrics Scientific) at 1 Hz and 0.5% strain amplitude and a heating rate of 1 °C/min, in a temperature range from -130 °C up to +40 °C.

This characterization was carried out in DIK's laboratories.

- Swelling test

From each 2-mm-thick strips of vulcanized sample, 3 disk of 1.5 cm of diameter were cut and placed in a sealed vessel with 20 mL of solvent (Toluene or DCM). Then the weight was recorded at 0 h, 6 h, 24 h, 48 h and 72 h, replacing the solvent with fresh one every 24 h.

After 72 h the swollen mass was dried in a vacuum oven at 60 °C for 24 h and weighted again.

Swelling ratio (Q%), absolute swelling ratio (q) and extractable fraction (f) were calculated from the data collected, with (Q%) defined as:  $\left(\frac{M_s - M_0}{M_0}\right) \cdot 100$ , where  $M_s$  is the mass of swollen sample and  $M_0$  is the starting mass of the sample.

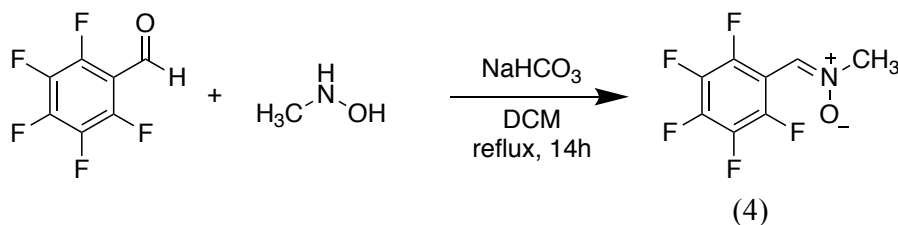
The absolute swelling ratio (q) was calculated as follow:  $\frac{M_s}{M_d}$  where  $M_d$  is the mass of the swollen sample after drying process.

Finally the extractable fraction (f) was calculated:  $\left(\frac{M_0 - M_d}{M_d}\right) \cdot 100$

The specimens for this test were cut using a Constant Volume Rubber Sample Cutter (Cutter 2000 from alpha technologies).

## 7. APPENDIX B – EXPERIMENTAL PART

### Synthesis of N-methyl- $\alpha$ -pentafluorophenylnitron (4)



Reagent	M.W. (g/mol)	Weight (g)	mmol	eq
Pentafluorobenzaldehyde	196.07	0.1	0.51	1
N-methylhydroxylamine	83.52	0.051	0.61	1.2
Sodium bicarbonate	84.01	0.130	1.53	2.5

Solvent: DCM dry

100 mg (0.51 mmol) of pentafluorobenzaldehyde, 51 mg (0.61 mmol) of N-methylhydroxylamine and 8 mL of dry DCM were added to a round bottom flask equipped with a water condenser under nitrogen atmosphere. The reaction mixture was refluxed under magnetic stirring for 14 hours. The reaction progress was followed by TLC, monitoring the disappearance of the perfluorobenzaldehyde spot.

The reaction mixture was allowed to cool down to room temperature and filtered on a short silica pad, eluting with DCM and Ethyl Acetate the product (4) in a pure form with 98% of yields.

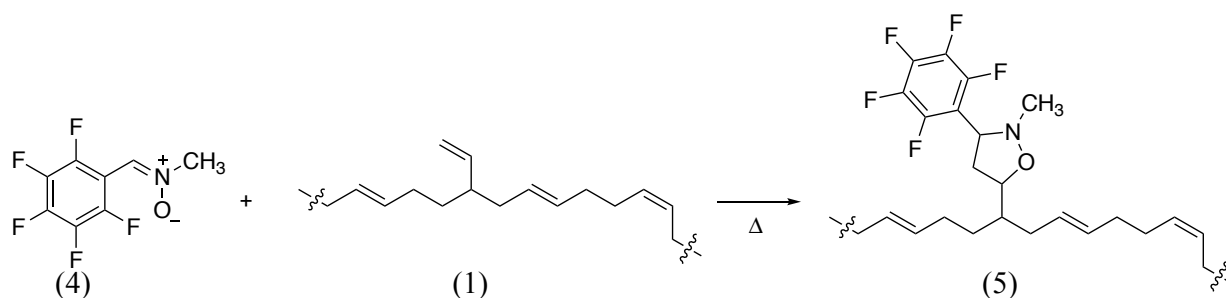
Physical aspect: Solid, white powder

R<sub>f</sub> (4) DCM = 0, EtOAc = 0.5

<sup>1</sup>H NMR (CDCl<sub>3</sub>, 300 MHz):  $\delta$  (ppm) = 3.96 (s, 3H, -CH<sub>3</sub>), 7.38 (s, 1H, CH=N)

FTIR-ATR (cm<sup>-1</sup>, intensity): 702, M; 734, M; 762, M; 805, M; 819, W; 846, W; 945, VS; 984, S; 999, S; 1020, W; 1036, W; 1049, W; 1102, M; 1132, W; 1139, M; 1154, M; 1198, S; 1315, M; 1353, W; 1368, W; 1385, M; 1400, M; 1418, S; 1464, M; 1494, VS; 1519, S; 1566, W; 1587, W; 1653, W; 3025, W; 3051, W; 3082, W.

### Synthesis of (5) - Functionalized PB oligomer with N-methyl- $\alpha$ -pentafluorophenylnitrone (4)



Reagent	M.W. (g/mol)	Weight (g)	mmol	eq
(1) – Polyvest vinyl double bonds	54.09	v.a.	v.a	1
(1) - Polyvest	54.09	v.a.	v.a	100
(4) - N-methyl- $\alpha$ -pentafluorophenylnitrone	225.12	v.a.	v.a	v.a.

#### (See table 5) – General procedure

v.a. various amount, Solvent: DCM, 1,2 – DCE, Heat source: Hot plate,  $\mu$ W oven

The proper amount of Polyvest was dissolved in the solvent chosen for the experiment at concentration of 15 mg/mL. The system was kept under vigorous stirring for 30 minutes, then the proper amount of (4) was added to the reaction mixture and heated at the condition stated in the table 5 – Section 3.1.

The work-up procedures were performed with three cycles of purification composed as follow:

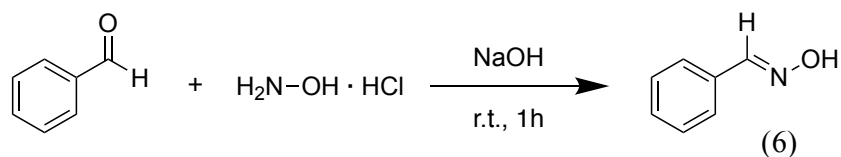
- Precipitation in MeOH - The amount of methanol used was 20 to 30 times the volume of the reaction solvent.
- Centrifugation - The suspension was centrifuged at 12'000 rpm for 20 min.
- Skimming – The solvent mixture was removed from the centrifuge tube.
- Dissolution in fresh DCM – The precipitated polymer was dissolved again in a fresh solvent and purified again.

After washing procedure, the sample was collected and dried under reduced pressure.

Physical aspect: yellowish viscous liquid.

<sup>1</sup>H NMR (CDCl<sub>3</sub>, 500 MHz):  $\delta$  (ppm) = 1.26, 1.41, 1.65, 2.08 (4H, CH<sub>2</sub>-CH=CH), 2.72, 4.03 (1H, Ph-CH-N, Nitronium), 4.05 (1H, Ph-CH-N, Nitronium), 4.98 (2H, CH=CH<sub>2</sub> vinyl PB), 5.38 (2H, cis + trans CH<sub>2</sub>-CH=CH).

### Synthesis of benzaldehydeoxime (6)



Reagent	M.W. (g/mol)	Weight (g)	mmol	eq
Benzaldehyde	106.12	2.1	20	1
Hydroxyl amine hydrochloride	69.19	1.4	20	1
Sodium Hydroxide	40.00	1.6	40	2

Solvent: mix of Ice, Water and Ethanol (2:1:1 ratio)

Freshly distilled benzaldehyde (2.1 g, 20 mmol) was added to a solution of hydroxyl amine hydrochloride (1.4 g, 20 mmol) dissolved in a mixture of 5 mL of water, 5 mL of ethanol and 10 mL of ice.

1.6 g of NaOH were solved in 5 mL of water and subsequently dripped into the reaction mixture.

After 20 minutes of stirring, the solution becomes clear and after 1 h the starting reagent was totally converted.

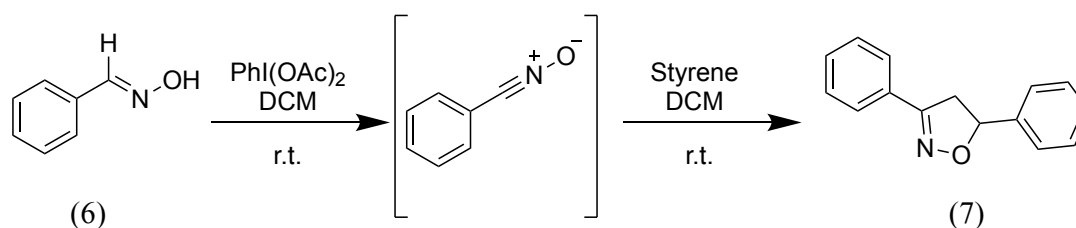
The reaction mixture was extracted 2 times with diethylether (Et<sub>2</sub>O) in order to remove the benzaldehyde, then the aqueous layer was acidified with HCl conc. to pH $\approx$ 5 and the solvent was removed under reduced pressure to afford the desired oxime in a pure form with excellent yield (95%).

Physical aspect: yellow oil.

<sup>1</sup>H NMR (CDCl<sub>3</sub>, 500 MHz):  $\delta$  (ppm) = 7.41 (m, 3H -C<sub>6</sub>H<sub>5</sub>), 7.63 (m, 2H -C<sub>6</sub>H<sub>5</sub>), 8.25 (s, 1H Ph-CH=N), 10.03 (s, 1H -OH).

FTIR-ATR (cm<sup>-1</sup>, intensity): 689, VS; 753, VS; 869, S; 946, S; 1075, W; 1177, VW; 1209, M; 1289, M; 1304, M; 1445, W; 1454, W; 1493, W; 1578, VW; 1599, W; 1632, W; 1694, W; 2920, W; 3028, W; 3064, W; 3294, bM;

### Synthesis of 3,5-diphenyl-4,5-dihydroisoxazole (7)



Reagent	M.W. (g/mol)	Weight (g)	mmol	eq
benzaldehydeoxime (6)	121.14	0.07	0.57	1
PhI(OAc) <sub>2</sub> - PIDA	322.1	0.18	0.55	0.98
Styrene	104.15	0.06	0.57	1

Solvent: DCM

70 mg (0.57 mmol) of benzaldehydeoxime (6), 180 mg of PIDA (0.55 mol) and 60 mg (0.57 mmol) of styrene were solved in 8 mL of DCM.

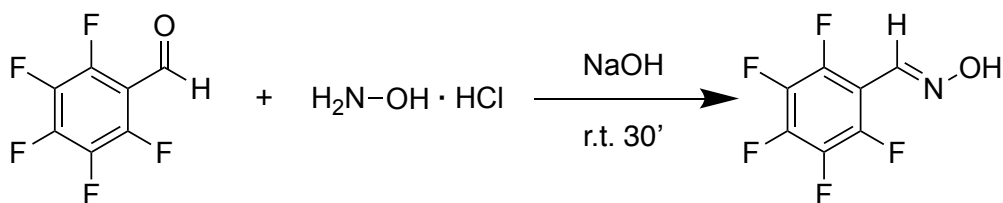
The reaction was followed by TLC (DCM as eluent) and, after 2 hours of stirring, the crude product was chromatographed over silica gel column (100% DCM), affording the desired isoxazole compound with 42% yield.

Physical aspect: white solid.

<sup>1</sup>H NMR (CDCl<sub>3</sub>, 500 MHz): δ (ppm) = 3.36 (dd, 1H C-CH<sub>2</sub>-CH), 3.79 (dd, 1H C-CH<sub>2</sub>-CH), 5.75 (dd, 1H CH<sub>2</sub>-CH-O), 7.33 (m, 1H -C<sub>6</sub>H<sub>5</sub>), 7.41 (m, 7H -C<sub>6</sub>H<sub>5</sub>), 7.70 (m, 2H -C<sub>6</sub>H<sub>5</sub>).

FTIR-ATR (cm<sup>-1</sup>, intensity): 685, VS; 695, S; 749, VS; 859, S; 892, S; 925, M; 974, W; 998, W; 1020, W; 1039, W; 1053, W; 1077, W; 1166, W; 1206, W; 1238, W; 1287, W; 1300, W; 1332, W; 1353, M; 1363, M; 1447, M; 1492, M; 1563, W; 1593, W; 2878, W; 2919, W; 2976, VW; 3028, W; 3062, W;

### Synthesis of pentafluorobenzaldehydeoxime (8)



Reagent	M.W. (g/mol)	Weight (g)	mmol	eq
Pentafluorobenzaldehyde	196.02	0.5	2.6	1
Hydroxyl amine hydrochloride	69.19	0.18	2.6	1
Sodium Hydroxide	40.00	0.11	5.2	2

Solvent: Mix of Water and MeOH (1:1 ratio)

Pentafluorobenzaldehyde (0.5 g, 2.6 mmol) and hydroxyl amine hydrochloride (0.18 g, 2.6 mmol) were dissolved in a mixture of 5 mL of water and 5 mL of methanol.

0.25 mL of aqueous NaOH (32% w/w) were subsequently dripped into the reaction mixture.

After 30 minutes of stirring, methanol was removed from the reaction mixture heating the crude under reduced pressure.

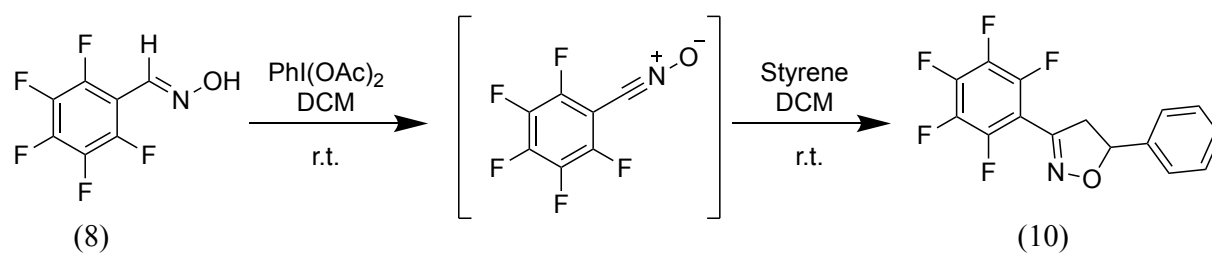
The product was extracted from the aqueous layer 3 times with AcOEt, the organic layers were collected then dried over Na<sub>2</sub>SO<sub>4</sub> and the solvent was removed under reduced pressure to afford the desired pentafluorobenzaldehydeoxime (8) with 90% yield.

Physical aspect: white solid.

<sup>1</sup>H NMR (CDCl<sub>3</sub>, 500 MHz): δ (ppm) = 8.23 (s, 1H Ph-CH=N), 8.28 (bs, 1H -OH).

FTIR-ATR (cm<sup>-1</sup>, intensity): 699, S; 785, M; 831, W; 939, S; 1025, S; 1134, S; 1158, M; 1304, M; 1319, M; 1381, M; 1422, S; 1493, VS; 1522, S; 1649, M; 2237, W; 3009, W; 3300, M.

### Synthesis of 3-(pentafluorophenyl)-5-phenyl-4,5-dihydroisoxazole (10)



Reagent	M.W. (g/mol)	Weight (g)	mmol	eq
pentafluorobenzaldehydeoxime (8)	211.08	0.08	0.4	1
PhI(OAc) <sub>2</sub> - PIDA	322.1	0.13	0.39	0.98
Styrene	104.15	0.04	0.4	1

Solvent: DCM

80 mg (0.4 mmol) of pentafluorobenzaldehydeoxime (8), 130 mg of PIDA (0.39 mol) and 41 mg (0.4 mmol) of styrene were solved in 10 mL of DCM.

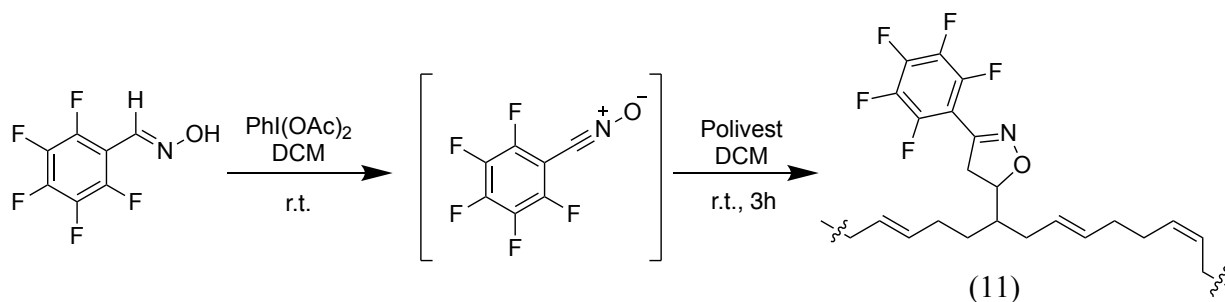
The course of the reaction was followed every hour by TLC (Hexane 50%, DCM 50% as eluent) until full conversion of pentafluorobenzaldehydeoxime (8). After 5 hours of stirring, the crude product was chromatographed over silica gel column (Hexane 50%, DCM 50%) afforded the desired compound with 61% yield.

Physical aspect: white solid.

<sup>1</sup>H NMR (CDCl<sub>3</sub>, 500 MHz): δ (ppm) = 3.38 (dd, 1H C-CH<sub>2</sub>-CH), 3.81 (dd, 1H C-CH<sub>2</sub>-CH), 5.79 (dd, 1H CH<sub>2</sub>-CH-O), 7.48-7.32 (m, 5H -C<sub>6</sub>H<sub>5</sub>).

FTIR-ATR (cm<sup>-1</sup>, intensity): 684, W; 700, S; 754, VS; 789, S; 830, M; 884, S; 918, S; 929, M; 980, VS; 990, VS; 1037, W; 1069, S; 1145, W; 1202, W; 1343, S; 1358, M; 1431, S; 1453, M; 1487, VS; 1524, S; 1585, M; 1654, W; 2855, VW; 2915, W.

### Synthesis of (11) - Functionalized PB oligomer with pentafluorobenzaldehydeoxime (8)



Reagent	M.W. (g/mol)	Weight (mg)	mmol	eq
(1) – Polyvest vinyl double bonds	54.09	0.77	0.001	1
(1) - Polyvest	54.09	76.9	1.42	100
pentafluorobenzaldehydeoxime (8)	211.08	300	1.42	100
PhI(OAc) <sub>2</sub> - PIDA	322.1	455	1.35	99

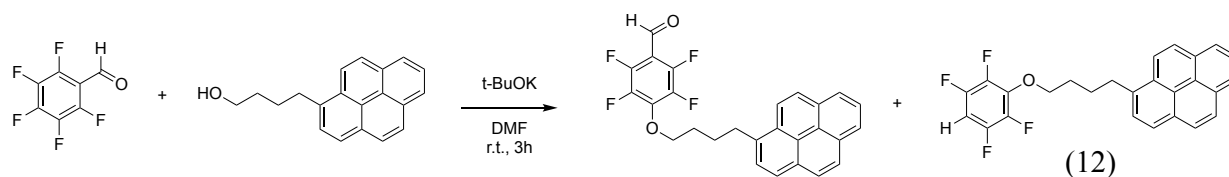
Solvent: DCM

300 mg (1.42 mmol) of pentafluorobenzaldehydeoxime (8) and 76.9 mg (1.42 mmol) of Polyvest were solved in 10 mL of DCM. Then, after 5 minutes of stirring, a solution of 455 mg of PIDA (1.35 mol) in 10 mL of DCM was dripped into the reaction mixture. After 3 hours of stirring it was no longer possible to detect the presence of the reactant (8) on TLC (100% DCM). 5 mL of solvent were evaporated off under reduced pressure, then the reaction mixture was poured into cold MeOH (125 mL). The next morning the presence of a precipitate was clear. The product was purified by 3 cycles of precipitation-centrifugation as described in the synthetic procedures of adduct (5).

<sup>1</sup>H NMR (CDCl<sub>3</sub>, 500 MHz): δ (ppm) = 1.42, 1.64, 2.08, 2.69, 3.32 - 3.54 (H-isoxazole), 4.51- 4.65 (H-isoxazole), 5.38.

FTIR-ATR (cm<sup>-1</sup>, intensity): 728, VS; 801, W; 907, S; 992, M; 1071, W; 1344, W; 1437, W; 1494, M; 1523, M; 1574, VW; 1655, VW; 2854, VW; 2936, W; 3007, VW.

### Synthesis of (12) - 1-[4-(2,3,5,6-tetrafluorophenoxy)butyl]pyrene



Reagent	M.W. (g/mol)	Weight (mg)	mmol	eq
pentafluorobenzaldehyde	196.07	50	0.255	1
1-Pyrenbutanol	274.36	77	0.290	1.1
Potassium <i>tert</i> -butoxide	112.21	69	0.617	2.2

Solvent: DMF

69 mg (0.62 mmol) of Potassium *tert*-butoxide were added to a solution of 50 mg (0.25 mmol) of pentafluorobenzaldehyde and 77 mg (0.29 mmol) of pyrenbutanol in 6 mL of DMF. 15 minutes after the addition of *t*-BuOK the reaction mixture had on a deep red color. The solution was stirred at room temperature for 3 h. After that, 10 mL of water were added to the reaction mixture, the resulting pink suspension was extracted three times with Et<sub>2</sub>O. The aqueous layer was still fluorescent under UV light, so it was extracted again for three times with AcOEt.

The combined organic fractions were washed with fresh water, then dried over MgSO<sub>4</sub> and the solvent was evaporated under reduced pressure affording a pale-yellow oil.

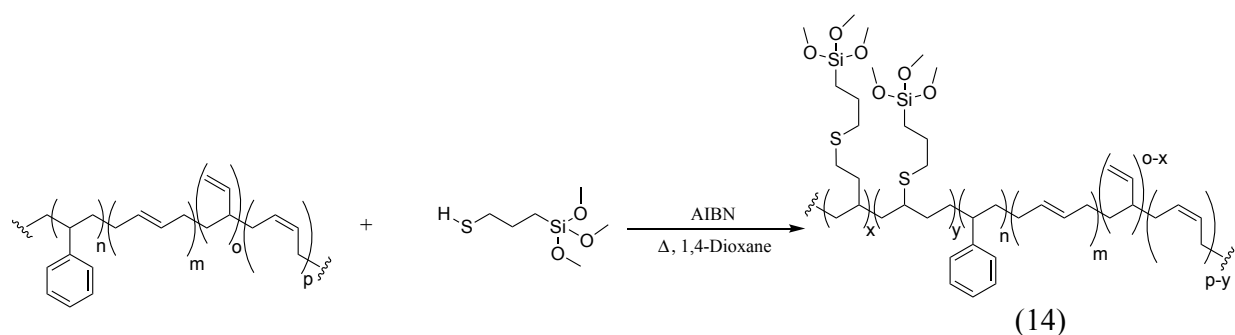
The crude product was purified by chromatographic column (80% Hexane, 20% DCM) affording 41 mg of 2,3,5,6-tetrafluoro-4-[4-(1-pyrenyl)butoxy]-benzaldehyde (12) instead of the desired product. (36% Yield)

Physical aspect: brown wax.

<sup>1</sup>H NMR (CDCl<sub>3</sub>, 500 MHz): δ (ppm) = 1.92-2.02 (m, 2H O-CH<sub>2</sub>-CH<sub>2</sub>-CH<sub>2</sub>), 2.06-2.09 (m, 2H O-CH<sub>2</sub>-CH<sub>2</sub>-CH<sub>2</sub>), 3.36 - 3.49 (m, 2H CH<sub>2</sub>-CH<sub>2</sub>-C), 4.27 (t, 2H O-CH<sub>2</sub>), 6.67 – 6.77 (m, 1H 4F-Ph-H), 7.88 (d, 1H), 7.99 (t, 1H), 8.03 (d, 2H), 8.10 – 8.14 (m, 2H), 8.15 – 8.20 (m, 2H), 8.29 (d, 1H).

FTIR-ATR (cm<sup>-1</sup>, intensity): 678.00, M; 690.00, M; 710.00, VS; 763.00, S; 820.00, VS; 839.00, VS; 917.00, S; 964.00, S; 1044.00, S; 1097.00, S; 1174.00, S; 1243.00, W; 1261.00, M; 1297.00, W; 1355.00, M; 1386.00, M; 1414.00, M; 1436.00, M; 1460.00, S; 1471.00, S; 1494.00, VS; 1510.00, VS; 1600.00, W; 1635.00, M; 1649.00, M; 2870.00, W; 2894.00, W; 2937.00, W; 2961.00, W; 3042.00, W; 3093.00, W

**Synthesis of (14) – Functionalized polymers with 3-Mercaptopropyl)-trimethoxysilane (See table X) – General procedure**



Entry	Polimer	n (%wt)	m+p (%mol)	o (%mol)	MPTES eq.	AIBN eq.
1	Polyvest	0	99	1	0.1	0
2	Polyvest	0	99	1	0.01	0.001
3	Polyvest	0	99	1	0.1	0.01
4	Polyvest	0	99	1	0.2	0.02
5	BR40 - Neocis	0	97 cis	0.1<	0.2	0.02
6	SBR Ricon 100	25	27	73	4.7	0.47

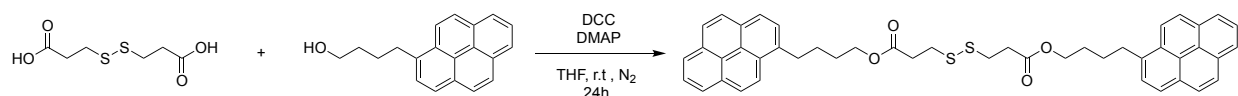
Solvent: 1,4 – Dioxane dry

The proper amount of polymer was dissolved into the solvent at concentration of 25 mg/mL (250 mg in 10 mL) in a sealed vessel. After the addition of the right amount of AIBN, the reaction mixture was degassed by three cycles of freeze-pump-thaw (FPT) and heated at 80 °C for 24 h, under vigorous stirring.

After 24 h the reaction was cooled down in an ice bath, the amount of solvent was reduced to 5 mL and the crude was purified with three cycles of precipitation-centrifugation with the same protocol used for functionalized polymer (5).

The isolated polymers were analyzed, if possible, with <sup>1</sup>H-NMR and FTIR spectroscopy.

## Synthesis of bis[4-(1-pyrenyl)butyl]-3,3'-disulfaneyldipropoanoate (15) – Steglich esterification



Reagent	M.W. (g/mol)	Weight (mg)	mmol	eq
1-Pyrenbutanol	274.36	100	0.36	1
Tiopropildicarboxyle acid	112.21	30.7	0.15	0.4
DCC	206.33	60.2	0.29	0.8
DMAP	122.17	2.3	0.02	0.05

Solvent: THF

100 mg (0.36 mmol) of 1-Pyrenbutanol, 30.7 mg (0.15 mmol) of tiopropylidicarboxyle acid and 60.2 mg (0.29 mmol) of DCC were dissolved in 6 mL of THF in a sealed flask under nitrogen atmosphere. After 15 min of stirring, a solution of 2.3 mg (0.05 mmol) of DMAP in 6 mL of THF was added to the reaction mixture.

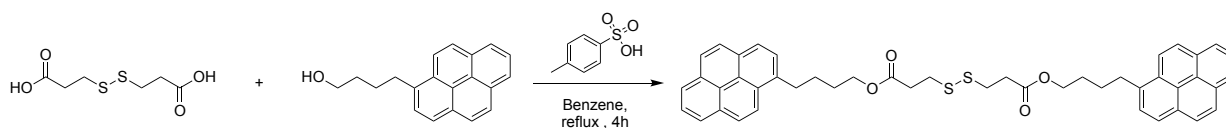
After 24 h the starting materials were consumed as indicated by TLC, and the reaction was worked up. The white precipitate (diphenylurea), due to the uptake of water from DCC, was removed by suction filtration on Hirsch funnel. The reaction solvent was removed under reduced pressure, then the residue was dissolved in DCM and purified by silica gel chromatography (100% DCM) to provide the desired compound (36 mg, 33% yield).

Physical aspect: brown wax

$^1\text{H}$  NMR ( $\text{CDCl}_3$ , 500 MHz):  $\delta$  (ppm) = 1.71-1.84 (m, 2H –O-CH<sub>2</sub>-CH<sub>2</sub>-CH<sub>2</sub>), 1.90-1.93 (m, 2H –O-CH<sub>2</sub>-CH<sub>2</sub>-CH<sub>2</sub>), 2.70 (t, 2H –CO-CH<sub>2</sub>-CH<sub>2</sub>-S), 2.89 (t, 2H –CO-CH<sub>2</sub>-CH<sub>2</sub>-S), 3.35 (t, 2H –CH<sub>2</sub>-Py), 4.16 (t, 2H –O-CH<sub>2</sub>-CH<sub>2</sub>), 7.84 (d, 1H Py), 7.96 – 8.04 (m, 3H Py), 8.07-8.12 (m, 2H Py), 8.13 – 8.18 (m, 2H Py), 8.23 (d, 1H Py).

FTIR-ATR ( $\text{cm}^{-1}$ , intensity): 620.00, W; 681.00, W; 708.00, M; 720.00, M; 758.00, M; 818.00, M; 841.00, VS; 970.00, W; 1137.00, M; 1170.00, S; 1181.00, M; 1210.00, M; 1235.00, M; 1348.00, M; 1417.00, W; 1463.00, W; 1587.00, W; 1603.00, W; 1728.00, S; 2866.00, W; 2925.00, W; 3040.00, W;

## Synthesis of bis[4-(1-pyrenyl)-butyl]-3,3'-disulfanediyldipropoate (15) – Fischer esterification



Reagent	M.W. (g/mol)	Weight (mg)	mmol	eq
1-Pyrenbutanol	274.36	790.0	2.88	1
tiopropylidicarboxylic acid	210.27	302.8	1.44	0.5
p-toluen sulfonic acid	172.2	49.6	0.29	0.1

Solvent: Benzene

790 mg (2.88 mmol) of 1-Pyrenbutanol and 302.8 mg (1.44 mmol) of tiopropylidicarboxylic acid were dissolved in 10 mL of benzene in a round bottom flask equipped with dean stark trap. After 15 min of stirring, 49.6 mg (0.29 mmol) of p-toluene-sulfonic acid were added to the reaction mixture and heated to reflux. The course of the reaction was monitored by TLC, and after 4 hours all the starting materials were consumed.

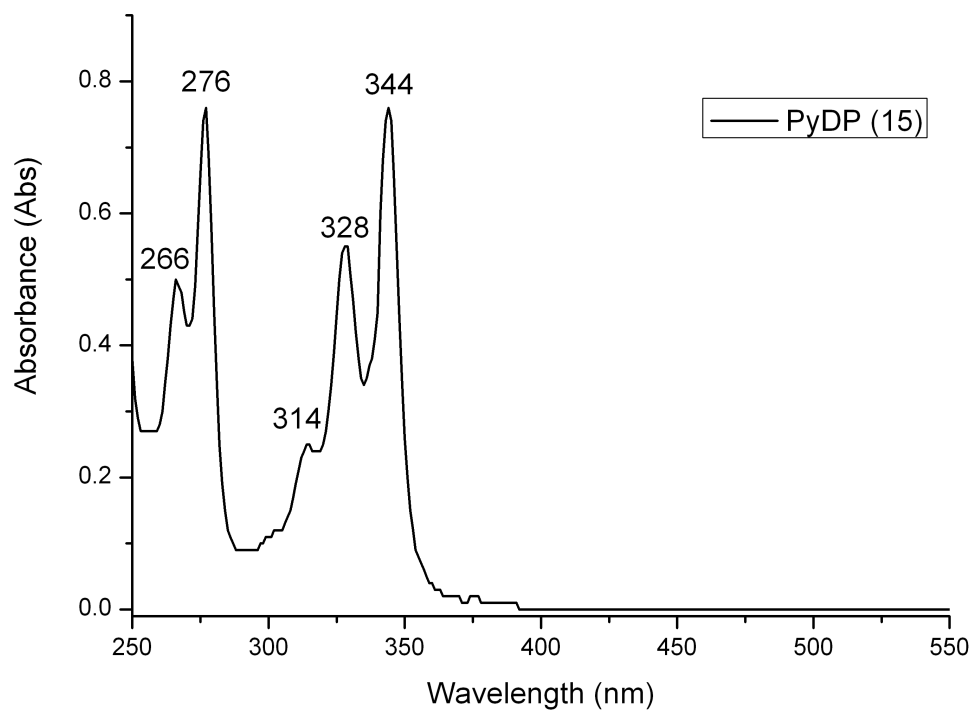
The benzene was evaporated under reduced pressure than the residue was dissolved in DCM. The organic layer was washed twice with aqueous NaHCO<sub>3</sub>, twice with H<sub>2</sub>O, dried over Na<sub>2</sub>SO<sub>4</sub>, and purified by silica gel chromatography (70% hexane 30% DCM) to provide the desired compound (938 mg, 91% yield).

Physical aspect: brown wax

<sup>1</sup>H NMR (CDCl<sub>3</sub>, 500 MHz): δ (ppm) = 1.71-1.84 (m, 2H –O-CH<sub>2</sub>-CH<sub>2</sub>-CH<sub>2</sub>), 1.90-1.93 (m, 2H –O-CH<sub>2</sub>-CH<sub>2</sub>-CH<sub>2</sub>), 2.70 (t, 2H –CO-CH<sub>2</sub>-CH<sub>2</sub>-S), 2.89 (t, 2H –CO-CH<sub>2</sub>-CH<sub>2</sub>-S), 3.35 (t, 2H –CH<sub>2</sub>-Py), 4.16 (t, 2H –O-CH<sub>2</sub>-CH<sub>2</sub>), 7.84 (d, 1H Py), 7.96 – 8.04 (m, 3H Py), 8.07-8.12 (m, 2H Py), 8.13 – 8.18 (m, 2H Py), 8.23 (d, 1H Py).

FTIR-ATR (cm<sup>-1</sup>, intensity): 620.00, W; 681.00, W; 708.00, M; 720.00, M; 758.00, M; 818.00, M; 841.00, VS; 970.00, W; 1137.00, M; 1170.00, S; 1181.00, M; 1210.00, M; 1235.00, M; 1348.00, M; 1417.00, W; 1463.00, W; 1587.00, W; 1603.00, W; 1728.00, S; 2866.00, W; 2925.00, W; 3040.00, W;

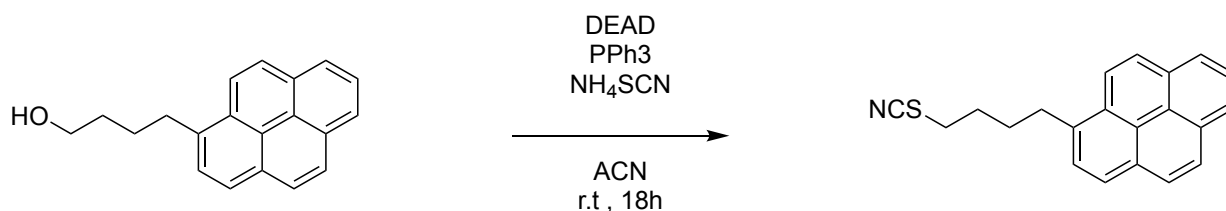
UV-VIS spectra:



Solution of PyDP in DCM:  $2.5 \cdot 10^{-4}$  M

$$\epsilon_{344} = 0.76361 / (1 \text{ cm} \cdot 2.5 \cdot 10^{-4} \text{ mol/L}) = 0.76361 / 0.00025 = 3054 \text{ M}^{-1} \text{ cm}^{-1}.$$

### Synthesis of 4-(1-pyrenyl)-butyl thiocyanate (16)



Reagent	M.W. (g/mol)	Weight (mg)	mmol	eq
1-Pyrenbutanol	274.36	500.00	1.82	1
DEAD	174.15	571	3.28	1.8
PPh <sub>3</sub>	262.29	860	3.28	1.8
NH <sub>4</sub> SCN	76.12	347	4.56	2.5

Solvent: Acetonitrile (ACN)

To a solution of 500 mg (1.82mmol) of 1-Pyrenbutanol in 10 mL of ACN, under vigorous stirring, each reagent was added into the reaction mixture at 5 minute intervals in this order: Diethyl azodicarboxylate (DEAD) 571 mg (3.28 mmol), Triphenylphosphine (PPh<sub>3</sub>) 860 mg (3.28 mmol) and ammonium thiocyanate (NH<sub>4</sub>SCN) 347 mg (4.56 mmol).

Starting from the addition of PPh<sub>3</sub>, the reaction mixture colour bleached from an intense orange to a pale yellow in few hours. This is due to the reduction of the aza-bridge of the DEAD moiety.

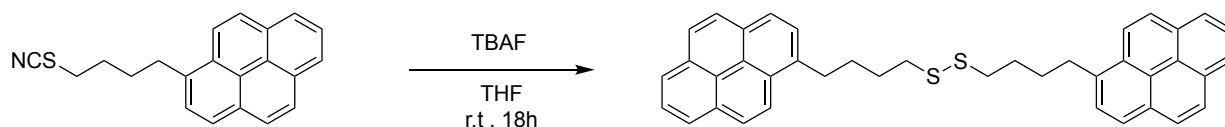
After 18 h the ACN was evaporated under reduced pressure, then the residue was dissolved in DCM. The crude product was purified by silica gel chromatography (70% hexane 30% DCM) to provide the desired compound (497 mg, 87% yield).

Physical aspect: Solid, White powder

<sup>1</sup>H NMR (CDCl<sub>3</sub>, 400 MHz):  $\delta$  (ppm) = 2.05 (m, 4H CH<sub>2</sub>-CH<sub>2</sub>-CH<sub>2</sub>-SCN), 3.01 (m, Py-CH<sub>2</sub>, 2H), 3.44 (s, 2H CH<sub>2</sub>-SCN), 7.89 (d, 1H), 8.03 (t, 1H), 8.06 (s, 2H), 8.13 – 8.17 (m, 2H), 8.20 (dt, 2H), 8.27 (d, 1H).

FTIR-ATR (cm<sup>-1</sup>, intensity): 557.00, W; 589.00, W; 679.00, M; 701.00, M; 710.00, S; 741.00, M; 752.00, W; 819.00, M; 840.00, VS; 903.00, W; 970.00, W; 1101.00, W; 1183.00, M; 1204.00, W; 1241.00, W; 1306.00, W; 1339.00, W; 1373.00, W; 1417.00, M; 1427.00, M; 1460.00, W; 1586.00, W; 1602.00, W; 2149.00, M; 2865.00, W; 2941.00, W; 3043.00, W.

### Synthesis of bis[4-(1-pyrenyl)butyl] disulfide (17)



Reagent	M.W. (g/mol)	Weight (mg)	mmol	eq
4-(1-pyrenyl)-butyl thiocyanate (16)	315.43	468.00	1.48	1
TBAF sol	261.46	775.85	2.97	2

Solvent: THF

468 mg (1.48 mmol) of 4-(1-pyrenyl)-butyl thiocyanate (16) and 2.97 mL of TBAF solution (1 M in THF) were dissolved in 8 mL of THF, under vigorous stirring.

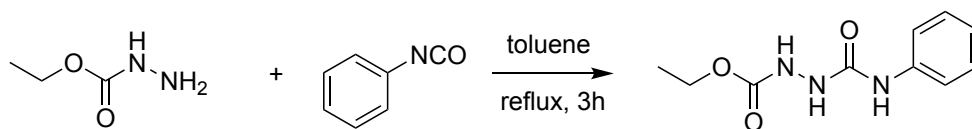
The reaction mixture was kept at room temperature for 18 hours, then the solvent was evaporated under reduced pressure and the residue was dissolved in DCM. The crude product was purified by silica gel chromatography (90% hexane 10% DCM) to provide the desired compound (421 mg, 98% yield).

Physical aspect: brown wax

$^1\text{H NMR}$  ( $\text{CDCl}_3$ , 400 MHz):  $\delta$  (ppm) = 1.76 – 1.94 (m, 4H  $\text{CH}_2\text{-CH}_2\text{-CH}_2\text{-S}$ ), 2.69 (t, 2H, Py- $\text{CH}_2$ ), 3.33 (t, 2H - $\text{S-CH}_2$ ), 7.84 (d, 1H), 7.98 (dd, 1H), 8.02 (d, 2H), 8.09 (d, 1H), 8.11 (d, 1H), 8.15 (d, 2H), 8.25 (d, 1H).

FTIR-ATR ( $\text{cm}^{-1}$ , intensity): 555.00, W; 587.00, M; 607.00, W; 677.00, M; 706.00, S; 727.00, W; 746.00, M; 757.00, M; 787.00, W; 797.00, W; 817.00, M; 835.00, VS; 872.00, VW; 896.00, W; 953.00, W; 962.00, W; 1044.00, W; 1067.00, W; 1099.00, W; 1138.00, W; 1158.00, W; 1184.00, M; 1198.00, W; 1235.00, W; 1243.00, W; 1254.00, W; 1260.00, W; 1305.00, W; 1332.00, W; 1363.00, W; 1373.00, W; 1413.00, M; 1431.00, W; 1458.00, W; 1487.00, W; 1509.00, W; 1585.00, W; 1602.00, W; 2864.00, W; 2900.00, W; 2930.00, W; 3037.00, W;

### Synthesis of ethyl 2-(anilincarbonyl)hydrazinecarboxylate (18)



Reagent	M.W. (g/mol)	Weight (mg)	mmol	eq
Ethyl carbazate	104.11	3018	28.99	1
Phenyl -isocyanate	119.12	3453	28.99	1

solvent: Toluene

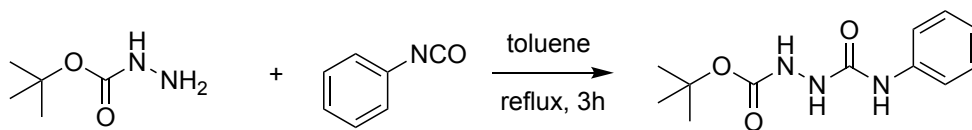
Ethylcarbazate (3.02 g, 29 mmol) was dissolved in 125 mL of toluene, under nitrogen atmosphere. The solution was cooled to 0 °C, then Phenyl -isocyanate (3.45 g, 29 mmol), in 15 mL of toluene, was added over a period of 10 min. The mixture was rinsed to r.t. and stirred for 30 min, then refluxed for 3 h. After cooling to r.t., the product was recovered by filtration, washed with cold toluene, and dried at 80 °C overnight (6.34 g, 98%).

Physical aspect: Solid, white crystals

<sup>1</sup>H NMR (DMSO-*d*<sub>6</sub>, 400 MHz): δ (ppm) = 1.20 (t, 3H -CH<sub>3</sub>), 4.06 (q, 2H -CH<sub>2</sub>-CH<sub>3</sub>), 6.83-7.01 (m, 1H), 7.17 – 7.33 (m, 2H), 7.46 (d, 2H), 7.98 (s, 1H -NH), 8.70 (s, 1H -NH), 8.91 (s, 1H -NH),

FTIR-ATR (cm<sup>-1</sup>, intensity): 667.00, W; 694.00, S; 743.00, S; 761.00, M; 787.00, W; 855.00, W; 897.00, W; 910.00, W; 1026.00, M; 1054.00, S; 1079.00, W; 1096.00, W; 1116.00, W; 1204.00, VS; 1227.00, VS; 1306.00, M; 1318.00, M; 1368.00, W; 1393.00, W; 1443.00, S; 1492.00, S; 1503.00, S; 1527.00, S; 1556.00, VS; 1596.00, S; 1622.00, M; 1642.00, S; 1688.00, M; 1745.00, S; 2910.00, W; 2933.00, W; 2982.00, W; 3036.00, W; 3096.00, W; 3146.00, W; 3291.00, M;

### Synthesis of *tert*-butyl 2-(anilincarbonyl)hydrazinecarboxylate (19)



Reagent	M.W. (g/mol)	Weight (mg)	mmol	eq
Tert-Butyl carbazate	132.16	202.08	1.53	1
Phenyl -isocyanate	119.12	182.14	1.53	1

solvent: Toluene

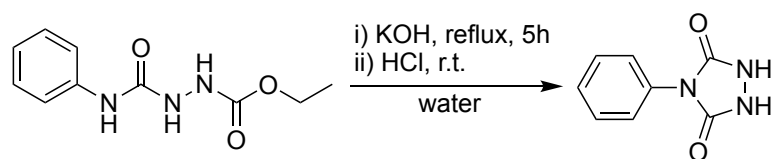
Tert-Butyl carbazate (202 mg, 1.53 mmol) was dissolved in 20 mL of toluene, under nitrogen atmosphere. The solution was cooled to 0 °C, then Phenyl -isocyanate (3.45 g, 29 mmol), in 5 mL of toluene, was added over a period of 10 min. The mixture was rinsed to r.t. and stirred for 30 min, then refluxed for 3 h. After cooling to r.t., the product was recovered by filtration, washed with cold toluene, and dried at 80 °C overnight (365 mg, 95%).

Physical aspect: Solid, white powder

<sup>1</sup>H NMR (CDCl<sub>3</sub>, 500 MHz): δ (ppm) = 1.49 (s, 9H -tBut), 6.49 (s, 1H, -NH), 6.76 (s, 1H, -NH), 7.04 (t, 1H), 7.25 (t, 2H), 7.36 (d, 2H), δ 7.43 (s, 1H -NH),

FTIR-ATR (cm<sup>-1</sup>, intensity): 673.00 ,W; 679.00 ,W; 697.00 , S; 751.00 , S; 787.00 ,W; 852.00 W; 884.00 M; 912.00 W; 1014.00 M; 1029.00 W; 1039.00 M; 1047.00 M; 1080.00 W; 1157.00 VS; 1239.00 VS; 1267.00 M; 1308.00 M; 1318.00 M; 1366.00 M; 1394.00 W; 1440.00 M; 1492.00 S; 1500.00 S; 1553.00 VS; 1598.00 S; 1620.00 W; 1651.00 S; 1685.00 M; 1738.00 VS; 2935.00 W; 2989.00 W; 3295.00 M; 3330.00 M.

### Synthesis of 4-phenyl-1,2,4-triazolidine-3,5-dione (4-Phenylurazole) (20)



Reagent	M.W. (g/mol)	Weight (g)	mmol	eq
Ethylsemicarbazate (18)	223.23	6.05	27.1	1
KOH 4M	54.11	-	-	-

Solvent: water

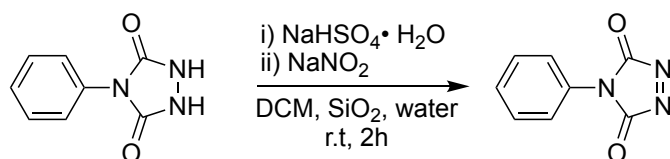
(6 g, 27.1 mmol) of ethylsemicarbazate (18) was solved in KOH<sub>aq</sub> (25 mL, 4 M) and heated at 100 °C for 5 h. The mixture was then cooled with an ice bath and acidified with concentrated HCl (37%) until pH ≈ 1. The residue was collected by filtration and dried overnight at 80 °C under vacuum (10 torr) (4.68 g, 98%).

Physical aspect: Solid, white crystals

<sup>1</sup>H NMR (DMSO-d<sub>6</sub>, 500 MHz): δ (ppm) = 7.32 – 7.56 (m, 5H –C<sub>6</sub>H<sub>5</sub>), 10.46 (s, 2H –NH),

FTIR-ATR (cm<sup>-1</sup>, intensity): 689.00, S; 757.00, VS; 788.00, S; 912.00, W; 1011.00, W; 1035.00, W; 1069.00, M; 1118.00, M; 1154.00, M; 1179.00, M; 1224.00, M; 1295.00, M; 1439.00, S; 1494.00, S; 1505.00, S; 1598.00, M; 1679.00, S; 1779.00, W; 2809.00, W; 3053.00, M; 3102.00, M; 3155.00, M;

### Synthesis of 4-phenyl-3*H*-1,2,4-triazole-3,5(4*H*)-dione (PhTAD) (21)



Reagent	M.W. (g/mol)	Weight (mg)	mmol	eq
4-Phenylurazole	177.16	550.00	3.10	1
Sodium Hydrogen sulfate hydrate	138.08	1286.02	9.31	3
Sodium Nitrite	68.98	642.45	9.31	3
Silica	-	1240		

Solvent: DCM

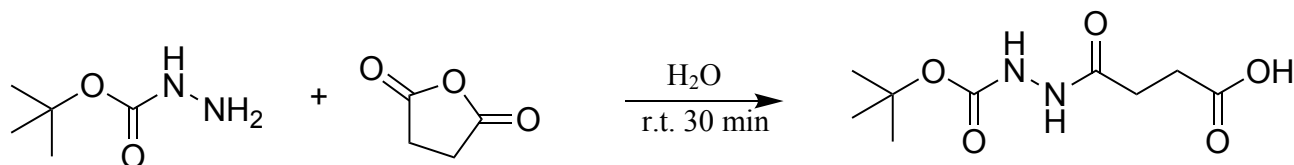
550 mg of 4-phenylurazole (3.1 mmol) was grinded into a mortar with NaHSO<sub>4</sub> · H<sub>2</sub>O (3 eq.) and SiO<sub>2</sub> (1240 mg, 70 - 200 μm). Water (600 μL) was added to the fine powder obtained, and the resulting mixture was stirred for 5 min. CH<sub>2</sub>Cl<sub>2</sub> (25 mL) was then added and the suspension was kept in the dark and in a sealed vessel for the whole reaction time. Every 30 min NaNO<sub>2</sub> (1 equiv) was added to the reaction mixture (3 eq. overall). The inorganic salts were removed by filtration and the solvent was removed under reduced pressure to afford PhTAD in a pure form (470 mg, 88%).

Physical aspect: Solid, pink-red powder

<sup>1</sup>H NMR (CDCl<sub>3</sub>, 500 MHz): δ (ppm) = 7.08 – 7.12 (m, 2H), 7.23 – 7.28 (m, 1H), 7.41 – 7.48 (m, 2H)

FTIR-ATR (cm<sup>-1</sup>, intensity): 663.00, S; 674.00, S; 687.00, M; 721.00, VS; 767.00, M; 898.00, M; 914.00, W; 1006.00, M; 1012.00, M; 1024.00, M; 1031.00, W; 1073.00, W; 1158.00, S; 1173.00, VS; 1290.00, M; 1317.00, W; 1395.00, S; 1455.00, M; 1466.00, W; 1501.00, S; 1527.00, M; 1596.00, M; 1626.00, W; 1737.00, VS; 1745.00, VS;

### Synthesis of 4-(*N'*-*tert*-butoxycarbonyl-hydrazino)-4-oxo-butyric acid



Reagent	M.W. (g/mol)	Weight (g)	mmol	eq
tertButyl carbazate	132.16	1	7.6	1
Succinic anhydride	100.07	0.76	7.6	1

Solvent: Water

0.76 g (7.6 mmol) of succinic anhydride and 1 g (7.6 mmol) of *tert*-butyl carbazate were dissolved in 20 mL water under magnetic stirring at room temperature. Within 30 min the solution became clear.

The reaction proceeded smoothly and fast in quantitative yields.

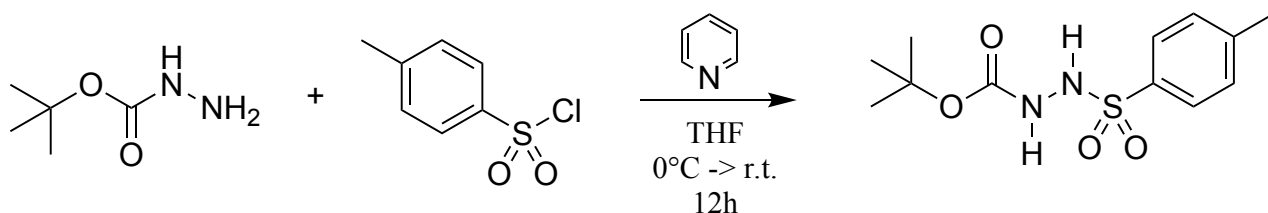
The reaction mixture was lyophilized in 72 hours and used without further purification.

Physical aspect: Solid, white powder

<sup>1</sup>H NMR (dms<sub>o</sub>-d<sub>6</sub>, 500 MHz): δ (ppm) = 1.40 (s, 9H, C(CH<sub>3</sub>)<sub>3</sub>), 2.32 (t, 2H, CH<sub>2</sub>COOH), 2.43 (t, 2H, CH<sub>2</sub>C=ONH), 8.71 (s, 1H, NH-*t*Boc), 9.54 (s, 1H, NHC=OCH<sub>2</sub>).

FTIR-ATR (cm<sup>-1</sup>, intensity): 779, W; 863, W; 918, VW, 1017, W; 1050, W; 1151, VS; 1245, S; 1368, S; 1394, M; 1496, M; 1501, M; 1671, S; 1709, S; 2937, W; 2982, M; 3271, W;

## Synthesis of *tert*-butyl 2-[(4-methylphenyl)-sulfonyl]-hydrazine-carboxylate



Reagent	M.W. (g/mol)	Weight (g)	mmol	eq
<i>tert</i> -butyl hydrazinecarboxylate	132.16	0.1	0.076	1
4-methylbenzenesulfonyl chloride	190.67	0.159	0.085	1.1
Pyridine	79.1	0.359	4.54	6

Solvent: THF

100 mg (0.076 mmol) of *tert*-butyl carbazate were added to a solution of 159 mg (0.085 mmol) of 4-methylbenzenesulfonyl chloride in 10 mL of THF, cooled in an ice bath at 0 °C, under magnetic stirring. After 15 min, the reaction was allowed to reach room temperature and stirred for 12 hours.

HCl (aqueous, 1 M) was added to the solution till pH  $\approx$ 3, then the organic layer was extracted with DCM three times. Once extracted, the organic phase was dried adding MgSO<sub>4</sub>. The sulfate was filtered off and the product was collected after the evaporation of the solvent heated under reduced pressure, with 71% of yield.

Physical aspect: Solid, white powder

<sup>1</sup>H NMR (CDCl<sub>3</sub>, 400 MHz):  $\delta$  (ppm) = 1.26 (s, 9H t-But), 2.44 (s, 3H -CH<sub>3</sub>), 6.53 (s, 2H), 7.33 (d, 2H), 7.83 (d, 2H),

FTIR-ATR (cm<sup>-1</sup>, intensity): 556.00, W; 599.00, W; 614.00, VW; 667.00, M; 705.00, W; 752.00, W; 775.00, W; 800.00, W; 812.00, M; 856.00, W; 1019.00, W; 1049.00, W; 1091.00, M; 1151.00, VS; 1184.00, M; 1255.00, M; 1287.00, M; 1305.00, M; 1335.00, S; 1369.00, M; 1396.00, M; 1420.00, W; 1456.00, W; 1496.00, M; 1599.00, W; 1710.00, M; 2935.00, W; 2980.00, W; 3231.00, W; 3301.00, W; 3343.00, W;

## BIBLIOGRAPHY

---

- <sup>1</sup> V. Coessens, T. Pintauer, K. Matyjaszewski, *Prog. Polym. Sci.* **2001**, *26*, 337-377.
- <sup>2</sup> T. Curtius, *Ber. Dtsch. Chem. Ges.* **1883**, *16*, 2230.
- <sup>3</sup> E. Buchner, *Ber. Dtsch. Chem. Ges.* **1888**, *21*, 2637.
- <sup>4</sup> A. Michael, *J. Prakt. Chem.* **1893**, *48*, 94.
- <sup>5</sup> H.V. Pechmann, *Ber. Dtsch. Chem. Ges.* **1894**, *27*, 1888.
- <sup>6</sup> A. Werner, H. Buss, *Ber. Dtsch. Chem. Ges.* **1894**, *27*, 219.
- <sup>7</sup> E. Beckmann, *Ber. Dtsch. Chem. Ges.* **1890**, *23*, 3331.
- <sup>8</sup> R. Huisgen, *Angewandte Chemie* **1963**, *75*, 604–637.
- <sup>9</sup> R.A. Firestone, *J. Chem. Soc., A*, **1970**, *92*, 1570.
- <sup>10</sup> G. Mloston, E. Langhals, R. Huisgen, *J. Am. Chem. Soc.* **1986**, *108*, 6401–66402. doi:10.1021/ja00280a053.
- <sup>11</sup> S. A. Siadati, *Tetrahedron Letters*, **2015**, *56*, 4857–4863. doi:10.1016/j.tetlet.2015.06.048.
- <sup>12</sup> R. Huisgen, *Angewandte Chemie International Edition* **1963**, *2*, 565-598. doi: 10.1002 / anie.196305651.
- <sup>13</sup> A. Cox, L. Thomas, J. Sheridan, *Nature* **1958**, *181* (4614): 1000-1001. doi: 10.1038 / 1811000a0.
- <sup>14</sup> P. Hilberty, C. Leforestier, *J. Am. Chem. Soc.* **1978**, *100*, 2012-2017. doi: 10.1021 / ja00475a007.
- <sup>15</sup> R. Sustmann, *Pure and Applied Chemistry* **1974**, *40*, 569-593. doi: 10.1351 / pac197440040569.
- <sup>16</sup> R. Huisgen, G. Szeimies, L. Mobius, *Chemische Berichte* **1967**, *100*, 2494-2507. doi: 10.1002 / cber.19671000806.
- <sup>17</sup> D.G. Williamson, R.J. Cvetanovic, *J. Am. Chem. Soc.* **1968**, *90*, 3668-3672. doi: 10.1021 / ja01016a011.
- <sup>18</sup> R. Huisgen, *Angew. Chem.* **1963**, *75*, 604; *Angew. Chem. Intern. Ed.* **1963**, *2*, 565.
- <sup>19</sup> KBG Torssell, Nitrile Oxides, Nitrones, and Nitronates in Organic Synthesis. Novel Strategies in Synthesis **1988**, VCH, Weinheim, ch. 1, 1; ch. 2, 55; ch. 5, 129.
- <sup>20</sup> L. Gaisler, R.M. Paton, J.H. Hall, D.J. Harper, *J. Polym. Sci., Polym. Lett. Ed.* **1980**, *18*, 635.
- <sup>21</sup> C.E. Hoyle, T.Y. Lee, T. Roper, *J. Polym. Sci., Part A: Polym. Chem.* **2004**, *42*, 5301-5338.

- 
- <sup>22</sup> J.-F. Lutz, H. Schlaad, *Polymer* **2008**, *49*, 817–824.
- <sup>23</sup> G.E. Serniuk, F.W. Banes, M.W. Swaney, *J. Am. Chem. Soc.* **1948**, *70*, 1804–1808.
- <sup>24</sup> B. Boutevin, Y. Hervaud, G. Mouledous, *Polym. Bull.* **1998**, *41*, 145–152
- <sup>25</sup> J. Justynska, Z. Hordyjewicz, H. Schlaad, *Polymer* **2005**, *46*, 12057–12064.
- <sup>26</sup> R.L. Ameri David, J.A. Kornfield, *Macromolecules* **2008**, *41*, 1151–1161
- <sup>27</sup> C.E. Hoyle, C.N. Bowman, *Angewandte Chemie International Edition* **2010**, *49* (9), 1540-1573. doi: 10.1002 / anie.200903924.
- <sup>28</sup> C.E. Hoyle, A.B. Lowe, C.N. Bowman, *Chem. Soc. Rev.* **2010**, *39*, 1355-1387.
- <sup>29</sup> A.B. Lowe, *Polym. Chem.* **2010**, *1*, 17-36.
- <sup>30</sup> B. D. Mather, K. Viswanathan, K. V. Miller, T. E. Long, *Prog. Polym. Sci.* **2006**, *31*, 487 - 531.
- <sup>31</sup> H. Kakwere, S. Perrrier, *J. Am. Chem. Soc.* **2009**, *131*, 1889 - 1895.
- <sup>32</sup> O. Diels, J.H. Blom, W. Koll, *Justus Liebigs Ann. Chem.* **1925**, *443*, 242–262.
- <sup>33</sup> O. Diels, K. Alder, *Justus Liebigs Ann. Chem.* **1928**, *460*, 98–122.
- <sup>34</sup> J. Thiele, O. Stange, *Justus Liebigs Ann. Chem.* **1894**, *283*, 1–46.
- <sup>35</sup> R.C. Cookson, S.S.H. Gilani, I.D.R. Stevens, *Tetrahedron Lett.* **1962**, *3*, 615–618.
- <sup>36</sup> G. Zinner, W. Deucker, *Arch. Pharm.* **1961**, *294*, 370–372.
- <sup>37</sup> G.B. Butler, *Ind. Eng. Chem. Prod. Res. Dev.* **1980**, *19*, 512–528.
- <sup>38</sup> W.H. Pirkle, J.C. Stickler, *Chem. Commun.* **1967**, 760–761.
- <sup>39</sup> S. Ohashi, K.-W. Leong, K. Matyjaszewski, G.B. Butler, *J. Org. Chem.* **1980**, *45*, 3467–3471.
- <sup>40</sup> A.G. Williams, G.B. Butler, *J. Org. Chem.* **1980**, *45*, 1232–1239.
- <sup>41</sup> M.A. Zolfigol, H. Nasr-Isfahani, S. Mallakpour, M. Safaiee, *Synlett* **2005**, 761–764.
- <sup>42</sup> J. Sauer, *Angew. Chem., Int. Ed. Engl.* **1967**, *6*, 16–33.
- <sup>43</sup> G.B. Butler, *Polym. Sci. U.S.S.R.* **1981**, *23*, 2587–2622.
- <sup>44</sup> M.E. Burrage, R.C. Cookson, S.S. Gupte, I.D.R. Stevens, *J. Chem. Soc., Perkin Trans. 2* **1975**, 1325–1334.
- <sup>45</sup> K. De Bruycker, S. Billiet, H.A. Houck, S. Chattopadhyay, J.M. Winne, Filip E. Du Prez, *Chem.*

---

Rev. **2016**, *116*, 3919–3974.

<sup>46</sup> R.L. Sowerby, Patent WO8707892, **1987**.

<sup>47</sup> M. Furdik, S. Mikulase, M. Livar, S. Priehrad, *Chem. Zvesti* **1967**, *21*, 427–442.

<sup>48</sup> W. Ried, S.-H. Lim, *Justus Liebigs Ann. Chem.* **1973**, 129–133.

<sup>49</sup> J.C. Stickler, W.H. Pirkle, *J. Org. Chem.* **1966**, *31*, 3444–3445.

<sup>50</sup> J.L. Riebsomer, *Chem. Rev.* **1945**, *36*, 157–233.

<sup>51</sup> M.A. Zolfigol, S.E. Mallakpour, E. Madrakian, E. Ghaemi, *Indian J. Chem., Sect. B: Org. Chem. Incl. Med. Chem.* **2000**, *39*, 308–310.

<sup>52</sup> R.M. Moriarty, I. Prakash, R. Penrnasta, *Synth. Commun.* **1987**, *17*, 409–413.

<sup>53</sup> R.J. Pounder, M.J. Stanford, P. Brooks, S.P. Richards, A.P. Dove, *Chem. Commun.* **2008**, 5158–5160.

<sup>54</sup> N. Roy, J.-M. Lehn, *Chem. - Asian J.* **2011**, *6*, 2419–2425.

<sup>55</sup> A.F. Holleman, E. Wiberg, N. Wiberg, *Inorganic Chemistry; Academic Press: New York*, **2001**; p 1884.

<sup>56</sup> P.S. Baran, C.A. Guerrero, E.J. Corey, *Org. Lett.* **2003**, *5*, 1999–2001.

<sup>57</sup> W. Adam, O. De Lucchi, *Tetrahedron Lett.* **1981**, *22*, 929–932.

<sup>58</sup> D.A. Singleton, C. Hang, *J. Am. Chem. Soc.* **1999**, *121*, 11885–11893.

<sup>59</sup> A.G. Leach, K.N. Houk, *Chem. Commun.* **2002**, 1243–1255.

<sup>60</sup> M.J.S. Dewar, S. Olivella, J.J.P. Stewart, *J. Am. Chem. Soc.* **1986**, *108*, 5771–5779.

<sup>61</sup> F.A. Carey, R.J. Sundberg, *R. J. Advanced Organic Chemistry-Part B: Reactions and Synthesis, 5th ed.*; Springer: New York, **2007**; p 1322.

<sup>62</sup> B. Rickborn, In *Organic Reactions; John Wiley & Sons, Inc.*: New York, **2004**.

<sup>63</sup> R.I. Yakhimovich, N.F. Fursaeva, V.E. Pashinnik, *Chem. Nat. Compd.* **1985**, *21*, 98–103.

<sup>64</sup> M.L. Poutsma, P.A. Ibarbia, *J. Am. Chem. Soc.* **1971**, *93*, 440–450.

<sup>65</sup> A.P. Henderson, E. Mutlu, A. Leclercq, C. Bleasdale, W. Clegg, R.A. Henderson, B.T. Golding, *Chem. Commun.* **2002**, 1956–1957.

<sup>66</sup> K. Alder, F. Pascher, A. Schmitz, *Ber. Dtsch. Chem. Ges. B* **1943**, *76*, 27–53.

- 
- <sup>67</sup> M.L. Clarke, M.B. France, *Tetrahedron* **2008**, *64*, 9003–9031.
- <sup>68</sup> L.J. Watson, Pericyclic Reactions of Vinyl-Heteroaromatics: Multi-Component Domino and Sequential Processes. Ph.D. Thesis, Newcastle University, **2013**.
- <sup>69</sup> Y. Hayashi, T. Shibata, K. Narasaka, *Chem. Lett.* **1990**, *19*, 1693–1696.
- <sup>70</sup> M. Squillacote, M. Mooney, J. De Felippis, *J. Am. Chem. Soc.* **1990**, *112*, 5364–5365.
- <sup>71</sup> M.M. Roubelakis, G.C. Vougioukalakis, Y.S. Angelis, M. Orfanopoulos, *Org. Lett.* **2006**, *8*, 39–42.
- <sup>72</sup> O. Acevedo, M.E. Squillacote, *J. Org. Chem.* **2008**, *73*, 912–922.
- <sup>73</sup> M.E. Squillacote, C. Garner, L. Oliver, M. Mooney, Y.-L. Lai, *Org. Lett.* **2007**, *9*, 5405–5408.
- <sup>74</sup> G.W. Breton, K.R. Hoke, *J. Org. Chem.* **2013**, *78*, 4697–4707.
- <sup>75</sup> H. Ban, J. Gavriyuk, C.F. Barbas, *J Am Chem Soc.* **2010**, *132(5)*, 1523-5. DOI: 10.1021/ja909062q
- <sup>76</sup> H. Ban, M. Nagano, J. Gavriyuk, W. Hakamata, T. Inokuma, C.F. Barbas, *Bioconjug Chem.* **2013**, *24(4)*, 520-32. DOI: 10.1021/bc300665t
- <sup>77</sup> S. Vandewalle, R. De Coen, B.G. De Geest, F.E. Du Prez, *ACS Macro Lett.* **2017**, *6*, 1368–1372, DOI: 10.1021/acsmacrolett.7b00795
- <sup>78</sup> C.M. Rasik, M.K. Brown, *J. Am. Chem. Soc.* **2013**, *135*, 1673– 1676.
- <sup>79</sup> G.B. Butler, A.G. Williams, *J. Polym. Sci., Polym. Chem. Ed.* **1979**, *17*, 1117– 1128.
- <sup>80</sup> B. Ostermayer, Thermoplastic Moulding Compositions. Patent EP0412414A2, **1990**.
- <sup>81</sup> E. Baumgartner, Graft Copolymers and Process for Producing the Same. Patent EP0390028A2, **1990**.
- <sup>82</sup> J. Blackborow, Substituted Azo-Dicarbonylo Derivatives. EP0728766A2, **1996**.
- <sup>83</sup> K.-W. Leong, G.B. Butler, *J. Macromol. Sci., Chem.* **1980**, *14*, 287–319.
- <sup>84</sup> T.C.S. Chen, G.B. Butler, *J. Macromol. Sci., Chem.* **1981**, *16*, 757–768.
- <sup>85</sup> R. Stadler, M.M. Jacobi, W. Gronski, *Makromol. Chem., Rapid Commun.* **1983**, *4*, 129– 135.
- <sup>86</sup> W. Gronski, R. Stadler, M. Maldaner Jacobi, *Macromolecules* **1984**, *17*, 741–748.
- <sup>87</sup> R. Stadler, J. Burgert, *Makromol. Chem.* **1986**, *187*, 1681–1690.
- <sup>88</sup> R. Stadler, L. de Lucca Freitas, *Colloid Polym. Sci.* **1986**, *264*, 773–778.

- 
- <sup>89</sup> R. Stadler, L. de Lucca Freitas, *Polym. Bull.* **1986**, *15*, 173–179.
- <sup>90</sup> U. Seidel, R. Stadler, G.G. Fuller, *Macromolecules* **1994**, *27*, 2066–2072.
- <sup>91</sup> C.I.D. Bica, W. Burchard, R. Stadler, *Macromol. Chem. Phys.* **1996**, *197*, 3407–3426.
- <sup>92</sup> M. Müller, U. Seidel, R. Stadler, *Polymer* **1995**, *36*, 3143–3150.
- <sup>93</sup> S. Mallakpour, F. Rafiemanzelat, B. Sheikholeslami, *Iran. Polym. J.* **1997**, *6*, 235–241.
- <sup>94</sup> T. Sabu, S. Ranimol, *Rubber Nanocomposites: Preparation, Properties and Applications*, (2010), John Wiley & Sons.
- <sup>95</sup> T. Sabu, J.M. Hanna, *Progress in rubber nanocomposites*, Woodhead Publishing Series in Composites Science and Engineering: Number 75, (2017) Elsevier.
- <sup>96</sup> K. Nagdi, *Rubber as an Engineering Material: Guideline for Users*, Carl Hanser Verlag (1993).
- <sup>97</sup> J. Brinke, S. Debnath, L. Reuvekamp, J. Noordermeer, (2003) *Compos. Sci. Technol.* **2003**, *63*, 1165–1174.
- <sup>98</sup> C.G. Moore and M. Porter *Rubber Chem. Technol.* (1963), *36*, 547–557.
- <sup>99</sup> A.R. Payne, *Rubber Plast Age* **1961**, 963.
- <sup>100</sup> A.R. Payne, *Rubber Chem. Technol.* **1971**, *44*, 440.
- <sup>101</sup> M. Klüppel, G. Heinrich, *Rubber Chem. Technol.* **1995**, *68* (4), 623–651.
- <sup>102</sup> M. Klüppel, R.H. Schuster, G. and Heinrich, *Rubber Chem. Technol.* **1997**, *70* (2), 243–255.
- <sup>103</sup> A.I. Medalia, *J. Interface. Sci.*, **1970**, *32*, 115.
- <sup>104</sup> G. Kraus, *Rubber Chem. Technol.*, **1971**, *44*, 199.
- <sup>105</sup> P.P.A. Smit, *Rubber Chem. Technol.*, **1968**, *41*, 1194.
- <sup>106</sup> I. Pliskin, N. Tokita, *J. Appl. Sci.*, **1972**, *16*, 473.
- <sup>107</sup> J.L. Leblanc, *Prog. Polym. Sci.* **2002**, *27*, 627–687.
- <sup>108</sup> K. Smirnov, *Vib. Spectrosc.* **1993**, *4*, 255–259.
- <sup>109</sup> W. Hertl, M. Hair, *J. Phys. Chem.* **1969**, *83*, 2372–2378.
- <sup>110</sup> M. Trombetta, T. Armaroli, A.G. Alejandre, J.R. Solis, G. Busca, *Appl. Catal., A* **2000**, *192*, 125–136.
- <sup>111</sup> M.J. Wang, S. Wolff, J.B. Donnet, *Rubber Chem. Technol.* **1991**, *64*, 559–576.

- 
- <sup>112</sup> E. Papirer, H. Balard, A. Vidal, *Eur. Polym. J.* **1988**, *24*, 783–790.
- <sup>113</sup> M. Castellano, L. Falqui, G. Costa, A. Turturro, B. Valenti, G. Castello, *J. Macromol. Sci.* **2002**, *41* (3), 451–471.
- <sup>114</sup> Y.-J. Heo, *Carbon letters*. **2015**, *18*, 1-10. Doi: 10.5714 / CL.2016.18.001.
- <sup>115</sup> C.-C. Peng et al. *Polym. Adv. Technol.* **2005**, *16*, 770-782.
- <sup>116</sup> Dicken and DeShong, *J. Org. Chem.* **1982**, *47*, No. 11, 2047–2051.
- <sup>117</sup> **Patent n°**: WO2015/114997, A1, 2015 – Yokohama Rubber Co.
- <sup>118</sup> A. Bâdoiu, E. P. Kündig, *Org. Biomol. Chem.* **2012**, *10*, 114.
- <sup>119</sup> Patent no. WO2014 / 72747, A1, 2014 by Medpharm Limited
- <sup>120</sup> Harding, Marcuccio, Savage, *Beilstein J. Org. Chem.* **2012**, *8*, 606-612.
- <sup>121</sup> Jawalekar, Reubsæet, Van Delft, *Chem. Commun.* **2011**, *47*, 3198.
- <sup>122</sup> W. Zhang, H. Sun, L. Wang, *Soil and Sediment Contamination* **2013**, *22*, 469–482.
- <sup>123</sup> Ayush Gupta *J. Phys.: Condens. Matter* **2016**, *28*, 094002
- <sup>124</sup> N. Brummelhuis, C. Diehl, H. Schlaad *Macromolecules* **2008**, *41*, No. 24, 9946-9947.
- <sup>125</sup> R.L. Ameri David, J.A. Kornfield, *Macromolecules* **2008**, *41*, 1151– 1161.
- <sup>126</sup> J. Justynska, Z. Hordyjewicz, H. Schlaad, *Polymer* **2005**, *46*, 12057– 12064.
- <sup>127</sup> L. Herczynska, L. Lestel, S. Boileau, J. Chojnowski, S. Polowinski, *Eur. Polym. J.* **1999**, *35*, 1115–1122.
- <sup>128</sup> M. Mihelčič, A.K. Surca, A. Kreta, M. Gaberšček, *Croat. Chem. Acta* **2017**, *90*(2), 169–175, DOI: 10.5562/cca3161
- <sup>129</sup> B. Neises, W. Steglich, *Angew. Chem. Int. Ed.* 1978, *17* (7): 522-524. doi: 10.1002 / anie.197805221.
- <sup>130</sup> E. Fischer, A. Speier, *Chemische Berichte* **1895**, *28*, 3252-3258. doi: 10.1002 / cber.189502803176.
- <sup>131</sup> M. S. Fellet, J. Bartels, B. Bi, K. D. Moeller, *J. Am. Chem. Soc.* **2012**, *134*, 16891-16898.
- <sup>132</sup> N. Iranpoor, H. Firouzabadi, B. Akhlaghinia, R. Azadi, *Synthesis* **2004**, *1*, 92–96.
- <sup>133</sup> N. Iranpoor et al., *Tetrahedron Letters* **2012**, *53*, 6913–6915.

- 
- <sup>134</sup> C. J. Bums, L. D. Field, J. Morgan, D. D. Ridley, V. Vignevich, *Tetrahedron Letters* **1999**, *40*, 6489-6492.
- <sup>135</sup> Mallakpour, *Synthetic Comm.* **2007**, *37*, 1927-1934 & *Molecules* **2003**, *8*, 359-362.
- <sup>136</sup> M.A. Zolfigol, M. Bagherzadeh, S. Mallakpour, G. Chehardoli, A. Ghorbani-Choghamarani, N. Koukabi, M. Dehghanian, M. Doroudgar, *J. of Molecular Catalyst A: Chemical* **2007**, *270*, 219-224.
- <sup>137</sup> C.C. Cheng, C.A. Seymour, M.A. Petti, F.D. Greene, J.F. Blount, *J. Org. Chem.* **1984**, *49*, 2910–2916.
- <sup>138</sup> V.D. Kiselev, I.I. Shakirova, D.A. Kornilov, H.A. Kashaeva, L.N. Potapova, A.I. Konovalov, *J. Phys. Org. Chem.* **2013**, *26*, 47–53.
- <sup>139</sup> V.D. Kiselev, D.A. Kornilov, L.N. Potapova, H.A. Kashaeva, A.I. Konovalov, *Russ. J. Phys. Chem.* **2014**, *88*, 890–892.
- <sup>140</sup> V.D. Kiselev, D.A. Kornilov, I.I. Lekomtseva, A.I. Konovalov, *Int. J. Chem. Kinet.* **2015**, *47*, 289–301
- <sup>141</sup> X.A.J. Marzocca, A.L. Rodriguez Garraza, P. Sorichetti, H.O. Mosca, *Polymer Testing* **2010**, *29*, 4, 477-482.
- <sup>142</sup> T. Goffrey, M. Knight, J.L. Loadman, B. Saville, J.J.C.S. Wildgoose, *Chem. Commun.* **1974**, 193-194.
- <sup>143</sup> A. Dirksen, S. Dirksen, T.M. Hackeng, P.E. Dawson, *J. Am. Chem. Soc.* **2006**, *128*, 15602 – 15603.
- <sup>144</sup> Wunde M., Klüppel M., *Rubber Chemistry And Technology*, **2016**, *89*, **4**, 588–607 .
- <sup>145</sup> S.-H. Chouch, D.-H. Chang, *J. of Appl. Polym. Sci.*, **1996**, *61*, 449-454.